OMV Australia

VIC/RL 5

Australia - Gippsland Basin

BALEEN 2

WELL COMPLETION REPORT
INTERPRETIVE DATA

- VOLUME 3 -

Prepared by:
Alex Warris and Mark Adamson

CONFIDENTIAL

OMV Australia

908080 002

Cultus Timor Sea Pty Ltd
(ACN 064 126 138)
Level 29, 44 St George's Tce
Perth WA 6000
Australia
Tel: (61 8) 9223 5000
Fax: (61 8) 9223 5004

AUSTRALIA
GIPPSLAND BASIN

VIC/RL5

BALEEN-2

WELL COMPLETION REPORT
INTERPRETIVE DATA
VOLUME 3

Prepared by:
Alex Warris and Mark Adamson

CONFIDENTIAL

OMV Australia

908080 003

Cultus Timor Sea Pty Ltd
(ACN 064 126 138)

AUSTRALIA
GIPPSLAND BASIN

VIC/RL5

BALEEN-2

WELL COMPLETION REPORT
INTERPRETIVE DATA
VOLUME 3

Prepared by:
Alex Warris and Mark Adamson

Approved by:

Exploration Manager

October, 2000

CONFIDENTIAL

Copy No. 3

WELL SUMMARY CARD – BALEEN-2

WELL:	**BALEEN-2**	**SPUD**	02:15 hrs 11/10/99
WELL TYPE:	APPRAISAL	**TD REACHED:**	02:45 hrs 16/10/99
BLOCK/LICENCE:	VIC/RL5 Gippsland Basin	**RIG RELEASE:**	19/10/99
RIG:	SEDCO 702	**COMPLETION:**	n/a
WATER DEPTH:	55m (BMSL)	**STATUS:**	Plugged and abandoned appraisal well with gas and trace oil shows
RT (MSL):	26.0m	**TRAP TYPE**	Faulted anticline
TD:	895 m (driller) 895 m (TVD corrected)	**ZONE:**	Gurnard Formation
SURFACE LATITUDE:	38° 01' 55.76" S	**SURFACE Y coord:**	5 789 663.9 mN
SURFACE LONGITUDE:	148° 24' 37.55" E	**SURFACE X coord:**	623 781.4 mE
OBJECTIVE LATITUDE:	38° 01' 55.79" S	**OBJECTIVE Y coord:**	5 789 663 N
OBJECTIVE LONGITUDE:	148° 24' 37.57" E	**OBJECTIVE X coord:**	623 782 E
		Spheroid/Datum:	UTM Zone 55, CM 147°E ANS / AGD 66
SURFACE Seismic Station:	GL88-62, coincident with intersecting line GL88-55	**OBJECTIVE OFFSET:**	1.08m at 326°T

REMARKS: Vertical Well
Drilled without riser to 650m

CASING SIZE	SHOE DEPTH (mRT):	TYPE
30x20"	126m	Drill quip / SWF60
9 5/8"	646m	LTC/Buttress

LOG INTERPRETATION (Weighted Averages)

ZONE	INTERVAL m RT	THICKNESS	Net Pay (m)	POR Av%	Av Sw %
Gurnard	747.8-759	11.2m	10.6m	29.5%	59%

DST	Flow rate	Choke	GOR
No tests			

PERFORATIONS

No Perforations

CORES

ZONE	No.	INTERVAL mRT	CUT m	REC m
Gurnard	1	746 – 762.2	16.3	16.3
Gurnard	2	763.7 – 779.5	18	15.9

MUD DATA

SUITE	SUITE 1
TYPE	NaCl / PHPA / Polymer
DENSITY	1.21 g/cm3
VISCOSITY	49 sec/qt
FLUID LOSS	3.4 cc / 30 min
pH	9
RM	0.134 ohm.m @21°C
RMF	0.115 ohm.m @22°C
RMC	0.213 ohm.m @22°C
Chlorides	46 500 mg / L
Barite	3.7% by volume
NaCl	7.6% by volume

WIRELINE LOGS

LOG TYPE	SUITE / RUN	INTERVAL mRT	BHT °C /TIME	COMMENTS
PEX-HALS-DSI-NGS	1 / 1	888.5-90	46.7°C/5:21hrs	Logged GR from 640-90. Full PEX-DSI high resolution data recorded at 1800ft/h.
FMI-GR	1 / 2	887-647	48°C/8:35hrs	Logged open hole interval
MDT (pretests and samples)	1 / 3,5	823-748	52°C/18:25hrs	32 pretests, 16 normal, 8 supercharged, 5 lost seal, 2 pumpout failure, 1 dry test
CSAT-GR (VSP Survey)	1 / 4	885-100	50°C/22hrs	47 checkshot levels acquired, including 3 repeat levels at 300m, 663m and 795m
Junk Basket & Bridge Plug (GR and CCL record)	6,7	200-100		Run prior to setting cement abandonment plug 3

STRATIGRAPHY

AGE	FORMATION TOPS	MEASURED DEPTH mRT	SUBSEA mSS	THICKNESS (m)	PROGNOSED DEPTH mSS	DIFFERENCE (m)	DIFFERENCE High/low
Miocene	Gippsland Limestone -Seafloor	81	55	643	53	2	L
Oligocene	Lakes Entrance Formation	724	698	17	650	48	L
Eocene	Latrobe Group	741*	715	131	710	5	L
Eocene	- Gurnard Formation	741*	715	51	710	5	L
Eocene	- Coarse Clastics (Barracouda Formation)	792	766	80	755	11	L
Early Cretaceous	Strzelecki Group	872	846	23+	820	26	L
	Total Depth (T.D.)	**895**	**869**	-	**870**	**1**	**H**

*Revised top Gurnard pick.

WELL SUMMARY

Baleen-2 was an appraisal well drilled in the northern Gippsland Basin on the southwest extension of the Baleen portion of the Patricia-Baleen Gas Field. The well was drilled 3.31 km southwest and structurally downdip of the Baleen-1 discovery well which encountered dry gas accumulations in the Gurnard Formation and Latrobe Group Coarse Clastics.

The well was spudded at 2:15am on the 11th of October 1999 in 55 metres of water, and was drilled to a total depth of 895mRT at 2:45am on the 16th of October 1999. The 12 ¼" hole was drilled to 650mRT without the marine riser installed. 30"x20" casing set at 126mRT, and 9 5/8" casing set at 646mRT. An FIT was performed at 654mRT to 15.1ppg EMW, then the 8 ½" hole section was drilled to T.D.

The Patricia-Baleen Gas Field was mapped using several vintages of reprocessed data from 1979 to 1992. Good horizon continuity and a direct hydrocarbon indicator amplitude anomaly are observed at the discovery location and extend to Baleen-2. The pre-drill prognosis inferred the GWC at 734mSS. The observed DHI and 'flat lying event' gave the interpretation a high degree of confidence that at least a 7m gas column would be intersected. The depth conversion, based on a depth of burial average velocity trend, proved very accurate (just over 1.3% error) and 16.2m of gross gas column were intersected in the well.

The stratigraphy was very similar to prediction, however there appears to be some channeling or erosion at the top of the Lakes Entrance Formation resulting in approximately 31m reduction in thickness of the Lakes Entrance Formation, and 41m increase in Gippsland Limestone thickness at the Baleen-2 location. The objective Gurnard Formation was intersected 5m low to prognosis at 741mRT (715mSS). It should be noted that the top Gurnard pick was changed from the top porosity to the baseline shift in resistivity, approximately 5-7 metres above the previous top. This is consistent across the Patricia-Baleen Gas Field.

The Gurnard Formation is a shallow marine, transgressive greensand unit with a high proportion of silt and clays. The complex mineralogy adversely affects the petrophysical analysis with mica, glauconite, siderite and pyrite present. Overall, reservoir quality is slightly better at the Baleen-2 location compared to the Patricia-1 and Baleen-1 wells. There are less of the siderite cemented bands and therefore a higher net reservoir to gross formation ratio of 78.7% versus 64%, and net effective porosities are slightly better at 29% versus 27%.

The secondary objective was the Latrobe Group Coarse Clastics where gas had been intersected by the Baleen-1 and Patricia-1 wells. However, in the Baleen-2 well, no hydrocarbons were found in the Latrobe Group Coarse Clastics.

The top of the reservoir quality sandstones occurs at 747.8mRT (721.8mSS), with the base of the reservoir sands at 788mRT (762mSS). Net reservoir to gross formation thickness is 35.4/45m (78.7%), gross pay is from 747.8mRT (721.8mSS) to 759.0mRT (733mSS), i.e 11.2m with net pay of 10.6m. The maximum drilling gas occurred through the cored interval where 5.7% total gas (C_1 and C_2) was recorded. C_2 (ethane) was present only over the interval 749mRT to 763mRT (723mSS – 737mSS). Below 763 mRT (737mSS), total gas declines and remains between 0.3% and 1.0%. Fluorescence shows were recorded from the core chip samples from 756 mRT to 764 mRT (730mSS – 738mSS). The best shows have a strong gassy odour, dull to moderately bright yellow green patchy direct fluorescence, slow bluish white blooming cut fluorescence, thick yellowish white residual ring fluorescence. These shows occur in the poor visual porosity silty sandstones.

Petrophysical analysis of the logs and pressure data confirm a dry gas column in the upper part of the Gurnard Formation from 747.8mRT to 764.2mRT (721.8mSS – 738.2mSS), a water wet lower Gurnard Formation and Latrobe Group sandstones. Average net porosity in the gas column is 29.5% with associated average gas saturations of 41%. The low gas saturation appears to be a function of the very fine grained, clay rich rock in close proximity to the GWC and is therefore expected.

Wireline pressure data also demonstrated a regional drop in aquifer pressure of the Latrobe Group and consequent drop in Gurnard Formation reservoir pressure in the last 18 years. Since 1981 when the Baleen-1 well was drilled until this well Baleen-2 in 1999, the pressure in the Gurnard Formation gas reservoir has fallen from 1107psia to 1071 psia. This is most likely due to Bass Strait production and onshore abstraction.

The well was plugged and abandoned on the 18th of October 1999.

BALEEN-2
INTERPRETIVE REPORT

LIST OF TABLES

LIST OF FIGURES

LIST OF APPENDICES

LIST OF ENCLOSURES

BALEEN-2

WELL COMPLETION REPORT
INTERPRETIVE DATA
VOLUME 3

DISTRIBUTION LIST

Copy No 1	OMV Australia Pty Ltd Library, Perth
Copy No 2	OMV Australia Pty Ltd Exploration Department, Perth
Copy No 3	OMV, Vienna
Copy No 4 & 5	Department of Natural Resources & Environment - VIC (2 copies)
Copy No 6	AGSO, Canberra

1 INTRODUCTION

1.1 RATIONALE AND OBJECTIVES

The Baleen-2 well was drilled as an appraisal well in Retention Licence VIC/RL5, 350 kilometres east of Melbourne in the northern Gippsland Basin (Figure 1). The well was drilled 3.31 kilometres southwest and structurally downdip of the Baleen-1 gas discovery well, on the southwest extension of the Baleen portion of the Patricia-Baleen Gas Field (Figure 2). The Patricia-Baleen Gas Field is located 23 kilometres offshore, south of the town of Orbost in southeastern Victoria, and lies in 50-60 metres of water.

The Baleen portion of the gas field is thought to contain approximately 70% of the gas-in-place for the Patricia-Baleen Gas Field. Only a small proportion of this had been in the proven / undeveloped category as the Baleen-1 well found "gas on rock" in both the Gurnard Formation and Latrobe Group Coarse Clastics reservoirs, so no definite Gas Water Contact (GWC) had been determined for that structure. The reservoir target for the Baleen-2 well was the transgressive marine, fine grained sands of the Gurnard Formation. A GWC had been inferred at 760mRT (734mSS) from the RFT pressure data in the offset wells but relied on a postulated common water pressure gradient in both the Latrobe Group Coarse Clastics and Gurnard Formation. The GWC observed in the Patricia-1 well over the Patricia portion of the Patricia-Baleen Gas Field occurs at 729mSS in the Latrobe Group Coarse Clastics.

The main objective of the Baleen-2 well was therefore to locate the GWC of the Gurnard Formation gas accumulation. It would also test the reservoir distribution, quality and continuity within the gas field. A summary of the objectives are listed below.

Objectives of the Baleen-2 well:

- Locate the gas water contact (GWC) in the Gurnard Formation
- Core the Gurnard Reservoir
- Obtain sufficient wireline data for petrophysical and geophysical analysis
- Obtain reservoir pressure data
- Determine fluid gradients and pressure continuity between wells
- Confirm reservoir thickness, continuity and quality
- Obtain gas samples from the Gurnard Formation
- Obtain water samples from the Gurnard Formation
- Evaluate any Latrobe Group hydrocarbon accumulations

Well Results

The GWC was located in the Gurnard Formation at 764.2mRT (738.2mSS), 4 metres below prognosed depth.

The Gurnard Formation Reservoir was cored over the interval 746mRT – 780.3mRT. Due to the unconsolidated nature of the core, only 93.7% was recovered, resulting in a final length of 32.2 metres.

Good quality wireline data was acquired in good borehole conditions, allowing confident petrophysical analysis to be performed.

Reservoir pressure data was obtained through two MDT runs in the hole with 12 successful readings over the reservoir interval 747.8mRT - 764.2mRT. The reservoir pressure at the Free Water Level (FWL) was recorded at 1072 psia.

Fluid gradients were established in the Gurnard Formation and Latrobe Group Coarse Clastics, with the water gradient at 1.416psi/m, and the gas gradient at 0.0722psi/m. The Gurnard Formation Reservoir pressure was found to be some 38 psi below that which was expected given the results of the Baleen-1 well. This pressure depletion is caused by the production from the Bass Strait Fields and onshore abstraction.

The Baleen-2 well confirmed the extent and continuity of the Gurnard reservoir, intersecting 40 metres of silty sandstones with good to excellent porosities and moderate permeabilities.

Gas samples were attempted during the MDT runs, however none were successful due to a combination of friable, low permeability reservoir and the MDT pumpout module pump dynamics.

Water samples were also attempted during the MDT runs in the Gurnard Formation but were unsuccessful. One successful 1 gallon water sample was acquired at 797mRT in the Latrobe Group Coarse Clastics.

No Latrobe Group Coarse Clastics hydrocarbons were intersected.

1.2 PERMIT AND JOINT VENTURE INTERESTS

The Patricia-Baleen Gas Field is located in the Gippsland Basin, offshore Victoria, Australia, in Retention Licence VIC/RL5 (Figure 1). The permit containing Patricia-Baleen was originally granted to Gas and Fuel Corporation in 1978 as Exploration Permit VIC/P11. Interests held at that time were: Gas and Fuel Corporation (33.00%), Lasmo (Operator-29.17%), TCPL (4.16%) and Beach Petroleum NL (33.00%). Shell purchased Lasmo's interest in 1989 and Beach/TCPL sold their interests to Gas and Fuel Exploration NL (GFE). Both Lasmo and Shell worked to commercialise the Patricia-Baleen discovery during their term as Operator. Due to a limited gas market, low gas price and lack of infrastructure the project never proceeded. Development studies undertaken showed the potential for a commercial accumulation and in 1993, Shell gained approval from the Victorian government to declare the field as a Location. Shell operated the permit through to 1994 when their interest was transferred to GFE. In 1995 Cultus Petroleum purchased the assets of GFE and acquired a 100% interest in the Patricia-Baleen Gas Field as a result. Based on further study work undertaken by Cultus, the Retention Lease VIC/RL5 was granted to Cultus over the Patricia-Baleen Field on 14th November 1996. Baleen-2 was drilled by Cultus Timor Sea Ltd in October 1999, and was the first well to be drilled in VIC/RL5. It satisfied the Permit Year 3 commitment well drilled ahead of schedule.

In Late 1999, OMV gained full control of Cultus Petroleum and acquired a 100% interest in the Patricia-Baleen Gas Field.

1.3 EXPLORATION HISTORY

The Retention Licence VIC/RL5 was previously part of exploration permit VIC/P11 which was originally explored in the 1960's. The first well, Flathead-1 was drilled in April 1969 and discovered an approximate 30 metre residual oil column in the Latrobe and Strzelecki Groups. Little exploration was carried out during the 1970's, however, activity resumed following it's award to the Gas and Fuel Corporation in 1978. Three wells were drilled in November and December 1981, Baleen-1, Whale-1 and Sperm Whale-1. Well locations are provided in Figure 2.

The drilling of the Baleen-1 exploration well in November 1981 resulted in the discovery of the Baleen Gas Field. Baleen-1 was drilled on a culmination which discovered a 48 metre gas column, and with two production test flowed 1.8MMcf/D and 6.3 MMScf/d through a 1" choke from the Gurnard Formation. Patricia-1 was then drilled on the culmination to the south of the Baleen field in June 1987, and discovered a 54 metre gas column. On production test the well flowed 24.1 MMScf/d through a 1.25" choke from the Gurnard Formation, and 2.05 MMcf/d through a 5/8" choke from the Latrobe Group Coarse Clastics Formation, and was suspended as a potential gas producer.

The geophysical database over the Patricia-Baleen Gas Field is comprised of multi-vintage 2D and a recently acquired 3D seismic survey (post Baleen-2). The main 2D surveys utilised in the pre-drill mapping were the GB79, GB81 and GL88 surveys, which were acquired in 1979, 1981 and 1988 respectively. The combined surveys result in a line spacing of approximately 500 metres over the Baleen, Patricia and Sperm Whale features. The 2D dataset was reprocessed in 1991 by Shell Development Australia, and this dataset was used for the mapping.

In January 2000, a 3D seismic survey was shot over VIC/RL5. The 3D acquisition area measures 85 square kilometres full fold and consisted of shooting parallel lines spaced 12.5 metres apart with each line having a 12.5 metre group spacing. After processing, a 3D migrated data set with a 6.25 metre inline and 12.5 metre crossline grid spacing was achieved.

1.4 REGIONAL STRUCTURE AND STRATIGRAPHY

(Adapted from GFE, 1995)

The Gippsland Basin is an asymmetric East-West graben which initially formed during the break-up of Australia and Antarctica in the Early Cretaceous. During continental rifting the basin was filled by non-marine clastics of the Strzelecki Group, in part volcanolithic and containing coal beds.

The overlying alluvial sediments of the late Cretaceous Golden Beach Group represent a second phase of rift fill associated with the Tasman Sea rift. Following continental break-up in the Campanian, the Latrobe Group was deposited as a transgressive sequence of marine and coastal plain sediments. Thermal subsidence from the Oligocene to Recent was accompanied by the deposition of marine marls and limestones of the Lakes Entrance Formation and Gippsland Limestone.

The thickest deposition of the Latrobe Group and Golden Beach Group was in the "Central Deep" between the Rosedale and Foster faults, collectively exceeding 5 kilometres. North of the Emperor Fault the Latrobe Group is generally less than 500 meters in thickness and overlies the Strzelecki Group unconformably, with no Golden Beach Group present. The Latrobe Group is developed as a marginal marine "Coarse Clastic" facies. The Patricia-Baleen Gas Fields lie within this Northern Platform area.

Marine inundation of the Latrobe Group Coarse Clastics in the Middle Eocene, coupled with low subsidence and sediment input rates, resulted in deposition of a condensed, glauconitic, sandy siltstone known as the Gurnard Formation. This formation is widespread but discontinuous, and is overlain by the Oligocene Lakes Entrance Formation. The Lakes Entrance is the main regional seal for the Gippsland Basin. The generalised stratigraphy of the Gippsland Basin is shown in Figure 3.

While extensional rifting and thermal subsidence have dominated the depositional history of the Gippsland Basin, a dextral east-west wrench regime has been active intermittently from the late Paleocene to the Pleistocene, with the most intense effects evident in the Middle Miocene. This has resulted in anticlinal structuring on generally northeast – southwest axes, and the re-activation of many normal faults as reverse or wrench faults. A regional cross-section across the Gippsland Basin is shown in Figure 4.

VIC/RL5

Retention Licence VIC/RL5 is located on the northeastern flank of the Gippsland Basin, on the Northern Strzelecki Terrace. Over this area there was no Golden Beach Group deposited as shown in Figure 4. A structural cross-section of the VIC/RL5 area is shown in Figure 5. Formation tops intersected by the wells drilled on the Patricia-Baleen Gas Field are shown in Table 1.

Table 1 - Formation Tops over the Patricia-Baleen Field

	Patricia-1		Baleen-1		Baleen-2	
TOPS	mSS	Thick.	mSS	Thick.	mSS	Thick.
Gippsland Limestone (sea floor)	51	582	54.9	562.6	55	643
Lakes Entrance Formation	633	45	617.5	33	698	17
Gurnard Formation	678	44	650.5	39	715	51
Latrobe Group Coarse Clastics	722	56	689.5	8	766	80
Strzelecki Group	778	100+	697.5	323+	846	23+
Total Depth	878		1020.5		869	

Regional Reservoir

The marginal marine and coastal plain transgressive sequence of the Latrobe Group contains the main reservoirs of the Gippsland Basin.

The top Latrobe Group "Coarse Clastics", comprising coastal barrier and braided stream deposits, is present over the whole basin and contains the main regional aquifer. These sands constitute the reservoirs for 95% of Gippsland Basin oil and over 80% of the gas, and generally have very good reservoir quality (i.e. porosities and permeabilities). Intra-Latrobe reservoir, sands deposited as upper and lower-coastal plain facies, account for most of the remaining oil.

The Gurnard Formation, sporadically developed over the top Latrobe, is a reservoir of variable quality, grading to a seal facies. In the VIC/RL5 area, most of the Gurnard Formation exhibits good reservoir characteristics and contains the major part of the gas accumulation, with about 5% in the top Latrobe Group Coarse Clastics sands.

Source

Potential source rocks of the Gippsland Basin exist in the Strzelecki, Golden Beach and Latrobe Groups. The Golden Beach Group source potential is considered to be mainly gas and condensate-prone, while the Strzelecki is considered to be a gas source. By far the richest organic content is found in the Latrobe Group, particularly the upper part.

2.0 GEOLOGY

2.1 STRATIGRAPHY

In Baleen-2 , cuttings samples were collected from 650mRT to total depth at 895mRT, and two conventional cores were taken from 746mRT – 762.2mRT and 763.7mRT – 779.5mRT. Stratigraphic tops are presented in Table 2 and were defined using a combination of lithologic descriptions from cuttings and core, wireline logs, and biostratigraphic data (referring to spore-pollen, and microplankton). Core chip descriptions, cuttings descriptions, and the Basic Data Palynology Report are included as Appendices 2 and 3 and 10 respectively in the Baleen-2 BASIC Data Report. The Final Interpretive Palynology Report is included as Appendix 1 of this report.

For the purpose of this report, the Gurnard Formation is placed at the top of the Latrobe Group to provide consistency with previous wells' interpretation. Some workers have included the Gurnard Formation in the overlying Seaspray Group (Gilbert and Hill, 1994).

The following lithological descriptions are summarised according to regionally recognised lithostratigraphic units. The Baleen-2 well intersected the formation tops low to prognosis, with the predicted versus actual stratigraphy sections shown in Figure 6, and summary of the stratigraphy encountered presented in Table 2 below.

A well composite log for Baleen-2 is included as Enclosure 1.

Table 2 - Stratigraphic Table – Baleen-2

SYSTEM	STAGE	BIOZONE	FORMATION	LITHOLOGY	DEPTH mRT	Th. (m)
Tertiary	Early Miocene	Middle to Upper *P. tuberculatus (Operculodinium Superzone)*	Gippsland Limestone	Calcilutite becoming interbedded with calcareous claystone at the base	81 (seafloor)	636
Tertiary	Late Oligocene	Middle to Upper *P. tuberculatus (Operculodinium Superzone)*	Lakes Entrance Formation	Interbedded calcareous claystone and calcarenite	724	17
Tertiary	(Late) Middle Eocene	Lower *N. asperus (D. heterophlycta)*	LATROBE GROUP Gurnard Formation	Dominantly silty sandstone interbedded with sandy siltstone and claystone Interspersed with 1-2m siderite cemented zones	741	51
Tertiary	Late Paleocene	Upper *L. balmei*	LATROBE GROUP Coarse Clastics	Clean sandstone with thin claystone and siltstone interbeds	792	80
Early Cretaceous	Late Albian	Upper *C. paradoxa*	Strzelecki Group	Claystone grading to silty sandstone.	872	23+

Gippsland Limestone
Tertiary (Early Miocene)

81 (seafloor) – 724mRT
Thickness: 636m

Upper Boundary Pick: Seafloor

Biostratigraphy: Middle to Upper *Proteacidites tuberculatus* spore-pollen Zone and *Operculodinium* microplankton Superzone.

Lithology: The Baleen-2 well only recovered samples from below 650mRT, however from the gamma ray / Rate of Penetration (ROP) and regional correlation, we infer the Gippsland Limestone at this location to be dominated by calcilutite with occasional calcareous claystone interbeds near the base;

From 650mRT to 724mRT, the lithology descriptions are:

Calcilutite: light to medium grey, medium to dark olive grey, mottled in part, dominantly soft, dispersive, rare firm to moderately hard, amorphous to blocky, trace subfissile, trace carbonaceous specks, 20-35% siliceous content, trace quartz silt, trace to 5% calcisiltite, trace very fine glauconite, trace forams

Calcareous Claystone: light to medium grey, light olive grey, soft to firm, amorphous, dispersive in part, 20-30% micrite content, trace very fine glauconite, 5% carbonaceous specks.

Log Properties: Gamma ray was the only log to be run to the surface through pipe, and was steady at 20gAPI.

In the open hole, below 646mRT, where the casing was set and the other wireline logs were run, the gamma ray begins to fluctuate from 20gAPI – 50gAPI becoming more stable towards the base of this formation, increasing from 50gAPI to 60gAPI. Density and sonic velocity are very erratic ranging from 1.95g/cm^3 - 2.23g/cm^3 , and 80us/ft - 160us/ft respectively. Resistivity is also erratic ranging from 0.5ohm.m - 3ohm.m. This erratic behaviour is typical of limestones.

Some of the irregular nature of the wireline logs, especially the density and sonic, may also be due to washout, particularly near the base of the formation as recorded in the fluctuating caliper readings.

Drilling characteristics and mudgas: The ROP down to 646mRT was quite variable fluctuating between 80 and 150m/h, averaging around 100m/h. From 650mRT – 746mRT, controlled drilling was applied, and through this formation the ROP fluctuated slightly from 5m/h to 30m/h. Mudgas was only monitored below 650mRT as no marine riser was installed for the previous hole section.
Gas data was recorded from 650mRT. The chromatograph analysis gave the following range: Methane (C1): 0.2-2%, Ethane (C2): 0.04-0.1%, Butane (C3), Iso-Propane (IC4), Normal-Propane (NC4): all 0.04-0.06%, and Total gas 0.2-1.8%. C2-NC4 were all quite steady, while Methane

	and Total gas slowly increased throughout the section to the base of the formation. **Gas Ratios:** GWR: 19 ; LHR: 7.3 ; OCQ: 2
Pore Pressure:	Intermittent lost circulation in offset wells and lack of significant seal imply a normal pressure gradient through the formation.
Hydrocarbon Shows	No shows

Lakes Entrance Formation
Tertiary (Late Oligocene)

724 – 741mRT
Thickness: 24m

Upper Boundary Pick	Marked by an increase in gamma from 60gAPI to 80gAPI. Resistivity, density and sonic velocity all become quite steady, however the ROP is non-diagnostic due to controlled drilling. The lithology becomes more dominated by claystones with minor calcilutite.
Biostratigraphy	Middle to Upper *Proteacidites tuberculatus* spore-pollen Zone and *Operculodinium* microplankton Superzone.
Lithology	The Lakes Entrance Formation is characterized by calcareous claystone interbedded with calcilutite; *Calcareous Claystone:* Light to medium grey, light to medium olive grey, soft to firm, amorphous to rare blocky, 20-30% micrite content, trace very fine to medium pelletal glauconite, 5% carbonaceous specks. *Calcilutite:* light to medium grey, medium olive grey, mottled, dominantly soft, dispersive, rare firm to moderately hard, amorphous to blocky, trace carbonaceous specks, 30-35% siliceous clay content, grades to argillaceous calcilutite, trace quartz silt, trace to 5% calcisiltite, trace very fine glauconite, trace fossil fragments and forams.
Log Properties	Gamma ray is generally steady at 80gAPI, however there are common shaly peaks up to 200gAPI. Resistivity, density and sonic are all much steadier than the overlying Gippsland Limestone and have slightly curved pattern. At the top of the formation resistivity is 1ohm.m increasing to 1.8ohm.m at the middle of the formation then decreases back to 1ohm.m at the base of the formation. Sonic velocity also starts off at 140us/ft at the top of the formation slowly increasing to 120us/ft, then decreasing back to 140us/ft at the base. Density is slightly more irregular but has the same curved pattern, starting at 2.1g/cm^3 increasing to 2.35g/cm^3 then decreasing back to 2.15g/cm^3.
Drilling characteristics and mudgas:	The ROP throughout this formation is steady at 10-15m/h, with controlled drilling from 650-746mRT. The chromatograph analysis gave the following range: Methane (C1): 1.5-2%, Ethane (C2): 0.04-0.1%,

Propane (C3), Butane (C4), Pentane (C5): all 0.03-0.07%, and Total gas 1.5-1.8%. The mudgas readings in this formation were quite steady.

Gas Ratios: GWR: 11 ; LHR: 14 ; OCQ: 2

Pore Pressure: No abnormal trends indicating that this formation is normally pressured.

Hydrocarbon shows: No shows

Latrobe Group
Tertiary (Middle Eocene to Late Paleocene)

741 – 872mRT
Thickness: 131m

The Latrobe Group is subdivided into two formations in descending order, the Gurnard Formation, and the Coarse Clastics (Barracouta Formation Equivalent);

Gurnard Formation

741 – 792mRT
Thickness: 51m

Upper Boundary Pick: The top pick is an increase in resistivity, accompanied by an increase in density and sonic velocity. The lithology changes from claystones interbedded with calcilutite to claystones and sandy siltstones.

Mudgas also increases at the top of this formation.

It should be noted that the top Gurnard pick was changed from the top porosity to a baseline shift in resistivity, approximately 5-7 metres above the previous top (Figure 7). It is also the top of a higher density layer and slight increase in sonic velocity. The new top is very consistent across the Patricia-Baleen Field.

Biostratigraphy: From 741mRT – 792mRT- Middle *Nothofagidites asperus* spore-pollen Zone.

Lithology: The Gurnard Formation comprises predominantly silty sandstone interbedded with sandy siltstone and minor claystone. Only a couple of metres of claystone occur at the top of the formation grading into sandy siltstone to 746mRT, below which the silty sandstone dominates. The silty sandstone contains common siderite bands with thickness ranging from 15cm to 2m, commonly around 30cm thick. A zone of intense siderite cementation occurs between 747.7mRT – 772.5mRT. The bottom 10 metres of the formation becomes more silty, dominated by sandy siltstone, with a sideritic / pyritic band at 788mRT – 790mRT;

Silty Sandstone: moderate to dark yellowish brown, friable to locally firm, clear to translucent quartz grains, very fine to fine grained, moderately well sorted, angular to sub-rounded, trace to 5% patchy siderite cement,

20-30% dark yellowish brown quartz silt, 10-15% siliceous clay matrix, grades to sandy siltstone, 5% dark green glauconite, trace to 5% micromica, trace feldspar, trace lithics, homogeneously to moderately burrowed by *Thalassinoides* and *Ophiomorpha*, good to very good visual porosity. Contains abundant **siderite cemented bands**; yellow to orange, hard, very fine to fine grained, moderately well sorted.

Siltstone: dark yellowish brown to moderate yellowish brown, firm to locally moderately hard, blocky, 30-40% very fine to fine grained quartz sand, poorly sorted, trace to 5% glauconite with dispersed fine grained glauconite pellets, 5% siliceous clay, 5-10% micromica, common patchy siderite cement, trace to minor carbonaceous specks, trace lithics, intensively churned by *Thalassinoides* burrows, sporadic *Ophiomorpha* burrows.

Claystone: dark yellowish brown, soft, 25-30% very fine to fine grained quartz sand, 15-20% quartz silt, common faint lenticular wavy mudstone laminations, trace to 5% glauconite with dispersed fine grained glauconite pellets, 5% micromica, trace lithics, common *Skolithos* and *Zoophycos* burrows.

Log Properties

Density, sonic velocity, and resistivity all have increased log responses over the siderite cemented zones.

Gamma ray is irregular with values depending on the clay type and glauconite content of the formation. Through the silty sands it is 80gAPI, but through the more silty/claystone parts it ranges from 100-120gAPI.
Resistivity increases from the overlying formation to 2ohm.m at the top of the Gurnard Formation. It has a generally smooth pattern and slowly increases to 4ohm.m in the reservoir then slowly decreases back to 2ohm.m at the base of the formation. Siderite bands show as distinct peaks up to 10ohm.m. The sideritic/pyritic band at 788mRT –790mRT has a low resistivity value down to 1ohm.m, possibly due to the conductive clays and pyrite.

Density is irregular and also varies with lithology. Over the claystone/silty intervals, values are 2.25g/cm^3 - 2.55g/cm^3, while the more sandy parts are 2.05g/cm^3 - 2.25g/cm^3. Over the reservoir density is lower at 1.95g/cm^3 - 2.05g/cm^3, and the siderite peaks are 0.2-0.4 g/cm^3 above the average.

Sonic velocity has a smooth profile at 120us/ft but decreases to 160us/ft over the reservoir.
As mentioned above there is a difference in wireline log data over the gas and water intervals. Over the gas zone resistivity is 4ohm.m, whereas over the water zone it is 2ohm.m. Density is lower over the gas zone, at 1.95g/cm^3 - 2.1g/cm^3, while over the water zone it is 2.1g/cm^3 - 2.35g/cm^3. Sonic velocity is lower over the gas zone at 140us/ft - 160us/ft, whereas over the water zone it is steady on 120us/ft.

Drilling

The ROP starts to become erratic in this formation because most of this

characteristics and mudgas:

section was cored (over the interval 746mRT – 779.5mRT; refer to the Coring Report, Appendix 4 Baleen-2 BASIC Data Report). From the top of the formation to 746mRT, controlled drilling was applied. ROP slowly increases from 10m/h to 20m/h where coring begins at 746mRT, and ROP fluctuates from 8m/h to 42m/h. After coring ROP is quite steady over a sandy interval at 20m/h but then becomes very erratic in the interbedded clays and sands near the base where ROP fluctuates from 5m/h to 60m/h.

The chromatograph gave the following range: Methane (C1): 1.3-5%, Ethane (C2): 0.04-0.2%, Propane (C3): 0.05-0.09%, Butane (C4):0.04-0.08%, Pentane(C5): 0.03-0.06%, and Total gas 1.5-7%. The chromatograph analysis recorded the highest gas in this formation over the reservoir. All of the gas readings began to increase at the top of this formation peaking over the reservoir (747mRT-764mRT) then slowly decreased and steadied in the bottom half of this formation.

Gas Ratios – Gas pay interval:
GWR: 7 ; LHR: 29 ; OCQ: 1.25

Gas Ratios – Water column:
GWR: 11.5 ; LHR: 13 ; OCQ: 1.7

Pore Pressure:

The gas gradient was calculated as 0.0722psi/m and the water gradient at 1.416psi/m.

MDT pressure data indicates the Gurnard water is about 6-8psi above the Latrobe water. This difference could possibly be due to the basal siderite / pyrite cemented zone in the Gurnard Formation, which acts as a barrier to pressure losses from the Gurnard Formation into the slightly underpressured Latrobe Group Coarse Clastics.

Hydrocarbon shows

Oil shows were noted from core chips between the depths of 756mRT and 764mRT;

<u>756mRT-762mRT</u>: 70-90% dull to moderately bright yellowish green pinpoint to patchy direct fluorescence, slow to moderately fast yellowish white to bright bluish white blooming cut fluorescence, thick yellowish white residual ring fluorescence.

<u>762mRT-764mRT</u>: 30%, dull to moderately bright yellowish green pinpoint to patchy direct fluorescence, slow yellowish white streaming to blooming cut fluorescence, thin to thick yellowish white residual ring fluorescence.

Coarse Clastics **792 – 872mRT**
Thickness: 80m

Upper Boundary Pick: Marked by the first clean sand with a dramatic decrease in gamma ray from 120gAPI to around 20gAPI. ROP is slower and less erratic than the overlying Gurnard Formation in the upper sand at around 10m/h to 20m/h.

Biostratigraphy Upper *Lygistepollenites balmei* spore-pollen Zone.

Lithology The Latrobe Group Coarse Clastics is dominantly a clean sandstone with sporadic thin claystone and siltstone bands, and minor coal. Near the top are two distinctive claystone beds of 3-4 metres thickness;
Sandstone: white to opaque, clear to translucent quartz, fine to very coarse, dominantly medium to coarse, poorly sorted, sub-angular to sub-rounded, trace to 5% pyrite cement, 5-10% white kaolinite matrix, trace to 5% dark green pelloidal glauconite, trace reddish brown lithics (jasper), good inferred porosity.

Claystone: dark grayish black, dark grayish brown, hard to very hard, subfissile to fissile, siliceous, minor micromica.

Siltstone: moderate yellowish brown, medium olive grey, soft, dispersive, 15-20% siliceous clay content, grades to argillaceous claystone, 10-15% very fine to fine grained quartz sand, trace to 2% glauconite, trace nodular pyrite, trace micromica, trace lithics.

Between the depths of 800-810mRT, there is up to 2% coal;

Coal: black, firm to hard, occasionally brittle, dull to subvitreous.

Log Properties This formation is characterized by a smooth, low gamma ray for the clean sands at the top of the formation of 20gAPI, with shale peaks at 100gAPI, and siltstones at 60gAPI - 80gAPI. Towards the bottom of the formation gamma for the sands remains at 20gAPI, but there much more frequent silts and clays resulting in more erratic gamma ray profile with silt/clay peaks at 40-80gAPI.

Resistivity is erratic but consistent fluctuating between 1ohm.m – 3ohm.m, generally at 1ohm.m through the clean sands.

Density is also erratic fluctuating from 1.95g/cm^3 - 2.35g/cm^3 throughout this formation. Sonic velocity becomes more erratic than the overlying Gurnard Formation fluctuating by about 20us/ft as it slowly increases from 120us/ft at the top to 140us.ft at the base.

Towards the base of the formation, the caliper reading becomes more erratic indicating washout, possibly influencing the erratic nature of some of the wireline logs.

Drilling characteristics and mudgas: The ROP throughout this section is very erratic ranging from 7m/h to 100 m/h, faster through the sands and slower through the silts and claystones.
The chromatograph analysis gave the following range: Methane (C1): 1-3%, Ethane (C2): 0.05-0.1%, Propane (C3), Butane (C4), Pentane (C5): all 0.04-0.05%, and Total gas 1-3%. The mudgas recordings in this formation are consistently low.

Gas Ratios: GWR: 10 ; LHR: 14 ; OCQ: 2

Pore Pressure: The interbedded nature of this unit precludes any use of Dxc. The regional nature of this reservoir is well understood and is normally pressured save for the losses in pressure due to Bass Strait oil production and onshore abstraction.

The water gradient for the Latrobe is 1.416psi/m but from pressure data the pressure regime is 6-8psi lower than the Gurnard Formation in Baleen-2.

Hydrocarbon shows: No shows

Strzelecki Group
Early Cretaceous (Late Albian) **872 – 895mRT**
Thickness: 23m+

Upper Boundary Pick: Marked by a decrease in resistivity from 2ohm.m to 1ohm.m, and a decrease in sonic velocity from 120us/ft to 140us/ft from the overlying Latrobe Group. ROP decreases from 90m/h in the overlying Latrobe Group Coarse Clastics to 10-30m/h in this formation, and becomes much less erratic.

Biostratigraphy: Upper *Coptospora paradoxa* spore-pollen Zone in section penetrated.

Lithology: The Strzelecki Group is comprised of silty sandstones grading to claystones

Silty Sandstone: white to opaque, clear to translucent quartz grains, trace to 5% light bluish grey, loose, medium to coarse, poorly sorted, angular to sub-angular, moderately common siliceous cement, 40-50% white kaolinite matrix, trace pyrite nodules.

Claystone: dark grayish black, dark grayish brown, hard to very hard, subfissile to fissile, siliceous, minor micromica.

Log Properties: The only logs that are recorded in the Strzelecki Group are the resistivity and sonic, due to the minimal logging rathole.

Resistivity is less erratic than the overlying Latrobe Group Coarse Clastics with a generally smooth profile at 0.8ohm.m-1.1ohm.m at the top of the formation slowly increasing to 1.5ohm.m at the base of the

formation were the recording finish.

Sonic Velocity is also smoother than the overlying Latrobe Group Coarse Clastics, starting at 130us/ft slowly increasing to 118us/ft at the base of the formation were the recording finish.

Drilling characteristics and mudgas: The ROP is much less erratic than the overlying formation, although it still fluctuates from 10m/h to 29m/h.
The mudgas recording tails off in the Strzelecki Group with a smooth, consistent profile. The chromatograph analysis gave the following range: Methane (C1): 1-1.6%, Ethane (C2), Propane (C3), Butane (C4), Pentane (C5): all 0.05%, and Total gas 1-1.5%.

Gas Ratios: GWR: 12.5 ; LHR : 9.5 ; OCQ : 2

Pore Pressure: No abnormal Dxc trends. This formation is normally pressured at Baleen-2.

Hydrocarbon shows: No shows

2.2 RESERVOIR SEQUENCES

The primary reservoir target of the Baleen-2 well was the transgressional marine, very fine grained sands of the Gurnard Formation. This formation contains the majority of gas reservoired in the Patricia-Baleen Gas Field. Elsewhere on the Patricia-Baleen Gas Field, the Baleen-1 and Patricia-1 wells intersected gas in the Gurnard Formation. The Gurnard Formation is stratigraphically confined between the overlying calcareous claystones and calcilutites of the Lakes Entrance Formation, and the underlying medium to coarse sands and silts of the Coarse Clastics of the Latrobe Group. Elsewhere in the Gippsland Basin the Gurnard Formation is either a seal or a waste zone, but at the Patricia-Baleen location the unit thickens and develops into a reservoir facies. Table 1 shows the formation tops of the wells in the Patricia-Baleen Field.

Sedimentological analysis of the cores indicates deposition of the Gurnard Formation in a middle to outer shelfal marine setting. The entire reservoir is pervasively bioturbated by *Thalassinoides* and *Ophiomorpha*, and to a lesser extent, *Skolithos* and *Zoophycos*. The very fine to fine grained silty sandstones were deposited as a series of parasequence sets below fair-weather base with turbiditic and suspension deposition being the main mechanisms for sediment transport in the VIC/RL5 area (Barber, 2000). These sands are interspersed with several 1-2 metre thick siderite bands that could possibly represent flooding events (condensed sedimentation) related to parasequence boundaries. The siderite bands appear to be associated with low sedimentation rates, i.e, a low energy distal shelf setting, with intense bioturbation that has destroyed most of the original deposition fabric, giving resultant high clay matrix values. Figure 8 displays a hypothetical sedimentological model for the Gurnard Formation. There may be more than one mechanism for the deposition of siderite and associated minerals, and can also be the result of post-depositional diagenetic processes as discussed in the Reservoir Quality section.

The reservoir sequence of the Gurnard Formation thickens slightly in the Baleen-2 well to the southwest of the original discovery, with a total thickness of 51 metres. The Gurnard Formation is 39 metres thick in the Baleen-1 well, and 44 metres thick in the Patricia-1 well.

The secondary objective of the Baleen-2 well was the sandstones of the Latrobe Group Coarse Clastics, comprising coastal barrier and braided stream sediments deposited in a fluviodeltaic to nearshore marine environment. It is also the main regional aquifer. However, in the Patricia-Baleen Gas Field nearly all the gas reserves are in the Gurnard Formation, with only about 5% total GIIP (Gas-initially-in-place) in the top Latrobe Group Coarse Clastics.

Palynological analysis was performed on the cores and cuttings from the Baleen-2 well. From this analysis, depositional ages were determined for the Lakes Entrance Formation, Gurnard Formation, Latrobe Group Coarse Clastics Formation, and Strzelecki Group. The Lakes Entrance Formation contains *P. tuberculatus* (undiff.), however this is not diagnostic, with an age range from Early Miocene to Oligocene. It is most likely to be Early Oligocene in age by correlating with the Baleen-1 and Patricia-1 wells, whose ages are confined to Early Oligocene by the presence of Lower *P. tuberculatus*. The Gurnard Formation in Baleen-2 is confined to Middle Eocene in age by the presence of Lower *N. asperus*.. The Latrobe Group Coarse Clastics is interpreted to be Paleocene in age with the presence of *L. balmei*. The Strzelecki Group is confined to Late Albian in the Cretaceous by the presence of Upper *C. paradoxa*. The other wells in VIC/RL5, Patricia-1 and Baleen-1, have no recorded palynological data for the Latrobe Group Coarse Clastics and Strzelecki Group. The palynological analysis of core and cuttings samples from Baleen-2 is included as Appendix 1 of this report.

2.3 RESERVOIR QUALITY

The reservoir is generally a very fine grained, argillaceous sandstone which includes minor K-feldspar, mica, and glauconite. Hard, relatively impermeable siderite bands, ranging from 15 centimetres up to 2 metres in thickness, are common throughout the reservoir, and have much lower core measured porosities and permeabilities. Overall, reservoir quality is slightly better at the Baleen-2 location compared to the Baleen-1 and Patricia-1 wells.

Visible macroporosity, as defined in thin section analysis, ranges from 1.5% to 18.7% and is greatly reduced by the presence of clays and glauconite. As a result, reservoir quality is dependent on the detrital clay and glauconite content, indicating that most permeability variation is dependent on the original compositional differences.

From overburden corrected analysis of core samples taken across the reservoir sequence, permeability is quite variable, ranging from 33mD to 563mD, but are relatively low, averaging around 40md. Porosities are consistently high, with an average overburden corrected value of 31%. Despite having excellent porosities, these sands have low permeability due to the high clay matrix values resulting from intense bioturbation. The siderite bands have porosities of less than 15%, and permeabilities of 0.05mD to 0.13mD.

From petrographical techniques (Appendix 14, Baleen-2 BASIC Data Report), the main diagenetic process to have affected these sands appears to be glauconite formation with up to 11.3% by volume over the reservoir. The presence of glauconite indicates that deposition of these sands was most likely in a normal marine shelf setting during a slow sedimentation period. Common siderite zones are found across the reservoir, most likely formed as a result of a diagenetic process rather than a syn-sedimentological process. The evidence for this is that the siderite encloses both the pyrite and uncompacted glauconite. Energy Dispersive Spectrometer (EDS) analysis also reveals the siderite contains calcium and magnesium, which is consistent with siderite precipitation from marine porewater. Siderite is most likely to have formed before compaction at shallow burial, below the sulphate reduction zone. It could be the result of early methanogenesis or oxidation of early

formed, biogenic methane. More detailed petrology and reservoir quality results for Baleen-2 are found in the Petrology and Reservoir Quality Report in Appendix 14 of the Baleen-2 BASIC Data Report.
The siderite bands present in the reservoir adversely affect the reservoir quality. These bands have low porosities and permeabilities relative to the sandy sections, and likely form barriers to vertical fluid flow. Several siderite bands can be correlated to the nearby Patricia-1 and Baleen-1 wells indicating laterally extensive barriers to fluid flow within the reservoir. It is also observed that many of the siderite bands are discontinous, allowing some degree of vertical fluid migration. Figure 9 displays a Gurnard Reservoir Correlation Diagram from Baleen-2 to the other VIC/RL5 wells, Patricia-1 and Baleen-1.

The reservoir properties appear to be similar for the wells in the VIC/RL5 area. Production tests were performed on the Baleen-1 and Patricia-1 wells with the DST results summarised in Table 3. There was no production test performed on Baleen-2, however it is likely that production at Baleen-2 would be at least as good as at Baleen-1 and Patricia-1

Table 3 - Production tests on Patricia-Baleen wells

WELL	DST No.	Interval	Formation	Choke	Rate
Baleen-1	#1	700-706mRT	Coarse Clastics	1"	1.8MMcf/D
	#2	662-670mRT	Gurnard	1"	6.3MMcf/D
Patricia-1	#1	744-747mRT	Coarse Clastics	5/8"	2.05MMcf/D
	#2	719-728mRT	Gurnard	1"	6.1MMcf/D
	#3	703-738mRT	Gurnard	1 3/4"	8.3MMcf/D*
	#3A	703-738mRT	Gurnard	1 3/4" (with 5" drill pipe)	24.1MMcf/D

* flow restricted by down hole equipment.

2.4 SEAL

The calcareous claystones, minor marls and calcilutites of the Lakes Entrance Formation provides a very effective topseal, overlying the Gurnard Formation. The thickness of this topseal is in the Baleen-2 well is 24 metres

The Lakes Entrance Formation is the regional seal for the entire offshore Gippsland Basin and ensures that any valid structural high at top Latrobe (or Gurnard) level, in the path of oil or gas migration and not subsequently breached, will contain hydrocarbons. Sperm Whale-1, Baleen-1 and Patricia-1 all intersected gas columns sealed by the Lakes Entrance Formation in VIC/RL5. Baleen-1 intersected a 47 metre gas column, Patricia-1 intersected a 50 metre gas column, and Sperm Whale-1 intersected a gross hydrocarbon column of 45 metres, with a 26 metre gas column, a 2 metre oil column and a 11.5 metre transitional oil-water zone.

3.0 GEOPHYSICS (SEISMIC INTERPRETATION)

3.1 STRUCTURE AND TRAP

The Patricia-Baleen Gas Field is located on the northeastern flank of the Gippsland Basin, dominated by normal faults and tilted fault blocks. East-west wrench movement during the Middle to Late Paleocene resulted in anticlinal structuring and reactivation of many of the normal faults as high angle reverse faults. The Patricia and Baleen structures are interpreted to have developed at this time. The gas accumulations are in elongate compressional anticlines with reverse fault closure to the north and are separated by a structural saddle. The Baleen-2 well was drilled on the southwestern flank of the rollover anticline structure.

The trapping mechanism involves the fine grained, silty sands of the Gurnard Formation, sealed by the calcareous claystones of the Lakes Entrance Formation. The Lakes Entrance Formation unconformably overlies the Gurnard Formation providing an excellent seal over much of the Gippsland Basin area.

3.2 PRE-DRILL INTERPRETATION

The data used to interpret the Patricia-Baleen area comprised multi-vintage 2-D seismic surveys acquired over the area between 1979 and 1988. Shell Development Australia reprocessed this 2-D dataset in 1991.

The depth structure map on top Gurnard Formation Reservoir (Figure 10) shows the Baleen feature as a 3-way dip-closed anticline with a bounding fault on the northern side. The anticline trends WSW-ENE, and is approximately 6 kilometres in length and up to 2 kilometres in breadth at the widest point. Vertical relief was interpreted as approximately 83 metres from the highest known gas (HKG) at 651mSS to the most-likely GWC at 734mSS. At the Baleen-2 location to the southwest, the Baleen feature flattens out, with the well interpreted to intersect a 16.2 metre gas column.

3.3 POST-DRILL INTERPRETATION

Baleen-2 encountered the top of the Gurnard reservoir at 747.8mRT, about 5 metres low to prognosis. All the formation tops were intersected low to prognosis, with a 31 metre reduced thickness in the sealing Lakes Entrance Formation. Reinterpretation shows that an event can be seen cutting down into the Lakes Entrance Formation explaining the thinning from the top of that unit. The difference in pre-drill and post-drill formation tops is included in Table 4, with the predicted versus actual stratigraphic section shown as Figure 6.

A 16.4 metre gross gas column was confirmed with the (GWC) at 764.2mRT (738.2mSS) which proved to be very accurate from the interpreted column of 16.2 metres (just over 1.3% error).

TABLE 4 - Pre-Drill versus Post-Drill Formation Tops

	Baleen-2 Pre-drill (mSS)	Baleen-2 Post drill (mSS)
Top Lakes Entrance Formation	**650**	**698**
Top Gurnard Formation	**710**	**715**
Top Latrobe Coarse Clastics Formation	**755**	**766**
Top Strzelecki	**820**	**846**

3-D Seismic Interpretation

In early 2000, a 3D seismic survey was shot over approximately 140 square kilometres in VIC/RL5 which covered the Patricia-Baleen Gas Field. Interpretation of the 3D seismic was carried out between the 6th and 26th of June 2000. The main objectives of the interpretation were to estimate the Gross Rock Volumes (GRV's) for the Baleen and Patricia gas accumulations within the Gurnard Formation, identify any exploration potential and to provide depth grids for input to the reservoir simulation.

The seismic data has excellent resolution defining the Baleen and Patricia accumulations in much greater detail than the re-processed 2D data set. The Baleen structure is still a WSW-ENE trending anticline but can be subdivided into three compartments with individual crests (Figure 11). The major compartment comprises the large dome structure with highest relief where the Baleen-1 well was drilled. This structure contains the largest reserve with 68% of the GRV for the Baleen accumulation. Towards the southwest the structure flattens out with two smaller compartments each with approximately 16% of the GRV. Two smaller compartments are both bounded to the north by small throw reverse faults which trend WNW - ESE. The Baleen-2 well was drilled between the crests of these smaller compartments. A seismic section from Baleen-2 to Baleen-1 is also included as Figure 12.

4.0 HYDROCARBONS

The Baleen-2 well defined a gas column in the Gurnard Formation from 747.8mRT – 764.2mRT (721.8mSS – 738.2mSS) based on wireline logs, mudgas shows and MDT pressures. The FWL is defined at the intersection of the gas and water gradients in the Gurnard Formation. This point is within a siderite cemented zone so logs do not define the contact, however good gas saturation is defined above the main siderite cemented zone down to 762mRT, and water wet reservoir is defined up to 767.5mRT in the lower Gurnard.

Although attempts were made to sample the gas from the Gurnard Formation with the MDT tool, failure of the formation sandface and subsequent tool plugging and/or lost seals meant no samples were recovered.

Oil Shows were noted in core chips from 756mRT – 764mRT, and a faint fluorescence is observed on the core ultraviolet light (UV) photos over the interval 757.2mRT – 757.5mRT. Three plugs in this zone were extracted for hydrocarbons in an attempt to fingerprint the oil, but insufficient sample was recovered to produce a definitive chromatogram (Fluids Analysis Report, Appendix 13, Baleen-2 BASIC Data Report). The significance of this is unknown. No fluorescence was observed higher in the reservoir, therefore it seems unlikely that an initial oil charge was displaced by a later gas charge. Rather the reverse seems most likely, where a later oil charge has added to the initial gas in the reservoir. It is interesting to note a similar situation occurs at the Sperm Whale-1 well, 4 kilometres to the southwest. At Sperm Whale-1 however, some 30 litres of oil was recovered by FIT proving a moveable oil leg.

No producable hydrocarbons are interpreted in the Latrobe Group reservoirs, and water was recovered by MDT at 797mRT (771mSS) in the upper part of the Latrobe Group Coarse Clastics.

Hydrocarbon shows are documented on the Well Composite Log. Basic hydrocarbon indication data from the well can also be found under Section 3 of the Baleen-2 BASIC Data Well Completion Report.

5.0 WIRELINE LOGS AND SURVEYS

5.1 WIRELINE LOGS

The Baleen-2 wireline logging program consisted of 1 suite of wireline logs with 5 runs. The wireline logs did not reach the drilling T.D. due to soft fill. A list of the logs run are shown in Table 5.

TABLE 5 - Baleen-2 Wireline Logging Summary

LOG	DATE	SUITE / RUN	INTERVAL mRT	BHT-TIME
PEX-HALS-DSI-NGS	16/10/99	1/1	888.5-90	46.7°C/5:21hrs
FMI-GR	16/10/99	1/2	887-647	48°C/8:35hrs
MDT (pretests and samples)	17/10/99	1/3	823-748	52°C/18:25hrs
CSAT-GR (VSP Survey)	17/10/99	1/4	885-100	50°C/22hrs
MDT (pretests and samples)	17/10/99	1/5	757-749	52°C/18:25hrs
Junk Basket & Bridge Plug (GR and CCL record)	17/10/99	6,7	200-100	

5.2 SIDEWALL CORES

No sidewall cores were acquired in Baleen-2.

5.3 SEISMIC VELOCITY PROFILE

VSP data is summarized in section 4.3 and Appendix 11 of the Baleen-2 BASIC data Well Completion Report.

5.4 WIRELINE SAMPLING - MDT

A total of 32 MDT pretests were attempted over the two runs, of which 16 were successful, 8 were supercharged, 5 had lost seals, 1 was dry, and 2 had pumpout failure.

A total of 14 attempts with the MDT-pumpout were made to recover gas and water samples from the Gurnard Formation and Latrobe Group Coarse Clastics. One formation water sample recovery from the Latrobe Group Coarse Clastics at 797mRT was successful, with the properties discussed in Section 6.3. On transfer of the water sample, the exsolved gas was found to have 32 ppm H_2S (by Draeger tube). The presence of H_2S in the Latrobe Group Coarse Clastics in the Baleen-2 well is consistent with adjacent wells, with traces of H_2S found in the Latrobe Group Coarse Clastics in the Patricia-1 and Sperm Whale-1 wells. Failure to recover samples with the MDT from the Gurnard Formation seems to be a combination of friable, low permeability reservoir and the MDT pump out module pump dynamics.

Of the 32 pretests, 19 MDT mobility values were calculated for the Gurnard and Latrobe Group Coarse Clastics Formations. Over the Gurnard, 13 mobility readings were calculated ranging from 0.8mD/cP to 44.9mD/cP, averaging 9.3mD/cP. The increased porosity and permeability observed in the clean sandstones of the Latrobe Group Coarse Clastics, compared to the Gurnard

Formation, is evident with much higher calculated mobilities The 6 values determined over this interval range from 79.1mD/cP to 3399.6mD/cP, with an average of 1595mD/cP.
A plot of Mobilities versus Depth is included as Figure 13.

5.5 PETROPHYSICAL ANALYSIS

A petrophysical analysis was performed on the Baleen-2 well, which integrated the available wireline logs and core data, providing an interpretation of porosity, permeability, and water saturation with a high degree of confidence.

The logs available for the analysis included high-resolution density (RHO8 and PEF8), high-resolution neutron logs (HTNP/NPHU), high-resolution gamma ray logs (EHGR), spectral gamma ray logs (POTA, THOR, and URAN), compressional (DTCO) and shear (DTSM) sonic logs, and laterolog resistivities (MSFL, LLS, and LLD).

Core data consisted of core porosity, grain density, horizontal permeability, cation exchange capacity, and critical water saturation.

The final "Elan-Plus" analysis report for the Baleen-2 well is included as Appendix 2, with the results summarised in Table 6 below. Two plots of the petrophysical analysis results are included as a 1:100 scale Wide Display Composite Plot (Enclosure 2), an a 1:200 scale Standard Display with analysis parameters (Enclosure 3). The non-net zones are the siderite cemented zones.

Table 6 - Petrophysical Analysis Results

	Baleen-2
Top Interval	741.00 m
Bottom Interval	787.70 m
Gross Interval	46.70 m
Net Reservoir	40.31 m
Gross Pay	11.2m
Net Pay	10.6m
Average Effective Porosity (Net Reservoir)	0.260
Average Total Porosity (Net Reservoir)	0.297
Average Volume of Clay (Net Reservoir)	0.214
Average Log Calculated Permeability (Net Reservoir)	93 mD
Net / Gross Ratio	0.86
Formation water salinity	7.95ppk

6.0 CORE ANALYSIS

6.1 PRODUCTION STABILITY EVALUATION

Schlumberger performed a Production Stability Evaluation on the Baleen-2 well. The aim of this study was to assess the potential for sand production and mechanical stability of the Gurnard reservoir, to assess implications on the field development, and to support decisions on production well completion design. The work consisted of mechanical testing on five core samples from Baleen-2, and a study of formation integrity during production based on the core sample testing and on log data. The four vertical sample plugs, of diameter 42 millimetres and length 90-100 millimetres, were cut from the core at depths 750.82mRT, 756.52mRT, 760.23mRT, 769.67mRT, and 777.0mRT. The logs used included the compressional sonic and shear sonic, bulk density, and petrophysical analysis.

Rock compressive strengths were first measured on the core samples with measured unconfined compressive strengths of 3.41Mpa – 4.4Mpa, which is relatively low for sandstone. Single-stage tests were then performed to calibrate elasto-plastic properties of the core samples. The samples showed increases in strength up to 3.3 times the measured value, indicating the rocks are reasonably plastic (The physical tests were performed by CSIRO). Finally overburden and minimum horizontal stress have been calculated from log data, pore pressure profile and core measured strengths. The results show that the reservoir is likely to fail under any drawdown condition and any Patricia-Baleen development wells will require some form of sand control system. This is mainly a consequence of the low rock strength.

The Production Stability Evaluation Report is included as Appendix 3. A dynamic Elastic Moduli and Rock Properties log plot is included as Enclosure 4, and a Formation Integrity Sanding Production log plot is included as Enclosure 5.

6.2 SPECIAL CORE ANALYSIS (SCAL)

SCAL experiments were performed on core samples acquired from the Baleen-2 well. One plug for SCAL work was taken every metre throughout the core, with 30 samples acquired over the Gurnard Formation. 30 centimetre Format Core Photography is included as Appendix 4 and shows all the SCAL sample points. Cathodoluminscence (CT) scanning was initially performed on the core samples to note any internal inhomogeneities and/or drilling fluid invasion zones. The CT scanning Report is included as Appendix 5. After cleaning and drying all the samples, they were analysed for ambient base parameters. The samples were then split into 2 suites, a waterflood suite, and an electrical properties suite.

The electrical properties suite sequence was: pressure saturation followed by formation resistivity factor, and multi-salinity formation factor analyses. Finally the resistivity index and capillary pressure analyses were performed. The waterflood suite sequence also began with pressure saturation followed by brine permeability analysis. Single point desaturate to Swir was then performed, followed by Basic waterflood analysis.

All the samples were then cleaned and dried again. Base permeability and Klinkenberg permeability analysis was then performed on all the samples. Table 7 provides a summary of the results for the samples from the electrical properties suite, and Table 8 provides a summary of the results for the samples from the waterflood suite. The complete analysis and results of the Special Core Analysis is included in the SCAL Final Report in Appendix 6.

Table 7 - SCAL Results – Electrical Properties Suite

Sample	Depth	Formation Factor	Multi-salinity FF (@ Rw 0.1-0.9)	Resistivity Index (@ brine saturation of 50%)	Capillary pressure (@ brine saturation of 50%)	Perm. To Air (mD)	Porosity (%)	Klinkenberg Perm. (mD)	Grain Density (g/cm^3)
S1	746.63	7.2	1.1 – 5.9	3.8	540	27	31.2	22	2.83
S5	750.41	6.2	0.8 – 5.4	3.2	32	76	32.1	63	2.69
S9	754.41	5.6	0.7 – 5.4	3.4	10	313	35.8	280	2.68
S10	755.39	6.8	0.9 – 6.1	3.3	12	240	33.1	215	2.73
S20	767.87	12.2	1.8 – 10.7	3.4	98	30	23.3	25	2.99
S23	770.97	8.2	1.1 – 7.3	-	-	-	-	-	2.68
S25	772.99	6.3	0.8 – 5.6	3.8	22	79	33.3	64	2.74
S27	774.80	3.8	0.6 – 3.7	-	-	-	-	-	2.69
S28	775.82	5.5	0.7 – 5.2	-	12	213	35.3	176	2.68
S29	776.80	4.9	0.9 – 4.8	-	-	-	-	-	2.68

Table 8 - SCAL Results – Waterflood Suite

Sample	Depth	Gas saturation Sgr (percent)	Effective permeability to brine Kw@ Sgr (mD)	Relative permeability to brine	Perm. To Air (mD)	Porosity (%)	Klinkenberg Perm. (mD)	Grain Density (g/cm^3)
S2	747.41	16.8	0.26	0.531	42	31.5	33	2.71
S6	751.42	16.0	2.1	0.210	84	31.4	69	2.68
S11	756.40	14.8	2.3	0.117	149	33.9	128	2.68
S12	757.42	13.9	6.2	0.159	268	34.8	224	2.68
S21	768.79	12.3	0.53	0.408	22	29.9	17	2.69
S24	771.81	16.9	2.3	0.405	61	32.0	45	2.71
S26	773.79	15.8	1.7	0.221	86	34.2	73	2.71
S30	777.80	10.3	21	0.263	493	34.5	462	2.72

6.3 WATER SAMPLE CHEMISTRY

Water Sample Recovered by Wireline sample tool (MDT)

One water sample was obtained from the Baleen-2 well. During the MDT runs, 1 gallon of formation water was taken from 1 sample point at 797mRT within the Latrobe Group Coarse Clastics. The formation water sample was analysed by ACS laboratories in Brisbane with a summary of the results displayed in Table 9.

Table 9 - Formation Water Sample Results

Sample depth: 797mRT	
Resistivity	0.690 – 0.709 ohm.m @ 25°C
Conductivity	14 100 – 14 500 uS / cm @ 25°C
Reaction – pH	7.4
Specific Gravity	1.0040 @ 25.0°C

Fluids Extracted from Core

Two core plug samples were taken at 754.08mRT and 778.34mRT, divided into 5 sections, and pore water extracted from each of the sections. The extracted pore fluids were analysed by ACS Laboratories. The analyses performed on the extracted fluid samples include standard 10 ion plus nitrates and resistivity analysis. The purpose of these analyses was to examine the invasion of core by the drilling fluids. The nitrate invasion profile shown in Figure 14 indicates that the fluid invasion penetrates the entire core to some degree. Chlorides and Sodium Ion invasion profiles, and Resistivity are also shown in Figure 14.

The results of the ACS Laboratories analysis on the formation water and pore water samples is included in the Fluids Analysis Report in Appendix 13 of the Baleen-2 BASIC Data Well Completion Report.

6.4 GEOCHEMICAL EVALUATION

There was no geochemical source rock evaluation performed on samples from the Baleen-2 well.

7.0 FORMATION PRESSURE

MDT pretests for formation pressures were conducted across the Gurnard Formation and Latrobe Group Coarse Clastics. A gas gradient of 0.0220 psi/ft (0.0722 psi/m) was established in the upper Gurnard Fm from 749.3 mRT to 757.0 mRT. A water gradient of 0.432 psi/ft (1.416 psi/m) was established in the lower Gurnard Formation from 771.5 mRT to 785.0 mRT. A water gradient of 0.432 psi/ft (1.416 psi/m) was found in the upper sandstones of the Latrobe Group Coarse Clastics from 795.0 mRT to 823.0 mRT. Figure 15 displays the MDT data acquired from the Baleen-2 well with the calculated gas gradients, and water gradients for both the Gurnard Formation and Latrobe Group Coarse Clastics.

The Gurnard Formation reservoir pressure was found to be 38 psi below that which was expected given the results of the Baleen-1 well. Similarly the Latrobe Group Coarse Clastics pressures were found to be approximately 34 psi below that expected from data gathered in the Patricia-1 well. In Baleen-2, an offset of approximately 6 psi exists between the water gradients of the Latrobe Group Coarse Clastics and that of the Gurnard Formation (Figure 13). Pressure depletion of the main aquifer in the greater Gippsland Basin (Latrobe Group) through production at the nearby fields of Tuna, Marlin and others has reduced the formation pressures at Baleen-2 through the regional aquifer. The small offset of the water gradients in the Gurnard Formation and Latrobe Group Coarse Clastics appears to be due to the 3 metres to 5 metres of very strongly cemented zone at the base of the Gurnard Formation causing some small impediment to the loss of pressure from the Gurnard reservoir.

Resolved to a common depth of 738 mSS (746mRT) Gurnard reservoir pressures are:

Baleen-1	Drilled 1981	1110 psi
Patricia-1	Drilled 1987	1095 psi
Baleen-2	Drilled 1999	1072 psi

Intersection of the Gurnard Formation gas and water gradients indicates a FWL at 764.2 mRT (738.2 mSS). This point occurs within a non-net section of the reservoir.

Assuming a water gradient of 1.416psi/m from the surface, the expected pressure at the FWL (738.2mSS) would be 1045 psia. The recorded pressure was 1072 psia, indicating that the Gurnard Formation is slightly overpressured by 27psi. Using the recorded pressure at the FWL, the overall pressure gradient to surface is calculated at 1.452psi/m. The calculated pressure gradient from the surface (Mean Sea Level) to the top of the Gurnard Formation reservoir (1070psia, 741mRT) is 1.44psi/m (0.44psi/ft) or an Equivalent Mud Weight (EMW) of 1.016sg (8.46ppg).

Uncertainty exists over the connectivity between Baleen-2 and the other wells, Patricia-1 and Baleen-1, in the Patricia-Baleen Gas Field. This is due to the varying reservoir pressures for the 3 wells (Figure 16) resulting from pressure depletion by Bass Strait production and onshore ground water offtake. Baleen-2 is interpreted to have intersected the southwestern flank of the Baleen gas accumulation intersected by the Baleen-1 well, and from seismic data and well to well correlations, are interpreted to be in communication. It is also likely the Patricia and Baleen gas accumulations do not share the same GWC.

NOTE: Pressure data discrepancy is noted from the MDT runs, with the strain gauge reading 2-7psi less than the quartz gauge. The expected difference should be 14.7psi. Schlumberger performed tests on the gauges and advised that both gauges performed with expected specification, however, the recommendation was to use the pressure data from the quartz gauge. Communication from Schlumberger regarding the MDT pressure discrepancy is included as Appendix 7.

8.0 CONTRIBUTIONS TO GEOLOGICAL CONCEPTS

The principal conclusions and contributions to the geological knowledge of the Gippsland Basin region resulting from the drilling of the Baleen-2 well are:

(i) Baleen-2 was drilled structurally downdip of the Baleen-1 discovery well, and confirmed the southwest extension of the Patricia-Baleen gas accumulation. The top reservoir was intersected at 721.8mSS, 87.1 metres structurally lower than in the Baleen-1 well, and 58.5 metres structurally lower than in the Patricia-1 well. The FWL was defined at 738.2mSS (764.2mRT).

(ii) Baleen-2 intersected a 16.4 metre gas column in the Gurnard Formation over the interval 721.8mSS – 738.2mSS (747.8mRT – 764.2mRT), with an average log calculated porosity of 30.4%, and average water saturation of 59%.

(iii) Oil shows were noted in the lower part of Core #1 over the interval 730mSS – 738mSS (756mRT – 764mRT) in the Gurnard reservoir, with the best shows having dull to moderately bright yellowish green pinpoint to patchy direct fluorescence, slow to moderately fast yellowish white to bright bluish white blooming cut fluorescence, thick yellowish white residual ring fluorescence. The shows were extracted from core samples but could not be typed due to insufficient quantity.

(iv) Baleen-2 encountered 51 metres of Gurnard Formation and is slightly thicker than the Gurnard Formation intersected elsewhere on the Patricia-Baleen Gas Field. This infers good continuity of the Gurnard Formation between the wells in VIC/RL5.

(v) Palynological analysis performed on the cores and cuttings from the Baleen-2 well was able to determine the depositional ages for the Lakes Entrance Formation, Gurnard Formation, Latrobe Group Coarse Clastics Formation, and Strzelecki Group. The Lakes Entrance Formation contains *P. tuberculatus* (undiff.), with an age range from Early Miocene to Oligocene. It is most likely to be Early Oligocene in age by correlating with the Baleen-1 and Patricia-1 wells. The Gurnard Formation in Baleen-2 is confined to Middle Eocene in age by the presence of Lower *N. asperus.* The Latrobe Group Coarse Clastics is interpreted to be Paleocene in age with the presence of *L. balmei*. The Strzelecki Group is confined to Late Albian in the Cretaceous by the presence of Upper *C. paradoxa*.

(vi) The Gurnard Formation is interpreted to have been deposited in a middle to outer shelfal marine setting. The entire reservoir is pervasively bioturbated with abundant *Thalassinoides* and *Ophiomorpha*, and lesser, *Skolithos* and *Zoophycos*. The very fine to fine grained silty sandstones were likely deposited as a series of parasequence sets below fair-weather wave base with turbiditic and suspension deposition being the main mechanisms for sediment transport into the area.

(vii) The sands of the Gurnard Formation are interspersed with several 0.15 metre to 2 metre thick siderite bands. Petrographic analysis suggests the most likely origin of these siderite zones is through diagenesis, with siderite precipitation from marine porewater. Siderite is most likely to have formed before compaction at shallow burial, below a sulphate reduction zone. It is possibly the result of early methanogenesis or oxidation of early formed, biogenic methane.

(viii) Baleen-2 demonstrated persistence of the Lakes Entrance Formation topseal to the southwest of the original discovery well. In the Baleen-2 well this formational seal is only 17 metres thick, 20-30 metres thinner than seen in the other Patricia-Baleen wells due to channeling at the base of the overlying Gippsland Limestone.

(ix) Baleen-2 only intersected gas in the Gurnard Formation. No gas was intersected in the Latrobe Group Coarse Clastics as found in other wells in VIC/RL5 (Patricia-1, Baleen-1 and Sperm Whale-1). However, Latrobe Group Coarse Clastics gas was not expected at this downdip location.

(x) The presence of H_2S in the formation water sample from the Latrobe Group Coarse Clastics is consistent with observations from adjacent wells (Flathead-1, Patricia-1, Spermwhale-1 and Baleen-1), where H_2S is found in the Latrobe Group Coarse Clastics but not in the Gurnard Formation.

(xi) Rock Strength analysis suggests the Gurnard Formation is likely to fail under any drawdown conditions. Some sand control measures will be required in any Patricia-Baleen development wells.

(xii) A gas gradient of 0.0722 psi/m was established in the upper part of the Gurnard Formation reservoir. A water gradient of 1.416 psi/m was established for the Latrobe Group Coarse Clastics and Lower Gurnard Formation with a difference of 6psi between the Gurnard Formation water pressure gradient and the Latrobe Group Coarse Clastics water pressure gradient, with the Gurnard Formation "floating" on the Latrobe Group Coarse Clastics. The basal cemented zone of the Gurnard Formation therefore appears to be a partial pressure seal capable of maintaining a 6psi differential.

(xiii) Baleen-2 (1999) recorded a 38psi drop in regional aquifer pressure since the drilling of the Baleen-1 (1981) well. This is most likely due to Bass Strait production and onshore abstraction.

(xiv) Some uncertainty exists over the connectivity between Baleen-2 and the other wells in the Patricia-Baleen Gas Field due to the varying reservoir pressures for the 3 wells, and small-throw faults observed on the 3-D seismic data. Baleen-2 is most likely connected to the Baleen gas accumulation intersected by the Baleen-1 well. It is also likely the Patricia and Baleen gas accumulations do not share the same GWC.

9.0 REFERENCES

BARBER, P.B., 2000: Patricia – Baleen Gurnard Sedimentological Model. *Unpublished.*

GFE RESOURCES LTD, 1995: Exploration Summary, VIC/P11, Gippsland Basin, Victoria. *Unpublished.*

GILBERT, M.B., AND HILL, K.A – Gippsland, A Composite Basin-A case study from the Offshore Northern Strzelecki Terrace, Gippsland Basin, Australia. *APEA Journal,* 34, p495-512.

FIGURES

OMV

VIC/RL5 PERMIT LOCATION MAP

GIPPSLAND BASIN - OFFSHORE VICTORIA

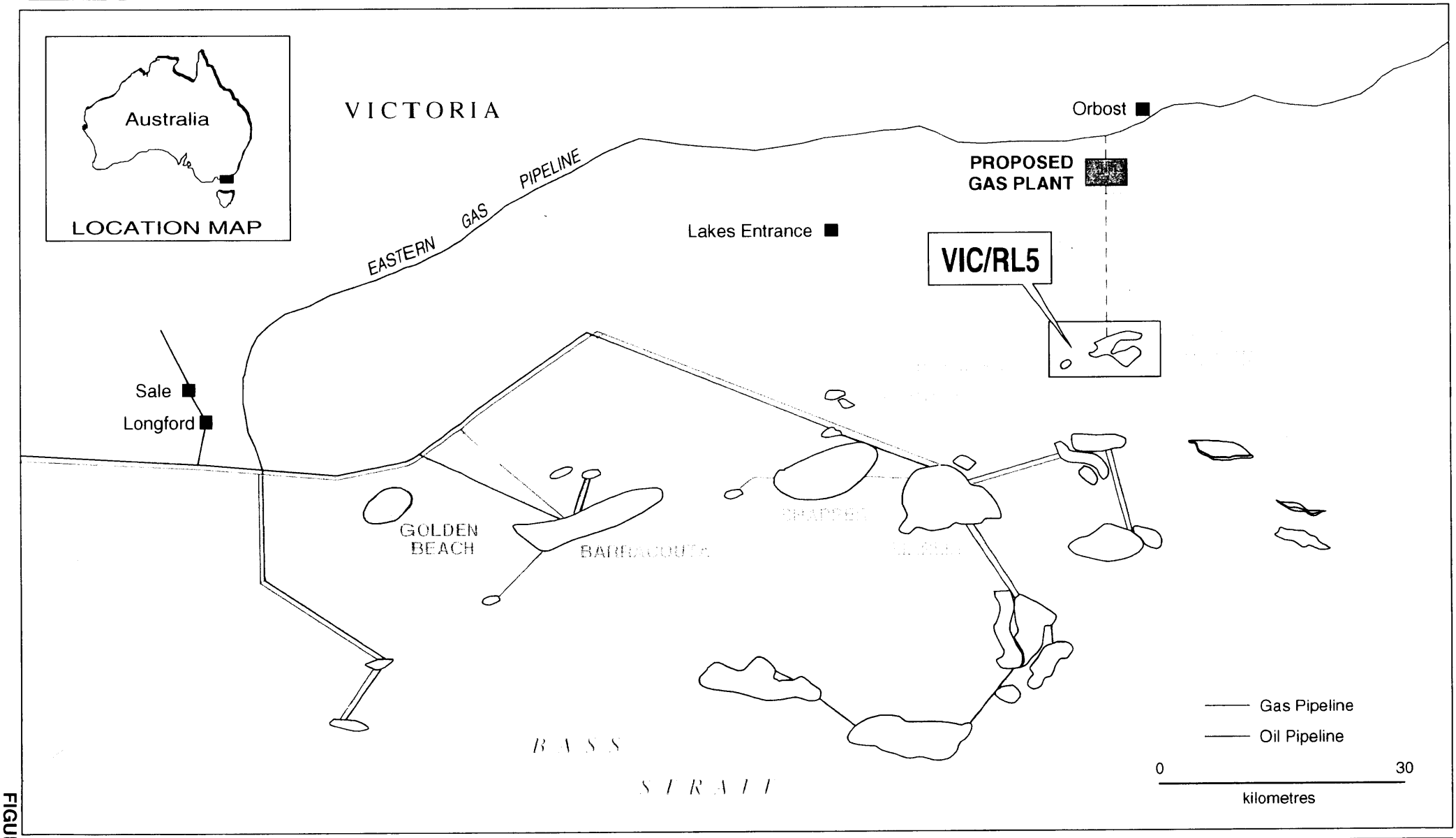

FIGURE 1

AUTHOR: OMV | DATE: MAY 2000 | FILENAME: GIPPSLAND \ A4S \ 21.DGN (V4)

BALEEN-2 LOCATION MAP

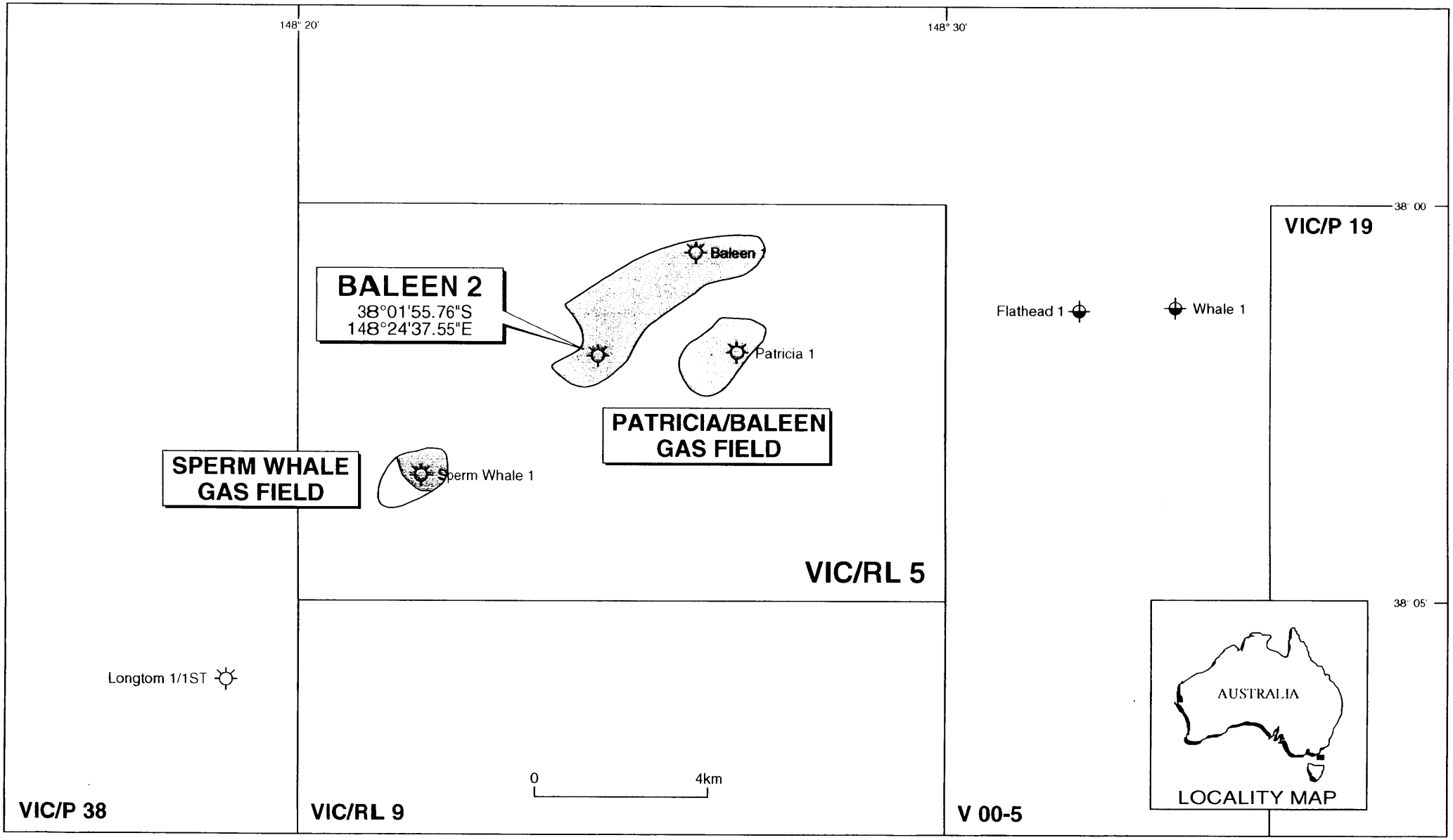

FIGURE 2

AUTHOR: OMV | DATE: JULY 2000 | FILENAME: GIPPSLAND \ VICRL5 \ A4S \ 81.DGN (V2)

OMV

GIPPSLAND BASIN

GENERALISED STRATIGRAPHY

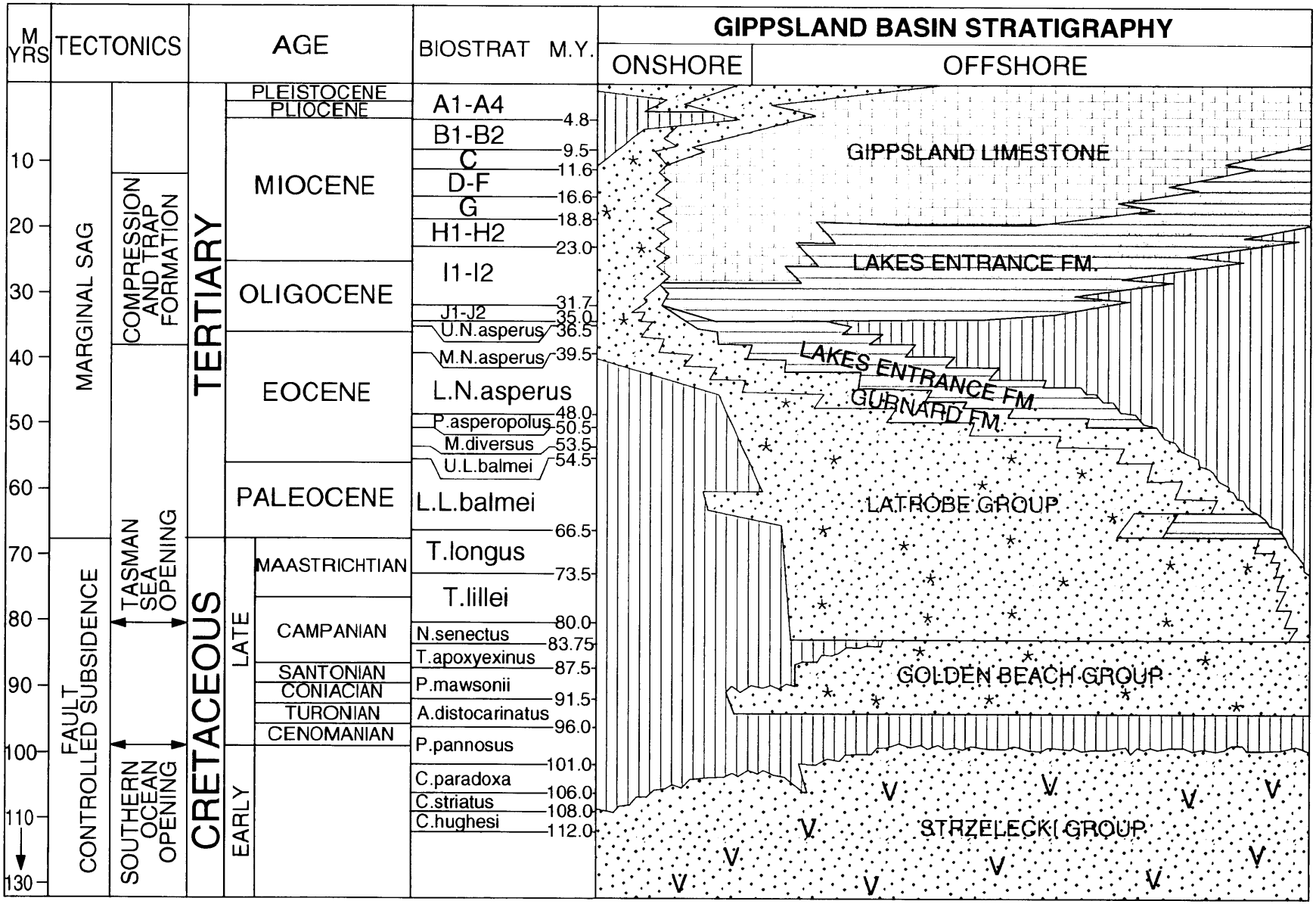

FIGURE 3

AUTHOR: OMV

DATE: MAY 2000

FILENAME: GIPPSLAND \ A4S \ 29.DGN

OMV

REGIONAL CROSS SECTION

GIPPSLAND BASIN - OFFSHORE VICTORIA

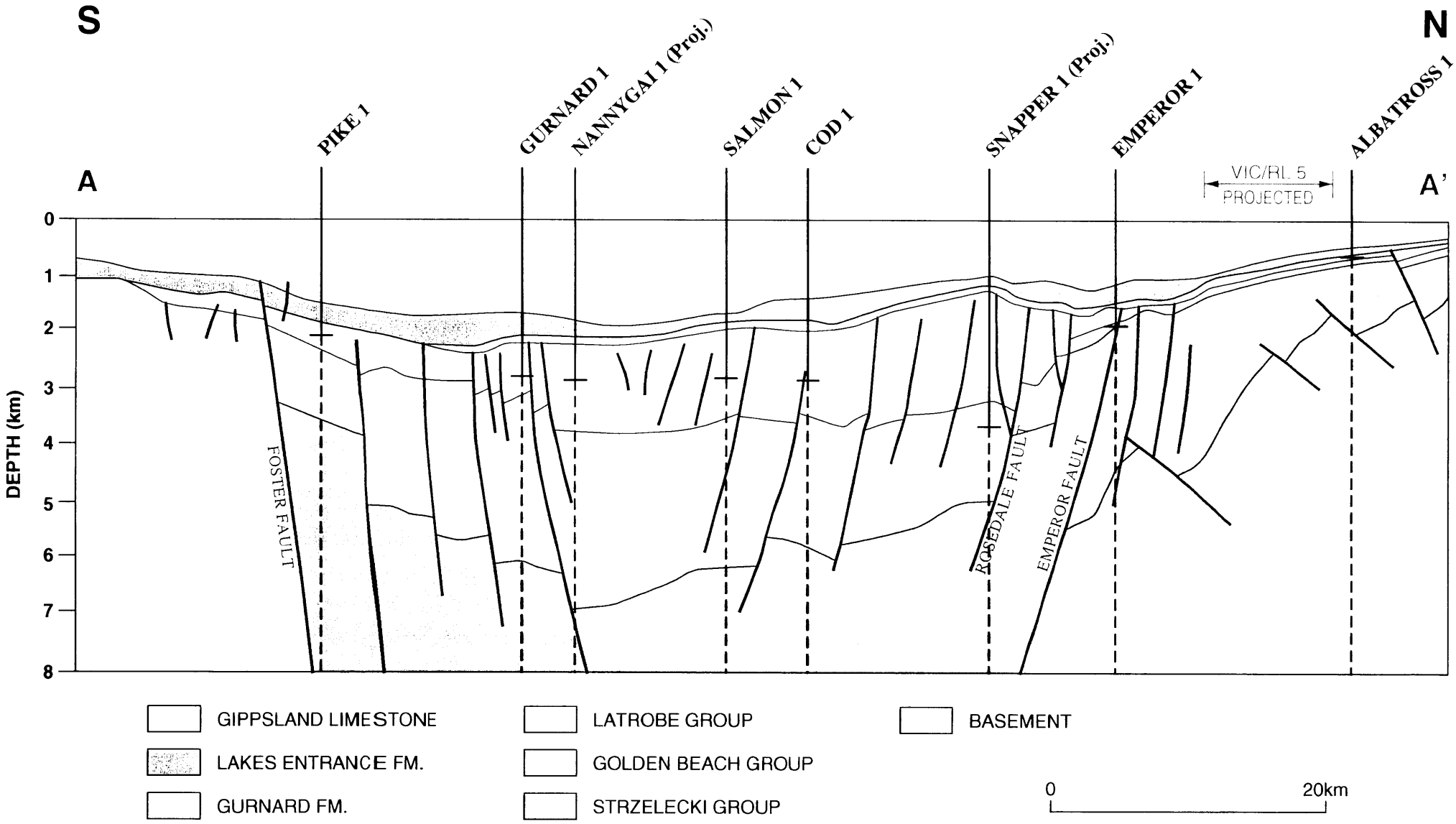

FIGURE 4

AUTHOR: OMV | DATE: MAY 2000 | FILENAME: GIPPSLAND \ A4S \ 31.DGN

OMV

STRUCTURAL CROSS-SECTION

SPERM WHALE 1, BALEEN 2, BALEEN1 and PATRICIA 1

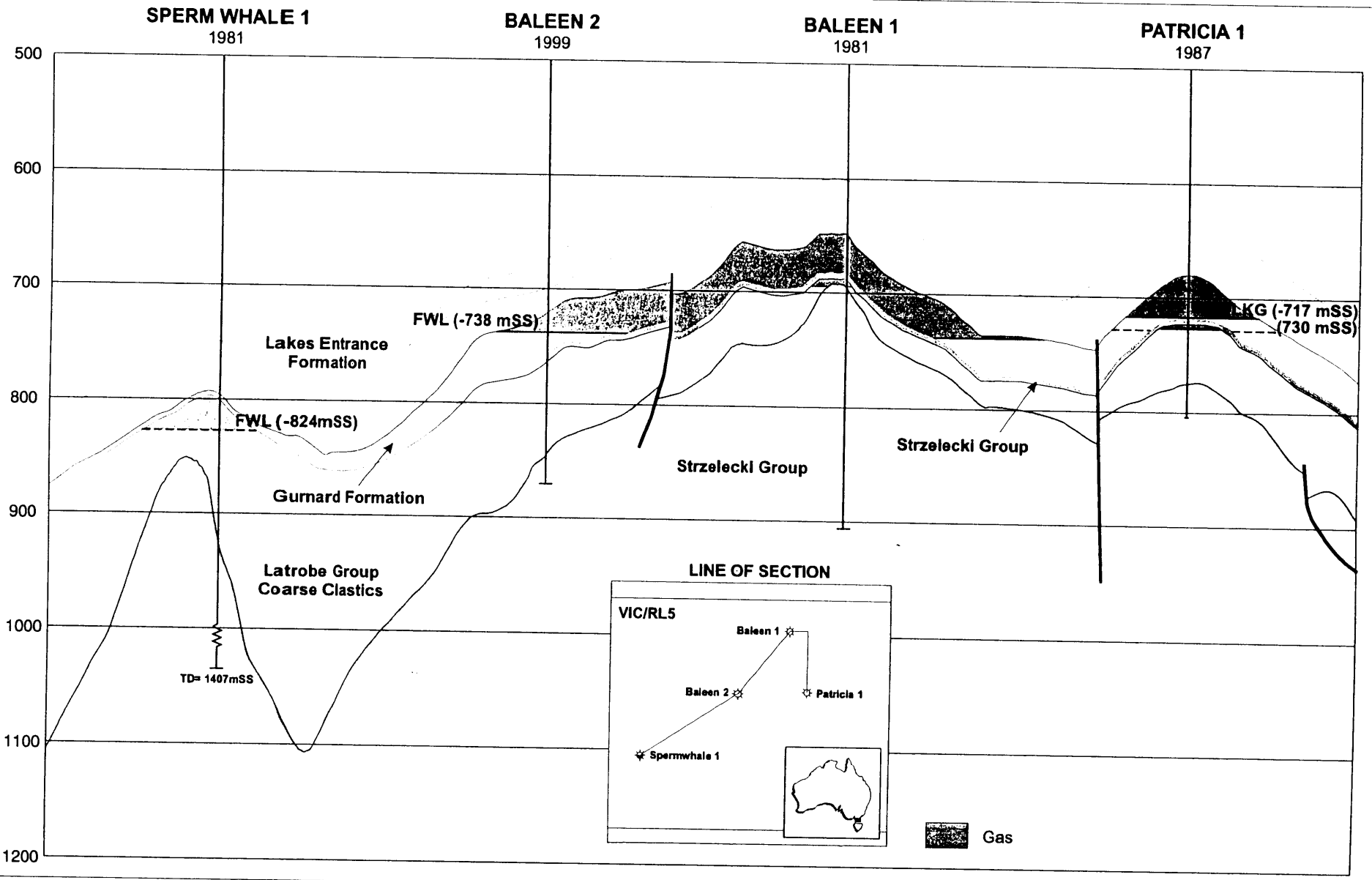

FIGURE 5

AUTHOR: OMV

DATE: JUNE 2000

FILENAME: GIPPSLAND \ A4S \ 230.CDR

908080 042

OMV

BALEEN 2

PREDICTED vs ACTUAL SECTION

Predicted Section

Actual Section

LOCATION: GL88-62 SP 366 | LATITUDE: 38° 01'55.79"S LONGITUDE: 148° 24'37.57"E | EASTING: 623782 NORTHING: 5789663 | WATER DEPTH: 55m RT: 26m AMSL

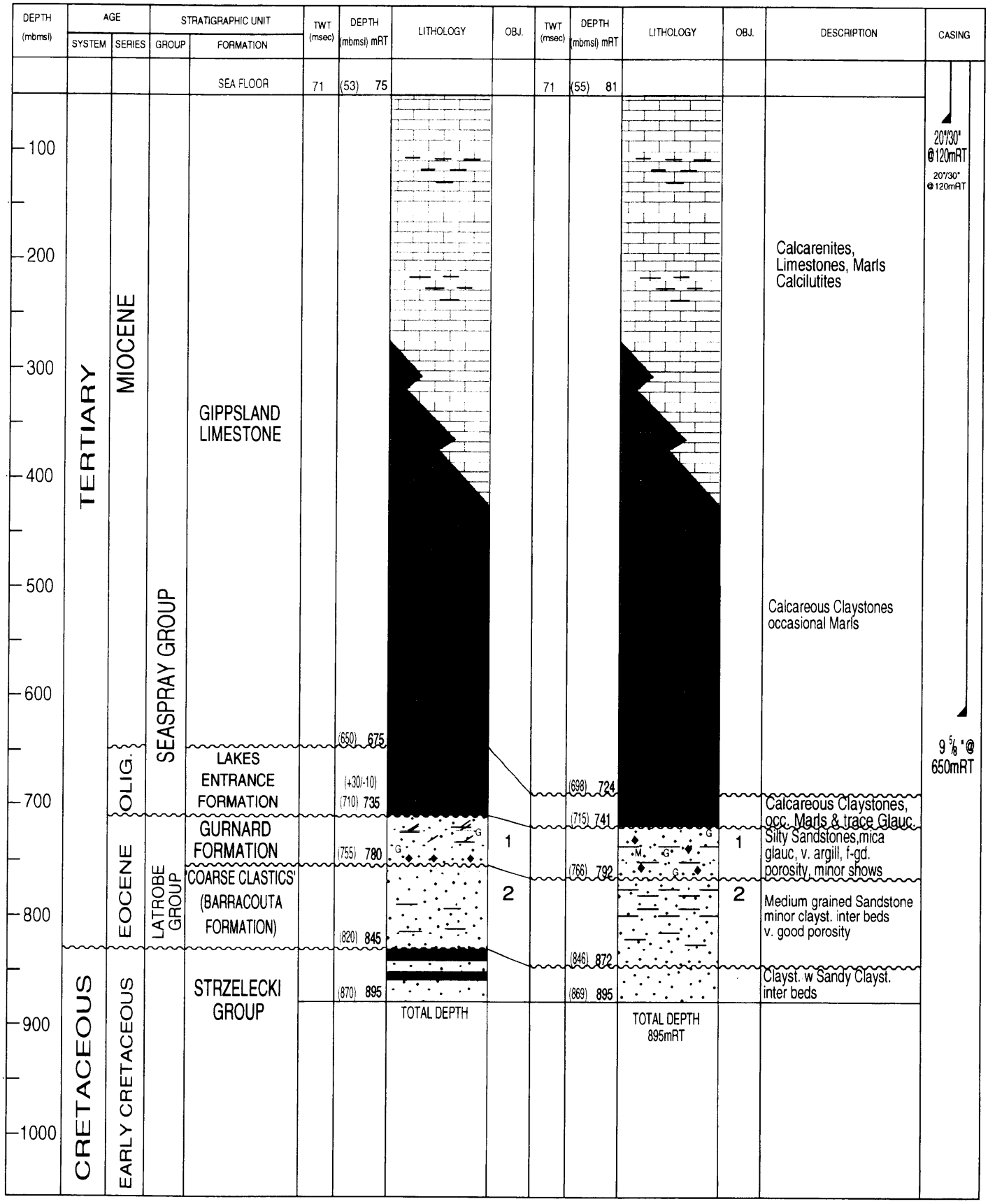

AUTHOR: OMV DATE: DECEMBER 2000 FILENAME: GIPPSLAND \ VICRL5 \ A4S \ 231.DGN

FIGURE 6

PE 908080_cc/cl 002

OMV

REVISED GURNARD FORMATION TOP PICK

GIPPSLAND BASIN

908080 044

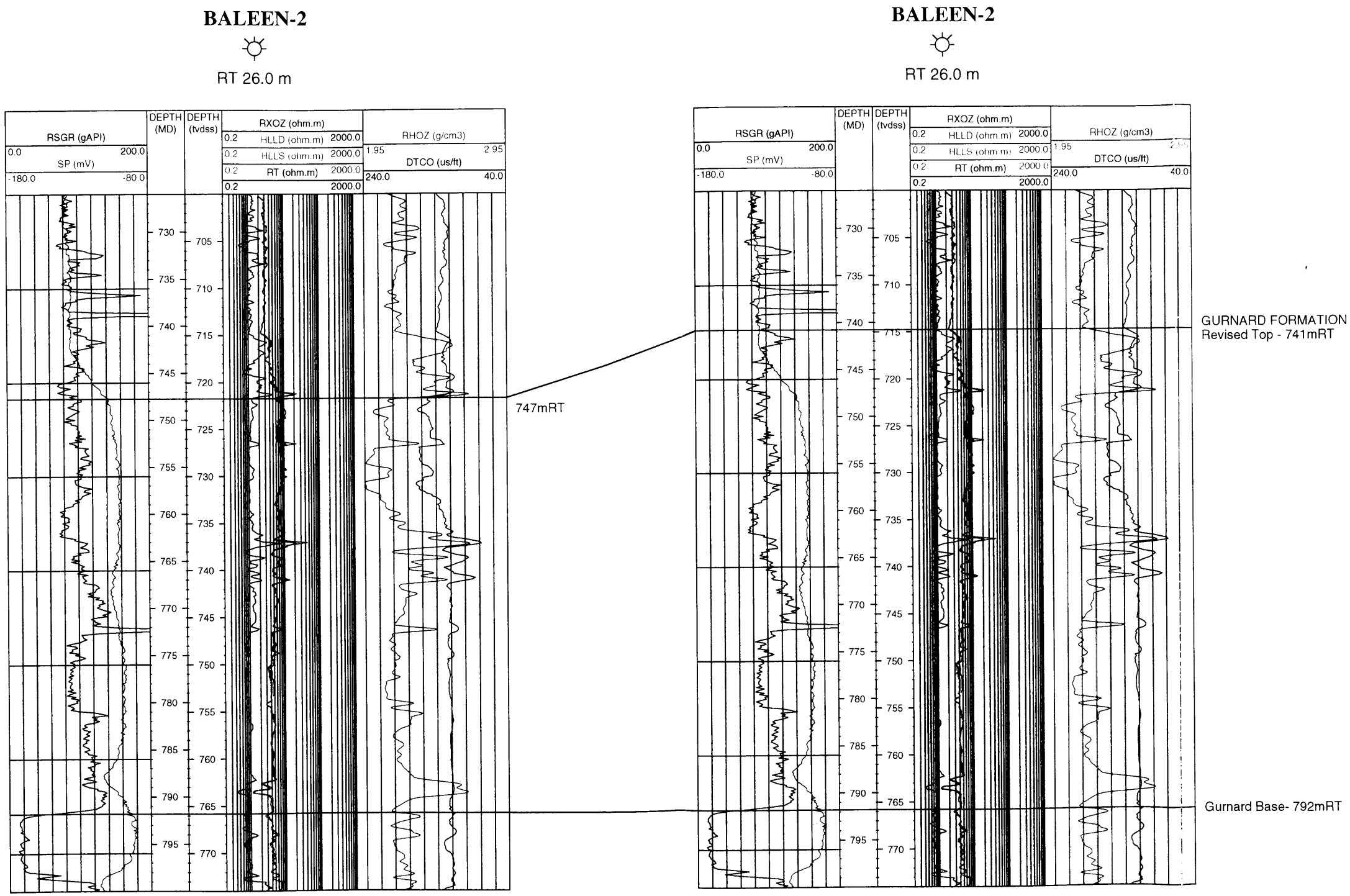

AUTHOR: OMV

DATE: DECEMBER 2000

FILENAME: GIPPSLAND \ VICRL5 \ A3S \ 233.DGN

FIGURE 7

HYPOTHETICAL SEDIMENTOLOGIC MODEL: GURNARD FORMATION

PATRICIA - BALEEN FIELD: GIPPSLAND BASIN

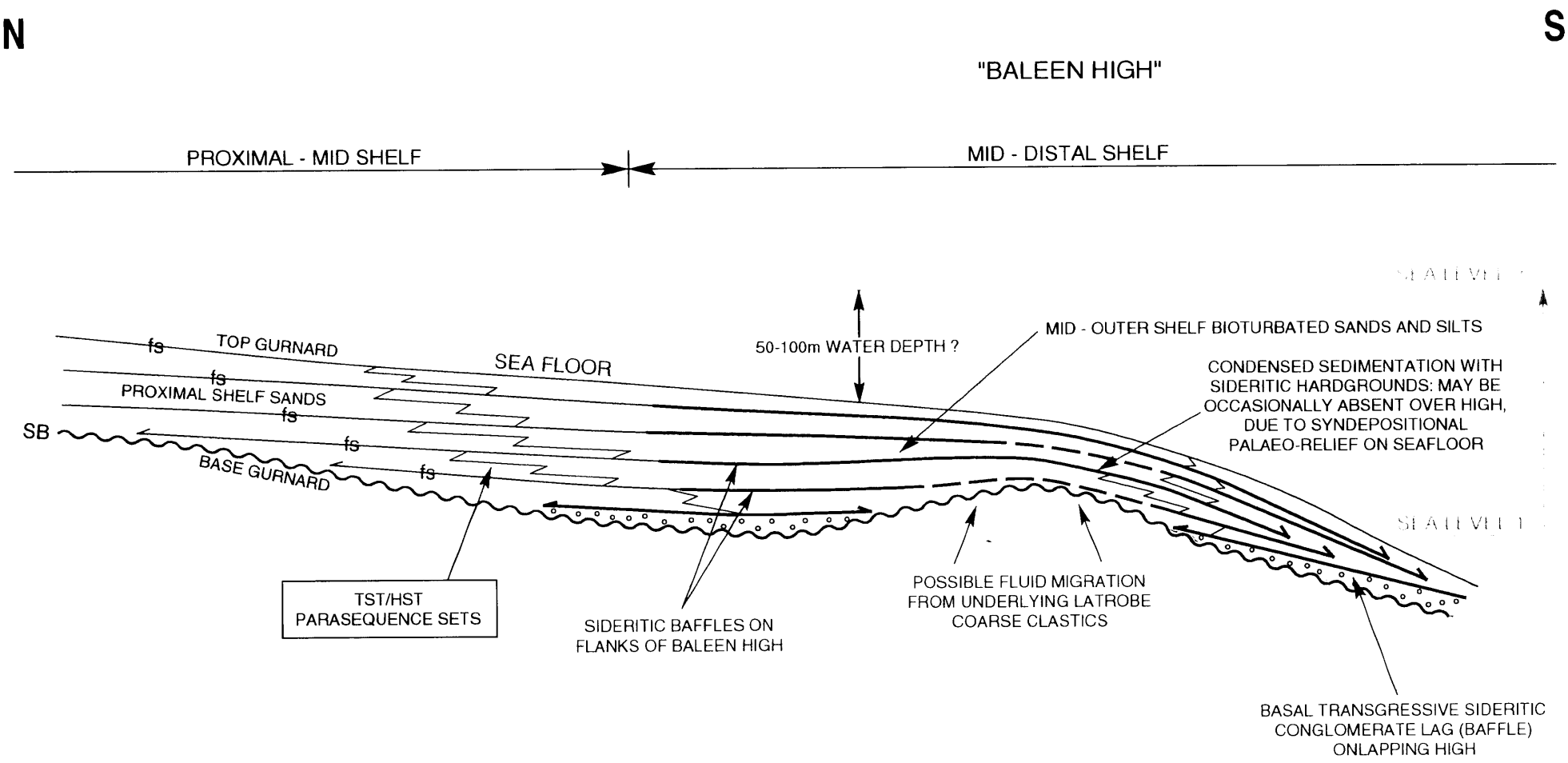

NOTES:
1. FAULTS OMITTED FOR CLARITY
2. MODEL SUBJECT TO VERIFICATION
3. VERTICAL SCALE EXAGERATED: MAXIMUM THICKNESS ~50m

SB: SEQUENCE BOUNDARY
fs: FLOODING SURFACE

FIGURE 8

AUTHOR: P.BARBER/ISIS PETROLEUM CONSULTANTS | DATE: AUGUST 2000 | FILENAME: GIPPSLAND \ VICRL5 \ A4S \ 102.DGN

PE908080_colour

OMV

GURNARD RESERVOIR CORRELATION

BALEEN-2, PATRICIA-1 and BALEEN-1

908080 046

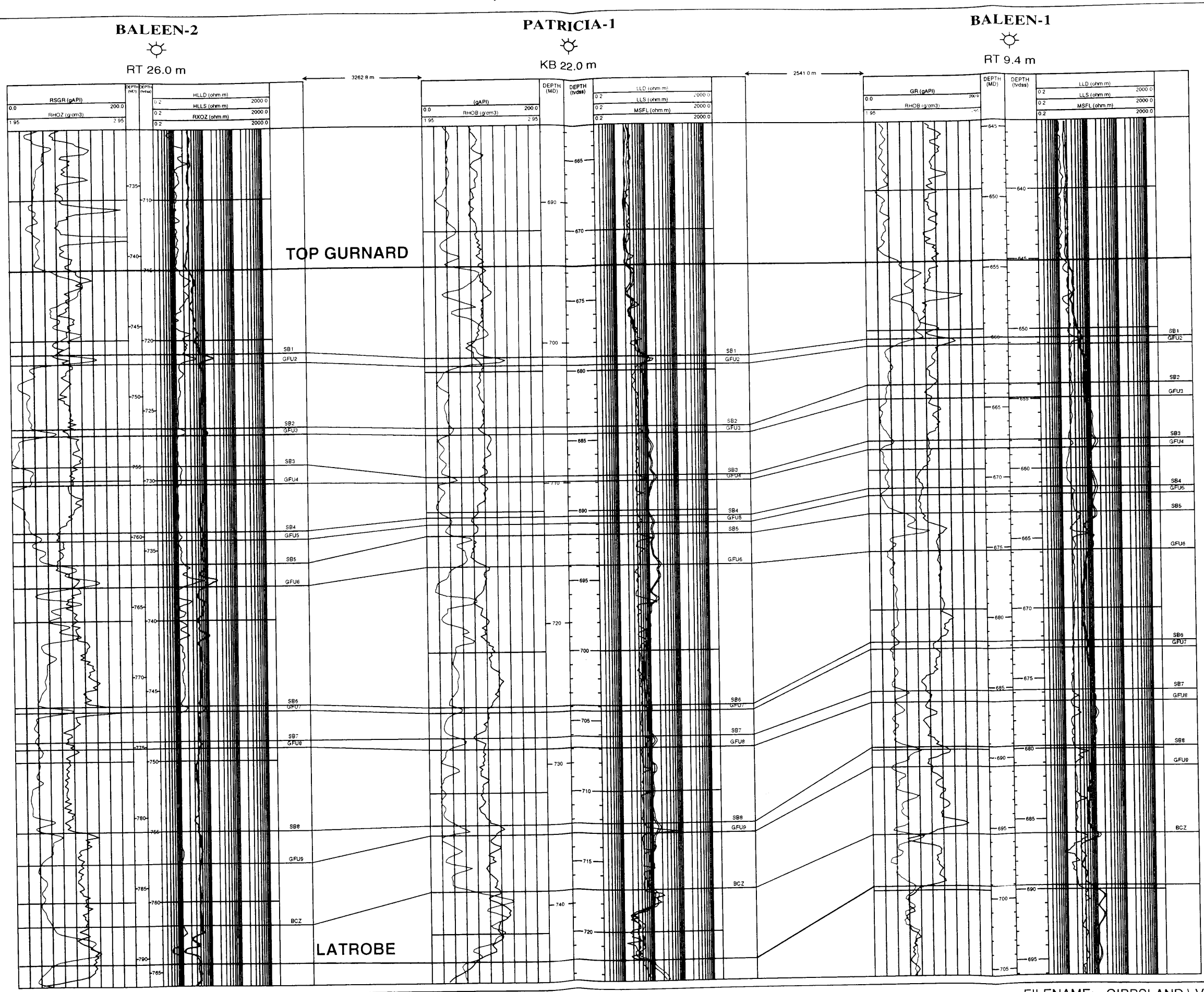

AUTHOR: OMV

DATE: DECEMBER 2000

FILENAME: GIPPSLAND \ VICRL5 \ A3S \ 236.DGN

FIGURE 9

PE904884 - color ΦΦ9

908080 047

VIC/RL5

BALEEN 1

Proposed Location

BALEEN 2

PATRICIA 1

SPERM WHALE 1

1:25000

0 1 2

KILOMETRES

UNIVERSAL TRANSVERSE MERCATOR PROJECTION
AUSTRALIAN NATIONAL SPHEROID
CENTRAL MERIDIAN 147 00 00 E
Mapsheet datum: 'AGD84'

CULTUS PETROLEUM N.L.

Gippsland Basin

VIC/RL5

Depth Structure Map

Top Reservoir

Author : mona	Date : 21/11/2000
Scale : 1:25000	Cont. Int. 10 metres
Spheroid : AUSTRALIAN NATIONAL	CM : 147 00 00E
Projection : UNIVERSAL TRANSVERSE MERCATOR	Projection File No.

FIGURE 10

OMV

TOP GURNARD DEPTH MAP

APPARENT POLARITY AMPLITUDES

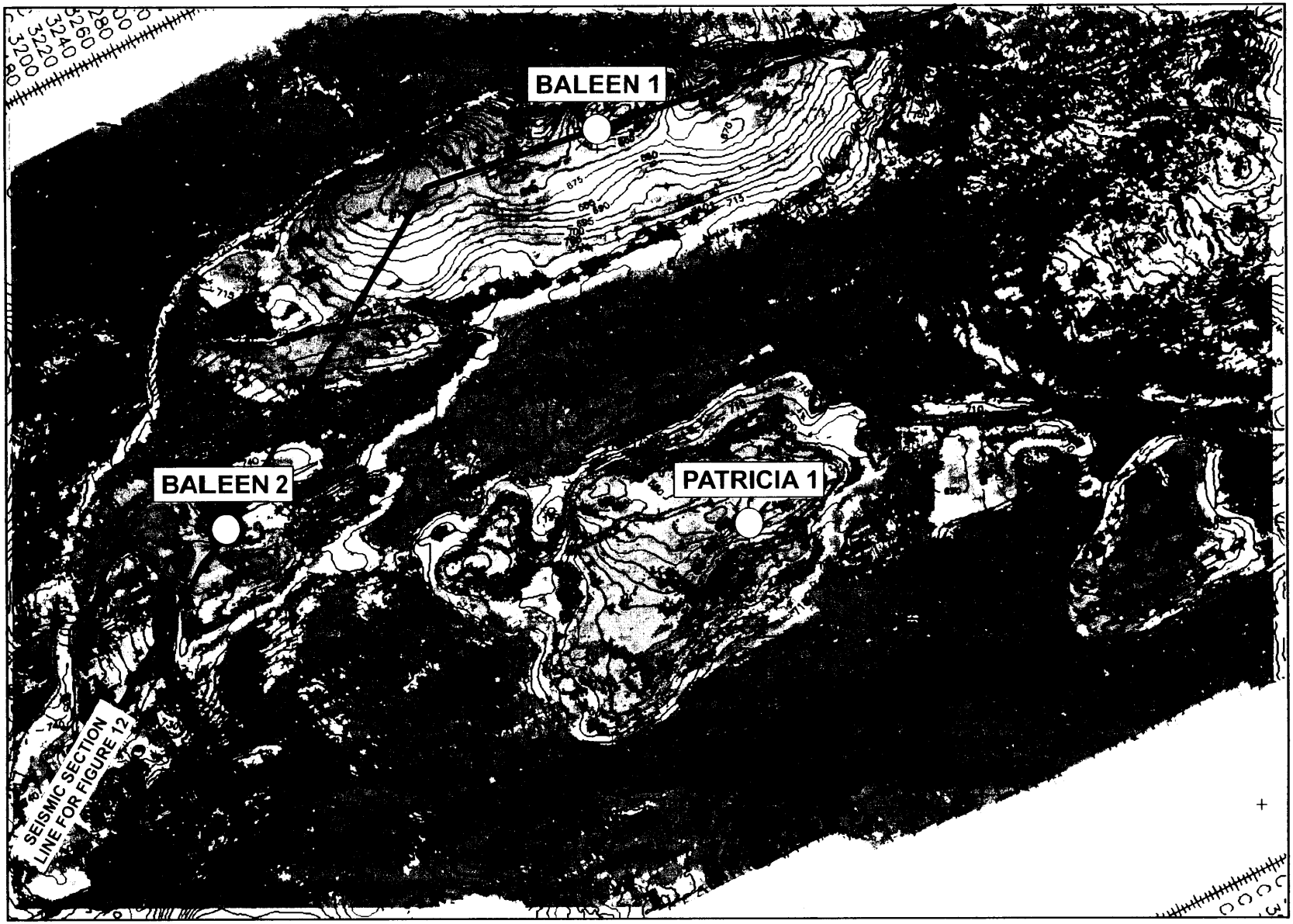

FIGURE 11

AUTHOR: OMV | DATE: DECEMBER 2000 | FILENAME: GIPPSLAND \ A4S \ 232.CDR

SEISMIC SECTION: BALEEN-2 to BALEEN-1

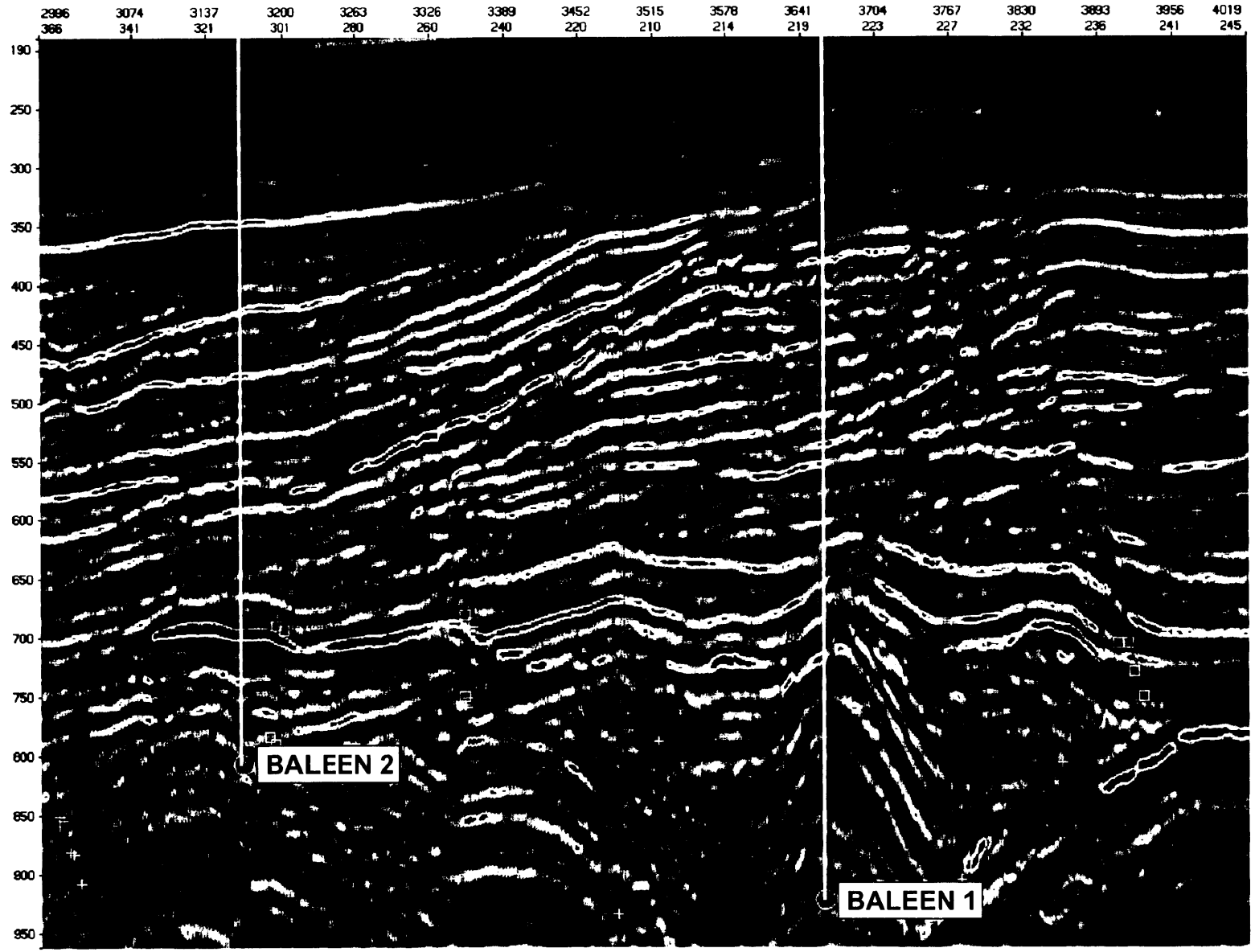

TOP GURNARD

TOP LATROBE
COARSE CLASTICS

TOP STREZELECKI

FIGURE 12

AUTHOR: OMV

DATE: DECEMBER 2000

FILENAME: GIPPSLAND \ VICRL5 \ A4S \ 235.CDR

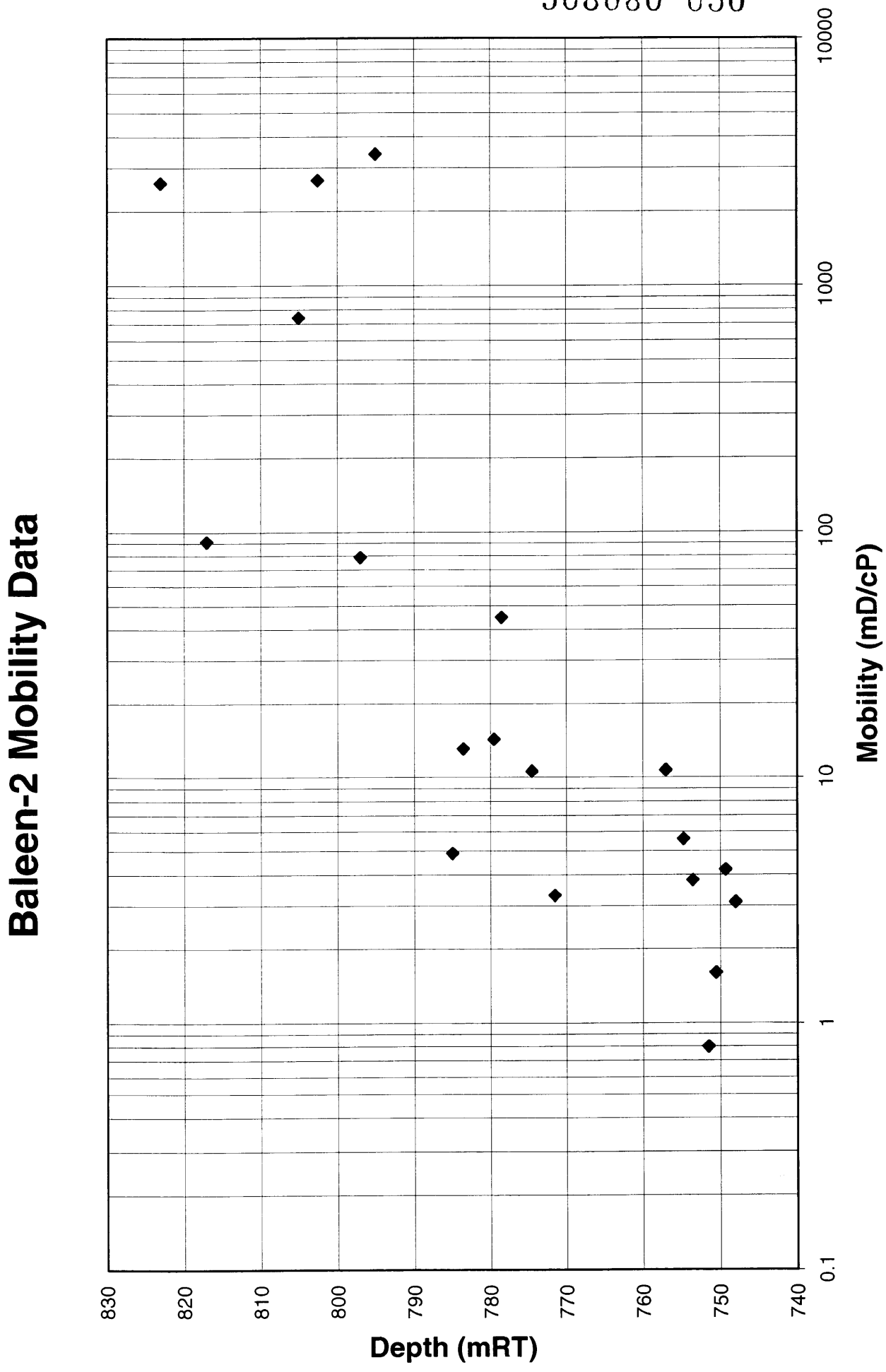
Baleen-2 Mobility Data
Depth (mRT)
830
820
810
800
790
780
770
760
750
740
Mobility (mD/cP)
10000
1000
100
10
1
0.1

FIGURE 13

OMV Australia

Fluids Invasion Profile - Core

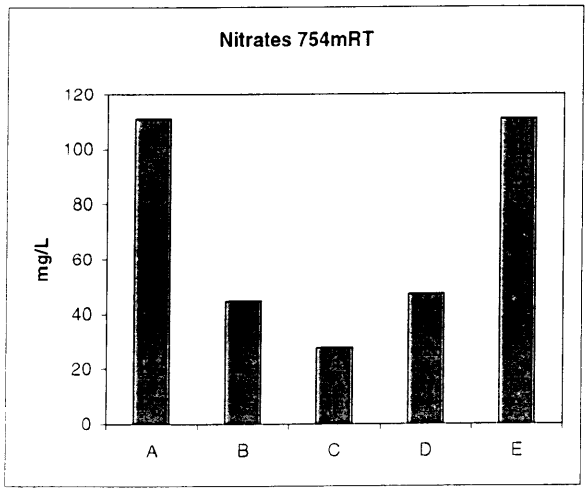

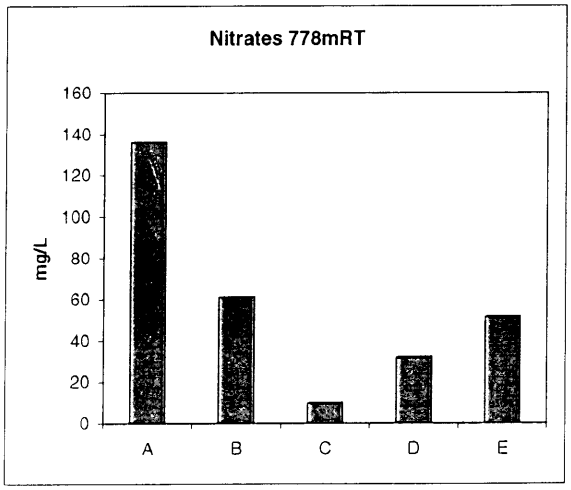

Nitrates Invasion Profile

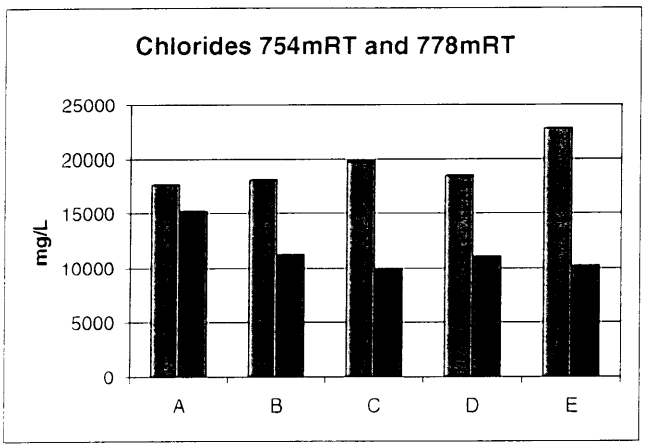

CORE
A = outer
C = centre
E = outer

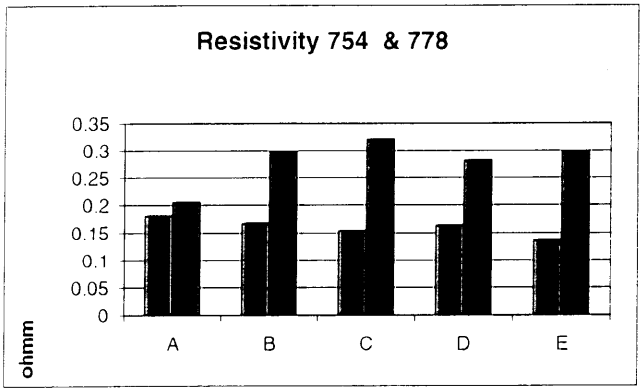

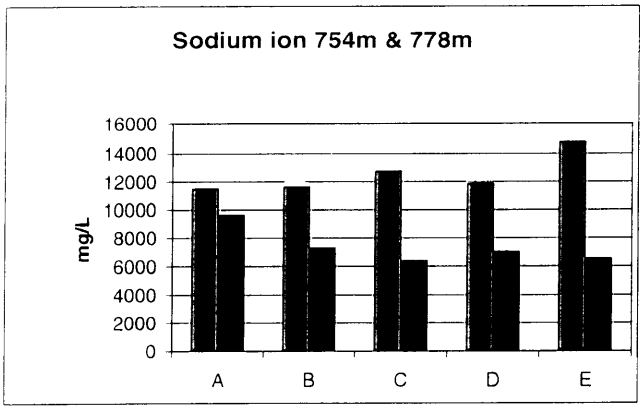

Figure 14

BALEEN 2
MDT PRESSURE SURVEY

908080 052

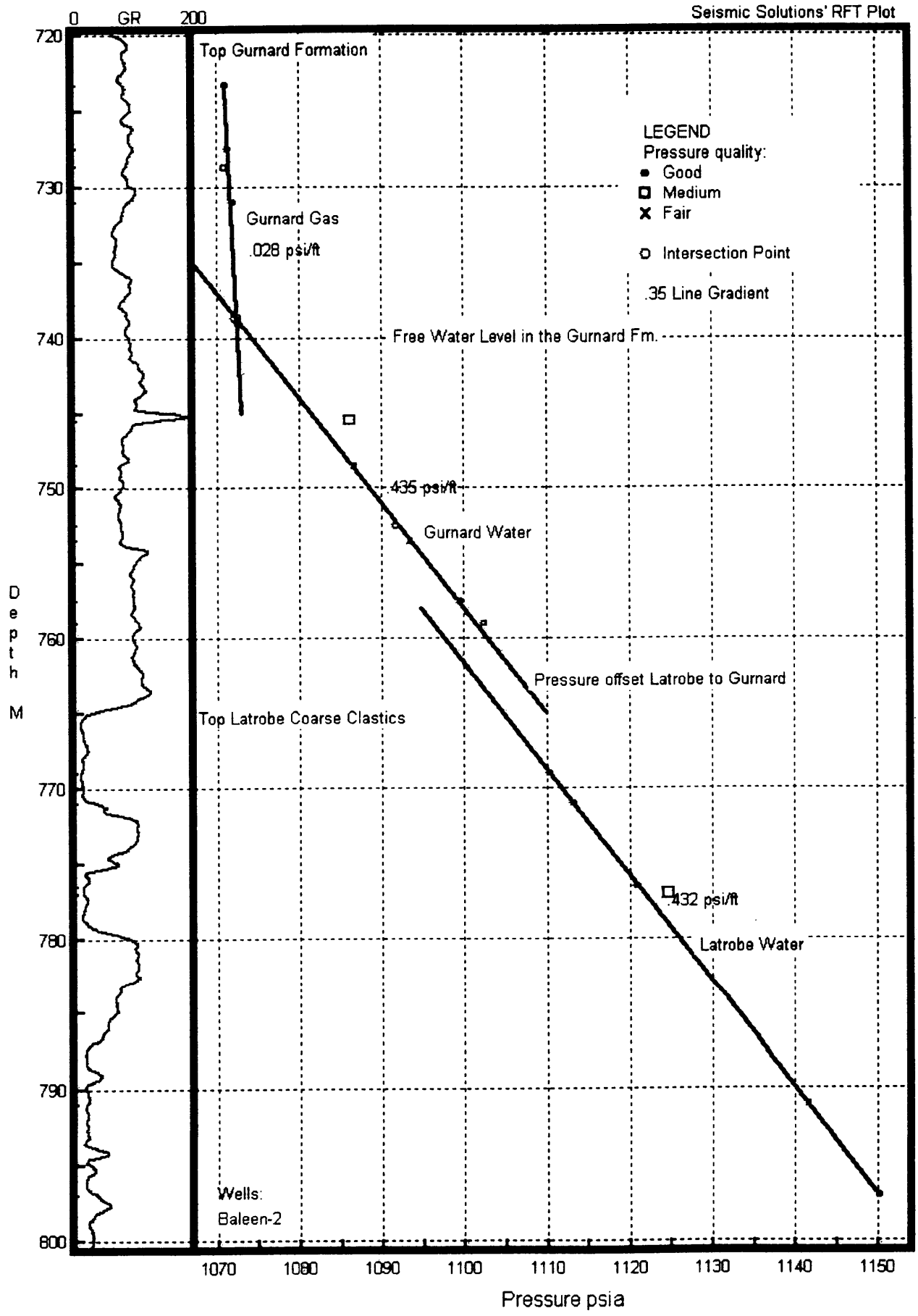

AUTHOR: OMV DATE: NOVEMBER 2000 FILENAME: GIPPSLAND\ VICRL5 \ A4S \ 234.CDR

FIGURE 15

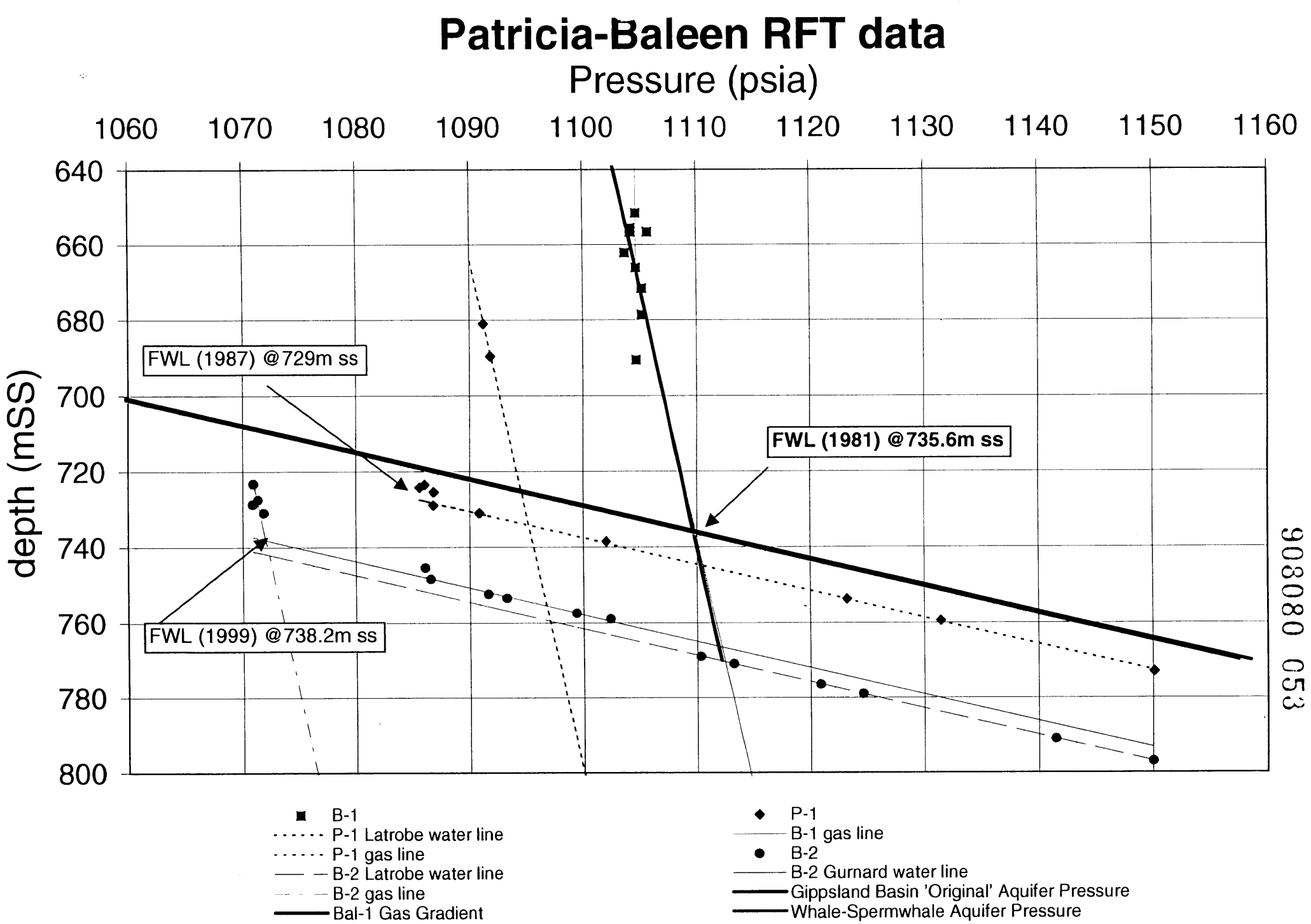
Patricia-Baleen RFT data
Pressure (psia)
1060
1070
1080
1090
1100
1110
1120
1130
1140
1150
1160
depth (mSS)
640
660
680
700
720
740
760
780
800
FWL (1987) @729m ss
FWL (1981) @735.6m ss
FWL (1999) @738.2m ss
9080080 053
B-1
P-1 Latrobe water line
P-1 gas line
B-2 Latrobe water line
B-2 gas line
Bal-1 Gas Gradient
P-1
B-1 gas line
B-2
B-2 Gurnard water line
Gippsland Basin 'Original' Aquifer Pressure
Whale-Spermwhale Aquifer Pressure

FIGURE 16

APPENDICES

APPENDIX 1

BALEEN-2

PALYNOLOGY FINAL REPORT

-BIOSTRATA-

Palynological analysis of core and cuttings samples from Baleen–2 well, Gippsland Basin.

by

Alan D. Partridge

Biostrata Pty Ltd
A.C.N. 053 800 945

Biostrata Report 2000/1

29 February 2000

Palynological analysis of core and cuttings samples from Baleen–2 well, Gippsland Basin.

by Alan D. Partridge

INTERPRETATIVE DATA

Summary

Six core and ten cuttings samples were analysed over a 235 metre interval from 660 to 895m in Baleen–2. The section is subdivided into Early Miocene to Late Oligocene Seaspray Group, a Middle Eocene part of the Latrobe Group (mainly Gurnard Formation), a Late Paleocene lower part of the Latrobe Group (bulk of coarse siliciclastics) and a short section near TD of Late Albian Strzelecki Group. Each of these each ages are separated by significant unconformities (Table 1).

Assemblages from the 45 metre thick Gurnard Formation represent only the upper part of the Lower *N. asperus* spore-pollen Zone and *D. heterophlycta* microplankton Zone, and are late Middle Eocene in age. In the underlying Latrobe coarse siliciclastics facies the uppermost sandstone from 791.5 to 798.5m is interpreted as no older than the Lower *N. asperus* Zone, while the two distinctive shale beds at 798.5 to 802m and 807 to 812.5m and underlying sandy section from 812.5 to ~873m are Late Paleocene in age.

Table 1: Palynological Summary of Baleen–2 well.

AGE	UNIT/FACIES	SPORE-POLLEN ZONES (MICROPLANKTON ZONES)	DEPTHS mKB
EARLY MIOCENE	GIPPSLAND LIMESTONE Seafloor to 724m	Middle to Upper *P. tuberculatus* (*Operculodinium* Superzone)	720m
LATE OLIGOCENE	LAKE ENTRANCE FORMATION 724 to 746m	Middle to Upper *P. tuberculatus* (*Operculodinium* Superzone)	Caved cuttings at 747m
late MIDDLE EOCENE	LATROBE GROUP Gurnard Formation 746 to 791m	Lower *N. asperus* (*D. heterophlycta*)	753 to 790m (753 to 772m)
MIDDLE EOCENE	LATROBE GROUP Undiff. coarse clastics 791 to 798.5m	No older than Lower *N. asperus*	795m
LATE PALEOCENE	LATROBE GROUP Undiff. coarse clastics 798.5m to 872.5m	Upper *L. balmei*	800 to 870m
LATE ALBIAN	STRZELECKI GROUP 872.5 to 895mTD	Upper *C. paradoxa*	880 to 895m

Introduction

An initial batch of twelve samples were received by the author on 3rd December 1999. However, as there was considered to be insufficient material from a number of the core samples from the Gurnard Formation (which typically gives low yields) additional material was requested. In addition, a cuttings sample at 780m, from within the Gurnard Formation, was rejected as unlikely to provide reliable age dating because it was composed almost entirely of 5–10mm long shards of light-grey marl interpreted to be caved from the Lakes Entrance Formation. Eight of these original samples were forwarded by courier to Laola Pty Ltd in Perth for palynological processing on the 6th December, with a replacement four core samples forwarded on the 8th December. The prepared palynological slides were returned on the 16th December and a Provisional Report issued on the 22nd December. The recovery of well preserved specimens of the index species *Lygistepollenites balmei* from the deepest cuttings and its absence from shallower samples at or above 795m, suggested the presence of a Paleocene section in the well, and therefore four additional cuttings samples were analysed from within the interval 795 to 895m. These samples were forwarded to Laola Pty Ltd on 14th February 2000, with the palynological slides returned on 22nd February and the Provisional Report issued on 23rd February.

Details of zone assignments, confidence ratings and key comments are given in Table 2, with basic sample data provided in Table 3, and visual residues yields, preservation and recorded species diversity provided in Table 4. Distribution of the spore-pollen and microplankton in the samples are arranged alphabetically in Tables 5 and 6, and the result of assemblage count provided in Table 7. Author citations for spore-pollen species are mostly sourced from Stover & Partridge (1973) and Dettmann (1963), and for the microplankton species from the index of Williams *et al.* (1998). Species names followed by "ms" are unpublished manuscript names.

Geological Comments

1. The sequence penetrated in Baleen–2 appears to be fairly typical of other offshore wells drilled on the Northern Strzelecki Terrace. It consists of a moderate thickness of Gippsland Limestone (643 metres), overlying a thin Lakes Entrance Formation (22 metres), which are both assigned to the Seaspray Group. These unconformably overlie a moderate thickness of

Gurnard Formation (45 metres), and a thin section of coarse siliciclastic facies assigned to the Latrobe Group (~82 metres). The latter, in turn, unconformably overlies about 20 metres of Early Cretaceous Strzelecki Group extending to T.D.

2. The palynological analysis indicates a time break of about 10 million years between the Seaspray and Latrobe Groups with the Late Eocene and Early Oligocene missing at the unconformity. In contrast, biostratigraphic data from the adjacent Baleen-1 well suggests an unconformity of much shorter duration. In the latter well a thin section of the Early Oligocene foram zone J-1 is recorded from the base of the Lakes Entrance Formation between 627 and 632m (Paltech, 1982), while the underlying Gurnard Formation is given a Late Eocene age (Harris, 1982). As neither of these ages were found in Baleen-2 an explanation of the different age sequences in the two wells is needed.

3. One possible explanation for the age discrepancy at the base of the Lakes Entrance Formation is that the older age is masked in Baleen-2 by downhole cavings, as no definitive Early Oligocene palynomorphs were recorded from the largely caved cuttings at 747m. An alternative explanation is that the older foraminifera recorded in Baleen-1 represent reworked Early Oligocene specimens, a common feature elsewhere in the basin (eg. Taylor, 1979). Although such reworking is acknowledged in Baleen-1 from the sample at 627m, it is impossible to evaluate whether the underlying sample at 632m may also be substantially reworked as only selected key species are recorded on the distribution chart in the Paltech report.

4. Explanation of the discrepancy in the age of the Gurnard Formation between Baleen-1 and 2 revolves around the interpretation of the recorded palynological assemblages. Overall, Baleen-2 is more thoroughly documented, with a total diversity of 103 spore-pollen species and average diversity of 55 species/sample, recorded from the seven samples analysed from the Gurnard Formation. This compares with a total diversity of just 60 species and average diversity of only 16 species/sample from over twice as many samples (15) analysed from the same unit in Baleen-1. Similarly, the microplankton have a total recorded diversity of 36 species and average

diversity of 15 species/sample in Baleen-2, compared to a total diversity of 21 species and average diversity of only 2 species/sample in Baleen-1. Notwithstanding these significant difference in diversity, the spore-pollen and microplankton assemblages are very similar with most species common between the two wells. Indeed, the only age significant palynomorphs recorded from Baleen-1 that are restricted to the Late Eocene are the dinoflagellates *Gippslandica* (al. *Vozzhennikovia*) *extensa* recorded at 658m and *Corrudinium incompositum* recorded at 693m. Of these, the former could easily be a misidentification of *Spinidinium macmurdoense* recorded in Baleen-2, while the latter is possibly a misidentification of the undescribed manuscript species *Corrudinium corrugatum*. In addition, negative evidence supporting an older age for the Gurnard Formation in Baleen-1 is the absence of key species considered diagnostic of the Middle and Upper *N. asperus* Zones, such as *Triorites magnificus* and *Proteacidites stipplatus*. Assuming that the two key dinoflagellate species in Baleen-1 are indeed misidentified my preferred interpretation is that the Gurnard Formation in both wells belongs to the upper part of the Middle *N. asperus* Zone and the equivalent *D. heterophlycta* Zone. To confirm this interpretation the palynological slides from Baleen-1 would need to be re-examined.

5. The relatively thin (~82 metres) section of coarse siliciclastic facies of the Latrobe Group penetrated in Baleen-2 is interpreted to be mostly Late Paleocene in age (Upper *L. balmei* Zone), overlain after a substantial time break by a thin sandstone bed (~7 metres) of probable Middle Eocene age (Lower *N. asperus* Zone). Although the cuttings sample at 795m within the latter bed gave only a meager yield (and therefore could be entirely caved), the absence of *L. balmei* Zone index species from this or shallow samples, in contrast to their consistent presence in all deeper cuttings between 800 and 895m, favours placement of a unconformity within the coarse siliciclastic facies. This interpretation is supported by the presence of a thin section of Middle Eocene age siliciclastics in Baleen-1 (Harris, 1982).

6. The presence of a Paleocene section in Baleen-2 was first hinted at by the recovery of well-preserved but rare specimens of the zone index species *Lygistepollenites balmei* in the deepest cuttings in the well. Subsequent analysis of four additional cuttings between 800 and 880m gave rich assemblages confirming the presence of the Upper *L. balmei* Zone. Those

recovered from the distinctive shaly intervals on the gamma log in Baleen–2 between 799–802m and 807–812m are particularly noteworthy for the negligible content of palynomorphs caved from higher in the well. The small amount of carbonaceous mudstone and coal picked from cuttings between 850 and 870m also gave a surprisingly good assemblage without obvious cavings from above the *L. balmei* Zone. The unusual dominance of *Phyllocladidites verrucosus* in this composite sample, in contrast to its rarity in the two higher cuttings, is strong evidence to suggest that the lithologies sampled are representative of the interval and are unlikely to have caved from higher in the well. The composite cuttings sample also contained a few rare Late Cretaceous species (eg. *Tricolporites lilliei*), that are interpreted as reworked. Equivalent Paleocene sections are recorded in Sperm Whale–1 and Sweep–1, but are absent in the other nearby wells Patricia–1, Flathead–1, Whale–1.

7. Penetration of the Strzelecki Group in the Baleen–2 well is confirmed by the recovery of good Late Albian *C. paradoxa* Zone assemblages from the two deepest cuttings analysed at 880 and 895m. From examination of the washed and dried cuttings the top of the Strzelecki Group is considered to lie between 870 and 880m, but it is not clear on the electric logs due to lack of reliable data below 870m.

Discussion of Assemblages

Middle to Upper *Proteacidites tuberculatus* spore-pollen Zone
and
***Operculodinium* microplankton Superzone**
Interval: 720 to 747 metres.
Age: Late Oligocene to Early Miocene

Both cuttings sample are dominated by microplankton (>40%) and contain only moderate diversity spore-pollen assemblages that are assigned to the Middle to Upper subdivisions of the *P. tuberculatus* Zone on the presence of the spore *Cyathidites subtilis*, which is not know to range below the Late Oligocene. An age no younger than the Early Miocene Upper *P. tuberculatus* Zone is suggested by the presence of the pollen *Proteacidites rectomarginis* in the shallower sample. The composition of the spore-pollen assemblages shows a dominance of the alete gymnosperm pollen *Araucariacites australis* and *Dilwynites granulatus*, as is typical

of most distal marine sections in the Gippsland Basin, and this is interpreted to be the manifestation of a Neves effect. The latter, is the tendency for certain more buoyant spores or pollen to have greater relative abundance in sediments deposited in more distal marine or lacustrine environments (Traverse, 1988).

The two cuttings samples are also assigned to the *Operculodinium* Superzone based on the common occurrence of the species *Operculodinium centrocarpum*, *Pyxidinopsis pontus* ms, *Protoellipsodinium simplex* ms and *Spiniferites* spp. The superzone is applicable to all microplankton assemblages from the Seaspray Group dominated by a mixture of chorate dinoflagellate cysts (eg. *Operculodinium centrocarpum* and *Spiniferites* spp.) and spherical, morphologically simple proximate dinoflagellate cysts (eg. *Pyxidinopsis pontus* ms). The superzone has a broad age range of Oligocene to Recent. Potential exists for subdivision of the superzone into a number of shorter range zones based on the many undescribed taxa in the assemblages, but as yet the necessary documentation studies have not been undertaken.

Middle *Nothofagidites asperus* spore-pollen Zone
Interval: 753 to 790 metres, probably extending to 795 metres.
Age: Middle Eocene
The six core sample and cuttings at 790m are confidently assigned to the broad *N. asperus* Zone of Stover & Partridge (1973) based on the dominance of *Nothofagidites* pollen (average 25%). An age no older than the Lower subzone is indicated by the consistent presence of the index species *Nothofagidites falcatus*, and sporadic occurrences of *Tricolpites simatus* and *Tricolporites leuros* as none of these species range below this subzone. An age no younger than the subzone is indicated by the fairly consistent presence of *Proteacidites pachypolus* (in 4 out of the 7 samples), the sporadic presence of *Proteacidites asperopolus* (at 758m and 790m) and rare occurrence of *Proteacidites reflexus* (only at 753m), as these species are not normally found above the Lower subzone. The only discordant species is the occurrence of a single specimen of *Anacolosidites sectus* at 753m, as this species is not normally found below the Late Eocene Middle *N. asperus* Zone.

The moderate diversity assemblage recorded from the cuttings a 795m, probably also belongs to the Lower *N. asperus* Zone, but the extremely low numbers of palynomorphs recovered from this sample does not allow confident zone or age assignment.

***Deflandrea heterophlycta* microplankton Zone**

Interval: 753 to 772 metres.

Age: Middle Eocene

The six core samples also contain marine microplankton assemblages, of low abundance (average 5% of combined SP and MP count) and moderate diversity (average 15+ species per sample), which can be assigned to the *D. heterophlycta* Zone on the inconsistent presence of the eponymous species (in three samples), and extremely rare occurrence of the acritarch *Paucilobimorpha* (al. *Tritonites*) *inaequalis* (Marshall & Partridge, 1988) comb. nov. in the shallowest sample. Associated species not known to range below this zone are *Corrudinium corrugatum* ms, *Rhombodinium glabrum*, *Phthanoperidinium comatum* and *Samlandia reticulifera*. Species showing anomalously young occurrences are *Diphyes colligerum* at 772m, which is not normally recorded above the Early Eocene, and *Enneadocysta partridgei* recorded from 4 of the 6 core sample. This last species is diagnostic of the *E. partridgei* Zone, and has previously been recorded in palynological reports and on stratigraphic tables from the Gippsland Basin as the informal *Areosphaeridium australicum* Zone. The name change is necessary as *Areosphaeridium australicum* is a manuscript species name that has been recently been described as a new genus and species by Stover & Evitt (1995).

The low diversity microplankton assemblages recorded from the core sample at 772m and the two cuttings at 790 to 795m, lack key species and therefore cannot be assigned to a microplankton zone.

Upper *Lygistepollenites balmei* spore-pollen Zone

Interval: 800 to 870 metres

Age: Late Paleocene.

Well preserved specimens of the eponymous species were initially recorded as caved specimens in the deepest cuttings sample examined in the well. Their identification prompted speculation that a section of Paleocene age strata could occur in Baleen-2, and the analysis of additional cuttings samples confirmed the presence of approximately 70 metres of Upper *L. balmei* Zone, representing most of the Latrobe Group coarse clastics. The two shallower cuttings assemblages are dominated by *Podocarpidites* (average 40%), with common *Phyllocladidites mawsonii* (average 15%) with minor but significant *Nothofagidites endurus* (average <3%). The deeper picked cuttings over the composite interval in contrast is overwhelmingly dominated by *Phyllocladidites verrucosus* (21%) and *P. mawsonii*

(27%), with a significant secondary abundance of the spore *Gleicheniidites circinidites* (24%). The commonest diagnostic species is the eponymous *Lygistepollenites balmei* with an abundance range of 4 to 11%. Other species that range no younger than the *L. balmei* Zone are *Gambierina rudata* and *Australopollis obscurus*, while the presence of the pollen *Proteacidites annularis* in the deeper cuttings is indicative of an age no older than the Upper subzone. The single palynological slide recovered from the picked cuttings at 850–870m also contained individual specimens of *Tricolporites lilliei*, *Camarozonosporites horrendus* ms, and possibly *Tetradopollis securus* ms, which are diagnostic of the latest Cretaceous *Forcipites* (al. *Tricolpites*) *longus* Zone. These specimens are considered to be reworked but they hint at the possibility of some Late Cretaceous sediments in the vicinity of the Baleen–2 location. The Paleocene *L. balmei* Zone section is interpreted to be non-marine.

Upper *Coptospora paradoxa* spore-pollen Zone
Interval: 880 to 895 metres
Age: Late Albian

The two cuttings sample from the bottom of the hole contained high diversity Albian spore-pollen assemblage assigned to the Upper *C. paradoxa* Zone (as recognised by Morgan *et al.*, 1995) based on the rare presence of *Pilosisporites grandis* in the shallower sample and the eponymous species in the deeper sample. Other species considered diagnostic of the zone are *Arcellites reticulatus* and *Perotrilites majus* based on ranges recorded by Dettmann (1963) and Dettmann & Playford (1969). The assemblages are dominated by smooth spores assigned to *Cyathidites* (23 to 37%) and bisaccate pollen broadly referred to *Podocarpidites* (19 to 47%). Rare freshwater algal cyst in the sample are not age diagnostic, but are indicative of probably ephemeral lacustrine environments within the Albian succession. As is typical of many Strzelecki Group samples the assemblage also contains rare reworked Permian and Triassic palynomorphs.

References

DETTMANN, M.E., 1963. Upper Mesozoic microfloras from southeastern Australia. *Proceedings Royal Society of Victoria, vol.77*, pt.1, p.1–148, pls 1–27.

DETTMANN, M.E. & PLAYFORD, G., 1968. Taxonomy of some Cretaceous spores and pollen grains from eastern Australia. *Proceedings of the Royal Society of Victoria, vol.81*, pt.1, p.69–93, pls 6–8.

HARRIS, W.K., 1982. Baleen No.1 well. Palynological examination and kerogen typing of sidewall cores. Unpublished report for Hudbay Oil (Australia) Ltd, 9p.

MARSHALL, N.G. & PARTRIDGE, A.D., 1988. The Eocene acritarch *Tritonites* gen. nov. and the age of the Marlin Channel, Gippsland Basin, southeastern Australia. *Association of Australasian Palaeontologists Memoir 5*, p.239–257.

MORGAN, R., ALLEY, N.F., ROWETT, A.I. & WHITE, M.R., 1995. Biostratigraphy. **In** *The Petroleum Geology of South Australia. Volume 1: Otway Basin*, J.G.G. Morton & J.F. Drexel, editors, *Mines and Energy South Australia, Report Book 95/12*, p.95–101.

PALTECH, 1982. Foraminiferal sequence in Baleen #1. *Paltech Report 1982/01*, 5p.

STOVER, L.E. & PARTRIDGE, A.D., 1973. Tertiary and late Cretaceous spores and pollen from the Gippsland Basin, southeastern Australia. *Proceedings Royal Society of Victoria 85*, p.237–286.

STOVER, L.E. & WILLIAMS, G.L., 1995. A revision of the Palaeogene dinoflagellate genera *Areosphaeridium* Eaton and *Eatonicysta* Stover & Evitt 1978. *Micropaleontology, vol.41*, no.2, p.97–141, pls 1–7.

TAYLOR, D., 1979a. The Foraminiferal sequence in Seahorse–1, Gippsland Basin. *Esso Australia Ltd Palaeontology Report 1979/2*, 20p. 4 charts (unpubl.).

TRAVERSE, A., 1988. *Paleopalynology*. Unwin Hyman Ltd, Boston. p.1–600.

WILLIAMS, G.L., LENTIN, J.K. & FENSOME, R.A., 1998. The Lentin and Williams index of fossil dinoflagellates 1998 edition. *American Association of Stratigraphic Palynologists, Contributions Series, no. 34*, p.1–817.

***Confidence Ratings used in STRATDAT database and applied to Table 2.**

Alpha codes: Linked to sample		**Numeric codes:** Linked to fossil assemblage		
A	Core	**1**	**Excellent confidence:**	High diversity assemblage recorded with key zone species.
B	Sidewall core	**2**	**Good confidence:**	Moderately diverse assemblage recorded with key zone species.
C	Coal cuttings	**3**	**Fair confidence:**	Low diversity assemblage recorded with key zone species.
D	Ditch cuttings	**4**	**Poor confidence:**	Moderate to high diversity assemblage recorded without key zone species.
E	Junk basket	**5**	**Very low confidence:**	Low diversity assemblage recorded without key zone species.

Table 2: Interpretative data from Baleen-2 well.

Sample	Depth Metres	Spore-Pollen Zone (Microplankton Zone)	CR*	Comments and Key Species Present
Cuttings	660	Indeterminate		Very low yielding sample.
Cuttings	720	Upper? *P. tuberculatus* (*Operculodinium* Superzone)	D4 D3	MP 42%. LAD of pollen *Proteacidites rectomarginis*, with *Pyxidinopsis pontus* ms most abundant microplankton.
Cuttings	747	*Middle P. tuberculatus* (*Operculodinium* Superzone)	D4 D2	MP 87%. FAD of spore *Cyathidites subtilis*, with *Spiniferites* and *Operculodinium* species most abundant microplankton.
Core-1	753	Lower *N. asperus* (*D. heterophlycta*)	A1 A2	MP 4% containing *Deflandrea heterophlycta*, *Paucilobimorpha inaequalis* and LAD of *Enneadocysta partridgei*. SP dominated by *Nothofagidites* at 36%.
Core-1	754	Lower *N. asperus* (*D. heterophlycta*)	A1 A4	MP 9% containing *Rhombodinium glabrum*. SP dominated by *Nothofagidites* at 36%
Core-1	758	Lower *N. asperus* (*D. heterophlycta*)	A1 A4	MP 3% not very diagnostic. SP dominated by *Phyllocladidites mawsonii* 31%, and containing LAD of *Proteacidites asperopolus*.
Core-1	764	Lower *N. asperus* (*D. heterophlycta*)	A1 A2	MP 7% containing *Deflandrea heterophlycta* and *R. glabrum*. SP dominated by *P. mawsonii* 24% and *Nothofagidites* 18%.
Core-2	768	Lower *N. asperus*	A1	MP <2% not diagnostic with *Haloragacidites harrisii* 21% and *Nothofagidites* 14% the dominant pollen.
Core-2	772	Lower *N. asperus* (*D. heterophlycta*)	A1 A4	MP 7% containing *Deflandrea heterophlycta* and *Enneadocysta partridgei*. SP dominated by *Haloragacidites harrisii* 21% and *Nothofagidites* 20%.
Cuttings	790	Lower *N. asperus*	A1	MP 40% but <2% of MP are in situ. SP dominated by *Nothofagidites* 23% and containing pollen *Proteacidites asperopolus*.
Cuttings	795	No older than Lower *N. asperus*		Very low yielding assemblage dominated by caved palynomorphs.
Cuttings	800	Upper *L. balmei*	D1	Assemblage dominated by *Podocarpidites* 45% with frequent *Lygistepollenites balmei* 4%.
Cuttings	810	Upper *L. balmei*	D1	Assemblage dominated by *Podocarpidites* 37% and *Phyllocladidites mawsonii* 17%, with *L. balmei* again 4%.
Composite picked cuttings	850-870	Upper *L. balmei*	D1	Very low yield assemblage dominated by *P. mawsonii/P. verrucosus* 48%, and *Gleicheniidites/Clavifera* 27%, with *L. balmei* 10%.
Cuttings	880	Upper *C. paradoxa*	D2	LAD of *Pilosisporites grandis* confirms upper subzone. Assemblage dominated by *Podocarpidites* 47% and *Cyathidites* 23%.
Cuttings	895	Upper *C. paradox*	D1	LAD *Coptospora paradoxa* in assemblage dominated by spores 73%.

MP %= microplankton expressed as % of combined SP & MP count.
Nothofagidites % = abundance expressed as % of SP count only.
FAD & LAD = Last & First Appearance Datums.

BASIC DATA

Table 3: Basic sample data from Baleen-2 well.

Sample Type	Depth metres	Lithology	Weight (grams)
Cuttings	660	Very light grey calcarenite	19.0
Cuttings	720	Light grey calcarenite	16.1
Cuttings	747	Light grey marl	23.9
Core-1	753	Medium brown-grey muddy glauconitic sandstone	32.6
Core-1	754	Medium brown-grey muddy glauconitic sandstone	33.3
Core-1	758	Medium brown-grey muddy micaceous and glauconitic? sandstone	31.5
Core-1	764	Hard light grey glauconitic sandstone	29.5
Core-2	768	Medium grey muddy glauconitic sandstone	18.4
Core-2	772	Medium grey muddy glauconitic sandstone	25.7
Cuttings	790	Medium grey quartz sandstone	29.9
Cuttings	795	Light grey quartz sandstone	37.5
Cuttings	800	Medium grey argillaceous quartz sandstone with ~1% coal or carbonaceous shale	28.9
Cuttings	810	Medium brown-grey argillaceous quartz sandstone with <1% coal or carbonaceous shale	27.9
Composite picked cuttings	850-870	Medium to dark grey carbonaceous mudstone and coaly fragments picked from cuttings	0.9
Cuttings	880	Medium grey clumped mudstone? with continued presence of significant coarse quartz sandstone	26.6
Cuttings	895	Clumps of light grey mudstones and sandstone	19.3
		Average:	**25.1**

Table 4: Basic assemblage data from Baleen-2 well.

Sample Type	Depth metres	Visual Yield	Palynomorph Concentration	Preservation	No. SP Species	No. MP Species
Cuttings	660	Very Low	Very Low	Poor	1+	1+
Cuttings	720	Very Low	Low	Fair	21+	6+
Cuttings	747	Low	Moderate	Good	23+	18+
Core-1	753	Moderate	High	Good	70+	21+
Core-1	754	Low	High	Fair-Good	55+	17+
Core-1	758	High	High	Good	62+	16+
Core-1	764	Low	Moderate	Good	52+	20+
Core-2	768	High	Low	Fair	45+	3+
Core-2	772	High	Low-Moderate	Fair-Good	46+	16+
Cuttings	790	Low	Moderate	Fair	38+	4+
Cuttings	795	Very Low	Low	Poor	15+	
Cuttings	800	High	High	Poor	30+	2+
Cuttings	810	Low	Moderate	Poor-fair	26+	
Composite picked cuttings	850-870	Very Low	Low	Good	25+	
Cuttings	880	High	High	Poor-good	22+	1
Cuttings	895	High	High	Good	44+	2+
				Averages:	**35+**	**9+**

Table–5: Tertiary Species Distribution in Baleen–2, Gippsland Basin.															
Sample/Depths (m)	Cts 660	Cts 720	Cts 747	C-1 753	C-1 754	C-1 758	C-1 764	C-2 768	C-2 772	Cts 790	Cts 795	Cts 800	Cts 810	Cts 850-870	Cts 895
SPORE-POLLEN SPECIES															
Anacolosidites sectus					X										
Araucariacites australis		X	X	X	X		X	X	X	X	X	X			
Australopollis obscurus													X		
Baculatisporites spp.	X			X	X	X	X	X	X	X					
Beaupreaidites elegansiformis					X	X									
Beaupreaidites verrucosus						X									
Camarozonosporites heskermensis				X	X	X							X	X	
Camarozonosporites horrendus ms														W	
Clavifera triplex				X	X								X	X	
Cranwellia striatus				cf											
Cupanicidites orthoteichus							X	X	X						
Cupressacites sp.				X											
Cyatheacidites annulatus		X								CV		CV			
Cyathidites australis		W	W						W		W				
Cyathidites paleospora		X		X	X	X	X	X	X	X	X	X		X	
Cyathidites splendens							X	X	X			X			
Cayathidites subtilis		X	X												
Dacrycarpites australiensis			X	X											
Dicotetradites clavatus				X	X	X	X		X	X		X			
Dictyophyllidites spp.						X	X		X	X					
Dilwynites granulatus		X	X	X	X	X	X		X	X	X	X	X		
Dilwynites tuberculatus			X	X		X	X		X	X					
Diporites delicatus ms													X		
Dryptopollenites semilunatus						X									
Ericipites crassiexinus			X	X		X									
Ericipites scabratus				X	X		X	X				X			
Foveotriletes balteus				X		X									
Gambierina rudata													X	X	
Gleichenlidites circinidites			X	X	X	X	X	X	X	X		X	X	X	
Haloragacidites harrisii		X	X	X	X	X	X	X		X	X	X	X	X	CV
Haloragacidites trioratus				X	X	X	X								
Herkosporites elliottii				X	X	X						X	X		
Ilexpollenites spp.				X		X		X	X	X					
Ischyosporites gremius		X	X	X					X		X				
Ischyosporites irregularis ms				X		X	X	X	X			X	X		
Laevigatosporites major		X	X		X	X	X	X	X			X			
Laevigatosporites ovatus		X	X	X	X		X		X	X	X	X	X	X	
Latrobosporites crassus													X	X	
Latrobosporites marginatus				X		X			X						
Liliacidites spp.				X	X										
Lygistepollenites balmei						W						X	X	X	CV
Lygistepollenites florinii		X	X	X	X	X	X	X	X	X	X	X	X	X	
Malvacipollis robustus ms				X	X	X	X	X							
Malvacipollis subtilis				X	X	X	X	X	X	X		X			
Matonisporites ornamentalis			X	X			X								
Microcachryidites antacticus				X	X	X	X			X		X		X	
Microalatidites paleogenicus				X								X	X		
Milfordia homeopunctatus					X										
Monosulcites gemmatus					cf										
Myrtaceidites parvus/mesonesus						X	X			X					
Nothofagidites asperus		X		X	X	X	X	X		X					
Nothofagidites brachyspinulosus				X	X	X		X	X						
Nothofagidites deminutus				X	X	X	X	X	X						
Nothofagidites emarcidus/heturus			X	X	X	X	X	X	X	X	X	X	X		CV
Nothofagidites endurus												X	X		
Nothofagidites falcatus			X	X	X	X	X	X	X	X					
Nothofagidites flemingii				X	X	X	X	X	X	X	X				
Nothofagidites goniatus				X	X	X	X	X	X	X					
Nothofagidites longispinosus					X										
Nothofagidites vansteenisii				X	X	X				X					
Paripollis ochesis														X	
Parvisaccites catastus		X		X	X	X									
Peninsulapollis gillii														X	
Periporopollenites demarcatus				X	X	X	X		X	X					
Periporopollenites polyoratus						X				X		X			
Periporopollenites vesicus								X							
Peromonolites densus												X			
Peromonolites vellosus				X	X			X		X					

Table-5: Tertiary Species Distribution in Baleen-2, Gippsland Basin.

Sample/Depths (m)	Cts 660	Cts 720	Cts 747	C-1 753	C-1 754	C-1 758	C-1 764	C-2 768	C-2 772	Cts 790	Cts 795	Cts 800	Cts 810	Cts 850-870	Cts 895
Perotrilites n.sp.							X								
Phyllocladidites mawsonii		X	X	X	X	X	X	X	X	X	X	X	X	X	
Phyllocladidites verrucosus													X	X	
Podocarpidites spp.		X	X	X	X	X	X	X	X	X	X	X	X	X	
Polypodiidites perverrucatus				X	X		X	X	X						
Proteacidites adenanthoides				X	X		X	X	X					X	
Proteacidites alveolatus				cf		cf									
Proteacidites annularis				X	X	X	X							X	
Proteacidites asperopolus						X				X					
Proteacidites callosus					X					X					
Proteacidites carobelindiae				X											
Proteacidites crassus						X	X		X						
Proteacidites grandis		W	W												
Proteacidites kopiensis								X	X						
Proteacidites latrobensis				X	X		X								
Proteacidites nasus						X									
Proteacidites obscurus				X	X	X	X	X	X						
Proteacidites pachypolus				X		X		X	X						
Proteacidites prodigus												X			
Proteacidites pseudomoides				X	X	X			X						
Proteacidites recavus								X	X						
Proteacidites rectomarginis		X													
Proteacidites reflexus				X											
Proteacidites reticuloscabratus				X		X	X	X							
Proteacidites tenuiexinus						X	X		X			X			
Proteacidites truncatus		X													
Proteacidites tuberculatus											CV				
Proteacidites tuberculiformis									X						
Proteacidites uncinatus ms								X							
Proteacidites spp.				X	X	X	X	X	X	X	X	X	X	X	CV
Pseudowinterapollis couperi					X										
Pseudowinterapollis cranwellae													X		
Reticuloidosporites escharus ms				X	X				X						
Retitriletes spp.			X	X	X	X	X	X							
Rhoipites alveolatus				X				X							
Ricciaesporites boxatus ms				X											
Rugulatisporites mallatus			X	X	X				X						
Santalumidites cainozoicus						X	X	X	X	X					
Sapotaceoidaepollenites rotundus						X									
Schizocolpus marlinensis								X							
Sparganiaceaepollenites barungensis				X											
Stereisporites antiquisporites		X		X	X	X		X	X	X				X	
Tetracolporites multistrixus ms														X	
Tetracolporites textus ms													X	X	
Tetradopollis securus ms														W	
Trichotomosulcites subgranulatus				X			X			X		X	X	X	
Tricolpites phillipsii				X		X		X		X		X	X		
Tricolpites simatus						X	X			X					
Tricolporites spp.			X	X	X	X	X	X	X	X	X	X	X		
Tricolporites adelaidensis		X	X	X	X	X		X							
Tricolporites leuros				X			X	X	X						
Tricolporites lilliei														W	
Tricolporites paenestriatus							X			X					
Tricolporites scabratus					X					X					
Tricolporites sphaerica							X					X			
Triletes tuberculiformis												X			
Triporopollenites ambiguus						X	X								
Tripunctisporis maastrichtiensis				X	X	X	X	X		X				X	
Verrucatosporites attinatus ms				cf		cf									
Verrucosisporites kopukuensis		X		X	X	X	X	X	X		X				
MICROPLANKTON SPECIES															
Achomosphaera spp.			X			X				X					
Apteodinium australiense										X		X			
Batiacasphaera amplectus ms				X		X	X								
Batiacasphaera denticulia ms				X					X						
Cooksonidium capricornum				cf											
Cordosphaeridium inodes						X									
Corrudinium corrugatum ms				X			X		X						
Cyclopsiella vieta			X												

Table–5: Tertiary Species Distribution in Baleen–2, Gippsland Basin.

Sample/Depths (m)	Cts 660	Cts 720	Cts 747	C-1 753	C-1 754	C-1 758	C-1 764	C-2 768	C-2 772	Cts 790	Cts 795	Cts 800	Cts 810	Cts 850-870	Cts 895
Dapsilidinium pseudocolligerum			X												CV
Deflandrea antarctica				X											
Deflandrea heterophlycta				X			X		X						
Deflandrea phosphoritica					cf		cf								
Deflandrea sp. indent.				X			X								
Diphyes colligerum									X			cf			
Enneadocysta arcuata					cf		cf		cf						
Enneadocysta partridgei				X	X	X			X						
Heteraulacacysta paxilla					X				X						
Hystiocysta variata ms				X			X		X						
Hystrichokolpoma rigaudae			X							CV					
Hystrichosphaeridium tubiferum							X								
Impagidinium spp.	X	X		X						X					
Impagidinium dispertitum					X		X		X						
Impagidinium maculatum			cf												
Impagidinium victorianum				X		X						CV			
Lingulodinium machaerophorum			X						X	CV					
Lingulodinium solarum			X			X				CV					
Micrhystridium sp.												X			
Nematosphaeropsis rhizoma ms			X												
Operculodinium centrocarpum		X	X	X	X	X	X	X	X	CV					CV
Operculodinium tabulatum ms			X												
Paralecaniella indentata				X	X	X	X	X	X						
Paucilobimorpha inaequalis				X											
Pentadinium laticinctum			X												
Phthanoperidinium comatum				X	X	X	X			X					
Phthanoperidinium eocenicum					X	X	X								
Protoellipsodinium simplex ms.		X	X							CV	CV	CV			
Pyxidinopsis pontus ms		X	X							CV	CV				
Rhombodinium glabrum					X		X								
Rottnestia borussica			X												
Samlandia reticulifera							X								
Spinidinium macmurdoense				X	X					cf					
Spiniferites ramosus		X	X	X	X	X	X	X	X	CV					CV
Stoveracysta sp.			cf												
Surculosphaeridium oceanica				cf	cf	cf	cf		cf						
Systematophora placacantha			X												
Tectatodinium marlum ms					X	X				X					
Tectatodinium scabroellipticus ms		cf													
Thalassiphora pelagica						X	X		X						
Valensiella clathroderma				cf	cf										
Vozzhennikova apertura				X	X	X	X								
Indeterminate Micro-dinoflagellates		X	X	X	X	X	X		X	CV					
OTHER PALYNOMORPHS															
Botryococcus braunii				X				X							X
Fungal fruiting bodies				X	X	X		X							
Fungal spores & hyphae			X	X	X	X	X	X	X	X		X			
Microforaminiferal liners		X	X	X			X	X	X	X	CV	X	X		CV
Scolecodonts		X	X												
ABBREVIATIONS															
X = Present															
W = Reworked															
CV = Caved															
cf = Compared with															

Table 6: Early Cretaceous Species Distribution in Baleen-2.		
Species List	**Cuttings**	**Cuttings**
Spore-Pollen	**880m**	**895m**
Aequitriradites spinulosus		0.5%
Aequitriradites verrucosus		X
Alisporites grandis	X	X
Antulisporites varigranulatus	X	
Aratrisporites sp.		Reworked
Araucariacites australis		0.5%
Arcellites reticulatus		Fragments
Baculatisporites spp.	2%	10%
Balmeisporites holodictyus		X
Ceratosporites equalis		X
Cicatricosisporites australiensis	X	X
Cicatricosisporites spp.	4%	8%
Clavatipollenites hughesii		X
Coptospora paradoxa		X
Corollina torosa		<1%
Couperisporites tabulata		**X**
Crybelosporites striatus	2%	3%
Cupresaccites sp.	X	
Cyathidites australis	2%	2%
Cyathidites minor	21%	35%
Cyathidites punctatus		X
Dictyophyllidites pectinaeformis		X
Dictyophyllidites spp.	1%	2%
Dictyotosporites speciosus		X
Falcisporites australis		Reworked
Foraminisporis asymmetricus		X
Foraminisporis wonthaggiensis		cf
Foveosporites cannalis	X	X
Gleicheniidites circinidites		<1%
Matonisporites cooksoniae	X	X
Microcachryidites antarcticus	3%	5%
Neoraistrickia truncata		X
Nevesisporites dailyi		X
Osmundacidites wellmanii	10%	6%
Perotrilites linearis		X
Perotrilites majus		X
Pilosisporites grandis	X	
Plicatipollenites spp.		Reworked
Podocarpidites spp.	47%	19%
Polycingulatisporites clavus		X
Retitriletes austroclavatidites	X	X
Retitriletes douglasii		X
Retitriletes eminulus		X
Retitriletes nodosus	X	X
Retitriletes spp.	X	1.5%
Stereisporites antiquisporites	7%	3%
Trichotomosulcites subgranulatus	1%	X
Trilobosporites tribotrys		X
Trilobosporites trioreticulosus		X
Triporoletes reticulatus	X	
Microplankton		
Schizosporis reticulatus		X
Sigmopollis carbonis		X
Other Palynomorphs		
Botryococcus braunii		X
Fungal hyphae		Rare

Table–7: Palynomorph Count Data from Baleen-2, Gippsland Basin.												
Sample Type	**Cts**	**Cts**	**C-1**	**C-1**	**C-1**	**C-1**	**C-2**	**C-2**	**Cts**	**Cts**	**Cts**	**Cts**
Depth (m)	**720**	**747**	**753**	**754**	**758**	**764**	**768**	**772**	**790**	**800**	**810**	**850-870**
SPORE-POLLEN SPECIES												
TRILETE SPORES undiff.	5.3%	13.3%		4.7%	1.6%	4.2%	0.9%	2.8%			2.0%	0.7%
Baculatisporites spp.			2.4%	2.4%	0.8%	1.7%			0.9%			
Clavifera triplex												2.6%
Cyatheacidites annulatus	1.3%											
Cyathidites spp. large >40µm	2.7%		0.8%									
Cyathidites spp. small <40µm	14.7%	20.0%	2.4%	3.1%	4.1%	4.2%	10.9%	6.5%	5.3%	3.8%	3.0%	2.0%
Dictyophyllidites spp.									0.9%			
Gleichenidites/Clavifera spp.		6.7%	2.4%		0.8%	0.8%	0.9%			2.9%	14.0%	24.2%
Stereisporites spp.	1.3%			1.6%	1.6%	0.8%	1.8%		1.8%			
Verrucosisporites kopukuensis							0.9%					
MONOLETES SPORES undiff:											1.0%	
Laevigatosporites spp.	6.7%	6.7%	0.8%	2.4%		0.8%	10.0%	5.6%	0.9%	5.8%		
Peromonolites spp.	1.3%						0.9%		0.9%			
TOTAL SPORES:	**33%**	**47%**	**9%**	**14%**	**9%**	**13%**	**26%**	**15%**	**11%**	**13%**	**20%**	**29%**
GYMNOSPERMS												
Araucariacites australis	28.0%	13.3%	0.8%			0.8%	0.9%	0.9%	3.5%			0.7%
Dilwynites spp.	6.7%	26.7%	2.4%	2.4%	3.3%	6.7%	2.7%	4.7%	3.5%	1.0%	1.0%	
Lygistepollenites balmei										3.8%	4.0%	10.5%
Lygistepollenites florinii	5.3%		4.8%	0.8%	1.6%	4.2%	5.5%	2.8%	3.5%	7.7%		0.7%
Microalatidites spp.										1.0%	1.0%	
Microcachyridites antarticus			0.8%	1.6%	0.8%	0.8%			0.9%	2.9%	4.0%	2.0%
Phyllocladidites mawsonii	1.3%		16.7%	11.8%	31.1%	23.5%	3.6%	5.6%	11.4%	13.5%	17.0%	27.5%
Phyllocladidites verrucosus											1.0%	20.9%
Podocarpidites spp.	16.0%		6.3%	11.0%	5.7%	7.6%	6.4%	9.3%	13.2%	43.3%	37.0%	3.9%
Trichotomosulcites subgranulatus								1.9%	3.5%		3.0%	
TOTAL GYMNOSPERM POLLEN:	**57%**	**40%**	**32%**	**28%**	**43%**	**44%**	**19%**	**25%**	**39%**	**73%**	**68%**	**66%**
ANGIOSPERM POLLEN			0.8%	1.6%			0.9%	1.9%	0.9%			2.6%
Australopollis obscurus											1.0%	
Casuarinaceae (H. harrisii)	1.3%	13.3%	11.1%	8.7%	13.1%	13.4%	20.9%	21.5%	14.9%	1.9%		
Cupanieidites orthoteichus							0.9%					
Dicotetradites clavatus			0.8%	1.6%	0.8%	1.7%	0.9%	0.9%	0.9%			
Gambierina rudata											1.0%	
Illexpollenites spp.			0.8%	0.8%	0.8%		0.9%	0.9%	0.9%			
Liliacidites spp.				0.8%								
Malvacipollis spp.			4.0%	3.1%	3.3%	1.7%			2.6%			
Myrtaceidites spp.					1.6%				0.9%			
Nothofagidites asperus/goniatus	1.3%		0.8%	0.8%	0.8%	0.8%	1.8%		3.5%	4.8%	1.0%	
N. brachyspinulosus/flemingii			4.0%	5.5%	2.5%	2.5%	1.8%	5.6%	1.8%			
N. emarcidus/heterus/falcatus			29.4%	26.0%	18.9%	14.3%	10.0%	13.1%	17.5%	2.9%	5.0%	
N. deminutus/vansteenisii			1.6%	3.9%	0.8%	0.8%		0.9%				
Periporopollenites spp.			0.8%	0.8%	0.8%	0.8%		1.9%	0.9%			
Proteacidites pachypolus							0.9%					
Proteacidites spp.	5.3%		4.0%	1.6%	2.5%	2.5%	8.2%	8.4%	2.6%	2.9%	3.0%	1.3%
Santalumidites cainozoicus					0.8%		1.8%	0.9%	0.9%			
Tricolp(or)ates spp.	1.3%		1.6%	3.1%	1.6%	5.0%	5.5%	3.7%	1.8%	1.9%	1.0%	0.7%
TOTAL ANGIOSPERM POLLEN:	**9%**	**13%**	**60%**	**58%**	**48%**	**44%**	**55%**	**60%**	**50%**	**14%**	**12%**	**5%**
TOTAL SPORE-POLLEN COUNT:	**75**	**15**	**126**	**127**	**122**	**119**	**110**	**107**	**114**	**104**	**100**	**153**
MAJOR CATEGORIES%												
Spores %	33%	47%	9%	14%	9%	13%	26%	15%	11%	13%	20%	29%
Gymnosperm Pollen %	57%	40%	32%	28%	43%	44%	19%	25%	39%	73%	68%	66%
Angiosperm Pollen %	9%	13%	60%	58%	48%	44%	55%	60%	50%	14%	12%	5%
MICROPLANKTON												
Dinoflagellates undiff:	42%	10%	20%	77%	50%	11%		75%	22%			
Deflandrea spp.			20%			22%						
Enneadocysta partridgei			20%									
Lingulodinium macharophorum									1%			
Operculodinium centrocarpum	4%	24%				11%			14%			
Paralecaniella indentata			40%	8%	25%	22%	50%	13%				
Phthanoperidinium comatum					25%							
Protoellipsodinium simplex ms		10%							16%			
Pyxidinopsis pontus ms.	36%	3%										
Microdino sphere	18%	11%							14%			
Spinidinium spp.				8%				13%	3%			
Spiniferites spp.		41%		8%		33%	50%		30%			
TOTAL MICROPLANKTON COUNT:	**55**	**97**	**5**	**13**	**4**	**9**	**2**	**8**	**77**			
Microplankton as % of SP + MP	**42%**	**87%**	**4%**	**9%**	**3%**	**7%**	**2%**	**7%**	**40%**			
OTHER PALYNOMORPHS as % of count												
Botryococcus braunii							0.8%					
Fungal spores and hyphae		0.8%	1.5%	4.8%	3.8%	1.5%	8.1%	10.0%	1.0%			
Microforaminiferal liners	5.1%	7.4%	0.7%				0.8%	1.5%	4.0%			
Scolecodonts	0.7%											
TOTAL Other Palynomorphs:	**8**	**10**	**3**	**7**	**5**	**2**	**12**	**15**	**10**			
TOTAL COUNT:	**138**	**122**	**134**	**147**	**131**	**130**	**124**	**130**	**201**	**104**	**100**	**153**

APPENDIX 2

BALEEN-2

PETROPHYSICS REPORT

-SCHLUMBERGER-

Schlumberger

Multi-Model Open Hole Analysis (ELAN) Report

Prepared for:

OMV Australia Pty Ltd

for

Baleen-2

18-JUL-2000

NOTE: This report presents the results of analysis for the Baleen-2 well as extracted from a "Baleen Field Study" performed on the Baleen-1, Baleen-2 and Patricia-1 wells.

Prepared by:
Don Clarke
Schlumberger Oilfield Australia Pty Ltd
Data Consulting Services
Level 5, 256 St George's Tce
PERTH WA 6000
Telephone: (08) 9420 4800
Facsimile: (08) 9322 3080

Table of Contents

List of Tables

Table of Figures

Executive Summary

A petrophysical analysis was performed on the Baleen-2 well, which integrated the available wireline logs and core data, providing porosity, permeability, and water saturation with a high degree of confidence.

The results are provided in Table 1 and Table 15, as well as in more detail by Gurnard Flow Units in the Appendix.

Table 1: Executive summary results of the Baleen-2 well.

	Baleen-2
Top Interval	741.00 m
Bottom Interval	787.70 m
Gross Reservoir	46.70 m
Net Reservoir	40.31 m
Gross Pay	11.2m
Net Pay	10.6m
Average PIGN	0.260 m3/m3
Average PHIT	0.297 m3/m3
Average VCL	0.214 m3/m3
Average KINT	93 mD
Net / Gross Ratio	0.86

We would like to recommend the following for any future wells:

- A cored interval with detailed analysis of the most clay rich fraction of the reservoir.
- The acquisition of CMR* to better understand pore-size distribution, the effective porosity in a clay rich environment, and a continuous permeability log.
- The acquisition of ECS* to better control the complex matrix mineralogy component and the complex clay component of the model.
- Continued acquisition of NGS/HNGS, FMI, and high-resolution logs.

Review of available data

A summary of the available data is in the following tables, with any discussion occurring below.

Wireline Data

Table 2: Summary of relevant wireline borehole parameters.

	Baleen-2
Date Logged	16-Oct-1999
RMS (ohm.m)	0.134
MST (degC)	21.4
RMFS (ohm.m)	0.115
MFST (degC)	21.6
RMCS (ohm.m)	0.213
MCST (degC)	21.7
DFD (g/cm3)	1.21
BHT (degC)	46.7
BS (in)	8.5

All relevant log data has been extracted from field print headers, or has been provided by OMV.

Table 3: Summary of available wireline logs.

	Baleen-2
Total Gamma Ray	EHGR
Spectral Gamma Ray	POTA/THOR/URAN
Bulk Density	RHO8
Photoelectric Factor	PEF8/U8
Thermal Neutron Porosity	HTNP/NPHU
Formation Resistivity	HART
Flushed Zone Resistivity	RXO8
Delta-T Compressional	DTCO

Baleen-2 was completely re-computed from the original field tape acquisition data, applying the latest correction algorithms available for the data. Reprocessing was done using the GeoFrame 3.7.1 baseline.
The invasion factor logs were computed from the new RHO8 log, the new HTNP log, and the diameter of invasion computed from the HALS processing.

Environmental Corrections

- CNT – After re-computation from counts, the TNPH porosity log had borehole size, mudcake thickness, mud density, borehole temperature, and borehole pressure corrections applied. No borehole salinity or formation salinity corrections were applied as they were applied during the evaluation.
- DLT – Borehole size, and tool position corrections were applied.

- FDC – No reprocessing was applied as the field-processing unit applies all of the relevant corrections.
- HRDD – The raw counts were reprocessed using the latest "environmental correction matrix" available in GeoFrame 3.7.1
- LDT – No reprocessing was applied as the field-processing unit applies all of the relevant corrections.
- NGT – The raw counts were re-processed, and correction estimates were computed for barite and potassium content in the mud.
- SGT – Borehole size, tool position, and mud weight corrections were applied.
- SRT – Mud cake corrections were applied.

Core Data

All available core data is summarised in Table 4, and a brief discussion is included to provide any additional relevant information.

Table 4: Summary of available core results.[1]

	Baleen-2
Core Porosity	CPOR
Core Grain Density	CGDN
Core Horizontal Permeability	CKH
Core Cation Exchange Capacity	CCEC
Critical Water Saturation from Core	CSWC

Baleen-2 had both routine and special core analysis results available. Several core-interval shifts were applied based on observations made by Colum Corless when comparing the FMI image to core. These shifts are documented in Table 5.

Table 5: Baleen-2 core interval depth shifts.

Core Section	Original Core Depth	Depth Shift	Revised Core Depth
Core 1	746.0m to 762.2m	+0.14m	746.14m to 762.34m
Core 2A	763.7m to 769.0m	-0.78m	762.92m to 768.22m
Core 2B	769.1m to 771.5m	NO SHIFT	769.1 m to 771.5m
Core 2C	771.6m to 779.0m	+0.77m	772.37m to 779.77m

The core porosities and permeabilities were available at ambient (400 psi) and overburden pressures (700 psi, 1040 psi). Only the data measured at 1040 psi was used for display and comparison purposes. The core porosities were measured after humidity drying, which should have preserved the clay bound waters, therefore the measured core-porosities should more closely match the effective porosity derived from the log analysis.

Core sample cation exchange capacities were also available for purposes of display and comparison to the log analysis, although only the crushed sample data was used.

[1] See Table 19 for core mnemonic descriptions.

The exponents "m", "n", and "c" derived by the electrical properties study of the core, incorporate the effects of the clay fraction in each sample. New exponents (m_{igws}, n_{igms}, and c_{igws})[2] that exclude the effects of the clay fraction were used in the Waxman Smitts saturation equation, and are summarised in Table 6.

Table 6: Baleen-2 derived (clay corrected) core electrical properties.

a	c_{igws}	m_{igws}	n_{igms}
1	1.4766	1.6086	1.84

Baleen-2 core petrology was also available. The information was used to come to a better understanding of the Gurnard formation mineral assemblages. Of most importance were the various descriptions of clay minerals, and their morphology. This information was central to the construction of the mineral model (described later).

[2] igws = Intergranular Waxman Smitts corrected exponent.

ELANPlus* Analysis

Since the previous Baleen-2 analysis, additional information has become available, and a more integrated analysis has been undertaken encompassing all available data.

The petrology and x-ray diffraction report helped to identify minerals that could be included in the complex mineralogy model. The following key minerals were identified, Biotite, Glauconite, Illite, Kaolinite, Orthoclase, Pyrite, Quartz, and Siderite although not all were included in the final complex model.

The special core analysis provided core-derived values of the saturation and cementation exponent's-m, n and c. These were clay corrected before they were used in the Waxman-Smits saturation equation.

Several Siderite cemented bands occur in the well and these were modelled differently. Two models were developed, a siderite model, and a pyrite model, with the "siderite" model used in the cemented zones and the "pyrite" model used in the silty sandstones (main reservoir type).

Baleen-2 Analysis

Table 7: Mineral model "pyrite".

Equations	Volumes	Constraints
RHOB	QUAR	WaterBaseMud_SXO_gt_SW
NPHU	ORTH	MinPyrite
U	PYRI	
CXDC_WS (RXO)	GLAU	
CUDC_WS (RT)	ILLI	
WWK (POTA)	KAOL	
CT1	XWAT	
CT2	UWAT	
	XGAS	
	UGAS	

Table 8: Mineral model "siderite".

Equations	Volumes	Constraints
RHOB	QUAR	WaterBaseMud_SXO_gt_SW
NPHU	ORTH	
U	SIDE	
CXDC_WS (RXO)	GLAU	
CUDC_WS (RT)	ILLI	
WWK (POTA)	KAOL	
CT1	XWAT	
CT2	UWAT	
	XGAS	
	UGAS	

Petrophysical Analysis input logs

The logs available for the analysis included high-resolution density (RHO8 and PEF8), high-resolution neutron logs (HTNP/NPHU), high-resolution gamma ray logs (EHGR), spectral gamma ray logs (POTA, THOR, and URAN), compressional (DTCO) and shear (DTSM) sonic logs, and laterolog resistivities (MSFL, LLS, and LLD).

The photoelectric factor (PEF8) was converted to a volumetric photoelectric factor (U8) before it was used in the analysis. ELANPlus* is able to use it in a linear form which simplifies the analysts understanding of its impact on the mineral volumes.

The neutron porosity log (NPHU) used in the analysis used the high-resolution count rates with all environmental corrections applied except for the formation salinity correction. This correction is left to the ELANPlus module itself, as the analyst has control over how much effect the invaded zone salinities verses the uninvaded zone salinities have on the log response.

Only the potassium log was used from the spectral gamma ray data. The potassium response of the minerals included in the model is well understood in the literature and in mineral response catalogues. The thorium log was not used since the generally accepted end-points from the literature cannot be used, as they are too low for the region (Gippsland Basin). Further characterisation of the thorium response to minerals found in the region would be required before the thorium log could be accurately incorporated into the ELANPlus* model. The uranium log was not used, as uranium is soluble in water, can be dissolved from a formation, transported through fluid movement, and then precipitated into another formation. For these reasons it is not a good mineral indicator.

Although a conventional total gamma ray curve was available in all three wells, it was not used as a clay indicator. The formation's radioactivity is derived from a complex clay mixture of varying radioactive properties as well as a "hot" potassium rich matrix.

The compressional and shear sonic logs were not used in the analysis as the formation is poorly consolidated (porosity in excess of 30%), and because they do not aid in the differentiation of the various minerals included in the model.

The laterolog resistivities were invasion corrected to true resistivity (RT) and flushed zone resistivity (RXO) logs, before they were used in the analysis.

As there were insufficient logs to resolve all of the minerals present in the model, two constant tools were used. A constant tool (CT1) was added to lock the volume of Orthoclase to the volume of Quartz, and another constant tool (CT2) was used to lock the volume of Illite to the volume of Glauconite.

Analysis volumes

Biotite was eventually dropped from the mineral model because its inclusion in the model masked the clay response within the reservoir sections.

The following matrix mineral volumes and their associated log responses (Table 9) were included in the mineral model. Note that Biotite is included in this table for comparison only.

Table 9: Matrix mineral log responses.

Mineral	RHOB (g/cm3)	NPHU (m3/m3)	U	POTA (m3/m3)
Quartz	2.65	-0.02	5.04	0.00
Orthoclase	2.57	-0.01	8.71	0.10
Pyrite	4.99	0.01	82.06	0.00
Siderite	3.96	0.18	72.20	0.00
Biotite	3.22	0.11	22.42	0.07

The volume of Orthoclase was locked to the volume of Quartz using a well-understood ratio of 87:13 that was derived from the petrology report (Table 10). The use of this constant tool (CT1) allowed the potassium log to be used within the model to better differentiate the other potassium rich clay minerals.

Table 10: Baleen-2 quartz and orthoclase relationship.

CNUM	MD (m)	VQUA (m3/m3)	VORT (m3/m3)	QUAR	ORTH
S5	750.41	0.4300	0.0600	88	12
S6	751.42	0.4130	0.0530	89	11
S9	754.41	0.4500	0.0680	87	13
S12	757.42	0.4680	0.0580	89	11
52	765.59	0.2830	0.0310	90	10
S21	768.79	0.4140	0.0650	86	14
S22	770.05	0.3430	0.0550	86	14
70	771.60	0.1780	0.0130	93	7
S24	771.81	0.4150	0.0680	86	14
S26	773.79	0.4290	0.0580	88	12
S28	775.82	0.4710	0.0550	90	10
S30	777.80	0.4630	0.0720	87	13

The volume of pyrite was controlled using a constraint that used a linear relationship between the volume of pyrite and the volumes of quartz and orthoclase as derived from a crossplot of the corresponding petrology data. A constraint allows the ratio of pyrite to quartz-orthoclase to vary while a constant tool would enforce a fixed ratio.

Table 11: Baleen-2 matrix to pyrite comparison.

CNUM	MD (m)	VMAT (m3/m3)	VPYR (m3/m3)	MATR	PYRI
S5	750.41	0.49	0.08	87	13
S6	751.42	0.47	0.06	89	11
S9	754.41	0.52	0.03	95	5
S12	757.42	0.53	0.03	94	6
S21	768.79	0.48	0.07	87	13
S22	770.05	0.40	0.08	83	17
S24	771.81	0.48	0.04	92	8
S26	773.79	0.49	0.04	93	7
S28	775.82	0.53	0.02	96	4
S30	777.80	0.54	0.02	96	4

Figure 1: Matrix and pyrite relationship.

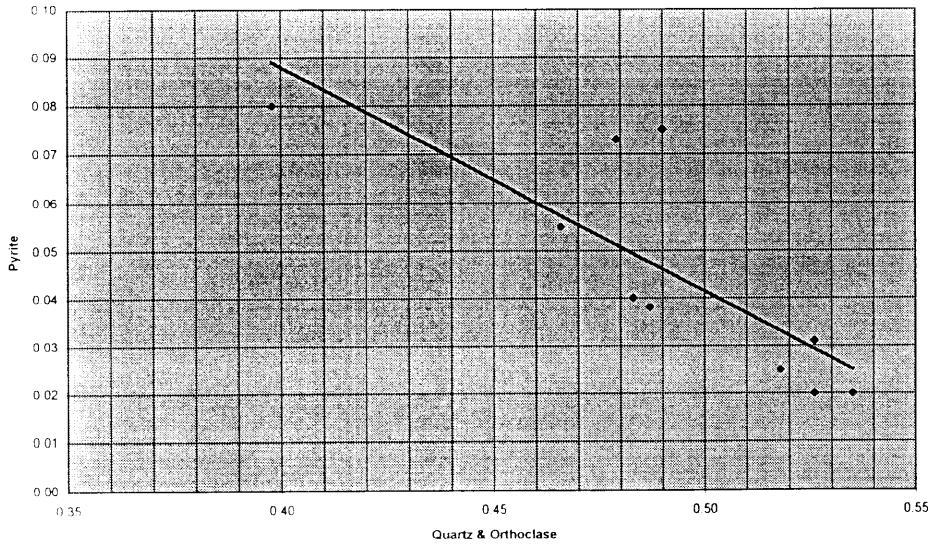

Siderite and Pyrite were evaluated in two separate models that were later combined into the final "answer" product. As siderite was primarily concerned with discrete bands within the reservoir, the pyrite model was used to evaluate the reservoir/shale intervals, and the siderite model was used to describe the tight streaks that occurred throughout the Gurnard formation.

The following dry clay mineral volumes and their parameters (Table 12) were also included in the complex mineral model.

Table 12: Dry clay mineral log responses.

Mineral	RHOB (g/cm3)	NPHU (m3/m3)	U	POTA (m3/m3)	CEC (meq/g)
Kaolinite	2.62	0.45	5.38	0.00	0.09
Illite	2.78	0.25	11.12	0.04	0.16
Glauconite	2.85	0.50	19.10	0.06	0.23

Kaolinite is described both by thin section observation in the petrology report, and by XRD analysis. A constant tool (CT2) was used to lock the volumes of Illite and Glauconite into a 1:1 ratio, which was based upon the XRD results describing Illite and Kaolinite as "abundant" in the distribution. The inclusion of Illite in this model is also supported by the description in the petrology report of a more "illitic Glauconite".

Water and gas were the only significant fluids included in the analysis, and both the invaded and undisturbed zones of the formation were analysed.

Formation Waters

A water sample taken from the Latrobe Group Coarse Clastics (below the Gurnard) had a resistivity of 0.7 ohm.m at 25 degC, and was confirmed by calculating an apparent water resistivity using the ratio method within the same sand interval. This corresponds to a formation water salinity of 7.95 ppk.
A further comparison of the pressure gradients in the Gurnard and Latrobe indicates that they have the same gradient therefore they are likely to have the same water salinity.

Core integration

The core data was integrated into the analysis using the following techniques.

Core porosities were displayed against the total porosity (PHIT) and the effective intergranular porosity (PIGN). As the cores had been humidity dried, the assumption is that only the non-clay bound waters are driven off in the drying process.

Core grain densities provided a good quality control on the total volume of dry-clay and heavy mineral included in the model.

Core CEC values provided a good quality control on the total volume of clays derived in the analysis. As the volume of clay is a direct input into the saturation equation and is included in the total conductivity/resistivity response of the formation, it was very important to have an external control on this volume.

Core irreducible water saturations, derived from the capillary pore measurements were an external check on the water saturation derived from the Waxman-Smits equation. Assuming that the gas reservoir had reached maximum gas saturation for that height above the free water level, the critical core water saturations (CSWC) should plot along the undisturbed-zone water saturation line. Each of these "critical saturations" were computed for their own unique formation type, and the points were plotted on depth against the computed water saturation.

Observations

Observations regarding the complex mineral model ELANPlus results are included in Table 13.

Table 13: Complex mineral model observations.

Interval	Observation
748m to 759m	Good fit to all of the available core data (porosity, water saturation, grain density, and CEC values).
	Saturation profile looks reasonable as we can see from the effect on the density and neutron logs that not all of the gas has been flushed from the near borehole.
	The flow units (GFU2, GFU3, and GFU4) within this interval, are dominated by Illite and Glauconite clays, and contain a lesser amount of Kaolinite when present.
759m to 762m	This interval is characterised by dispersed/nodular siderite as can be seen on the FMI image.
	The calculated porosity and grain density do not match well to the core data as the logs include an "averaged" response of the dispersed/nodular siderite.
762m to 768m	Several tight siderite bands dominate this interval. Although the logs used in the analysis have a high vertical resolution, they still include an "averaged" response of the siderite. The FMI image shows that these are discrete bands without dispersed siderite between them.
768m to 772m	The calculated porosity does not match the core porosity although all other core measurements agree with the logs.
772m to 788m	The clays within this interval are dominated by Kaolinite, although there are discrete packets of the reservoir sands that are more Glauconitic than other packets.

Permeability determination

After the completion of the ELANPlus* complex model analysis, the resulting mineral volumes were used to compute a permeability using the k-Lambda transform. K-Lambda primarily responds to two inputs, the pore throat size and the mineral surface areas (Herron, 1998). Total porosities are also used as an input to the k-Lambda transform.

The model was initially run on default values for the mineral surface areas, but it significantly overestimated the permeabilities compared to the core.

All of the matrix and clay minerals were examined to see if there were any significant correlations to the high permeabilities. The surface areas of Quartz, Kaolinite, Illite, Siderite and Pyrite were treated as defaults in the model. Glauconite is described as being "book-like" in form, and "illitic" in composition, therefore its surface area was changed to be the same as Illite. This helped to account for some of the permeability difference, but not the all of the over estimated permeability was associated with the more clay rich zones.

Another adjustment was required throughout the whole interval to further reduce the permeabilities. The thin section petrology reported the Orthoclase minerals as being weathered or chemically leached. Since Orthoclase alters to Kaolinite and Quartz, the surface area of Orthoclase was increased to be half way between its default response and the default response of Kaolinite. This had the desired effect of matching the computed permeability to most of the core permeabilities. The final surface areas used in the model are summarised in Table 14 along with the default values.

Table 14: K-Lambda surface area constants.

	VQUA (m^2/g)	VORT (m^2/g)	VSID (m^2/g)	VPYR (m^2/g)	VKAO (m^2/g)	VILL (m^2/g)	VGLA (m^2/g)
Default	0.22	0.3	2.0	0.3	23.0	101.0	23.0
Model	0.22	10.0	2.0	0.3	23.0	101.0	101.0

Analysis Results

A final reservoir summation was calculated based on the ELANPlus volumes and a flag curve that was used to discriminate between the reservoir intervals and the siderite bands. It is important to note that no other cut-offs (porosity, volume of clay, saturation, or permeability) were used in this reservoir summation.

Baleen-2 used a cut-off of greater than or equal to 2.35 g/cm3 on the 8" density log (RHO8) to identify siderite bands.

The results of the summations using the flag-curve are provided in more detail in Appendix 2. They are also available using both the effective porosity and the total porosity computed by each analysis.

It is important to note that "pay" as shown in the summary listing refers only to "reservoir". A water saturation cutoff was not applied for the summation as the results were also used to define reservoir in a simulation model

Table 15: Summary of Results

	Baleen-2 (Complex)
Top Interval	741.0 m
Base Interval	787.7 m
Total gross thickness	46.7 m
Total net thickness	40.3
Total net reservoir thickness	40.3
Total net pay thickness	10.6
Thickness-weighted net reservoir to gross ratio	0.86
Thickness-weighted average net pay porosity	0.26 v/v
Cumulative porosity thickness for all zones:	10.5 m
Cumulative permeability thickness for all zones:	10060 m
Cumulative hydrocarbon thickness for all zones:	2.04 m

References

A Robust Permeability Estimator for Siliciclastics, M.Heron, D. Johnson, and L. Schwartz, SPE 49301, 1998.

Baleen-2 CEC Excel Worksheet – ACS Laboratories, 2000.

Baleen-2 Fluids Analysis Final Report, ACS Laboratories Pty. Ltd., February 2000.

Baleen-2 petrology EXCEL Worksheet.

Baleen-2 Preliminary Log Analysis Report, Tom Neville, 1999.

Baleen-2 RCA Excel Worksheet – ACS Laboratories, 2000.

Baleen-2 SCAL Excel Worksheet – ACS Laboratories ,2000.

Electrical Conductivities in Shaly Sands, M. Waxman and E. Thomas, SPE 4094, 1972.

Elemental Composition and Nuclear Parameters of Some Common Sedimentary Minerals, M. Herron and A. Matteson, Nuclear Geophysics Vol.7 No.3 pp 383-406, 1993.

Estimating the Intrinsic Permeability of Clastic Sediments from Geochemical Data, M. Herron, SPWLA 1987.

Log Interpretation Charts, Schlumberger Oilfield Communications, SMP-7006, 2000.

The Theoretical and Experimental Bases for the "Dual Water" Model for the Interpretation of Shaly Sands, C. Clavier, G Coates, and J. Dumanoir, SPE 6859, 1977.

Appendix 1

Chronology of Models

- Preliminary model – built by Tom Neville.

Volumes: QUAR KAOL XWAT UWAT XGAS UGAS
Equations: RHOB NPHU U CXDC_WS CUDC_WS WWK CT1 CT2
Comments: This was the original model built by Tom Neville. No core descriptions or results were available at the time. The analysis also included several other models covering the different formations surrounding the Gurnard Formation. This model was missing several significant minerals that were described in the core Petrology report.

- First revised model – Complete model.

Volumes: QUAR ORTH BIOT PYRI GLAU ILLI KAOL XWAT UWAT XGAS UGAS
Equations: RHOB NPHU U CXDC_WS CUDC_WS WWK CT1 CT2 CT3
Comments: This first model was built with all of the relevant minerals described by the petrology report included. It was overly ambitious but was attempted in the hope that sufficient external controls (through the use of constant tools) could be applied. With more logging tools that are sensitive to the minerals in the formation, this would represent the "ideal" model for the Gurnard Formation.

- Second revised model – Biotite model.

Volumes: QUAR ORTH BIOT GLAU KAOL XWAT UWAT XGAS UGAS
Equations: RHOB NPHU U CXDC_WS CUDC_WS WWK CT1 CT2
Comments: The second model was cut down to the maximum number of volumes that could be resolved with the available logs. It also used "well understood" constant tools extracted from the petrology report.

- Third revised model – Rock model.

Volumes: SAND FELD CLA1 XWAT UWAT XGAS UGAS
Equations: RHOB NPHU U CXDC_WS CUDC_WS WWK
Comments: An attempt was made to characterise the reservoir in terms of rock types, which would allow us to simplify the complex mineralogy. This failed for the same reasons that the "lumped model" fails. The formation cannot be easily characterised into a "matrix" and "clay" as there is significant variability within both throughout the reservoir.

- Fourth revised model – Pyrite model, kaolinite and Illite bound.

Volumes: QUAR ORTH PYRI GLAU ILLI KAOL XWAT UWAT XGAS UGAS
Equations: RHOB NPHU U CXDC_WS CUDC_WS WWK CT1 CT2
Comments: Returned to the "complex model", having removed Biotite. Settled upon the three-clay mix of Kaolinite, Illite, and Glauconite, and added Pyrite back into the model, as a significantly dense matrix mineral was required. Initially bound Kaolinite and Illite together which had proved successful in several other sand/shale evaluations. It didn't provide the best fit to the petrology and core descriptions as Glauconite would come and go in the model replaced by Illite.

- Final revised model – Pyrite model, Illite and Glauconite bound.

Volumes: QUAR ORTH PYRI GLAU ILLI KAOL XWAT UWAT XGAS UGAS
Equations: RHOB NPHU U CXDC_WS CUDC_WS WWK CT1 CT2
Comments: Settled upon this final model, which bound Illite and Glauconite together. It provided the best fit between the minerals included in the model, the petrology descriptions, and the final results of porosity, permeability, and water saturation.

Gurnard Flow Units

The following table of Gornard Formation flow units was summarised from an Excel Worksheet provided by Mark Adamson.

Table 16: Summary of Gurnard Flow Units.

	Baleen-2
top Gurnard	741
GFU1	741
SB1	747
GFU2	747.7
SB2	752.3
GFU3	752.8
SB3	755
GFU4	756.3
SB4	759.7
GFU5	760.3
SB5	762
GFU6	763.6
SB6	772.1
GFU7	772.5
SB7	774.6
GFU8	775.1
SB8	781
GFU9	783.3
BCZ	787.7
top Latrobe	790.5
top Strzelecki	859

Mnemonic listings

Table 17: Parameter mnemonic listing.

Mnemonic	Description
RMS	Resistivity of the mud sample
MST	Mud sample temperature
RMFS	Resistivity of the mud filtrate sample
MFST	Mud filtrate sample temperature
RMCS	Resistivity of the mud cake sample
MCST	Mud cake sample temperature
DFD	Drilling fluid density
BHT	Bottom hole temperature
BS	Bit size

Table 18: Log-curve mnemonic listing.

Mnemonic	Description
GR	Total gamma ray
POTA	Potassium concentration
THOR	Thorium concentration
URAN	Uranium concentration
RHOB	Formation bulk density
PEF	Formation photoelectric factor
U	Formation volumetric photoelectric factor
TNPH	Thermal neutron porosity (ratio method)
NPHI	Thermal neutron porosity (original ratio method)
NPHU	Thermal neutron porosity uncorrected for salinity
RT	True formation resistivity
RXO	Flushed zone resistivity
LLD	Deep laterolog
LLS	Shallow laterolog
MSFL	Micro-spherically-focused resistivity
DT	Delta-T from first motion detection
DTCO	Delta-T from semblance processing
EHGR	Environmentally corrected high resolution total gamma ray
RHO8	HRDD high resolution formation bulk density
PEF8	HRDD high resolution photoelectric factor
U8	HRDD high resolution volumetric photoelectric factor
HTNP	High resolution thermal neutron porosity
HART	True formation resistivity from HALS/MCFL combination.
RXO8	MCFL high resolution invaded formation resistivity
IFRH	RHOB invasion factor
INPH	NPHI invasion factor

Table 19: Core-data mnemonic listing.

Mnemonic	Description
CNUM	Core Number
CPOR	Core Porosity
CKHA	Core Horizontal Permeability to Air
CKVA	Core Vertical Permeability to Air
CCEC	Core Derived Cation Exchange Capacity
CSWC	Core Critical Water Saturations

Appendix 2

Summary Listing of Results

Jul 27,2000 17:35:53

Baleen-2 Using PIGN as Porosity

OMV Australia

BALEEN_STUDY

SUMMARY REPORT

Reservoir Summation based on RHO8 discriminator.

LAYER SUMMATION DATA - MEASURED DEPTH
(ALL PROCESSED WELLS)

Reservoir Summation based on RHO8 discriminator.

Layer Data			Net - Average				Net Reservoir - Average					Net Pay - Average							
Name	Avg Gross Thick	Avg Gross PHI	Net Thick (m)	Net %	Shale Thick (m)	Shale %	Thick (m)	PHI-Thick (m)	Avg PHI	Avg Clay Vol	Net / Gross Ratio	Thick (m)	PHI-Thick (m)	HPHI-Thick (m)	Perm-Thick (mD-m)	Avg PHI	Avg Sw	Avg Clay Vol	Avg Perm	Net / Gross Ratio
GFU1	6.00	0.168	2.2	0.36	3.8	0.63	2.19	0.41	0.187	0.603	0.365	2.19	0.41	0.02	5	0.19	0.95	0.60	1	0.365
SB1	0.70	0.106	0.4	0.56	0.3	0.44	0.40	0.07	0.168	0.318	0.565	0.40	0.07	0.02	39	0.17	0.67	0.32	1	0.565
GFU2	4.60	0.280	4.6	1.00	0.0	0.00	4.60	1.29	0.280	0.131	1.000	4.60	1.29	0.50	2221	0.28	0.61	0.13	1	1.000
SB2	0.50	0.162	0.4	0.72	0.1	0.28	0.36	0.04	0.102	0.295	0.717	0.36	0.04	0.01	4	0.10	0.77	0.29	2	0.717
GFU3	2.20	0.324	2.2	1.00	0.0	0.00	2.20	0.71	0.324	0.134	1.000	2.20	0.71	0.39	481	0.32	0.46	0.13	1	1.000
SB3	1.30	0.276	1.3	1.00	0.0	0.00	1.30	0.36	0.276	0.173	1.000	1.30	0.36	0.19	192	0.28	0.48	0.17	1	1.000
GFU4	3.40	0.304	3.4	1.00	0.0	0.00	3.40	1.03	0.304	0.132	1.000	3.40	1.03	0.39	898	0.30	0.62	0.13	1	1.000
SB4	0.60	0.211	0.6	1.00	0.0	0.00	0.60	0.13	0.211	0.375	1.000	0.60	0.13	0.05	18	0.21	0.62	0.37	1	1.000
GFU5	1.70	0.214	1.7	1.00	0.0	0.00	1.70	0.36	0.214	0.384	1.000	1.70	0.36	0.14	37	0.21	0.62	0.38	1	1.000
SB5	1.60	0.085	0.6	0.35	1.0	0.65	0.56	0.07	0.130	0.429	0.353	0.56	0.07	0.00	1	0.13	0.98	0.43	2	0.353
GFU6	8.50	0.205	7.7	0.91	0.8	0.09	7.74	1.66	0.214	0.273	0.910	7.74	1.66	0.09	557	0.21	0.94	0.27	1	0.910
SB6	0.40	0.274	0.2	0.55	0.2	0.45	0.22	0.06	0.260	0.151	0.546	0.22	0.06	0.00	31	0.26	1.00	0.15	1	0.546
GFU7	2.10	0.305	2.1	1.00	0.0	0.00	2.10	0.64	0.305	0.113	1.000	2.10	0.64	0.08	614	0.31	0.87	0.11	1	1.000
SB7	0.50	0.281	0.5	1.00	0.0	0.00	0.50	0.14	0.281	0.131	1.000	0.50	0.14	0.01	103	0.28	0.91	0.13	1	1.000
GFU8	5.90	0.308	5.9	1.00	0.0	0.00	5.90	1.82	0.308	0.111	1.000	5.90	1.82	0.08	4021	0.31	0.96	0.11	1	1.000
SB8	2.30	0.224	2.1	0.93	0.2	0.07	2.15	0.49	0.226	0.265	0.934	2.15	0.49	0.01	147	0.23	0.98	0.27	1	0.934
GFU9	4.40	0.280	4.4	1.00	0.0	0.00	4.40	1.23	0.280	0.162	1.000	4.40	1.23	0.06	691	0.28	0.95	0.16	1	1.000

Jul 27,2000 17:35:53

WELL INFORMATION

Project:	BALEEN_STUDY	
Field:	VIC/RL5	
Operator:	CULTUS PETROLEUM NL	
Well:	Baleen-2	
Well Location:	Lat/Long (deg):	N/A /N/A
	X/Y (m):	-6.40126e+0/1e+07
	Legal:	N/A
	State:	N/A
	Country:	N/A
Elevation:	KB (m):	N/A
	GL (m):	4294945536.000
	MSL (m):	N/A

Reservoir Summation based on RHO8 discriminator.

SUMMARY FOR RESERVOIR Default_Summation_Reservoir SUMMATION MODEL BALEEN_2

	MD	TVD	TVT	TST
Top of zones (measured depth):	741			
Base of zones (measured depth):	787.7			
Total gross thickness for all zones:	46.7000	N/A	N/A	N/A
Total net thickness for all zones:	40.3122	N/A	N/A	N/A
Total net reservoir thickness for all zones:	40.3122	N/A	N/A	N/A
Total net pay thickness for all zones:	40.3122	N/A	N/A	N/A
Thickness-weighted net reservoir to gross ratio:	0.8632	N/A	N/A	N/A
Thickness-weighted average net pay porosity:	0.2604	N/A	N/A	N/A
Thickness-weighted average net pay Sw:	0.8054	N/A	N/A	N/A
Cumulative porosity thickness for all zones:	10.4993	N/A	N/A	N/A
Cumulative permeability thickness for all zones:	10060.2725	N/A	N/A	N/A
Cumulative hydrocarbon thickness for all zones:	2.0430	N/A	N/A	N/A

Jul 27,2000 17:35:53

ZONE SUMMATION PARAMETERS

Well: Baleen-2

Curves used:
- Clay Volume: VCL [A3459056]
- Porosity: PIGN [A3459017]
- Water Saturation: SUWI [A3459044]
- Permeability: KINT [A3316850]
- Discriminator 1: FLAG [A3455028]
- Discriminator 2: Not used

Discriminator Application Point 1: Initial
Discriminator Application Point 2: Initial

Averaging used for Permeability: Geometric

Zone Name	Top Depth (m)	Bottom Depth (m)	Gross Thick. (m)	Net Res. Thick. (m)	Net Pay Thick. (m)	Dip Correction Factors	VCL max	PIGN min	SUWI max	KINT min	Discr1 FLAG <	Discr2 Not used
GFU1_1	741.00	747.00	6.000	2.190	2.190		1.000	0.000	1.000	0.100	1.000	
SB1_1	747.00	747.70	0.700	0.395	0.395		1.000	0.000	1.000	0.100	1.000	
GFU2_1	747.70	752.30	4.600	4.600	4.600		1.000	0.000	1.000	0.100	1.000	
SB2_1	752.30	752.80	0.500	0.359	0.359		1.000	0.000	1.000	0.100	1.000	
GFU3_1	752.80	755.00	2.200	2.200	2.200		1.000	0.000	1.000	0.100	1.000	
SB3_1	755.00	756.30	1.300	1.300	1.300		1.000	0.000	1.000	0.100	1.000	
GFU4_1	756.30	759.70	3.400	3.400	3.400		1.000	0.000	1.000	0.100	1.000	
SB4_1	759.70	760.30	0.600	0.600	0.600		1.000	0.000	1.000	0.100	1.000	
GFU5_1	760.30	762.00	1.700	1.700	1.700		1.000	0.000	1.000	0.100	1.000	
SB5_1	762.00	763.60	1.600	0.565	0.565		1.000	0.000	1.000	0.100	1.000	

Jul 27,2000 17:35:53

Zone Name	Top Depth (m)	Bottom Depth (m)	Gross Thick. (m)	Net Res. Thick. (m)	Net Pay Thick. (m)	Dip Correction Factors	VCL max	PIGN min	SUWI max	KINT min	Discr1 FLAG <	Discr2 Not used
GFU6_1	763.60	772.10	8.500	7.738	7.738		1.000	0.000	1.000	0.100	1.000	
SB6_1	772.10	772.50	0.400	0.218	0.218		1.000	0.000	1.000	0.100	1.000	
GFU7_1	772.50	774.60	2.100	2.100	2.100		1.000	0.000	1.000	0.100	1.000	
SB7_1	774.60	775.10	0.500	0.500	0.500		1.000	0.000	1.000	0.100	1.000	
GFU8_1	775.10	781.00	5.900	5.900	5.900		1.000	0.000	1.000	0.100	1.000	
SB8_1	781.00	783.30	2.300	2.148	2.148		1.000	0.000	1.000	0.100	1.000	
GFU9_1	783.30	787.70	4.400	4.400	4.400		1.000	0.000	1.000	0.100	1.000	

ZONE SUMMATION DATA - MEASURED DEPTH

Reservoir Summation based on RHOB discriminator.

Zone / Interval Data				Net Reservoir				Net Pay								
Zone Name	Top Depth (m)	Bottom Depth (m)	Gross Thick. (m)	Thick. (m)	PHI-Thick. (m)	Avg PHI	Avg Clay Vol	Thick. (m)	PHI-Thick. (m)	HPHI-Thick. (m)	Perm-Thick. (mD-m)	Avg PHI	Avg Sw	Avg Clay Vol	Avg Perm	Net / Gross Ratio
GFU1_1	741.00	747.00	6.00	2.19	0.41	0.187	0.603	2.19	0.41	0.02	5	0.19	0.95	0.60	1	0.36
SB1_1	747.00	747.70	0.70	0.40	0.07	0.168	0.318	0.40	0.07	0.02	39	0.17	0.67	0.32	17	0.56
GFU2_1	747.70	752.30	4.60	4.60	1.29	0.280	0.131	4.60	1.29	0.50	2221	0.28	0.61	0.13	401	1.00
SB2_1	752.30	752.80	0.50	0.36	0.04	0.102	0.295	0.36	0.04	0.01	4	0.10	0.77	0.29	10	0.72
GFU3_1	752.80	755.00	2.20	2.20	0.71	0.324	0.134	2.20	0.71	0.39	481	0.32	0.46	0.13	191	1.00
SB3_1	755.00	756.30	1.30	1.30	0.36	0.276	0.173	1.30	0.36	0.19	192	0.28	0.48	0.17	101	1.00
GFU4_1	756.30	759.70	3.40	3.40	1.03	0.304	0.132	3.40	1.03	0.39	898	0.30	0.62	0.13	216	1.00
SB4_1	759.70	760.30	0.60	0.60	0.13	0.211	0.375	0.60	0.13	0.05	18	0.21	0.62	0.37	27	1.00
GFU5_1	760.30	762.00	1.70	1.70	0.36	0.214	0.384	1.70	0.36	0.14	37	0.21	0.62	0.38	14	1.00
SB5_1	762.00	763.60	1.60	0.56	0.07	0.130	0.429	0.56	0.07	0.00	1	0.13	0.98	0.43	1	0.35
GFU6_1	763.60	772.10	8.50	7.74	1.66	0.214	0.273	7.74	1.66	0.09	557	0.21	0.94	0.27	36	0.91
SB6_1	772.10	772.50	0.40	0.22	0.06	0.260	0.151	0.22	0.06	0.00	31	0.26	1.00	0.15	142	0.55
GFU7_1	772.50	774.60	2.10	2.10	0.64	0.305	0.113	2.10	0.64	0.08	614	0.31	0.87	0.11	252	1.00
SB7_1	774.60	775.10	0.50	0.50	0.14	0.281	0.131	0.50	0.14	0.01	103	0.28	0.91	0.13	200	1.00
GFU8_1	775.10	781.00	5.90	5.90	1.82	0.308	0.111	5.90	1.82	0.08	4021	0.31	0.96	0.11	515	1.00
SB8_1	781.00	783.30	2.30	2.15	0.49	0.226	0.265	2.15	0.49	0.01	147	0.23	0.98	0.27	52	0.93
GFU9_1	783.30	787.70	4.40	4.40	1.23	0.280	0.162	4.40	1.23	0.06	691	0.28	0.95	0.16	133	1.00
TOTALS/AVERAGES OVER ALL ZONES:			46.70	40.31	10.50	0.260	0.214	40.31	10.50	2.04	10060	0.26	0.81	0.21	93	0.86

Jul 27,2000 17:35:53

GLOSSARY

Abbreviations

Avg.	Average
GL	Ground Level
h	Depth Increment within Zone
HPHI	Hydrocarbon pore-thickness
KB.	Kelly Bushing
MSL	Mean Sea Level
Perm.	Permeability
PHI	Porosity
Sw	Water Saturation
Thick.	Thickness
TST	True Stratigraphic Thickness
TVT	True Vertical Thickness
Vcl	Clay Volume
ZGH	Gross Thickness for zone
ZH	Zone Thickness
ZNRH	Net Reservoir Thickness for Zone
ZPHI	Average Porosity for Zone

Calculations/Cutoffs

Gross	Depths passing 'Initial' discriminator
Net	Depths passing Gross, Clay Volume cutoffs and 'Net' discriminator
Net Reservoir	Depths passing Net, Porosity cutoffs and 'Net_Reservoir' discriminator
Net Pay	Depths passing Net Reservoir, Sw, Permeability cutoffs and 'Net_Pay' discriminator

Summations

Thick.	Sum(h)
PHI-Thick.	Sum(Porosity * h)
HPHI-Thick.	Sum(Porosity * h * (1 - Water saturation))
Perm-Thick.	Sum(Permeability * h)

Averages

Avg PHI	Sum(Porosity * h)/Sum(h)
Avg Clay Vol	Sum(Clay Volume * h)/Sum(h)
Avg Perm (Arithmetic)	Sum(Permeability * h)/Sum(h)
Avg Perm (Geometric)	10**(Sum(LOG10(Permeability) * h)/Sum(h))
Avg Perm (Harmonic)	Sum(h) / Sum(h/Permeability)
Avg Sw	Sum(Porosity * Water Saturation * h)/Sum(Porosity * h)

Thickness-weighted Averages

Net Reservoir to Gross Ratio	Sum(ZNRH/ZGH * ZH)/Sum(ZH)
Average Porosity	Sum(ZPHI * ZH)/Sum(ZH)
Average Sw	Sum(ZSW * ZH)/Sum(ZH)

Ratios

Net / Gross Ratio	Net Pay Thickness / Gross Thickness

Output

SFLG	Sand Flag Curve
RFLG	Reservoir Flag Curve
PFLG	Pay Flag Curve

Jul 27,2000 17:41:50

Baleen-2 Using PHIT as Porosity

OMV Australia

BALEEN_STUDY

SUMMARY REPORT

Reservoir Summation based on RHO8 discriminator.

Jul 27,2000 17:41:50

LAYER SUMMATION DATA - MEASURED DEPTH
(ALL PROCESSED WELLS)

Reservoir Summation based on RHO8 discriminator.

Layer Data			Net - Average				Net Reservoir - Average					Net Pay - Average							
Name	Avg Gross Thick	Avg Gross PHI	Net Thick (m)	Net %	Shale Thick (m)	Shale %	Thick (m)	PHI-Thick (m)	Avg PHI	Avg Clay Vol	Net / Gross Ratio	Thick (m)	PHI-Thick (m)	HPHI-Thick (m)	Perm-Thick (mD-m)	Avg PHI	Avg Sw	Avg Clay Vol	Avg Perm	Net / Gross Ratio
GFU1	6.00	0.271	2.2	0.36	3.8	0.63	2.19	0.64	0.293	0.603	0.365	2.19	0.64	0.03	5	0.29	0.95	0.60	1	0.365
SB1	0.70	0.167	0.4	0.56	0.3	0.44	0.40	0.09	0.219	0.318	0.565	0.40	0.09	0.02	39	0.22	0.71	0.32	1	0.565
GFU2	4.60	0.304	4.6	1.00	0.0	0.00	4.60	1.40	0.304	0.131	1.000	4.60	1.40	0.54	2221	0.30	0.61	0.13	1	1.000
SB2	0.50	0.205	0.4	0.72	0.1	0.28	0.36	0.05	0.152	0.295	0.717	0.36	0.05	0.01	4	0.15	0.81	0.29	2	0.717
GFU3	2.20	0.352	2.2	1.00	0.0	0.00	2.20	0.77	0.352	0.134	1.000	2.20	0.77	0.42	481	0.35	0.46	0.13	1	1.000
SB3	1.30	0.309	1.3	1.00	0.0	0.00	1.30	0.40	0.309	0.173	1.000	1.30	0.40	0.21	192	0.31	0.48	0.17	1	1.000
GFU4	3.40	0.330	3.4	1.00	0.0	0.00	3.40	1.12	0.330	0.132	1.000	3.40	1.12	0.43	898	0.33	0.62	0.13	1	1.000
SB4	0.60	0.271	0.6	1.00	0.0	0.00	0.60	0.16	0.271	0.375	1.000	0.60	0.16	0.06	18	0.27	0.63	0.37	1	1.000
GFU5	1.70	0.272	1.7	1.00	0.0	0.00	1.70	0.46	0.272	0.384	1.000	1.70	0.46	0.18	37	0.27	0.62	0.38	1	1.000
SB5	1.60	0.160	0.6	0.35	1.0	0.65	0.56	0.11	0.200	0.429	0.353	0.56	0.11	0.00	1	0.20	0.98	0.43	2	0.353
GFU6	8.50	0.254	7.7	0.91	0.8	0.09	7.74	2.02	0.261	0.273	0.910	7.74	2.02	0.11	557	0.26	0.94	0.27	1	0.910
SB6	0.40	0.299	0.2	0.55	0.2	0.45	0.22	0.06	0.292	0.151	0.546	0.22	0.06	0.00	31	0.29	1.00	0.15	1	0.546
GFU7	2.10	0.325	2.1	1.00	0.0	0.00	2.10	0.68	0.325	0.113	1.000	2.10	0.68	0.09	614	0.33	0.87	0.11	1	1.000
SB7	0.50	0.307	0.5	1.00	0.0	0.00	0.50	0.15	0.307	0.131	1.000	0.50	0.15	0.01	103	0.31	0.90	0.13	1	1.000
GFU8	5.90	0.324	5.9	1.00	0.0	0.00	5.90	1.91	0.324	0.111	1.000	5.90	1.91	0.08	4021	0.32	0.96	0.11	1	1.000
SB8	2.30	0.264	2.1	0.93	0.2	0.07	2.15	0.57	0.265	0.265	0.934	2.15	0.57	0.01	147	0.26	0.98	0.27	1	0.934
GFU9	4.40	0.311	4.4	1.00	0.0	0.00	4.40	1.37	0.311	0.162	1.000	4.40	1.37	0.07	691	0.31	0.95	0.16	1	1.000

908080 103

Jul 27,2000 17:41:50
WELL INFORMATION

Project:	BALEEN_STUDY	
Field:	VIC/RL5	
Operator:	CULTUS PETROLEUM NL	
Well:	Baleen-2	
Well Location:	Lat/Long (deg):	N/A /N/A
	X/Y (m):	-6.40126e+0/1e+07
	Legal:	N/A
	State:	N/A
	Country:	N/A
Elevation:	KB (m):	N/A
	GL (m):	4294945536.000
	MSL (m):	N/A

Reservoir Summation based on RHO8 discriminator.

9080080 104

SUMMARY FOR RESERVOIR Default_Summation_Reservoir SUMMATION MODEL BALEEN_2

	MD	TVD	TVT	TST
Top of zones (measured depth):	741			
Base of zones (measured depth):	787.7			
Total gross thickness for all zones:	46.7000	N/A	N/A	N/A
Total net thickness for all zones:	40.3122	N/A	N/A	N/A
Total net reservoir thickness for all zones:	40.3122	N/A	N/A	N/A
Total net pay thickness for all zones:	40.3122	N/A	N/A	N/A
Thickness-weighted net reservoir to gross ratio:	0.8632	N/A	N/A	N/A
Thickness-weighted average net pay porosity:	0.2972	N/A	N/A	N/A
Thickness-weighted average net pay Sw:	0.8098	N/A	N/A	N/A
Cumulative porosity thickness for all zones:	11.9800	N/A	N/A	N/A
Cumulative permeability thickness for all zones:	10060.2725	N/A	N/A	N/A
Cumulative hydrocarbon thickness for all zones:	2.2781	N/A	N/A	N/A

Jul 27,2000 17:41:50

ZONE SUMMATION PARAMETERS

Well: Baleen-2

Curves used:
- Clay Volume: VCL [A3459056]
- Porosity: PHIT [A3459014]
- Water Saturation: SUWI [A3459044]
- Permeability: KINT [A3316850]
- Discriminator 1: FLAG [A3455028]
- Discriminator 2: Not used

Discriminator Application Point 1: Initial
Discriminator Application Point 2: Initial

Averaging used for Permeability: Geometric

Zone Name	Top Depth (m)	Bottom Depth (m)	Gross Thick. (m)	Net Res. Thick. (m)	Net Pay Thick. (m)	Dip Correction Factors	VCL max	PHIT min	SUWI max	KINT min	Discr1 FLAG <	Discr2 Not used
GFU1_1	741.00	747.00	6.000	2.190	2.190		1.000	0.000	1.000	0.100	1.000	
SB1_1	747.00	747.70	0.700	0.395	0.395		1.000	0.000	1.000	0.100	1.000	
GFU2_1	747.70	752.30	4.600	4.600	4.600		1.000	0.000	1.000	0.100	1.000	
SB2_1	752.30	752.80	0.500	0.359	0.359		1.000	0.000	1.000	0.100	1.000	
GFU3_1	752.80	755.00	2.200	2.200	2.200		1.000	0.000	1.000	0.100	1.000	
SB3_1	755.00	756.30	1.300	1.300	1.300		1.000	0.000	1.000	0.100	1.000	
GFU4_1	756.30	759.70	3.400	3.400	3.400		1.000	0.000	1.000	0.100	1.000	
SB4_1	759.70	760.30	0.600	0.600	0.600		1.000	0.000	1.000	0.100	1.000	
GFU5_1	760.30	762.00	1.700	1.700	1.700		1.000	0.000	1.000	0.100	1.000	
SB5_1	762.00	763.60	1.600	0.565	0.565		1.000	0.000	1.000	0.100	1.000	

Jul 27,2000 17:41:50

Zone Name	Top Depth (m)	Bottom Depth (m)	Gross Thick. (m)	Net Res. Thick. (m)	Net Pay Thick. (m)	Dip Correction Factors	VCL max	PHIT min	SUWI max	KINT min	Discr1 FLAG <	Discr2 Not used
GFU6_1	763.60	772.10	8.500	7.738	7.738		1.000	0.000	1.000	0.100	1.000	
SB6_1	772.10	772.50	0.400	0.218	0.218		1.000	0.000	1.000	0.100	1.000	
GFU7_1	772.50	774.60	2.100	2.100	2.100		1.000	0.000	1.000	0.100	1.000	
SB7_1	774.60	775.10	0.500	0.500	0.500		1.000	0.000	1.000	0.100	1.000	
GFU8_1	775.10	781.00	5.900	5.900	5.900		1.000	0.000	1.000	0.100	1.000	
SB8_1	781.00	783.30	2.300	2.148	2.148		1.000	0.000	1.000	0.100	1.000	
GFU9_1	783.30	787.70	4.400	4.400	4.400		1.000	0.000	1.000	0.100	1.000	

ZONE SUMMATION DATA - MEASURED DEPTH

Reservoir Summation based on RHO8 discriminator.

Zone / Interval Data				Net Reservoir				Net Pay								
Zone Name	Top Depth (m)	Bottom Depth (m)	Gross Thick. (m)	Thick. (m)	PHI-Thick. (m)	Avg PHI	Avg Clay Vol	Thick. (m)	PHI-Thick. (m)	HPHI-Thick. (m)	Perm-Thick. (mD-m)	Avg PHI	Avg Sw	Avg Clay Vol	Avg Perm	Net / Gross Ratio
GFU1_1	741.00	747.00	6.00	2.19	0.64	0.293	0.603	2.19	0.64	0.03	5	0.29	0.95	0.60	1	0.36
SB1_1	747.00	747.70	0.70	0.40	0.09	0.219	0.318	0.40	0.09	0.02	39	0.22	0.71	0.32	17	0.56
GFU2_1	747.70	752.30	4.60	4.60	1.40	0.304	0.131	4.60	1.40	0.54	2221	0.30	0.61	0.13	401	1.00
SB2_1	752.30	752.80	0.50	0.36	0.05	0.152	0.295	0.36	0.05	0.01	4	0.15	0.81	0.29	10	0.72
GFU3_1	752.80	755.00	2.20	2.20	0.77	0.352	0.134	2.20	0.77	0.42	481	0.35	0.46	0.13	191	1.00
SB3_1	755.00	756.30	1.30	1.30	0.40	0.309	0.173	1.30	0.40	0.21	192	0.31	0.48	0.17	101	1.00
GFU4_1	756.30	759.70	3.40	3.40	1.12	0.330	0.132	3.40	1.12	0.43	898	0.33	0.62	0.13	216	1.00
SB4_1	759.70	760.30	0.60	0.60	0.16	0.271	0.375	0.60	0.16	0.06	18	0.27	0.63	0.37	27	1.00
GFU5_1	760.30	762.00	1.70	1.70	0.46	0.272	0.384	1.70	0.46	0.18	37	0.27	0.62	0.38	14	1.00
SB5_1	762.00	763.60	1.60	0.56	0.11	0.200	0.429	0.56	0.11	0.00	1	0.20	0.98	0.43	1	0.35
GFU6_1	763.60	772.10	8.50	7.74	2.02	0.261	0.273	7.74	2.02	0.11	557	0.26	0.94	0.27	36	0.91
SB6_1	772.10	772.50	0.40	0.22	0.06	0.292	0.151	0.22	0.06	0.00	31	0.29	1.00	0.15	142	0.55
GFU7_1	772.50	774.60	2.10	2.10	0.68	0.325	0.113	2.10	0.68	0.09	614	0.33	0.87	0.11	252	1.00
SB7_1	774.60	775.10	0.50	0.50	0.15	0.307	0.131	0.50	0.15	0.01	103	0.31	0.90	0.13	200	1.00
GFU8_1	775.10	781.00	5.90	5.90	1.91	0.324	0.111	5.90	1.91	0.08	4021	0.32	0.96	0.11	515	1.00
SB8_1	781.00	783.30	2.30	2.15	0.57	0.265	0.265	2.15	0.57	0.01	147	0.26	0.98	0.27	52	0.93
GFU9_1	783.30	787.70	4.40	4.40	1.37	0.311	0.162	4.40	1.37	0.07	691	0.31	0.95	0.16	133	1.00
TOTALS/AVERAGES OVER ALL ZONES:			46.70	40.31	11.98	0.297	0.214	40.31	11.98	2.28	10060	0.30	0.81	0.21	93	0.86

Jul 27,2000 17:41:50

GLOSSARY

Abbreviations	
Avg.	Average
GL	Ground Level
h	Depth Increment within Zone
HPHI	Hydrocarbon pore-thickness
KB.	Kelly Bushing
MSL	Mean Sea Level
Perm.	Permeability
PHI	Porosity
Sw	Water Saturation
Thick.	Thickness
TST	True Stratigraphic Thickness
TVT	True Vertical Thickness
Vcl	Clay Volume
ZGH	Gross Thickness for zone
ZH	Zone Thickness
ZNRH	Net Reservoir Thickness for Zone
ZPHI	Average Porosity for Zone
Calculations/Cutoffs	
Gross	Depths passing 'Initial' discriminator
Net	Depths passing Gross, Clay Volume cutoffs and 'Net' discriminator
Net Reservoir	Depths passing Net, Porosity cutoffs and 'Net_Reservoir' discriminator
Net Pay	Depths passing Net Reservoir, Sw, Permeability cutoffs and 'Net_Pay' discriminator
Summations	
Thick.	Sum(h)
PHI-Thick.	Sum(Porosity * h)
HPHI-Thick.	Sum(Porosity * h * (1 - Water saturation))
Perm-Thick.	Sum(Permeability * h)
Averages	
Avg PHI	Sum(Porosity * h)/Sum(h)
Avg Clay Vol	Sum(Clay Volume * h)/Sum(h)
Avg Perm (Arithmetic)	Sum(Permeability * h)/Sum(h)
Avg Perm (Geometric)	10**(Sum(LOG10(Permeability) * h)/Sum(h))
Avg Perm (Harmonic)	Sum(h) / Sum(h/Permeability)
Avg Sw	Sum(Porosity * Water Saturation * h)/Sum(Porosity * h)
Thickness-weighted Averages	
Net Reservoir to Gross Ratio	Sum(ZNRH/ZGH * ZH)/Sum(ZH)
Average Porosity	Sum(ZPHI * ZH)/Sum(ZH)
Average Sw	Sum(ZSW * ZH)/Sum(ZH)
Ratios	
Net / Gross Ratio	Net Pay Thickness / Gross Thickness
Output	
SFLG	Sand Flag Curve
RFLG	Reservoir Flag Curve
PFLG	Pay Flag Curve

Jul 27,2000 12:54:38

Reservoir Summation Based on Discriminator
and Using PIGN

OMV AUSTRALIA

BALEEN_STUDY

SUMMARY REPORT

Presentation of Data From Workshop (27-JUL-2000)

Jul 27,2000 12:54:38

LAYER SUMMATION DATA - MEASURED DEPTH
(ALL PROCESSED WELLS)

Presentation of Data From Workshop (27-JUL-2000)

Layer Data			Net - Average				Net Reservoir - Average					Net Pay - Average							
Name	Avg Gross Thick	Avg Gross PHI	Net Thick (m)	Net %	Shale Thick (m)	Shale %	Thick (m)	PHI-Thick (m)	Avg PHI	Avg Clay Vol	Net / Gross Ratio	Thick (m)	PHI-Thick (m)	HPHI-Thick (m)	Perm-Thick (mD-m)	Avg PHI	Avg Sw	Avg Clay Vol	Avg Perm	Net / Gross Ratio
GFU1	6.00	0.221	4.8	0.79	1.3	0.21	4.76	1.11	0.233	0.568	0.788	4.76	1.11	0.00	91	0.23	1.00	0.57	1	0.788
SB1	0.60	0.141	0.3	0.54	0.3	0.46	0.33	0.06	0.188	0.339	0.542	0.33	0.06	0.01	20	0.19	0.86	0.34	1	0.542
GFU2	3.93	0.283	4.1	1.00	0.0	0.00	4.10	1.15	0.283	0.163	1.000	4.10	1.15	0.37	1201	0.28	0.68	0.16	1	1.000
SB2	0.67	0.245	0.7	0.93	0.0	0.07	0.71	0.19	0.241	0.229	0.929	0.71	0.19	0.06	145	0.24	0.67	0.23	1	0.929
GFU3	2.73	0.305	2.8	1.00	0.0	0.00	2.79	0.85	0.305	0.134	1.000	2.79	0.85	0.41	1667	0.30	0.52	0.13	1	1.000
SB3	0.77	0.270	1.0	1.00	0.0	0.00	0.96	0.26	0.270	0.194	1.000	0.96	0.26	0.11	224	0.27	0.53	0.19	1	1.000
GFU4	2.90	0.312	2.9	1.00	0.0	0.00	2.95	0.92	0.312	0.158	1.000	2.95	0.92	0.37	2121	0.31	0.59	0.16	1	1.000
SB4	0.53	0.256	0.5	1.00	0.0	0.00	0.54	0.14	0.256	0.302	1.000	0.54	0.14	0.06	50	0.26	0.53	0.30	1	1.000
GFU5	1.27	0.258	1.4	1.00	0.0	0.00	1.37	0.35	0.258	0.287	1.000	1.37	0.35	0.13	147	0.26	0.61	0.29	1	1.000
SB5	2.17	0.187	1.6	0.69	0.6	0.31	1.61	0.35	0.210	0.346	0.691	1.61	0.35	0.15	105	0.21	0.63	0.35	1	0.691
GFU6	8.33	0.250	8.1	0.95	0.4	0.05	8.14	2.07	0.255	0.255	0.951	8.14	2.07	0.60	993	0.26	0.74	0.26	1	0.951
SB6	0.43	0.204	0.3	0.69	0.1	0.31	0.31	0.08	0.213	0.307	0.689	0.31	0.08	0.03	83	0.21	0.71	0.31	1	0.689
GFU7	2.30	0.290	2.4	1.00	0.0	0.00	2.41	0.71	0.290	0.199	1.000	2.41	0.71	0.24	656	0.29	0.68	0.20	1	1.000
SB7	0.70	0.249	0.5	0.71	0.2	0.29	0.49	0.13	0.263	0.273	0.708	0.49	0.13	0.06	42	0.26	0.55	0.27	1	0.708
GFU8	4.83	0.293	5.0	0.97	0.1	0.03	4.99	1.47	0.294	0.172	0.968	4.99	1.47	0.39	1569	0.29	0.68	0.17	1	0.968
SB8	1.47	0.231	1.4	0.68	0.4	0.32	1.36	0.34	0.246	0.263	0.680	1.36	0.34	0.03	129	0.25	0.74	0.26	1	0.680
GFU9	4.40	0.260	4.2	0.94	0.3	0.06	4.17	1.10	0.263	0.258	0.942	4.17	1.10	0.30	794	0.26	0.71	0.26	1	0.942

9030080 111

Jul 27,2000 12:54:38

WELL INFORMATION

Project:	BALEEN_STUDY	
Field:	VIC/RL5	
Operator:	CULTUS PETROLEUM NL	
Well:	Baleen-2	
Well Location:	Lat/Long (deg):	N/A /N/A
	X/Y (m):	-6.40126e+0/1e+07
	Legal:	N/A
	State:	Victoria
	Country:	N/A
Elevation:	KB (m):	N/A
	GL (m):	4294945536.000
	MSL (m):	N/A

Presentation of Data From Workshop (27-JUL-2000)

Baleen-2

SUMMARY FOR RESERVOIR Default_Summation_Reservoir SUMMATION MODEL JULY_27_OMV

	MD	TVD	TVT	TST
Top of zones (measured depth):	741			
Base of zones (measured depth):	787.7			
Total gross thickness for all zones:	46.7000	N/A	N/A	N/A
Total net thickness for all zones:	40.3122	N/A	N/A	N/A
Total net reservoir thickness for all zones:	40.3122	N/A	N/A	N/A
Total net pay thickness for all zones:	40.3122	N/A	N/A	N/A
Thickness-weighted net reservoir to gross ratio:	0.8632	N/A	N/A	N/A
Thickness-weighted average net pay porosity:	0.2670	N/A	N/A	N/A
Thickness-weighted average net pay Sw:	0.8704	N/A	N/A	N/A
Cumulative porosity thickness for all zones:	10.7619	N/A	N/A	N/A
Cumulative permeability thickness for all zones:	6305.6626	N/A	N/A	N/A
Cumulative hydrocarbon thickness for all zones:	1.3951	N/A	N/A	N/A

Jul 27,2000 12:54:38

ZONE SUMMATION PARAMETERS

Well: Baleen-2

Curves used:
- Clay Volume: VCL [A3453962]
- Porosity: PIGN [A3453950]
- Water Saturation: SUWI [A3453958]
- Permeability: KINT [A3454165]
- Discriminator 1: FLAG [A3455028]
- Discriminator 2: Not used

Discriminator Application Point 1: Initial
Discriminator Application Point 2: Initial

Averaging used for Permeability: Geometric

Zone Name	Top Depth (m)	Bottom Depth (m)	Gross Thick. (m)	Net Res. Thick. (m)	Net Pay Thick. (m)	Dip Correction Factors	VCL max	PIGN min	SUWI max	KINT min	Discr1 FLAG <	Discr2 Not used
GFU1_1	741.00	747.00	6.000	2.190	2.190		1.000	0.000	1.000	0.100	1.000	
SB1_1	747.00	747.70	0.700	0.395	0.395		1.000	0.000	1.000	0.100	1.000	
GFU2_1	747.70	752.30	4.600	4.600	4.600		1.000	0.000	1.000	0.100	1.000	
SB2_1	752.30	752.80	0.500	0.359	0.359		1.000	0.000	1.000	0.100	1.000	
GFU3_1	752.80	755.00	2.200	2.200	2.200		1.000	0.000	1.000	0.100	1.000	
SB3_1	755.00	756.30	1.300	1.300	1.300		1.000	0.000	1.000	0.100	1.000	
GFU4_1	756.30	759.70	3.400	3.400	3.400		1.000	0.000	1.000	0.100	1.000	
SB4_1	759.70	760.30	0.600	0.600	0.600		1.000	0.000	1.000	0.100	1.000	
GFU5_1	760.30	762.00	1.700	1.700	1.700		1.000	0.000	1.000	0.100	1.000	
SB5_1	762.00	763.60	1.600	0.565	0.565		1.000	0.000	1.000	0.100	1.000	

908080 114

Jul 27,2000 12:54:38

Zone Name	Top Depth (m)	Bottom Depth (m)	Gross Thick. (m)	Net Res. Thick. (m)	Net Pay Thick. (m)	Dip Correction Factors	VCL max	PIGN min	SUWI max	KINT min	Discr1 FLAG <	Discr2 Not used
GFU6_1	763.60	772.10	8.500	7.738	7.738		1.000	0.000	1.000	0.100	1.000	
SB6_1	772.10	772.50	0.400	0.218	0.218		1.000	0.000	1.000	0.100	1.000	
GFU7_1	772.50	774.60	2.100	2.100	2.100		1.000	0.000	1.000	0.100	1.000	
SB7_1	774.60	775.10	0.500	0.500	0.500		1.000	0.000	1.000	0.100	1.000	
GFU8_1	775.10	781.00	5.900	5.900	5.900		1.000	0.000	1.000	0.100	1.000	
SB8_1	781.00	783.30	2.300	2.148	2.148		1.000	0.000	1.000	0.100	1.000	
GFU9_1	783.30	787.70	4.400	4.400	4.400		1.000	0.000	1.000	0.100	1.000	

ZONE SUMMATION DATA - MEASURED DEPTH

Presentation of Data From Workshop (27-JUL-2000)

Zone / Interval Data				Net Reservoir				Net Pay								
Zone Name	Top Depth (m)	Bottom Depth (m)	Gross Thick. (m)	Thick. (m)	PHI-Thick. (m)	Avg PHI	Avg Clay Vol	Thick. (m)	PHI-Thick. (m)	HPHI-Thick. (m)	Perm-Thick. (mD-m)	Avg PHI	Avg Sw	Avg Clay Vol	Avg Perm	Net / Gross Ratio
GFU1_1	741.00	747.00	6.00	2.19	0.50	0.229	0.593	2.19	0.50	0.00	25	0.23	1.00	0.59	7	0.36
SB1_1	747.00	747.70	0.70	0.40	0.07	0.184	0.365	0.40	0.07	0.02	9	0.18	0.76	0.36	9	0.56
GFU2_1	747.70	752.30	4.60	4.60	1.29	0.280	0.191	4.60	1.29	0.37	906	0.28	0.71	0.19	174	1.00
SB2_1	752.30	752.80	0.50	0.36	0.05	0.130	0.313	0.36	0.05	0.01	15	0.13	0.80	0.31	11	0.72
GFU3_1	752.80	755.00	2.20	2.20	0.70	0.320	0.184	2.20	0.70	0.29	757	0.32	0.59	0.18	338	1.00
SB3_1	755.00	756.30	1.30	1.30	0.34	0.265	0.241	1.30	0.34	0.13	139	0.26	0.63	0.24	95	1.00
GFU4_1	756.30	759.70	3.40	3.40	1.05	0.310	0.239	3.40	1.05	0.30	850	0.31	0.71	0.24	198	1.00
SB4_1	759.70	760.30	0.60	0.60	0.14	0.230	0.397	0.60	0.14	0.03	9	0.23	0.80	0.40	13	1.00
GFU5_1	760.30	762.00	1.70	1.70	0.39	0.231	0.401	1.70	0.39	0.07	32	0.23	0.81	0.40	13	1.00
SB5_1	762.00	763.60	1.60	0.56	0.10	0.178	0.372	0.56	0.10	0.00	3	0.18	0.96	0.37	3	0.35
GFU6_1	763.60	772.10	8.50	7.74	1.79	0.232	0.319	7.74	1.79	0.06	412	0.23	0.97	0.32	25	0.91
SB6_1	772.10	772.50	0.40	0.22	0.02	0.103	0.536	0.22	0.02	0.00	0	0.10	1.00	0.54	0	0.55
GFU7_1	772.50	774.60	2.10	2.10	0.60	0.285	0.272	2.10	0.60	0.03	291	0.28	0.94	0.27	111	1.00
SB7_1	774.60	775.10	0.50	0.50	0.14	0.273	0.233	0.50	0.14	0.01	59	0.27	0.93	0.23	115	1.00
GFU8_1	775.10	781.00	5.90	5.90	1.82	0.308	0.177	5.90	1.82	0.05	2047	0.31	0.97	0.18	314	1.00
SB8_1	781.00	783.30	2.30	2.15	0.54	0.251	0.250	2.15	0.54	0.00	191	0.25	1.00	0.25	61	0.93
GFU9_1	783.30	787.70	4.40	4.40	1.21	0.274	0.241	4.40	1.21	0.02	561	0.27	0.99	0.24	105	1.00
TOTALS/AVERAGES OVER ALL ZONES:			46.70	40.31	10.76	0.267	0.273	40.31	10.76	1.40	6306	0.27	0.87	0.27	73	0.86

903080 116

Jul 27,2000 18:04:59

WELL INFORMATION

Project:	BALEEN_STUDY	
Field:	VIC/RL5	
Operator:	CULTUS PETROLEUM NL	
Well:	Baleen-2	
Well Location:	Lat/Long (deg):	N/A /N/A
	X/Y (m):	-6.40126e+0/1e+07
	Legal:	N/A
	State:	N/A
	Country:	N/A
Elevation:	KB (m):	N/A
	GL (m):	4294945536.000
	MSL (m):	N/A

Presentation of Data From Workshop (27-JUL-2000) PHIT

SUMMARY FOR RESERVOIR Default_Summation_Reservoir SUMMATION MODEL JULY_27_OMV

	MD	TVD	TVT	TST
Top of zones (measured depth):	741			
Base of zones (measured depth):	787.7			
Total gross thickness for all zones:	46.7000	N/A	N/A	N/A
Total net thickness for all zones:	40.3122	N/A	N/A	N/A
Total net reservoir thickness for all zones:	40.3122	N/A	N/A	N/A
Total net pay thickness for all zones:	40.3122	N/A	N/A	N/A
Thickness-weighted net reservoir to gross ratio:	0.8632	N/A	N/A	N/A
Thickness-weighted average net pay porosity:	0.3008	N/A	N/A	N/A
Thickness-weighted average net pay Sw:	0.8734	N/A	N/A	N/A
Cumulative porosity thickness for all zones:	12.1279	N/A	N/A	N/A
Cumulative permeability thickness for all zones:	6305.6626	N/A	N/A	N/A
Cumulative hydrocarbon thickness for all zones:	1.5356	N/A	N/A	N/A

Jul 27,2000 18:04:59

ZONE SUMMATION PARAMETERS

Well: Baleen-2

Curves used:
- Clay Volume: VCL [A3453962]
- Porosity: PHIT [A3453946]
- Water Saturation: SUWI [A3453958]
- Permeability: KINT [A3454165]
- Discriminator 1: FLAG [A3455028]
- Discriminator 2: Not used

Discriminator Application Point 1: Initial
Discriminator Application Point 2: Initial

Averaging used for Permeability: Geometric

Zone Name	Top Depth (m)	Bottom Depth (m)	Gross Thick. (m)	Net Res. Thick. (m)	Net Pay Thick. (m)	Dip Correction Factors	VCL max	PHIT min	SUWI max	KINT min	Discr1 FLAG <	Discr2 Not used
GFU1_1	741.00	747.00	6.000	2.190	2.190		1.000	0.000	1.000	0.100	1.000	
SB1_1	747.00	747.70	0.700	0.395	0.395		1.000	0.000	1.000	0.100	1.000	
GFU2_1	747.70	752.30	4.600	4.600	4.600		1.000	0.000	1.000	0.100	1.000	
SB2_1	752.30	752.80	0.500	0.359	0.359		1.000	0.000	1.000	0.100	1.000	
GFU3_1	752.80	755.00	2.200	2.200	2.200		1.000	0.000	1.000	0.100	1.000	
SB3_1	755.00	756.30	1.300	1.300	1.300		1.000	0.000	1.000	0.100	1.000	
GFU4_1	756.30	759.70	3.400	3.400	3.400		1.000	0.000	1.000	0.100	1.000	
SB4_1	759.70	760.30	0.600	0.600	0.600		1.000	0.000	1.000	0.100	1.000	
GFU5_1	760.30	762.00	1.700	1.700	1.700		1.000	0.000	1.000	0.100	1.000	
SB5_1	762.00	763.60	1.600	0.565	0.565		1.000	0.000	1.000	0.100	1.000	

Jul 27,2000 18:04:59

Zone Name	Top Depth (m)	Bottom Depth (m)	Gross Thick. (m)	Net Res. Thick. (m)	Net Pay Thick. (m)	Dip Correction Factors	VCL max	PHIT min	SUWI max	KINT min	Discr1 FLAG <	Discr2 Not used
GFU6_1	763.60	772.10	8.500	7.738	7.738		1.000	0.000	1.000	0.100	1.000	
SB6_1	772.10	772.50	0.400	0.218	0.218		1.000	0.000	1.000	0.100	1.000	
GFU7_1	772.50	774.60	2.100	2.100	2.100		1.000	0.000	1.000	0.100	1.000	
SB7_1	774.60	775.10	0.500	0.500	0.500		1.000	0.000	1.000	0.100	1.000	
GFU8_1	775.10	781.00	5.900	5.900	5.900		1.000	0.000	1.000	0.100	1.000	
SB8_1	781.00	783.30	2.300	2.148	2.148		1.000	0.000	1.000	0.100	1.000	
GFU9_1	783.30	787.70	4.400	4.400	4.400		1.000	0.000	1.000	0.100	1.000	

ZONE SUMMATION DATA - MEASURED DEPTH

Presentation of Data From Workshop (27-JUL-2000) PHIT

Zone / Interval Data				Net Reservoir				Net Pay							
Zone Name	Top Depth (m)	Bottom Depth (m)	Gross Thick. (m)	Thick. (m)	PHI-Thick. (m)	Avg PHI	Avg Clay Vol	Thick. (m)	PHI-Thick. (m)	HPHI-Thick. (m)	Perm-Thick. (mD-m)	Avg PHI	Avg Sw	Avg Clay Vol	Avg Perm	Net / Gross Ratio
GFU1_1	741.00	747.00	6.00	2.19	0.66	0.303	0.593	2.19	0.66	0.00	25	0.30	1.00	0.59	7	0.36
SB1_1	747.00	747.70	0.70	0.40	0.09	0.229	0.365	0.40	0.09	0.02	9	0.23	0.78	0.36	9	0.56
GFU2_1	747.70	752.30	4.60	4.60	1.40	0.304	0.191	4.60	1.40	0.41	906	0.30	0.71	0.19	174	1.00
SB2_1	752.30	752.80	0.50	0.36	0.06	0.168	0.313	0.36	0.06	0.01	15	0.17	0.82	0.31	11	0.72
GFU3_1	752.80	755.00	2.20	2.20	0.75	0.343	0.184	2.20	0.75	0.31	757	0.34	0.59	0.18	338	1.00
SB3_1	755.00	756.30	1.30	1.30	0.38	0.295	0.241	1.30	0.38	0.14	139	0.29	0.63	0.24	95	1.00
GFU4_1	756.30	759.70	3.40	3.40	1.15	0.339	0.239	3.40	1.15	0.33	850	0.34	0.71	0.24	198	1.00
SB4_1	759.70	760.30	0.60	0.60	0.17	0.279	0.397	0.60	0.17	0.03	9	0.28	0.80	0.40	13	1.00
GFU5_1	760.30	762.00	1.70	1.70	0.48	0.281	0.401	1.70	0.48	0.09	32	0.28	0.81	0.40	13	1.00
SB5_1	762.00	763.60	1.60	0.56	0.13	0.224	0.372	0.56	0.13	0.01	3	0.22	0.96	0.37	3	0.35
GFU6_1	763.60	772.10	8.50	7.74	2.10	0.271	0.319	7.74	2.10	0.07	412	0.27	0.97	0.32	25	0.91
SB6_1	772.10	772.50	0.40	0.22	0.04	0.169	0.536	0.22	0.04	0.00	0	0.17	1.00	0.54	0	0.55
GFU7_1	772.50	774.60	2.10	2.10	0.67	0.318	0.272	2.10	0.67	0.04	291	0.32	0.94	0.27	111	1.00
SB7_1	774.60	775.10	0.50	0.50	0.15	0.302	0.233	0.50	0.15	0.01	59	0.30	0.93	0.23	115	1.00
GFU8_1	775.10	781.00	5.90	5.90	1.95	0.331	0.177	5.90	1.95	0.05	2047	0.33	0.97	0.18	314	1.00
SB8_1	781.00	783.30	2.30	2.15	0.61	0.282	0.250	2.15	0.61	0.00	191	0.28	1.00	0.25	61	0.93
GFU9_1	783.30	787.70	4.40	4.40	1.34	0.304	0.241	4.40	1.34	0.02	561	0.30	0.99	0.24	105	1.00
TOTALS/AVERAGES OVER ALL ZONES:			46.70	40.31	12.13	0.301	0.273	40.31	12.13	1.54	6306	0.30	0.87	0.27	73	0.86

APPENDIX 3

BALEEN-2

PRODUCTION STABILITY EVALUATION REPORT

-SCHLUMBERGER-

Schlumberger

Production Stability Evaluation

Patricia Baleen

Company: OMV Australia Pty Ltd.

Field Location: Gippsland Basin - Offshore Victoria

Country: Australia

Reference: G12270LM

by L. Murphy & J.Fuller

February 2000

Table of Contents

0.0 SUMMARY

The objective of the study was to assess the potential for sand production in the Patricia Baleen Gasfield, offshore Victoria, Australia using data from the Baleen-2 well. Data from the main gas bearing reservoir, the Gurnard formation, has been analysed to determine the critical draw-down pressure differential during production where formation failure will occur and sand production can result. The results from the study will be used to assess mechanical stability during production on the field and support decisions on completion design.

A geomechanical model of the reservoir has been constructed, quantifying the in-situ stress state and the rock strength. Rock compressive strengths have been measured on core from the reservoir section of the well to calibrate log estimates of uniaxial compressive strength. Results of these mechanical tests on three sets of samples from three depth points from Baleen-2 give an unconfined compressive strength of 3.41 - 4.4 MPa, which is relatively low for Sandstone. Estimates of rock strength from sonic log data in the well, computed independently, agreed very closely with core measurements.

Further single stage core tests have been performed to calibrate an elasto-plastic model of sand failure during production drawdown. Plasticity gives the rock an apparent increase in strength and hence improves stability during production. Particularly plastic sandstones can appear to be up to six times stronger under production than their nominal rock strength. Samples from Baleen-2 in this study showed increases in apparent strength of 3.3 times the measured value, which indicates that the reservoir rocks are reasonably plastic.

Overburden and minimum horizontal stress have been calculated from log data integrated with core and a direct measurement from Baleen-2. A pore pressure profile was also input, which was necessary to estimate the effective stress caused by internal fluid support.

A depth indexed continuous critical drawdown profile has been produced for Baleen-2 indicating the safe (no sand) drawdown limit. The results show that the reservoir is likely to fail under any drawdown condition and the Patricia-Baleen wells will require some form of sand control system. This is mainly a consequence of low rock strength. The results also include discussion on perforation tunnel scale effects on stability. Given that the formation is predicted to fail under initial reservoir pressures, no depletion estimates were necessary.

1.0 INTRODUCTION

This study assesses the potential for sand production in the Patricia Baleen Gurnard reservoir. The reservoir has been analysed to find the critical draw-down pressure and to identify intervals where formation failure will occur and sand production will result. The study also considered how the point of failure is altered as a result of stress changes induced by reservoir depletion.

A geomechanical model of the reservoir has been constructed, quantifying the in-situ stress state, rock strength and other constitutive properties. The study also evaluated the mechanical properties of the reservoir. The input data used were: the wireline logs, including sonic compressional, shear measurements and density logs, and core measurements of strength, friction angle and elastic properties computed for Baleen-2.

The analysis of formation failure combines a continuous, depth-indexed elasto-brittle solution, which also gives a qualitative assessment of relative stability within the reservoir, with the single point results from elasto-plastic modelling calibrated with the core measurements. The procedure provides a continuous, depth-indexed estimate of the draw-down required to cause formation failure at the perforation tunnel (Bradford et al, 1998). The results are obtained using ROXAN[1] software.

Geomechanical and other log evaluation was performed by Schlumberger Holditch Reservoir Technologies, Gatwick and Schlumberger Cambridge Research. The laboratory core measurements were performed by CSIRO, Melbourne, Australia.

The report includes appendices which further explain steps in the analysis and give more general geomechanics information.

[1] ROXAN is a multi-application mechanical properties evaluation software

2.0 GEOMECHANICAL ANALYSIS

2.1 Input Data

The study of formation integrity during production was conducted on log data acquired in Baleen-2. The logs include compressional sonic and density required for the calculation of elastic properties. Shear sonic data, required to calculate elastic properties, was available also used.

The sonic data was gas corrected using Biot-Gassmann equations, which correct for fluid effects on the sonic results, so that mechanical properties are consistent throughout the reservoir sands regardless of the saturating fluid.

Mechanical testing was performed on core samples from Baleen-2 and details of these tests are described in Appendix 2

The petrophysial evaluation of Baleen-2 included in the analysis of mechanical properties was provided by Schlumberger GeoQuest, Melbourne.

OMV Australia Pty Ltd further provided reports on well summary information, reservoir modelling and core analysis for the Patricia Baleen wells Patricia-1 and Baleen-1.

2.2 Rock Strength

Rock strength calculations were based on laboratory tests of core samples recovered from the reservoir section of Baleen-2 and a strength correlation using work by Plumb, 1994[2]. The core samples were analysed using triaxial compression testing conducted by Bailin Wu with equipment at CSIRO, Melbourne. Results of these tests are included in Appendix 2.

Rock strength has been computed from empirical equations derived from log measurements and from laboratory tests on cores, giving a continuous log of unconfined compressive strength. The form of the correlation used in this study between elastic moduli and rock strength was first observed by Deere and Miller[3].

Deere and Miller's work led to the assertion that unconfined compressive strength (UCS) was proportional to Young's Modulus, the constant of proportionality being

[2] Plumb R.A., Influence of Composition and Texture on the Failure Properties of Clastic Rocks, SPE/ISRM 28022, Eurock Aug. 1994.

[3] Deere D.U. and Miller R.P., 1966, Engineering Classification and Index Properties for Intack Rock, Technical Report No. AFWL-TR-65-116, Air Force Weapons Laboratory, Kirtland, New Mexico.

a function of the clay content, and to the internal friction coefficient of the rock, as shown below.

$$UCS = Young's\ Modulus*A + B$$

Due to the nature of the data used, the approach to derive a rock strength log involves two steps: Firstly a conversion of log elastic moduli from dynamic to static. The second step involves the correlation of the elastic property to strength. The conversion of dynamic Young's Modulus from logs to a static equivalent is based on a North Sea correlation of core (static) points to log (dynamic) points (Fuller)[4].

$$YME.stat = 0.032 * YME.dyn ** 1.623$$

where YME.stat = Young's Modulus from core
YME.dyn = Young's Modulus from log

The static elastic modulus can now be correlated to unconfined compressive strength. Work by Plumb 1994[2], using a world-wide data-base of borehole recovered core samples confirms the trend first observed by Deere and Miller. Their work was based on rock well above 5000 psi, however Plumb's correlation is more widely applicable to less strong, reservoir sandstones in the range 100 to 5000 psi unconfined compressive strength.

The equation is as follows:

$$UCS = 2.280 + 4.1089*YME\ stat.$$

where UCS = unconfined compressive strength
and YME.stat.= Young's Modulus from core
the coefficient of regression is 0.925.

2.3 In-situ State of Stress

The overburden gradient was estimated from the integrated density measurement extrapolated to surface. It is assumed the maximum principal stress is vertical. The minimum horizontal stress was computed from a frictional slip model based on the Mohr-Coulomb failure model. The model assumes the formation is at failure and uses a friction angle derived from the volume of clay, pore pressure and the overburden stress as inputs.

[4] Fuller J.A., Schlumberger Holditch-Reservoir Technologies, Internally communicated publication.

The direction of the minimum horizontal stress was not specifically considered in the study. There were no stress orientation data available from the wells studied. For vertical wells in this case, perforations orientated towards the maximum horizontal stress would have the highest levels of stress and as a consequence the greatest risk of sanding. This "worst case" has been considered in the sand production analysis.

The pore pressure used to estimate effective stress was from RFT data over interval 749.3m to 823.0m in Baleen-2. Reduction in the reservoir pressure due to depletion will increase the mean effective stress in the reservoir, inducing earlier formation failure and reducing safe draw-down limits. Estimates of these effects are included in the results.

2.4 Formation Failure

Draw-down failure analysis calculates the point at which the formation will fail during production as the pressure in the wellbore is reduced. The analysis provides a continuous, depth indexed, log of the *Critical Draw-down* (presented on the enclosed *Production Stability* log) required to cause formation failure. The analysis combines two approaches: elasto-brittle modelling, which is based on rock strength, elastic properties and in-situ stresses, and a single point calibration using elasto-plastic modelling (Bradford and Cook, 1994)[5]. The elasto-plastic model was calibrated using a single stage core test performed on core from Baleen-2.

Plastic deformation of the reservoir rock occurs after yielding and appears to raise the strength of the rock making the reservoir more stable than predicted from pure elasto-brittle analysis. To practically present a continuous *Critical Draw-down* log including the effects of the plastic behaviour observed in the core tests, the elasto-brittle analysis has been modified with the effects of plasticity by applying an offset or boost factor, since the failure model is linear, to the unconfined compressive strength. The approach makes the assumption that the plastic behaviour observed in the laboratory test remains constant throughout the reservoir interval. In this case a series of single stage tests characterised specific units.

[5] Bradford I.D.R., Cook J.M., A Semi-analytic Elastoplastic Model for Wellbore Stability with Applications to Sanding, SPE/ISRM Eurock 94, Delft, 1994.

3.0 DISCUSSION OF RESULTS

Formation failure leading to the onset of sanding in the Baleen-2 well has been calculated with a continuous, depth-indexed, elasto-brittle model calibrated with elasto-plastic. The results are displayed in the enclosed logs. Enclosure 1, *Dynamic Elastic Moduli and Rock Properties* shows mechanical properties and stress data. Enclosure 2, *Formation Integrity Sanding Production* provides the crtical drawdown profile.

3.1 Elastic Properties and Rock Strength

Elastic properties and rock strength were calculated from log and core measurements. Table 1 shows the rock strength, UCS, estimated from Young's Modulus (YME) using Plumb and the UCS and Poisson's Ratio calculated from multiple stage core tests.

Core Test	Depth, m mdbrt	YME core (Gpa)	Poissons Ratio	UCS Plumb (Mpa)	UCS core (Mpa)
1	750.82	0.30	0.486	3.71	3.125
2	756.52	0.60	0.475	4.4	4.215
3	760.23	0.75	0.474	4.33	4.18
4	769.67	0.30	0.48	4.28	0.48
5	777.00	0.25	0.39	3.41	1.65

Table 1. Elastic Properties and Rock Strength from Baleen-2 Core samples.

Log derived vlues of elastic moduli and rock strength have been verified with core measurements and calculations. There was close agreement between both for the first three tests, however the core estimates of rock strength were lower than the log estimates in tests 4 and 5, although the estimates of Young's modulus still closely agreed. Both these samples were from the water leg and the high water saturation may have influenced rock strength.

These values have been displayed in Enclosure 1 with the log-derived values for comparison.

3.2 In-situ State of Stress

The overburden stress gradient was estimated to be 0.93 psi/ft from the integrated bulk density log data, extrapolating the top most value to surface. The least principal stress (minimum horizontal stress) was calculated from a frictional slip model using

Mohr Coulomb failure criteria. Inputs were the overburden stress (assumed maximum principal stress), pore pressure and friction angle. Results are displayed on the enclosed logs. The initial reservoir pressure, required to estimate the effective stress caused by internal fluid support, was taken as 1074 psi at 750.72 m.

The maximum horizontal stress was estimated to be 1.05 times higher than the minimum horizontal stress, although the precise level of this stress is not required in the stability calculations for the Baleen-2 well. The horizontal stress ratio estimate is based on the mechanical properties of the rock: The reservoir has a very low Young's modulus or stiffness and therefore will not be expected to sustain any significant lateral stress anisotropy. Although the region may be under compression, high regional stresses will be barely transmissible through these rocks and it is reasonable to assume that most of the horizontal stress is generated by gravitational loading.

For vertical wells in this case, perforations orientated towards the maximum horizontal stress would have the highest levels of stress and as a consequence the greatest risk of sanding. This "worst case" has been considered in the sand production analysis below, although due to the minimal stress anisotropy there is expected to be little difference in the stability for horizontal perforations in any direction.

3.3 Critical Draw-down

The measurements of stress and strength were used to derive an elasto-brittle model of the critical drawdown pressure to fail the formation. The elasto-brittle models are generally too conservative and predict failure earlier than is normally observed. Rocks normally show some degree of plasticity which allows the rock to strengthen after yielding. Two single stage core tests were performed on core from Baleen-2 to calibrate an elasto-plastic model. These tests were conducted with confining pressures of 6 MPa, close to the initial mean effective stress6 of the reservoir, and 9 MPa, which will represent the stress state later during depletion.

3.3.1 Elasto-plastic Modelling

Elasto-plastic effects were calculated using an analytical model of elasto-plasticity (Bradford & Cook, 1994)5. Single stage core tests conducted at approximately the mean effective reservoir stress: 6 MPa, were used to calibrate elastic and plastic parameters. Plastic hardening parameters a1, b1 and n are power law terms from

[6] Mean effective stress of the reservoir, is the average of the three stress magnitudes (Vertical, Maximum Horizontal and Minimum Horizontal) minus the pore pressure of the reservoir.

the best fit of the post yield section of the core test. Elasto-plastic constitutive parameters from the 6 MPa test at each depth are shown below in Table 2.

Elasto-plastic parameter	Sample 1	Sample 2	Sample 3	Sample 4	Sample 5
Depth	750.82	756.52	760.23	769.67	777.0
Young's Modulus (Gpa)	1.02	1.213	0.96	1.04	1.02
Poisson's Ratio	0.241	0.176	0.201	0.223	0.244
Friction Angle (degs)	24.74	19.8	13.25	17.6	20.6
Dilation Angle (degs)	-0.9403	-	2.2882	-9.4164	-6.6721
Plastic hardening offset, a1	0.09	-	3.20	0.91	0.62
Plastic hardening gain, b1	12.18	-	4.34	23.61	16.93
Plastic hardening exponent, n	0.38	-	0.25	0.37	0.30
maximum plastic millistrain	36.7783	-	56.9592	23.7878	16.6719
UCS calibration factor	3.08	No peak	3.4694	2.52	3.24

Table 2. Elastoplastic parameters calculated from 6 MPa stage core test on Baleen-2

The UCS calibration factor is the ratio of calculated rock strength and the apparent rock strength. This factor is used to boost the log-derived estimates of sand strength for use in sand prediction calculations.

Elasto-plastic calculations for Sample 2 could not be made because the sample did not achieve a peak strength (No peak).

As a general note, the elasto-plastic modelling reveals that this material yields almost as soon as it is subjected to any load. In addition it compacts and has massive ductility.

3.3.2 Calculation of Critical Drawdown

Formation failure occurs when the effective hoop stress or tangential stress to the perforation exceeds the rock strength ($\sigma_{\theta f} > UCS_{boosted}$). For a vertical wellbore, with perforations lying along the minimum stress direction, the maximum hoop stress is:

$$\sigma_{\theta f} = 3.\sigma_v - \sigma_h - P_p - P_w$$

so the wellbore pressure is:

$$P_w = 3.\sigma_v - \sigma_h - P_p - \sigma_{\theta f}$$

$= 3.\sigma_v - \sigma_h - P_p - UCS_{boosted}$ for sand production.

and the critical draw-down is:

$C_{dd} = P_p - P_w$

where σ_v = vertical stress
σ_h = min. horizontal stress
P_p = pore pressure
P_w = well pressure

The critical draw-down prediction based on this modelling and the log derived measurements is displayed on the *Production Sanding* log.

The critical drawdown profile for Baleen-2 indicates that the reservoir is likely to fail early in production as a consequence of the low rock strength calculated from the elasto-plastic modelling work.

Results of the critical drawdown analysis are shown in Enclosure 2. The critical drawdown log in track 2 indicates the well pressure required to fail the formation. Positive drawdowns are shown to the right of the zero line in MPa.

3.4 Sanding Process

These results indicate formation failure at the sand face during production, however it is important to consider how sand is produced. Sand production is generally the result of two extrinsic parameters: stress and flow (Cook 1993)[7]. When a perforation tunnel is in a failed state due to applied stress, material can only be carried from the perforation if there is sufficient flow. The contribution of flow to the stress state is negligible in itself and therefore will not fail the rock, however flow along the perforation tunnel can remove damaged/yielded material from the wall if the flow is fast enough. The flow rate through a perforation required to transport sand is approximately 200 mm/sec. By comparison, the average flow through a producing perforation, when all perforations are contributing, is only between 1-10 mm/sec. or for an average perforation tunnel, approximately 25 bopd. Therefore although a zone may be in a failed state, if the flow is not high enough material will not be transported into the wellbore and no sanding will occur. However poor clean-up after perforating can lead to only a limited number of producing perforations, which results in higher than expected flows in these perforation tunnels, possibly leading to removal of yielded material. Therefore perforations in zones with draw-downs below the critical level are at risk of sanding. In gas wells the flow rates tend to be

[7] Cook J.M., A Study of Physical Mechanisms of Sanding and Application to Sand Production Prediction, SPE, 1993.

higher increasing the transport capacity. However as with the oil case, if the rock is not in a failed state then sand production is unlikely.

In general stability can be improved by; changing perforation geometry. For instance, the state of stress around a vertical perforation from a horizontal well can be much lower than that of a horizontal perforation, making the onset of failure much later. Alternatively, stimulation methods such as frac/pack and screenless completions can increase productivity and at the same time reduce drawdown and sanding risk.

3.4.1 Perforation Size Effects

Large perforating guns will reduce velocity but, to some extent, at the expense of perforation tunnel stability. The calculations in the preceding results sections do not take account of the perforation tunnel dimensions. However new work from Schlumberger Cambridge Research, as yet unpublished, provides a quantitative estimate of the scale effect between wellbore dimensions and perf dimensions. As an example for Patricia Baleen:

Given the mechanical model at an average point as follows:

sig_v = 15.9 Mpa
sig_h = 10.8
Pp = 7.4
UCS = 4.2, UCS boosted for elasto-plastic effects is 14.5

Then,

Pw = 3sig_v - sig_h - Pp - UCS
Pw = 3x15.9 - 10.8 - 7.4 - 14.5
Pw = 15.

The well pressure required to maintain formation stability is 15 Mpa (2175 psi) as the reservoir pressure is 7.4 Mpa (1073 psi) then clearly the well cannot be produced without reducing the well pressure below the failure limit.

Using the SCR work on perforation tunnel stability , a perf oration of 1" diameter would have a boost factor (on the nominal UCS, elastoplastic modelling included) of approximately 5 in this case. Therefore the boosted UCS to take account of perf tunnel dimensions and elasto-plasticity is 21 Mpa. On this basis Pw = 8.5 Mpa, this still exceeds reservoir pressure of 7.4 Mpa. Therefore the well cannot be produced without formation failure.

3.5 Effects of Depletion

As fluid support is withdrawn from the reservoir during depletion the level of stress will increase and the onset of sand failure will be expected earlier.

Given that the formation is predicted to fail under initial reservoir pressures, no depletion estimates were necessary.

4.0 CONCLUSIONS

1. Mechanical properties have been calculated on well Baleen-2 to assess the formation integrity during production on these wells.

2. Rock compressive strengths and friction angles have been measured on core from the reservoir section and have been used to validate log estimates.

3. A continuous depth-indexed, elasto-brittle model of formation failure from logs has been calibrated with elasto-plastic modelling, to calculate a critical draw-down pressure log for each well.

4. The critical drawdown profile for Baleen-2 indicates that the reservoir will fail when any draw down is put on the formation (i.e at any flow rate). This is mainly a consequence of low rock strength. Results indicate that sand management or prevention will be required from the outset.

5. Calculations of sanding for perforation tunnel dimensions indicate that the formation stability is higher than at wellbore dimensions, however the well still cannot be produced without exceeding the failure limit.

6. Core tests show evidence of compaction at initial reservoir pressure conditions, as inferred by the 6MPa single stage tests. These effects will increase during depletion as the stress state increases, which is evident in the 9MPa single stage tests. This increase in stress state is likely to have adverse effects on porosity and permeability.

5.0 RECOMMENDATIONS

1) In order to prevent sand from entering the wellbore during production it is recommended that a sand control system review is undertaken. Possible options include:

(i) Screens will exclude sand from the wellbore, however, any fines migration can cause plugging and eventual screen failure.

(ii) As an alternative, stimulating the well with a Frac and Pack technique provides a screen and allows zone isolation.

2) To estimate the effects of compaction on porosity and permeabilty, it is recommended to couple the stress model to the flow simulator (ECLIPSE).

APPENDIX 1

GEOMECHANICS EVALUATION AND TECHNIQUE

Rock mechanics analysis in this report includes several evaluation and processing steps which are detailed in this appendix.

1.0 Evaluation Programs

A computer processed volumetric interpretation is generated from the open hole logs and core information, where available. This analysis, which includes effective porosity and saturations, is used to correct sonic data for elastic properties and for strength correlations. The volumetric analysis can be conducted by Schlumberger or using the customer's in-house CPI product.

Waveforms from suitable sonic logging tools such as the Dipole Shear Sonic, DSI* or the Array Sonic, SDT* are analysed by the Slowness-Time-Coherence method (STC) to provide Compressional Slowness (DT) and Shear Slowness (DTSM). These outputs are then available to calculate elastic properties

The final phase of log evaluation is processed with ROXAN, linking log-derived dynamic mechanical properties with static values measured on cores and fracture data. ROXAN provides a complete depth-indexed database of deviation, log, core, pressure and triaxial test data. In-situ stresses, near-wellbore stresses and critical well pressures and gradients were computed according to ROXAN's internal models. External models can be substituted, if preferred.

ROXAN input data, including core data, and computed results are displayed in depth-indexed continuous log form. The output channels are too numerous to be presented simultaneously, therefore a sequential format has been adopted.

2.0 Input Data

The input compressional and shear slownesses (DT, DTSM) were obtained from waveform analysis. Bulk and shear moduli are computed from wireline logs 'investigating' the invaded zone, i.e. the annulus around the wellbore invaded by mud-filtrate.

Gassman equation (see section on Elastic Properties), conversions are made to the bulk and shear moduli according to the specified fluid content, and the acoustic properties recomputed. These conversions provide elastic properties free from the influence of fluid effects. Conversions are made to Dry frame i.e. as if effective pore

space contained a vacuum or gas, and wet frame transforms of DT, DTshear and RHOB. Wet frame equates to the pore space 100% saturated with formation water (if oil-based mud) or with mud filtrate (if water-based mud).

3.0 Elastic Properties

Dynamic elastic properties are computed from bulk density and the ratio of the shear slowness to compressional slowness (or their reciprocals, the velocities of the P-wave and S-wave). For stress determination purposes and also for input to strength relationships the dynamic values of the rock skeleton or 'dry-frame' are computed. This requires knowledge of the formation porosity, clay percentage, invaded zone saturation, fluid densities and compressibilities. The depths of investigation of the sonic and density tools are assumed to be less than the depth of invasion. Hence the water saturation of the invaded zone, is used in Wood's Law to compute the compressibility of the hydrocarbon/water mixture.

Gassman's Equation leads to a 'dry-frame' dynamic bulk modulus, modulus of the solid rock matrix is calculated from the grain density and sonic velocities of the non-clay fraction of the rock at zero porosity, adjusted for the dry clay percentage. It is feasible for bulk moduli to be calibrated to values obtained from laboratory compressibility tests.

The Biot poro-elastic constant; Alpha appears in the computations of effective overburden and body force created by the radial pore pressure gradient. A calibrated form of the Biot constant, Alpha is available to adjust to laboratory measurements of the constant. Alpha can be set to one for production stability calculations. G, shear modulus, of the dry-frame is assumed to be equal to the measured shear modulus.

Combining bulk modulus in the dry frame and the shear modulus with the bulk density of the dry-frame, compressional and shear velocities of the dry-frame, and hence the dry Poisson's Ratio and Young's Modulus are obtained. In this manner, the minimum horizontal stress, computed according to a biaxial strain model and calibrated whenever possible with `mini-frac' or leak-off test data, can be independent of the artifacts caused by the influence of fluid content on the sonic and density log responses.

4.0 Laboratory Testing

4.1 Uniaxial Compression Tests

Uniaxial (unconfined) compression tests are performed by loading samples axially to their peak strength for zero effective confining pressure. Pore pressures may be drained to atmosphere. Tests conducted under these conditions tend to fail in some cases under tension rather than shear and therefore do not truly reflect the uniaxial compressive strength of the rock.

4.2 Biaxial Compression Tests

Biaxial compression tests are conducted by keeping the axial stress zero, and increasing the confining stress. Pore pressures are drained to atmosphere.

4.3 Triaxial Compression Tests

These tests can be conducted as single stage tests, where a sample is stressed with an axial load to failure using a pre-set confining stress. Alternatively, as multiple failure triaxial compression tests, which are performed on a single plug at a series of confining stresses by not carrying the test beyond the peak differential stress (failure) point. The latter technique enables a complete set of points delineating a failure envelope to be obtained from a single plug.

Pore pressure inside the plug may be maintained at zero. Effective confining stress for a five-stage triaxial compression test is typically set in stages: at 145, 725, 1450, 2900 and 5800 psi. for instance. Low confining pressures and small incremental steps are chosen in order to be able to accurately define the failure envelope at low effective stress.

The specification to keep effective confining stress in these tests at somewhat low levels requires an explanation. The problem of formation collapse, addressed in these evaluations, entails the state of stress around the wellbore. The total radial stress at the sand face during production for instance, is equal to the well pressure. In a flowing well, pore pressure in an element close to the sandface is equal to the well pressure. Allowing for Biot's Constant being slightly less than one, and accounting for the body force i.e. component of tensile stress caused by the pore pressure gradient from the far-field to the wellbore, we would expect the effective radial stress to be close to zero.

4.4 Triaxial Extension Test

Three stresses representing the stress state of an element in the borehole wall, or perforation tunnel surface, can only be accurately simulated in a laboratory by means of a 'true triaxial test', also referred to as a polyaxial test. However, it can be assumed that, when drilling with underbalanced mud, the intermediate stress is closer to the major stress than to the minor stress (i.e. the radial stress). The same would be true in the case of a producing well. The triaxial extension test described below, in which the major and intermediate stresses are equal and are exerted by the confining pressure, is a viable alternative to the polyaxial test.

In the triaxial extension tests the axial and confining stresses are built-up simultaneously, so as not to cause premature failure, to a pre-determined hydrostatic level which is the 'starting point' of the test. During the next phase, the confining stress is maintained at this high level. The axial piston is gradually withdrawn at a constant axial strain rate, causing extension - or more accurately, a reducing compression - in the plug's axial direction.

Axial extension maybe continued while the axial stress passes through a minimum i.e. the differential between confining stress and axial stress reached a peak. With further axial strain, the axial stress adopts a near-constant value corresponding to residual strength.

5.0 Formation Strength

The correlation between Young's Modulus and rock strength was first observed by Deere and Miller (1966), using samples gathered from outcrops in the deserts of New Mexico and Deere and Merritt (1969) in which tested rock samples were found to fall into various ``modulus ratio'' classifications. This led to the assertion that uniaxial compressive strength was proportional to Young's Modulus, the constant of proportionality being a function of the clay content, and to the internal friction coefficient.

More recent investigations have shown that the function to compute the uniaxial compressive strength of many rocks can be expressed in the form:

UCS = Young's Modulus*A + B

The first term, related to Young's Modulus, represents the contribution to strength of the fraction of the rock behaving elastically. This is normally considered to be the brittle component in which the grains are bonded i.e. cemented together. It has long been recognised that well-cemented rocks have higher acoustic velocities than poorly-cemented or granular sediments. It is thus reasonable to use the Young's

Modulus in the above equation. Naturally, using a dynamic value requires different coefficients A and B than would have been applicable had the modulus been used.

The data for the Deere and Miller correlation was populated with higher strength samples and the trend is not completely applicable to sandstones typically found in hydrocarbon reservoirs. Further work by Plumb, using a world-wide data-base of borehole recovered core samples, has confirmed the Deere and Miller trend. However his correlation is much more applicable to less strong, reservoir sandstones. The same work observed the loss of strength with the introduction of clay for sandstones of similar porosities.

Performing a regression on the Plumb data generates the following equation:

UCS = 2.280 + 4.1089*YME stat.

where UCS = uniaxial compressive strength
and YME.stat.=. Youngs Modulus from core
the coefficient of regression is 0.925.

In more complex lithologies such as complex sandstones or shales it is necessary within a strength correlation to account for the influence of other minerals in addition to quartz. One of the first correlations to take account of percentages of shale in a sandstone was the Coates-Denoo Correlation.

The Coates-Denoo Equation, derived from observations in field development wells in the Gulf of Mexico, has been widely used for sanding predictions when rock mechanical data has been unavailable.

Initial Shear Strength = 10**6 x 0.025 x YME/Cb x [A x Vcl + B x (1 - Vcl)]

where YME is Young's Modulus, Cb is compressibility and Vcl is the volume of clay. Coefficients A and B in the Coates-Denoo equation are 0.008 and 0.0045 respectively.

6.0 In-situ State of Stress

6.1 Far Field Stresses

Rock in it's natural state is stressed in three principal directions; vertically from the overburden and horizontally in two orthogonal directions. The two horizontal stresses are generally not equal. There are three elements to estimating the insitu stress which need to be considered:

- Stress order: the order, in terms of magnitude of the three principal stresses, that is to say whether the overburden is the maximum, intermediate or indeed the minimum stress.

- Stress magnitudes, not only the size but the difference between principal stresses is also important in determining the onset of any failure

- Stress direction. Wellbore orientation with respect to the direction of the three principal stresses is also critical in determining the point at which failure will occur in a well.

The first step in making an accurate description of the insitu state of stress; the order of the three prinicpal stresses. This will determine whether a structure is under extension; the overburden will be the maximum principal stress or compression in which case the principal stress will be in the horizontal plane and the overburden will be either the intermediate stress; in Andersonian terms this would represent a strike-slip or wrench environment or if the overburden is the least principal stress; a thrust environment. There are several methods which can be applied to determine the stress order these include: seismic interpretation, extended leak-off tests and mini-fracs, and analysis of borehole shape using imaging tools like the UBI* (ultrasonic borehole imager).

Given an normal extentional stress regime vertical and horizontal far-field stresses can be computed using overburden gradient, calculated from either an integrated density to surface or a regional value or indeed a combination of both, elastic properties and pore pressure gradient. The minimum horizontal or least principal stress can be computed from a uniaxial elastic strain model, where the horizontal stress is driven from the overburden pressure and converted to a horizontal component by the Poisson's ratio. The minimum horizontal stress should be calibrated against measured closure stress, when known. In the case where the horizontal stresses are not the same, generally the case to a greater or lesser degree, the model needs to take some account of the tectonic element. This can be achieved by using a model which includes strain terms. These terms require

calibration through a direct measurement of the closure stress. Acceptable levels of stress can be calculated using failure criteria from laboratory core data. These data will set boundaries within a formation for the maximum sustainable difference between the major and least principal stresses.

When a structure is under compression, the insitu stress calculation becomes more complex. A pure elastic strain model is no longer applicable because the horizontal stress is no longer a function of the overburden alone but includes tectonically induced horizontal stress. Tectonic stresses are transmitted more effectively by rigid rocks such as sandstones than more ductile rocks such as claystones. This can produce a stress profile where the horizontal stress in a sandstone is higher than a claystone, the reverse to that expected in a normally stressed area. In this environment it is imperative that stress estimates are based on direct stress testing.

The last component of an insitu stress description is the orientation of the insitu stresses. The level of stress at the wellbore will be directly influenced by the orientation of the wellbore with respect to the insitu stress field and as a consequence will influence the stability of the wellbore. Therefore wellbore failure will vary for a given stress field depending on the well deviation and azimuth. The orientation of the horizontal stresses has been traditionally evaluated in vertical wells using break-out data with dual caliper measurements. In deviated wells this data is not applicable as a direct measurement although it can be applied through inversion techniques. Dual caliper data in these cases has to be treated with caution as other failures in the wellbore can be misinterpreted as break-outs. Image data from tools such as the UBI* give far more accurate data, not only break-out information but other failures such as slippage and drilling induced fractures which can be inverted to reveal the orientation of the insitu stress field. Mini-frac and extended leak-off test data in deviated wells can also be used to calculate stress direction through an inversion technique

6.2 Stresses around the Wellbore

With the introduction of a wellbore into the rock the hydraulic pressure of the mud replaces the support lost by the column of rock removed. The mud pressure however acts uniformly in all directions and cannot exactly balance the insitu stresses. The wellbore is distorted and may fail if the redistributed stresses exceed the rock strength. The mud pressure then has a major influence on mechanical failure of the wellbore and the level of mud pressure and the state of elastic behaviour in the near wellbore annulus will determine the when the wellbore fails.

The level of stress at the wellbore will also depend on the wellbore deviation. In a vertical well the level of tangential stress around the wellbore will be governed by the mud pressure and stresses acting normal to the wellbore axis; the horizontal stresses. In a deviated well the tangential stress, again determined by stresses

acting normal to its axis, will now include components of the horizontal and vertical stress.

7.0 Deformation Mechanisms

7.1 Formation Failure

As a wellbore is drilled the hydraulic pressure of the drilling mud must replace the support lost by the removal of the original column of rock, but as the mud pressure acts equally in all directions it cannot exactly balance the in-situ state of stress. Consequently rock surrounding the wellbore is distorted and strained, and may fail if the redistributed stresses exceed rock strength.

The mud pressure has a direct influence on the level of stress at the wellbore wall. When the hydraulic pressure of the mud becomes too high a tensile failure can occur. The formation stress at the wellbore goes into tension, exceeding the rock's tensile strength. This fractures the rock along a plane perpendicular to the least principal stress, normally one of the horizontal stresses, and potentially causes lost circulation. Axially-aligned cracks in the borehole wall, sometimes visible on the Formation Micro Scanner (FMI) or Ultasonic Borehole Imager (UBI), are indications of these limits having been exceeded.

Alternatively the formation can fail in compression. This is commonly predicted using model such as Mohr-Coulomb, in which factors controlling failure are the minimum and maximum stresses at the wellbore wall. Compressive failure may occur as a result of too lower mud weight or too higher mud weight. In either case, the formation caves or spalls, creating break-outs. The debris can accumulate in the borehole leading to stuck pipe or even hole collapse during drilling.

The failures just described represent damage to the rock which occurs as a result of the mud pressure being either too low or too high. It is important to bear in mind when assessing wellbore stability that these are not the only failures which can occur and initiate drilling delays and losses. Other failure mechanisms related to the rock or formation fabric such as laminations or fractures may be present and can be the dominant mode of failure in a wellbore section. The onset of such failures may be between boundaries defined by the compressive and tensile failures. For instance in a naturally fractured formation mud losses may be controlled by the least principal stress rather than a higher tensile failure stress.

A crucial element within the study of wellbore stability is accurate description of the failure that is occurring so that the correct remedial action can be taken. During any analysis it is important to define the potential failure types and boundary conditions

so that in the event of instability the responsible failure can be isolated. Incorrect diagnosis can lead to an inappropriate solution exacerbating the failure and leading to further damage and potential drilling losses. The solution may lie outside the mud weight altogether. Changes in drilling practices may provide stable conditions in a hitherto unstable interval.

Chemical instability, which may also be the dominant cause of failure in some sections, is not treated here. This report is primarily concerned with mechanical stability of rock but in isolating failure mechnisms it is important to recognise the potential for chemical as well as mechanical instability.

In discussing stresses at the wellbore wall and formation failure, the cases so far considered are those encountered in open hole during drilling. Under productions the mud pressure to support the formation is withdrawn and the radial stress acting on the formation or perforation is determined by the applied drawdown across the exposed, producing interval. If at the wellbore wall it is assumed that the pore pressure is equal to the bottom hole well pressure then the effective radial stress on the formation is zero.

Under production conditions, be they open or cased hole, the formation close to the wellbore wall is normally in some form of yielded state. Yield does not mean that the wellbore or perforation cavity will collapse but this yielded or plastic state generally reduces the state of stress at the wellbore wall and the formation is more stable than an elasto-brittle model would suggest. To predict the state of stress and the onset of failure it is more apropriate to apply elasto-plastic modelling to define the level of drawdown that would produce an influx of sand to the wellbore. This modelling analyses the plastic behaviour of the rock and calculates the reduced state of stress.

Having defined the point at which the formation will fail it is important to consider the mechanism that causes sanding. Sand production is generally the result of two extrinsic parameters: stress and flow (Cook 1994). When a perforation tunnel is in a failed state due to applied stress, material can only be carried from the perforation if there is sufficient flow. The contribution of flow to the stress state is negligable and therefore in itself will not fail the rock, however flow along the perforation tunnel can remove damaged/yielded material from the wall if the flow is fast enough. Poor clean-up after perforating can lead to only a limited number of producing perforations. This can result in high flows removing yielded material from a few perforations. Therefore effective critical drawdown in the zones expected to flow could be lower than calculated.

7.2 Elasto-Plastic Modelling

The elasto-plastic model (Bradford and Cook, Aug 1994) gives the critical draw-down that will produce formation failure. The model calibrates the elastic and plastic behaviour of the rock using data from single stage laboratory triaxial tests carried through to failure. These tests are conducted with confining stresses in the same order as the equivalent mean effective stress acting on the rock at reservoir conditions.

Loading and deformation data is used to calibrate both elastic and plastic parameters. Far-field boundary conditions are also included such as the far-field stresses and pore or reservoir pressure. The model calculates the stress and pore pressure profile radially from the wellbore giving the critical draw-down (far-field reservoir pressure - bottom hole well pressure) which will cause failure of the plastic annulus and sand influx during production.

7.3 Effect of Reservoir Depletion

Studies have shown that, at a certain point in the life of a field, the extent of reservoir pressure decline may begin to have a greater impact on formation collapse and solids influx, than the production drawdown itself. Reduction in pore pressure causes effective stresses to be increased. Thus it takes a smaller drawdown to exceed the failure criterion. If during production it is intended to allow the reservoir pressure to fall then by using reduced reservoir pressures the effect of depletion can be modelled before production begins.

APPENDIX 2

CSIRO Laboratory test
data and analyses

SINGLE- AND MULTI-STAGE DRAINED

TRIAXIAL COMPRESSION STUDIES -

BALEEN-2 (PATRICIA BALEEN GASFIELD)

LIST OF CONTENTS

Single and Multiple Stage Failure Triaxial Tests on Baleen-2 Cores

A proposal to Schlumberger

1 Introduction

This proposal has been prepared in response to an e-mail enquiry on 22 Dec. 1999 from Schlumberger concerning core testing for sand production studies in the Patricia Baleen reservoir. The test program includes one drained multiple stage failure triaxial test (five stages) and two single stage drained triaxial tests for each core section of poorly consolidated reservoir sands. A total of five core sections will be tested (15 tests in total). The tests will be conducted at room temperature.

2 Outline of proposed work

Sample size

The preferred sample size is 42 mm in diameter and 84 mm in length, due to the availability of the testing equipment in the proposed time frame.

Sample preparation

Four sample plugs (with one plug spare) with a diameter of 42 mm and a length slightly longer than 84 mm (say 90mm – 100mm) are to be prepared from each core section by ACS. The plugs are to be drilled along the core axis. Due to friable nature of the material, it is suggested that the plugs be cored under a frozen state using liquid nitrogen as the drilling fluid. They are then to be delivered to CSIRO in dry ice and stored in a deep freezer until required for testing.

Sample end surfaces will be prepared/lapped in a frozen state under the protection of a special core holder at CSIRO. The perpendicularity of the end surfaces to circumferential surface and flatness of the end surfaces of the finished sample will be in general accordance with the specifications recommended by ISRM.

Test equipment

A 45 MPa capacity triaxial cell will be made available for the proposed tests, with provisions for measurements of sample deformations, axial load, cell and pore pressures. The instruments used to measure the behaviour of the test sample are:

- two diametrically-opposed LVDTs (Linear Variable Differential Transformers) mounted between the sample end platens to measure axial deformation of the sample;
- four cantilever (orthogonal) radial gauges mounted at mid-height of the sample to measure radial deformation;
- a load cell located on top of the top platen to measure axial load;
- a pressure transducer to measure cell (confining) pressure; and
- two pressure transducers to measure pore pressures at both ends of the sample.

A computer-controlled system is used to control the axial displacement, and cell and pore pressures, and to conduct data acquisition.

Test procedure for single stage triaxial test

- Sample installation. The frozen sample is jacketed in a thin Viton rubber membrane (0.5 mm thick) and installed between top and bottom steel platens inside the triaxial cell. The transducers for measurements of radial and axial displacements, and axial load are then installed.
- Sample thawing. As soon as the triaxial cell is closed, a small confining pressure (0.5 MPa) is applied to maintain sample integrity while thawing.
- Sample saturation. Apply confining pressure and back pore pressure at a constant rate of 0.5 MPa/min. to 6 and 5 MPa respectively, while the pore pressure line at the other end of the sample is closed (undrained). A thin mineral oil (Shell process oil P874) will be used as the pore fluid. The cell and back pore pressures are maintained constant until the pore pressure measured at the other end of the sample reaches 5 MPa, when the sample is assumed to be fully saturated.
- Pressurization. This is conducted undrained (i.e., the pore pressure lines on both end of the sample are closed). Apply confining pressure at a rate of 0.5 MPa/min. until the required effective confining pressure level (6 MPa or 9 MPa) is established.
- Consolidation. After the pore pressure inside the sample stabilised, open the back pore pressure line and control the pressure at 5 MPa to allow the excess pore pressure to dissipate (consolidation). The consolidation is assumed to be completed when the pore pressure measured at the other (undrained) end of the sample is equal to the back pore pressure.
- Axial loading. Apply axial stress at a constant axial strain rate under computer control until residual strength is observed, while the confining and pore pressures are maintained constant. The loading rate selected will be sufficiently slow to allow an essentially uniform pore pressure distribution inside the sample during loading, as evidenced by the pore pressure measurement on the undrained end of the sample.

Test procedure for multiple stage failure triaxial test

The testing procedure is similar to that for a single stage triaxial test described above, except for the loading stage.

After the required cell and pore pressures are established, the axial stress is increased at a constant axial strain rate. The same strain rate as for the single stage triaxial tests will be applied. The axial stress vs axial strain curve will be displayed on the computer screen as the test progresses. Prior to failure of the sample, a curved response of the axial stress with the axial strain will be observed, indicating an imminent approach to failure. Where this non-linearity is observed, the axial stress is quickly reduced and the confining pressure is increased to the next level of effective confining pressure required. After the pore pressure is stabilised and equal to the back pore pressure, the axial load is increased again at a constant axial strain rate. This procedure is repeated at the effective confining pressures of 5, 10, 15 MPa. At the last stage (effective confining pressure of 25 MPa), the axial loading is allowed to proceed beyond the peak strength and until a residual strength is observed.

3 Schedule

The testing program can commence early in January 2000. It is estimated that approximately one week will be needed for the proposed 3 tests for each core section. Five weeks will be needed for the whole testing program. Summary results will be provided upon completion of the tests for each core section. A draft report will be produced within two weeks of completing the testing program.

4 Deliverables

A report containing:

- Test procedure.
- Axial stress vs axial strain, axial strain vs radial strain and axial strain vs volumetric strain curves.
- Young's modulus and Poisson's ratio (they will be determined based on ISRM suggested methods).
- Calculated UCS, peak and residual strength parameters such as cohesion, angle of internal friction, and Mohr circles.

Figure 1a Axial Stress-strain curves: 6 MPa confinement: Test 1 - Baleen-2, 750.82m

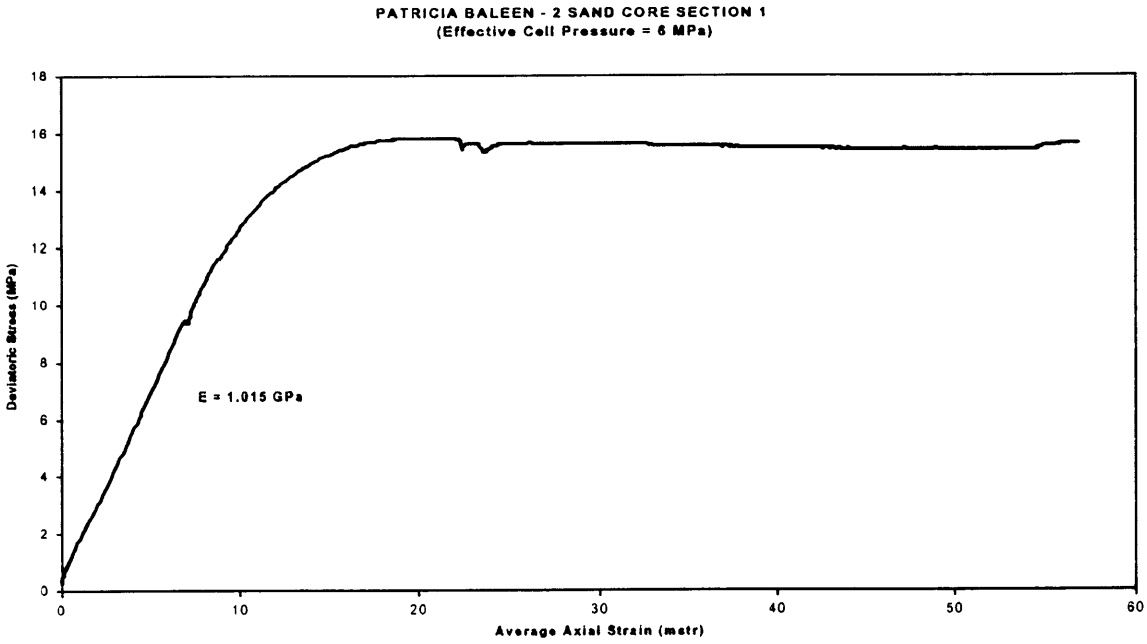

Figure 1b Radial strain-Axial strain curve: 6MPa confinement: Test 1 - Baleen-2, 750.82m

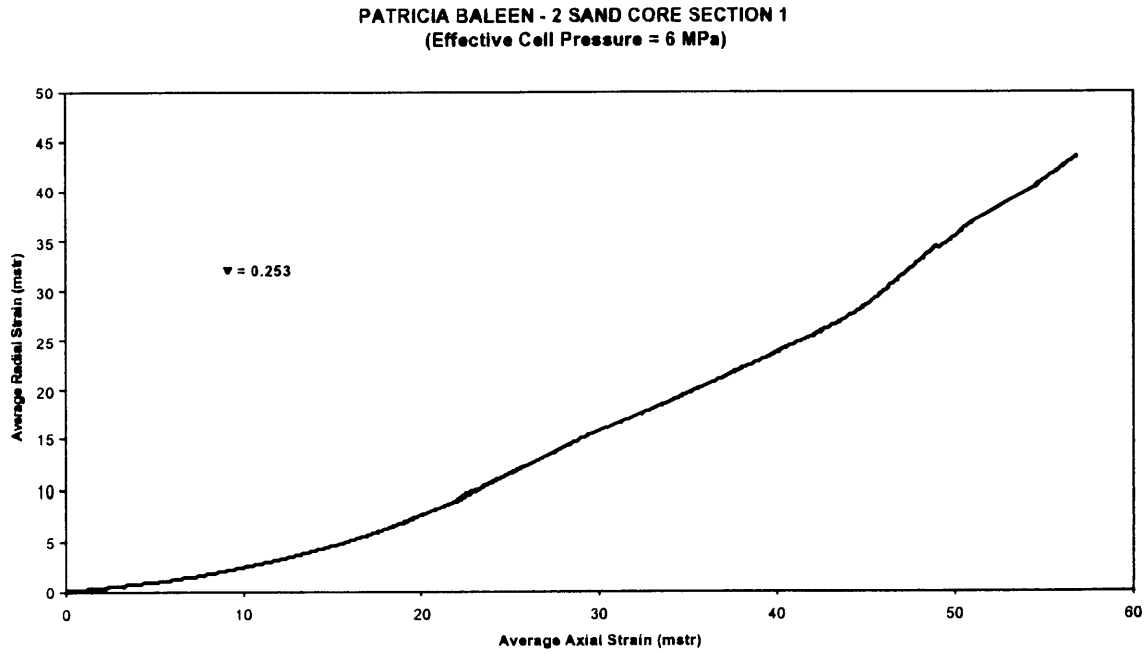

Figure 1c: Volumetric-Axial Strain curve: 6 MPa confinement:Test 1-Baleen-2, 750.82m

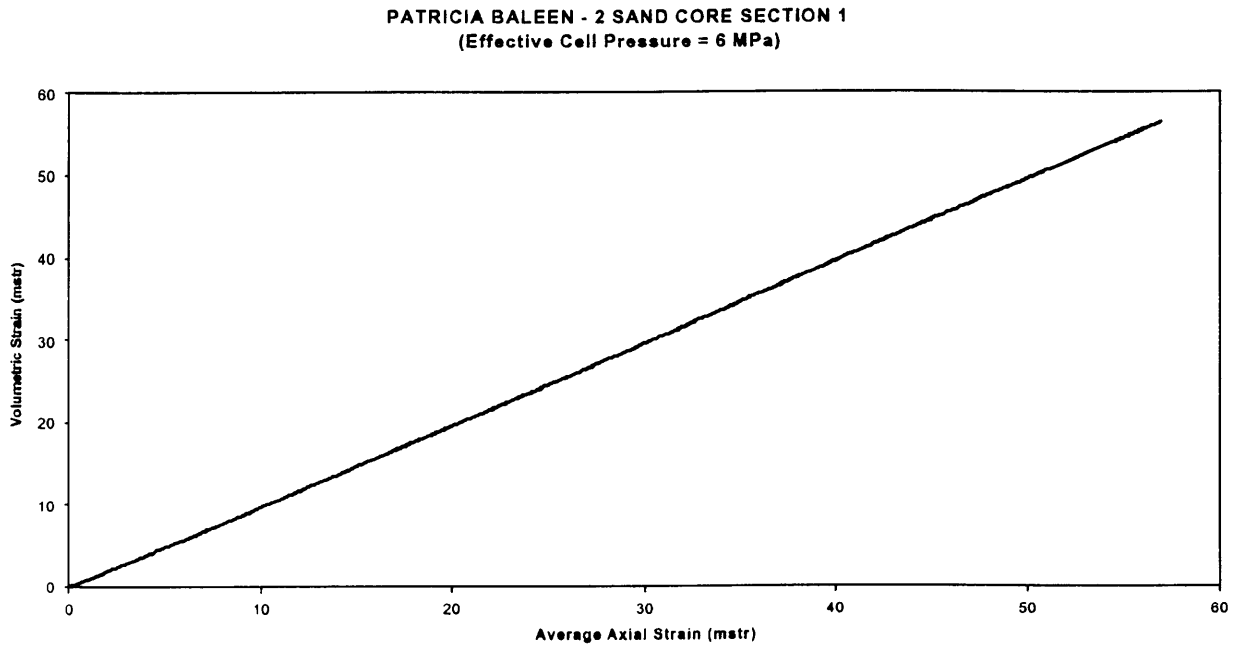

Figure 2a: Axial stress - strain curves; 9MPa confinement; Test 1 - Baleen-2, 750.82m

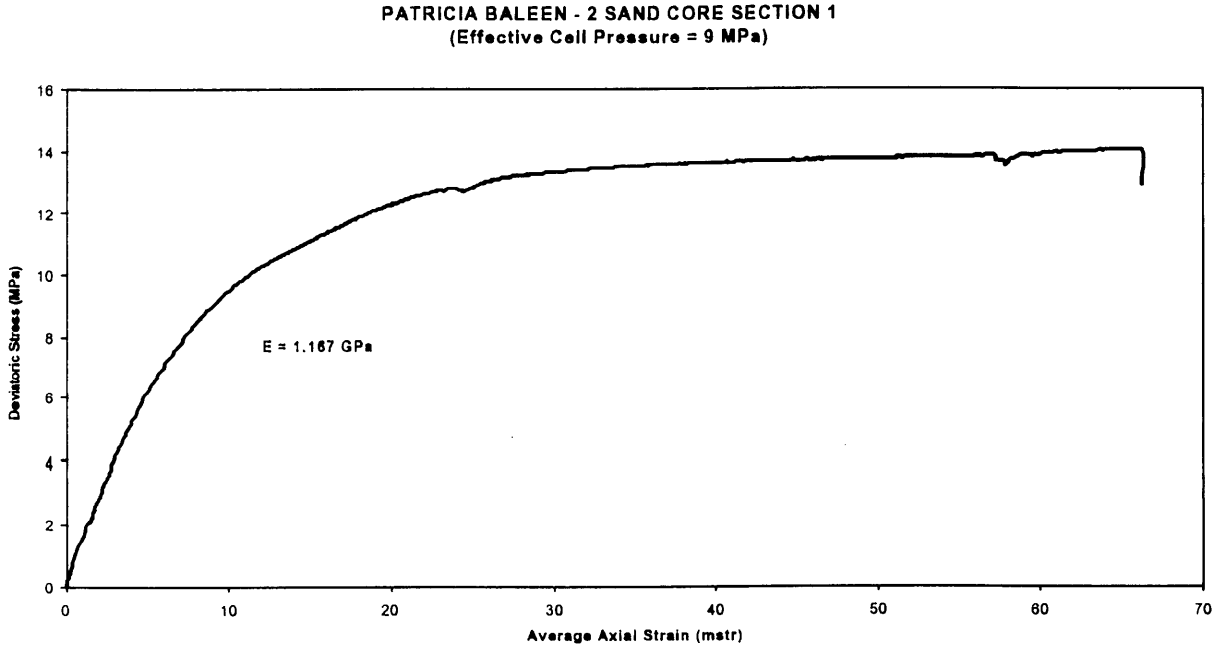

Figure 2b: Radial strain - axial strain: 9Mpa confinement: Test 1- Baleen-2, 750.82m

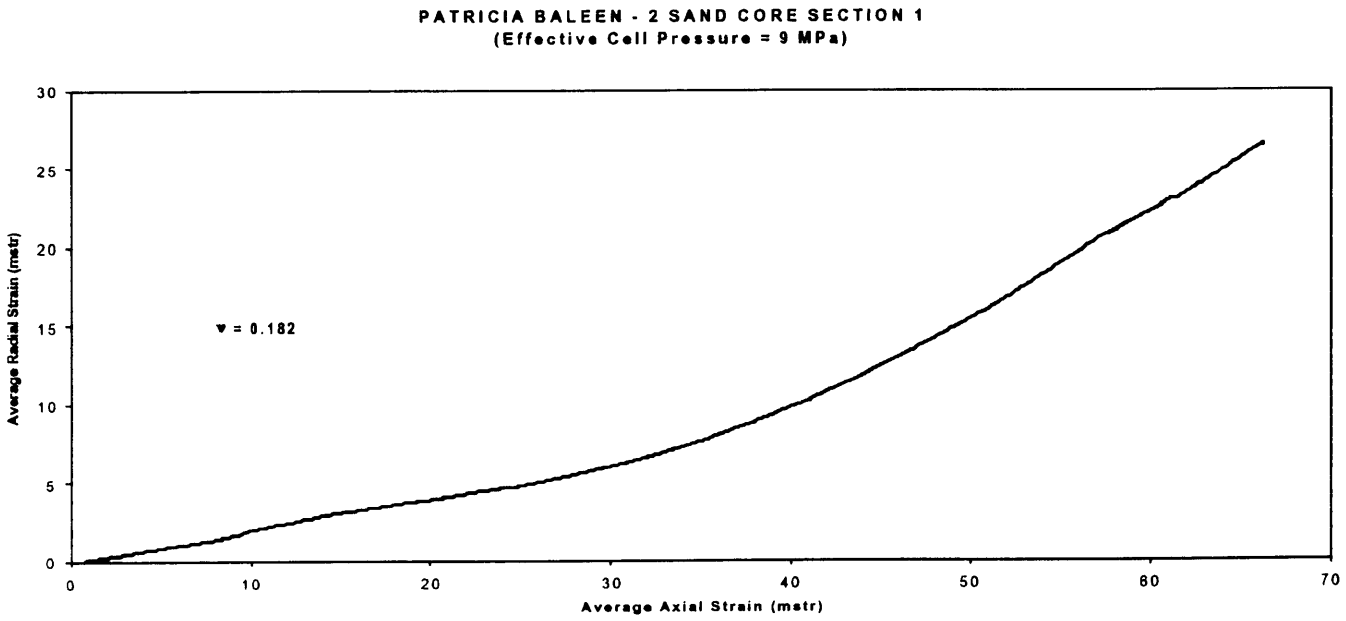

Figure 2c: Volumetric strain - Axial strain: 9 MPa confinement: Test 1 - Baleen-2, 750.82m

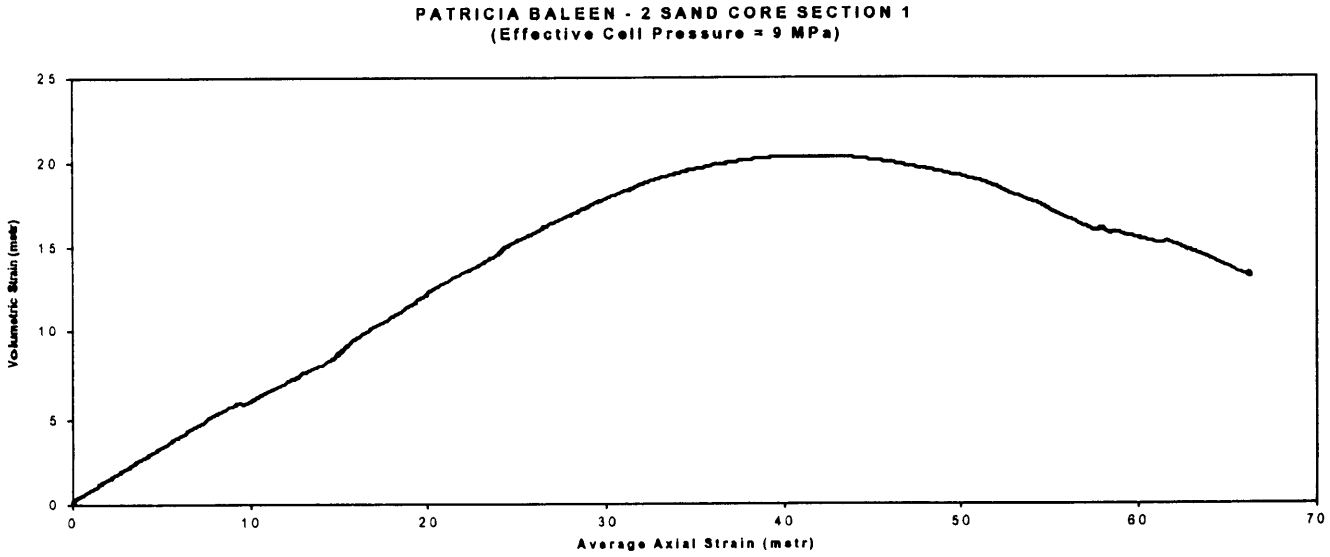

Figure 3a Radial vs Axial strain: Multi-stage Test: Test 1 - Baleen 2, 750.82m

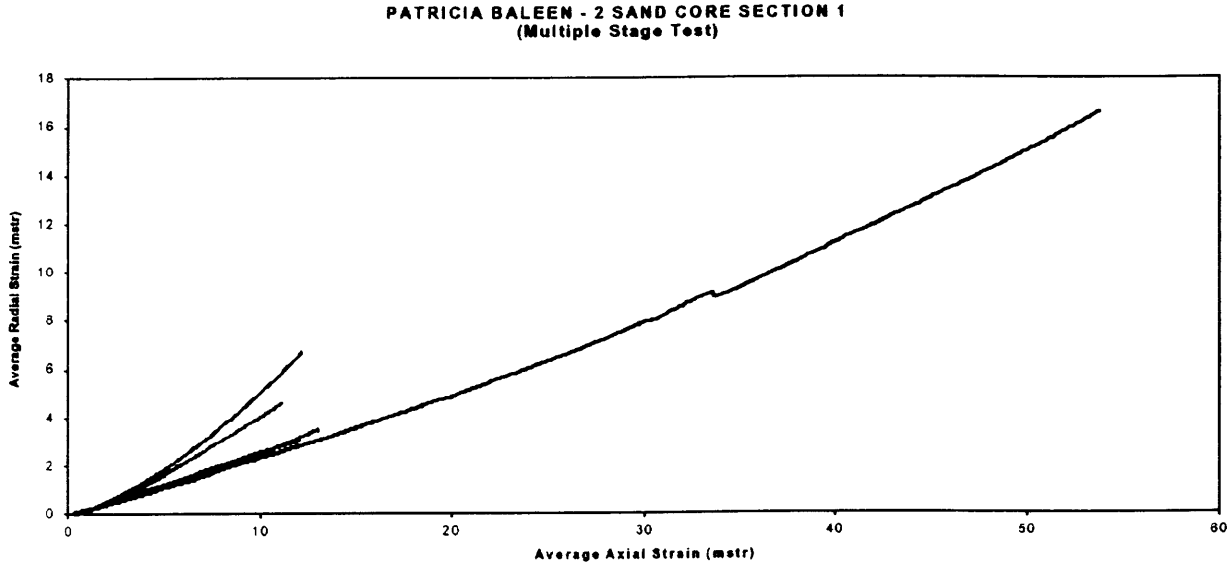

Figure 3b: Axial Stress vs Strain: Multi-Stage test: Test 1 - Baleen 2, 750.82m

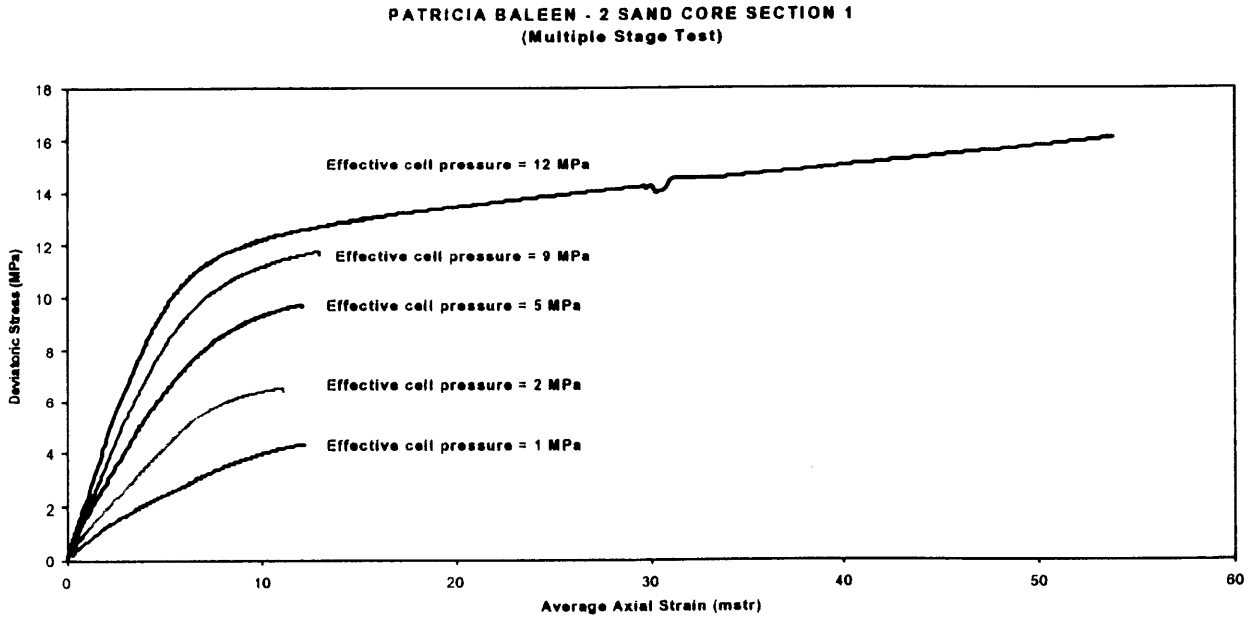

Figure 3c: Volumetric vs Axial Strain: Multi-stage Test: Test 1 - Baleen-2, 750.82m

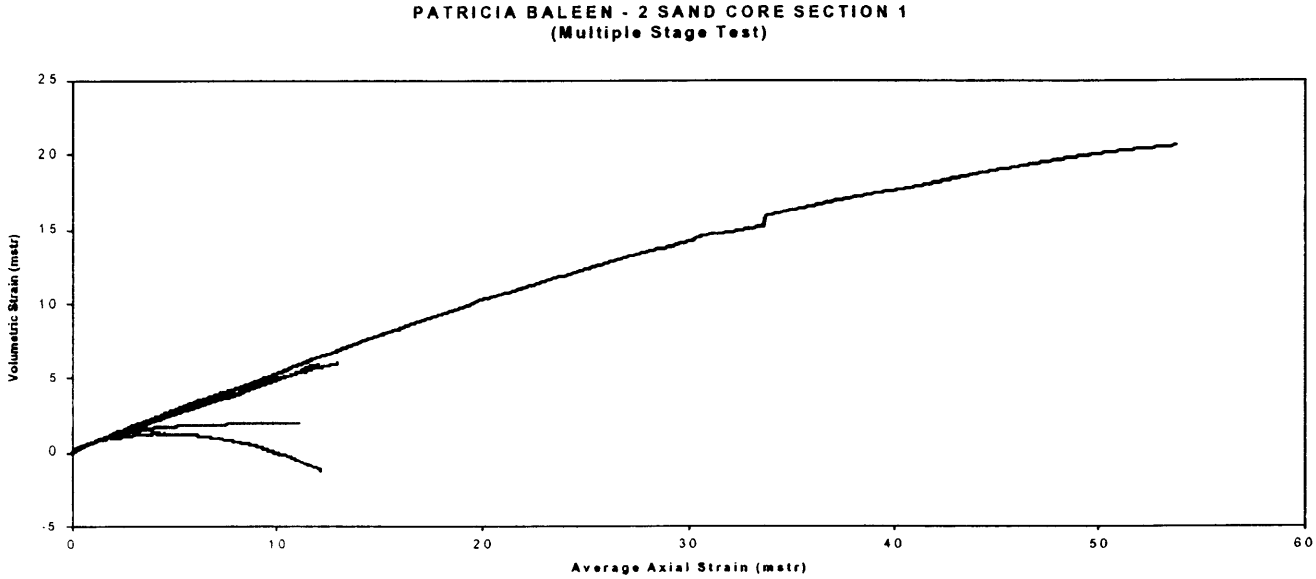

Figure 4a: Mohr Circles of Strength for Multi-stage tests : Test 1 - Baleen-2, 750.82m

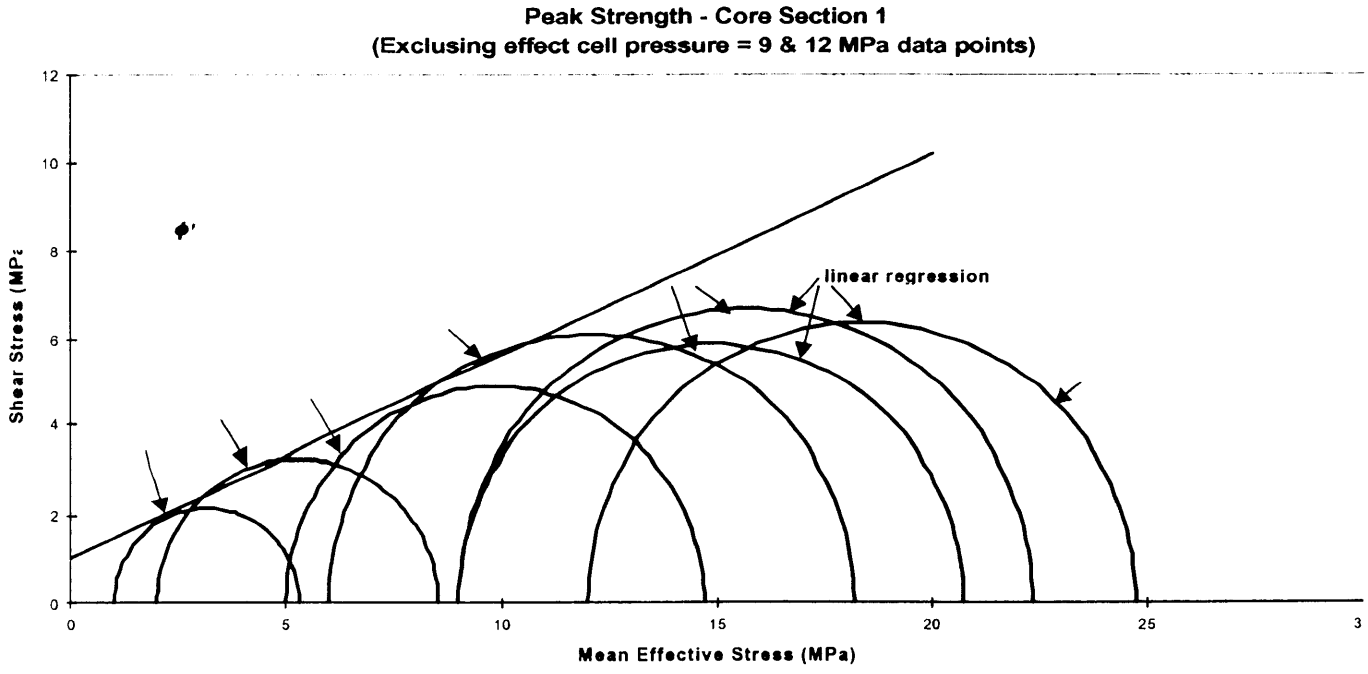

Figure 4b: Young's Modulus and Poisson's Ratio for Multi-Stage:Test 1 - Baleen-2, 750.82m

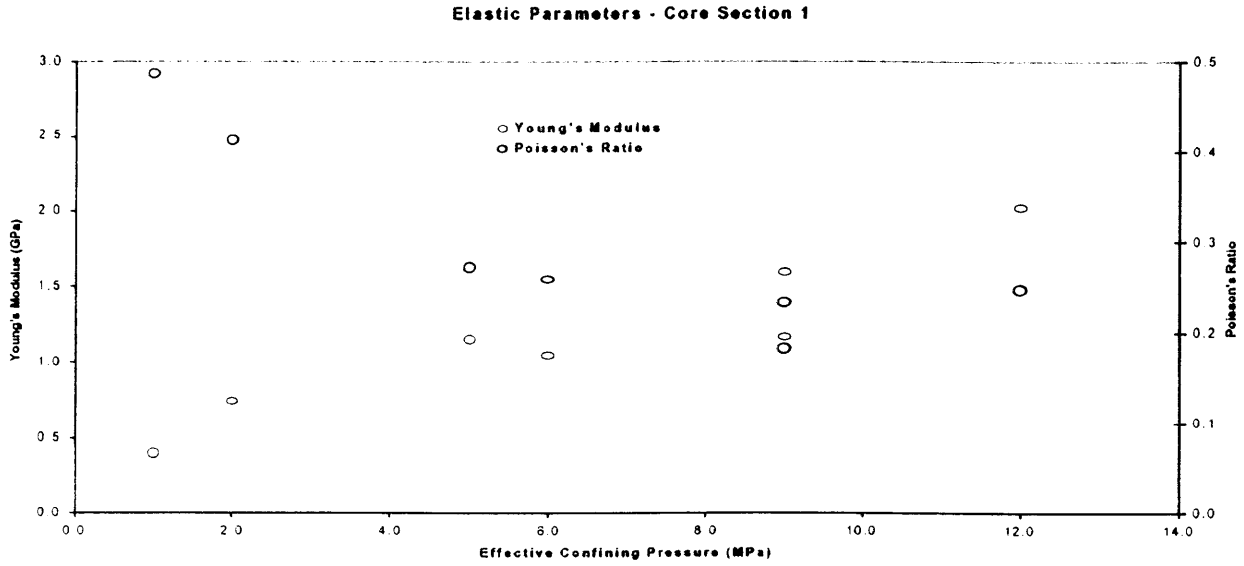

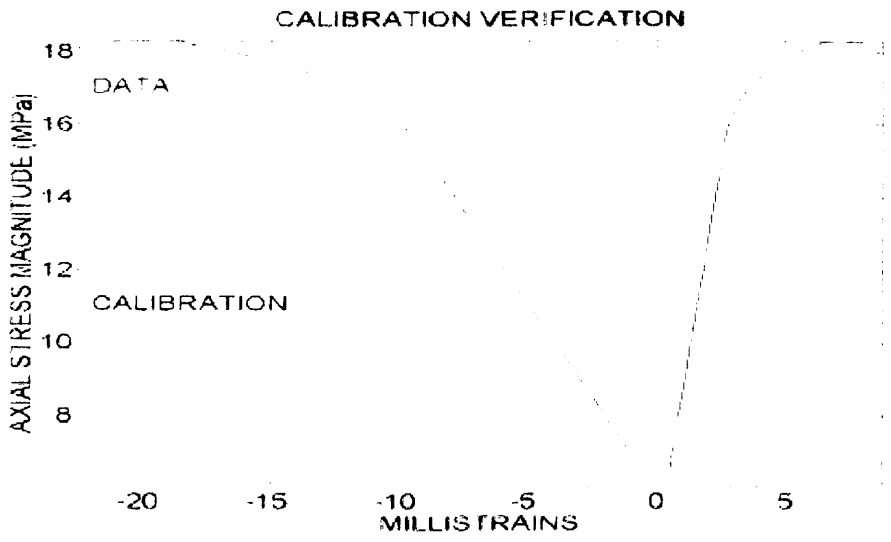

Figure 5: Elasto-plastic Modelling for 6MPa Test: Test 1 - Baleen-2, 750.82m

Figure 6a: Radial Strain vs Axial Strain: 6MPa confinement: Test 2 - Baleen-2, 756.52m

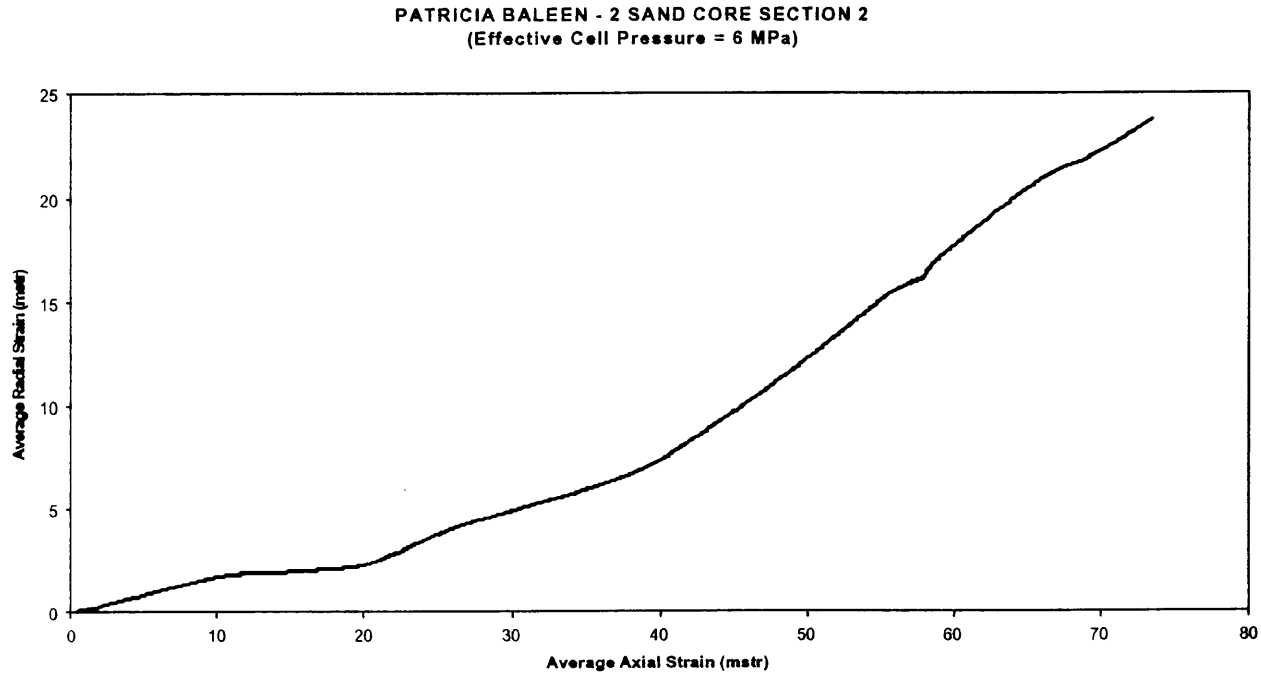

Figure 6b: Axial Stress vs Strain: 6 MPa confinement: Test 2 - Baleen-2, 756.52m

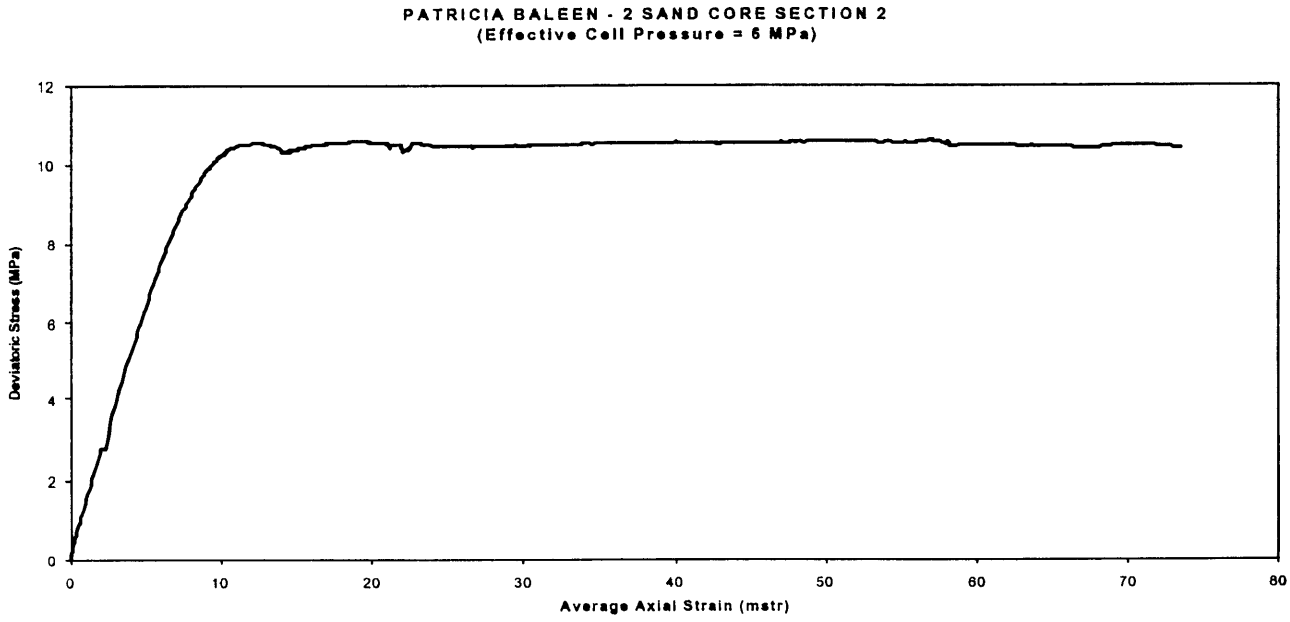

Figure 7a: Radial Strain vs Axial Strain: 9 MPa confinement: Test-2 - Baleen-2, 756.52m

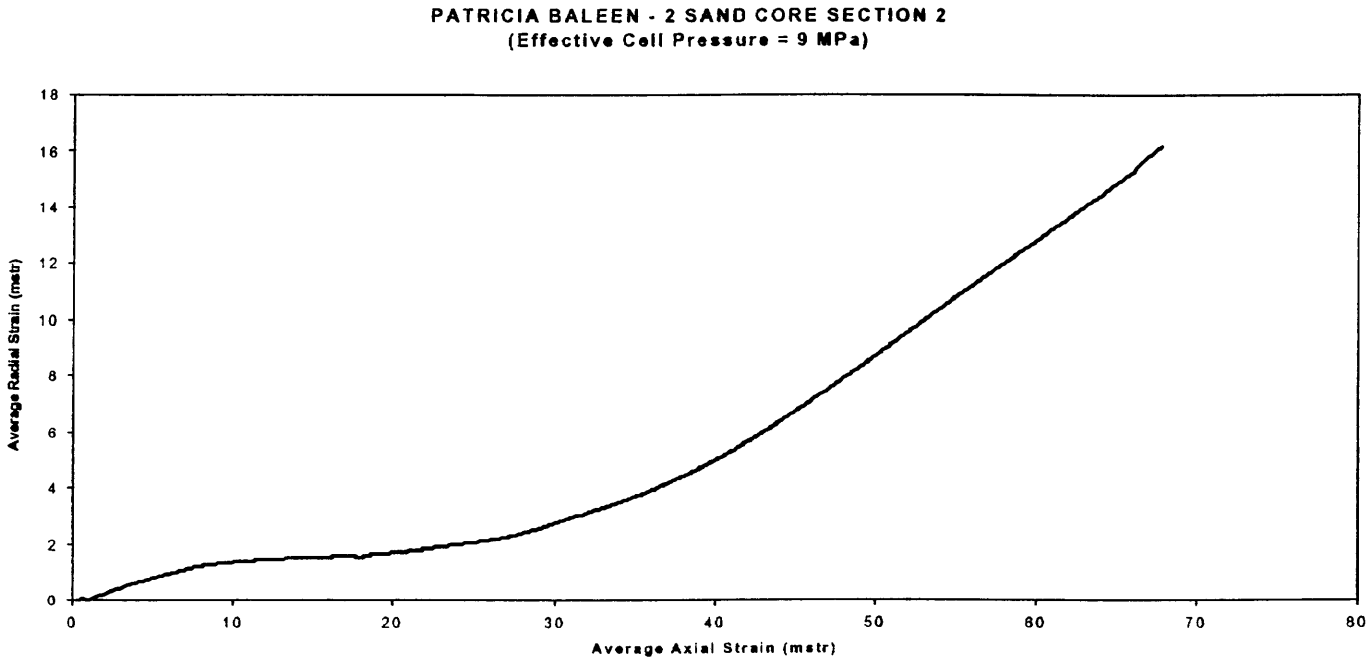

Figure 7b: Axial Stress vs Strain: 9 MPa confinement : Test 2 - Baleen-2, 756.52m

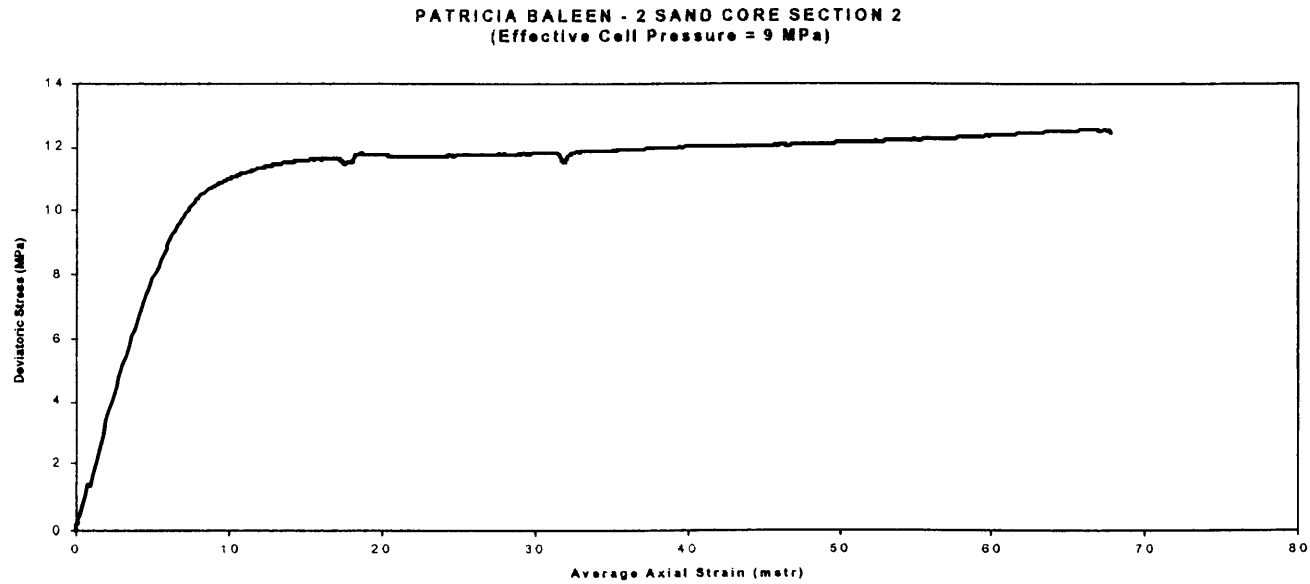

Figure 8a: Radial Strain vs Axial Strain: Multi-stage Tests : Baleen-2, 756.52m

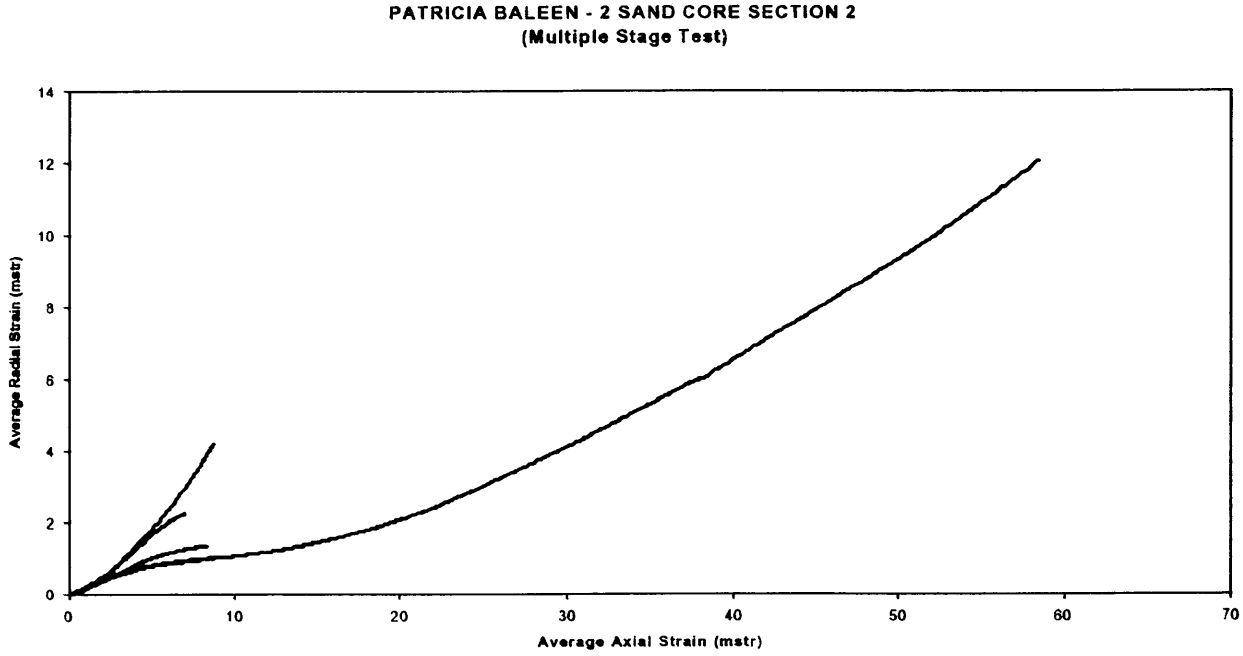

Figure 8b: Axial Stress vs Strain: Multi-stage Tests : Test 2 - Baleen-2, 756.52m

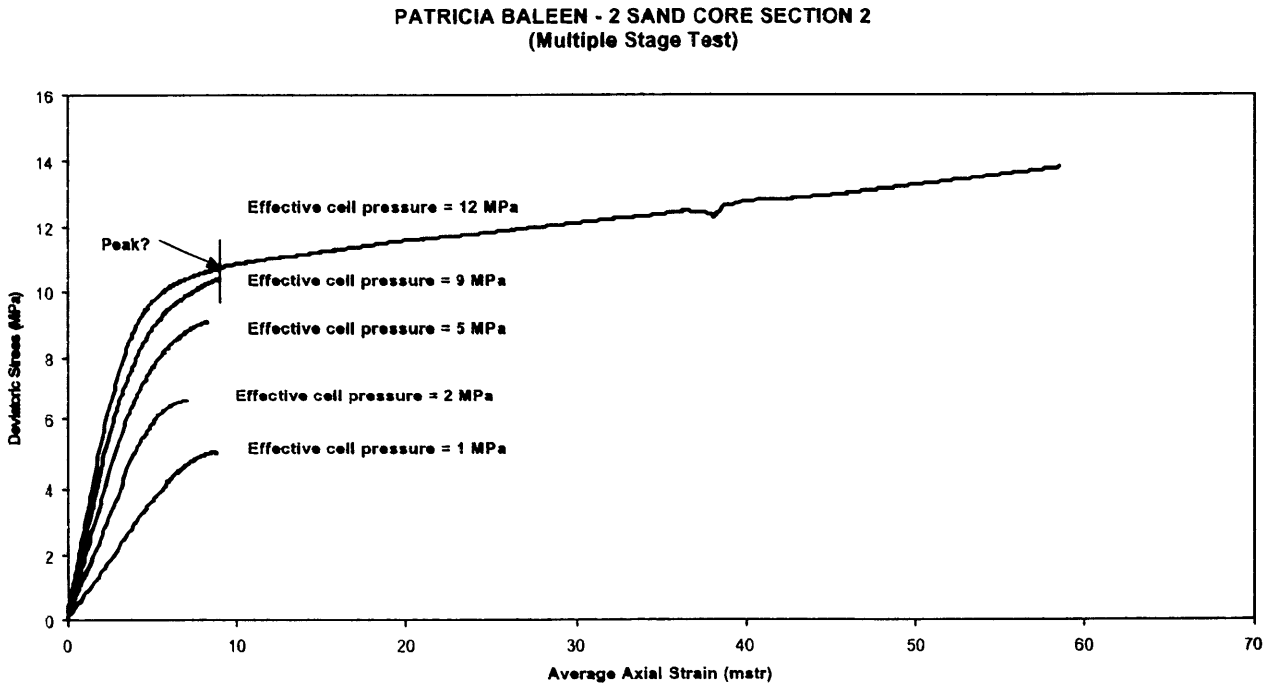

Figure 9a: Mohr's Circles of Strength for Multi-Stage Tests : Test 2 - Baleen-2, 756.52m

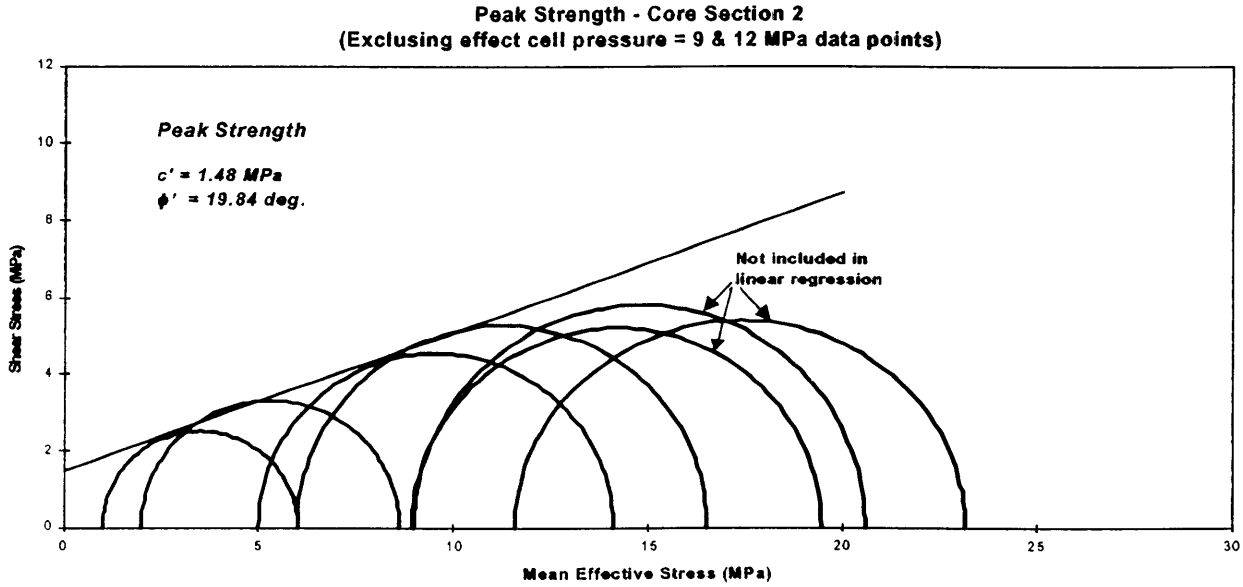

Figure 9b: Young's Modulus & Poisson's Ratio for Multi-Stage: Test 2 - Baleen-2, 756.52m

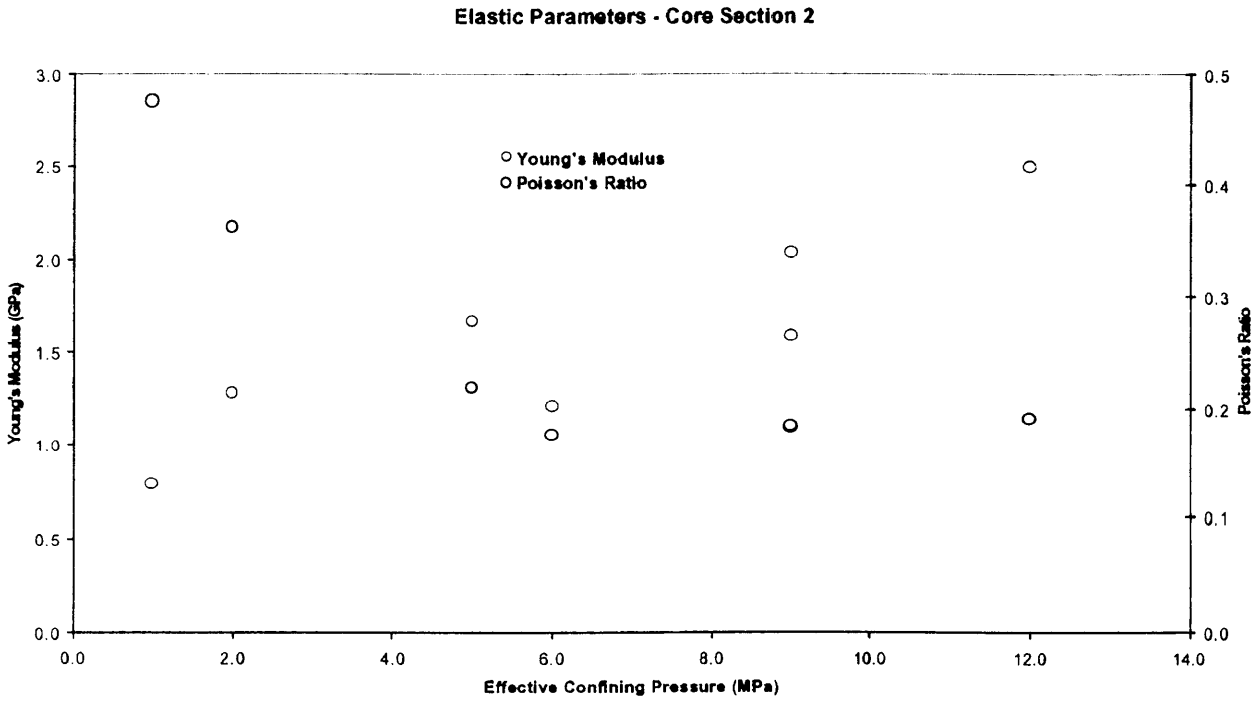

Figure 9c: Elasto-Plastic Modelling for 6 MPa Test : Test 2 - Baleen-2, 756.52m

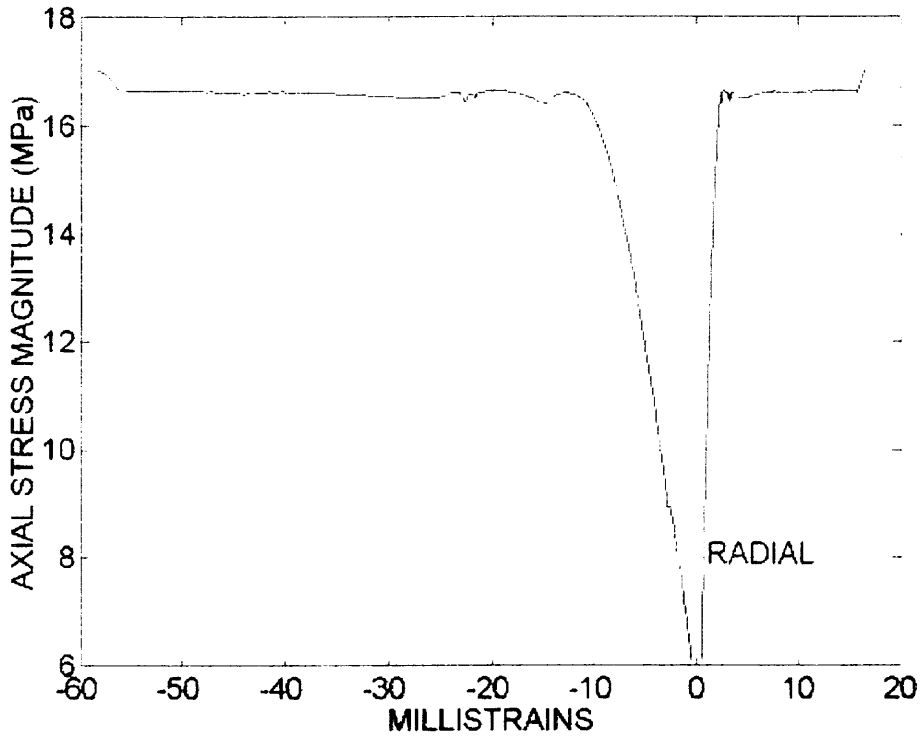

Figure 10a: Radial Strain vs Axial Strain : 6 Mpa confinement : Test 3 - Baleen-2, 760.23m

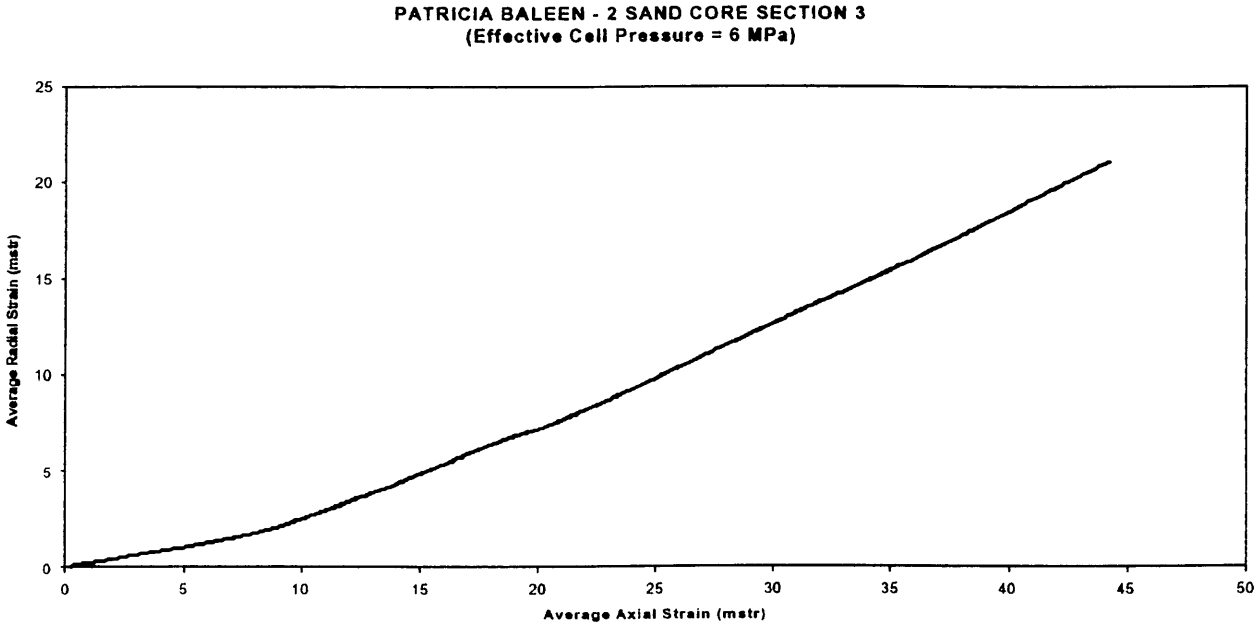

Figure 10b: Axial Stress vs Strain : 6 MPa confinement : Test 3 : Baleen-2, 760.23m

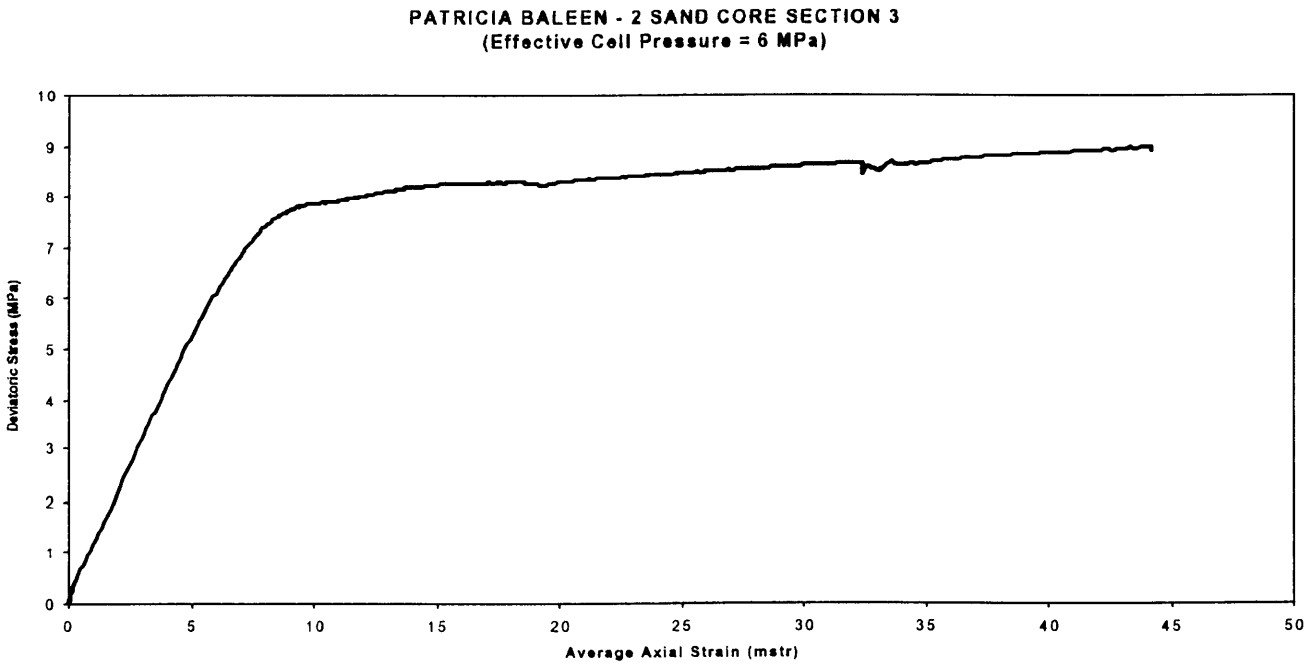

Figure 11a : Axial Stress vs Strain : 9 MPa confinement : Test 3 - Baleen-2, 760.23m

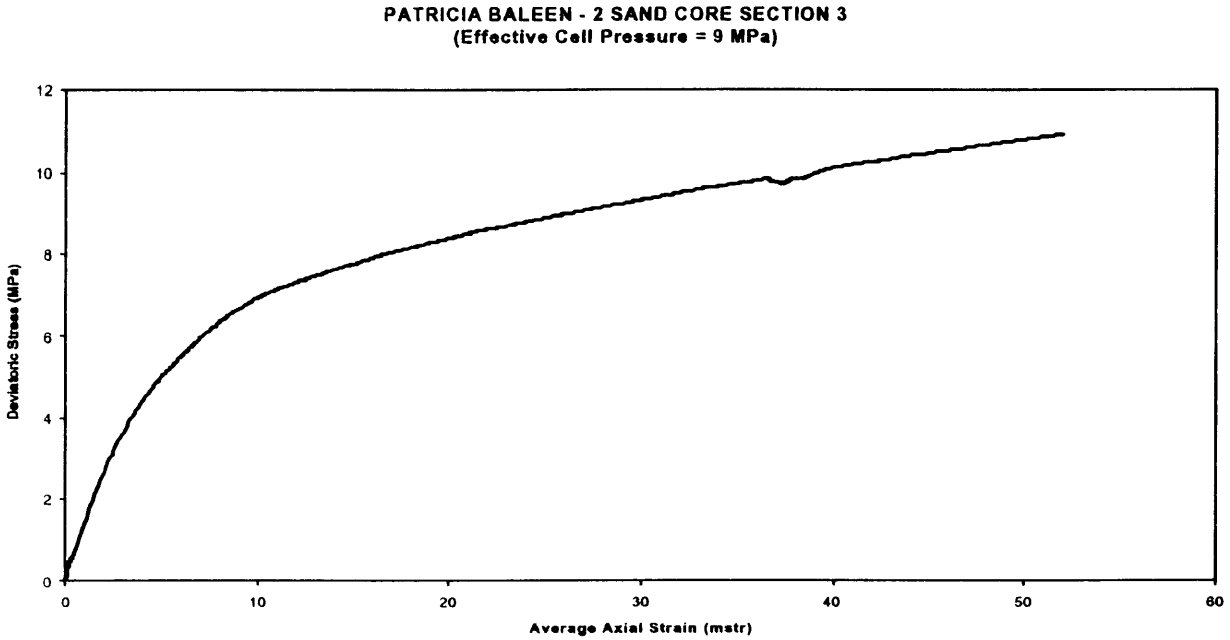

Figure 11b : Radial Strain vs Axial Strain : 9 MPa confinement : Test 3 - Baleen-2, 760.23m

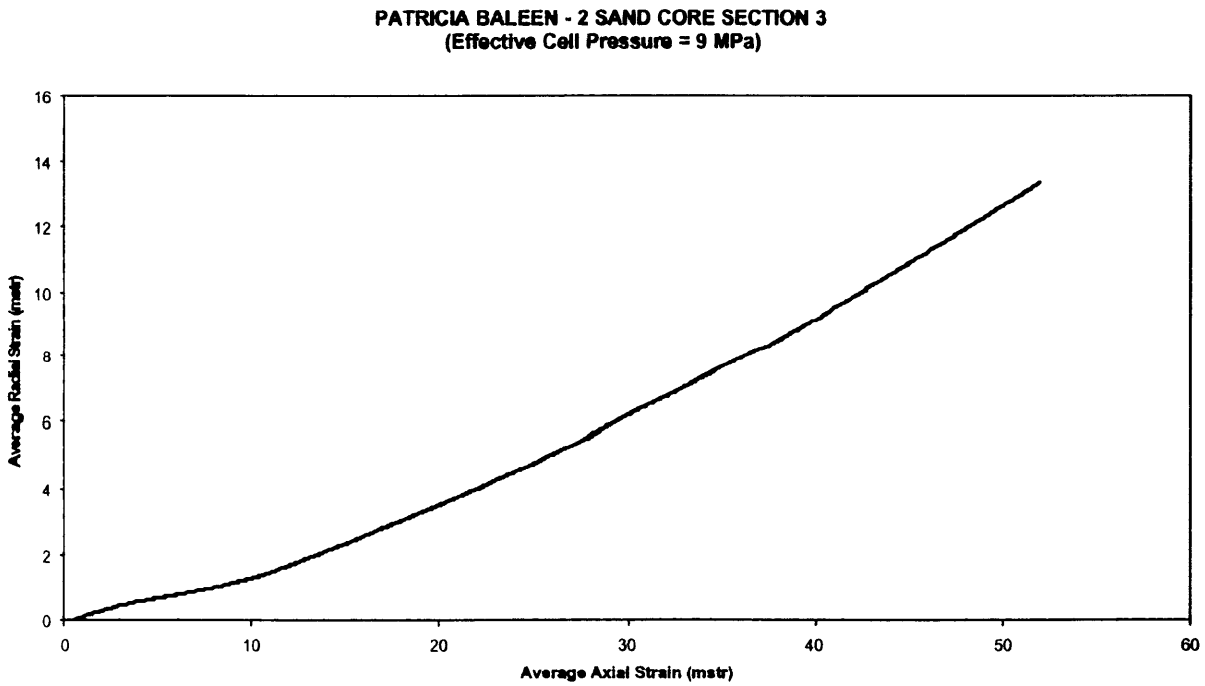

Figure 12a: Radial Strain vs Axial Strain ; Multi-Stage Tests ; Test 3 - Baleen-2, 760.23m

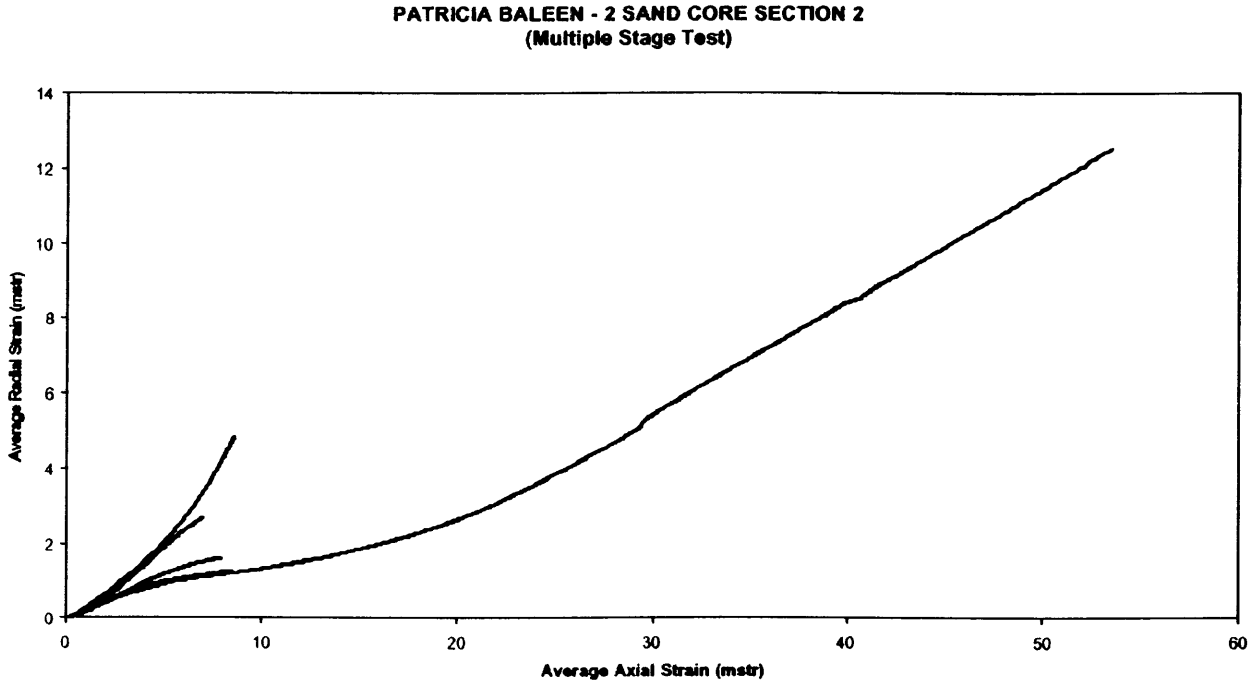

Figure 12b: Axial Stress vs Strain ; Multi-Stage Tests ; Test 3 - Baleen-2, 760.23m

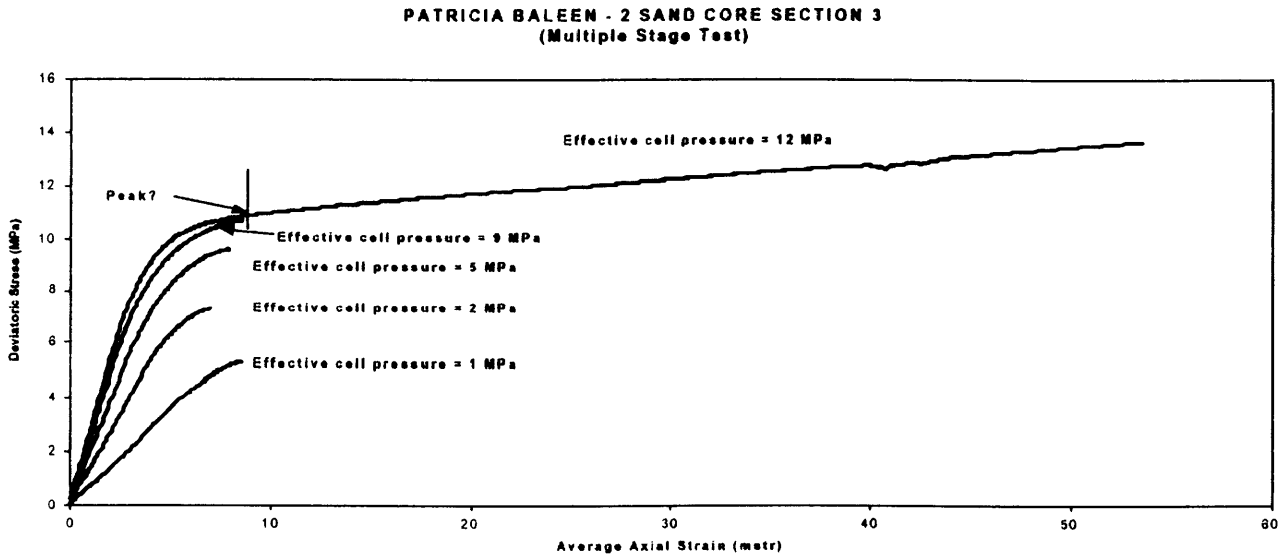

Figure 13a: Young's Modulus & Poisson's Ratio for Multi-Stage:Test 3 - Baleen-2, 760.23m

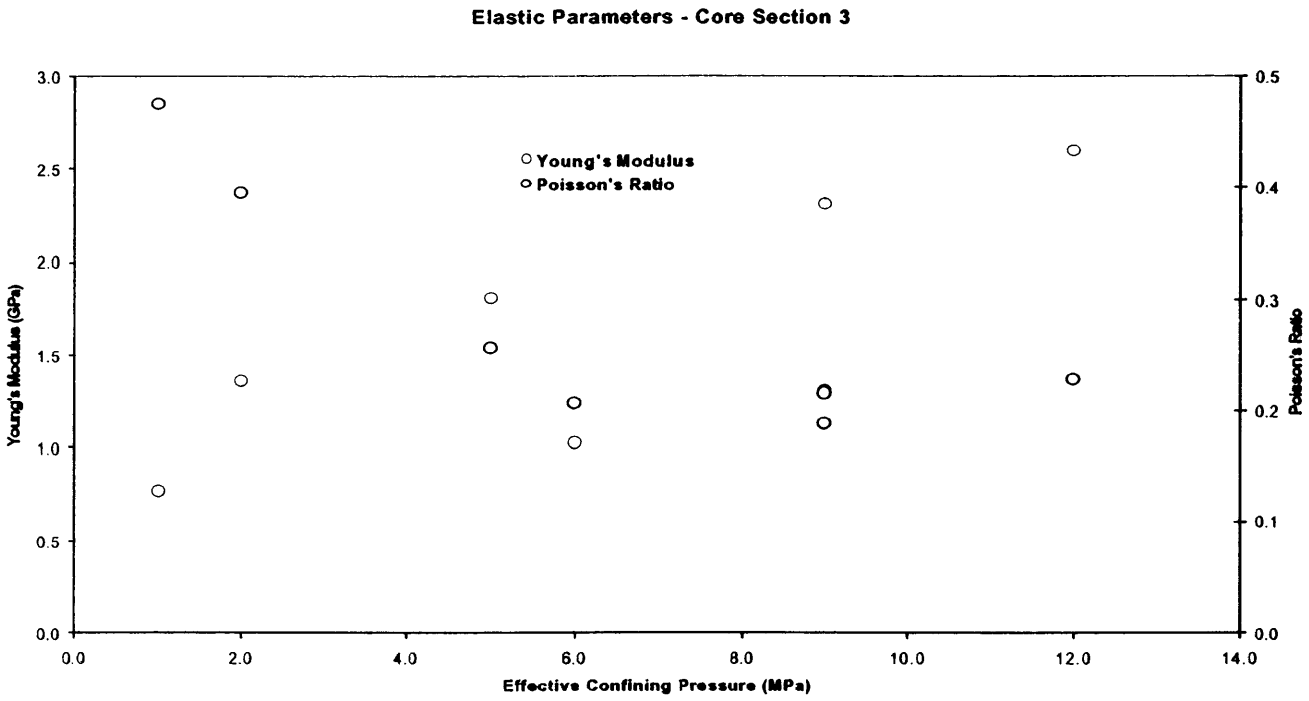

Figure 13b: Mohr's Circles of Strength for Multi-Stage : Test 3 - Baleen-2, 760.23m

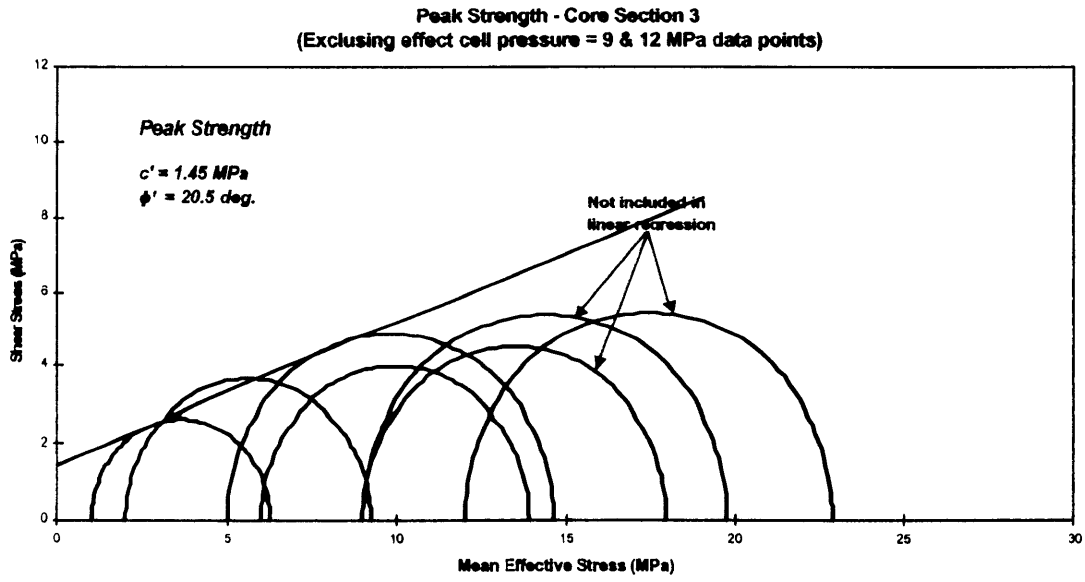

Figure 13c: Elasto-plastic Modelling for 6 MPa Test: Test 3 - Baleen-2, 760.23m

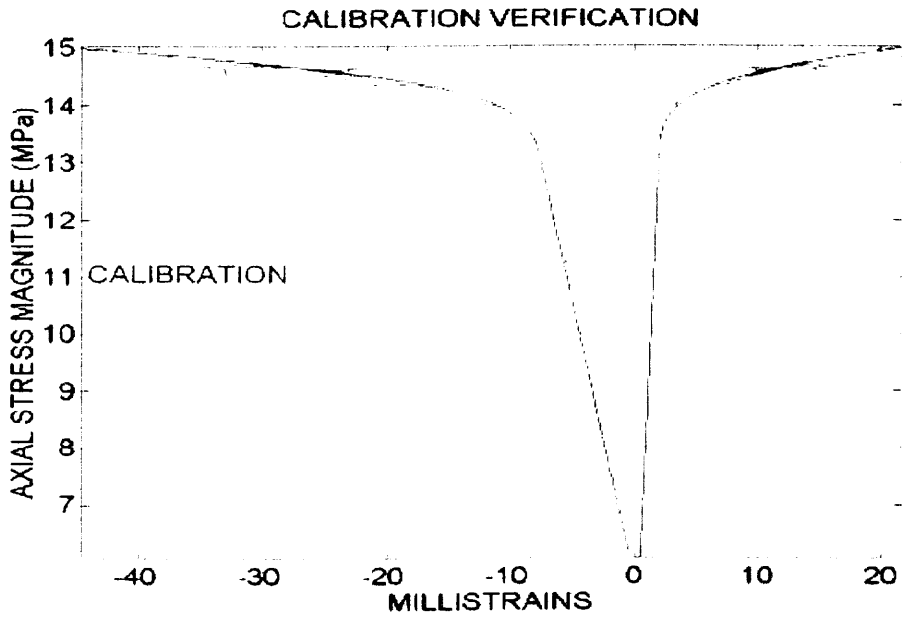

Figure 14a : Radial Strain vs Axial Strain : 6 MPa confinement : Test 4 - Baleen-2, 769.67m

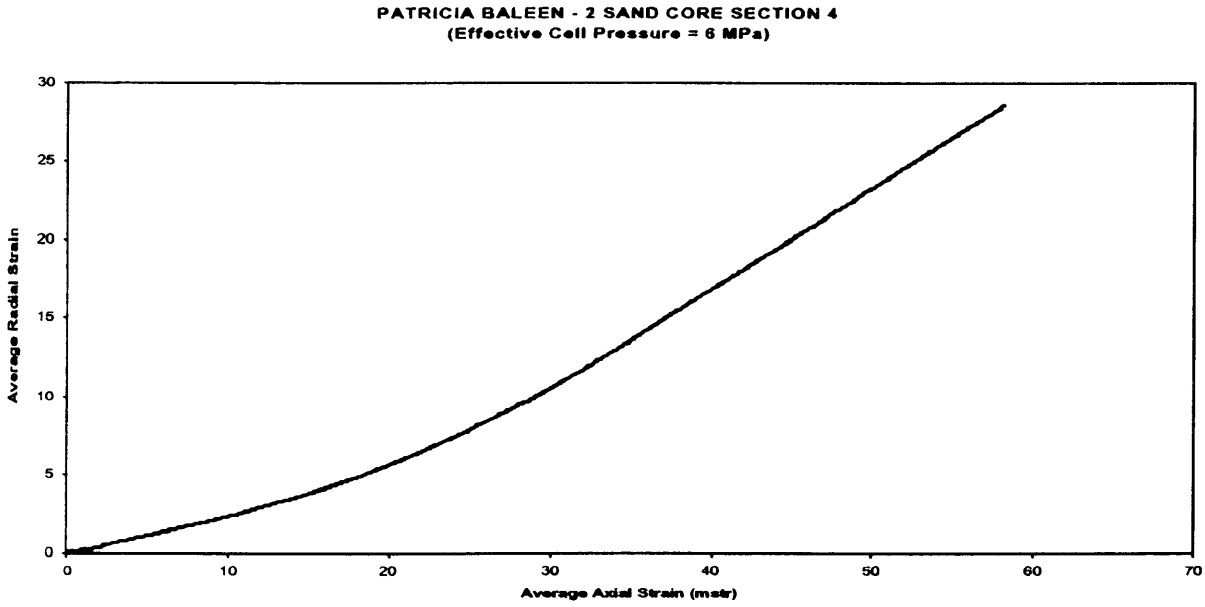

Figure 14b : Axial Stress vs Strain : 6 MPa confinement : Test 4 - Baleen-2, 769.67m

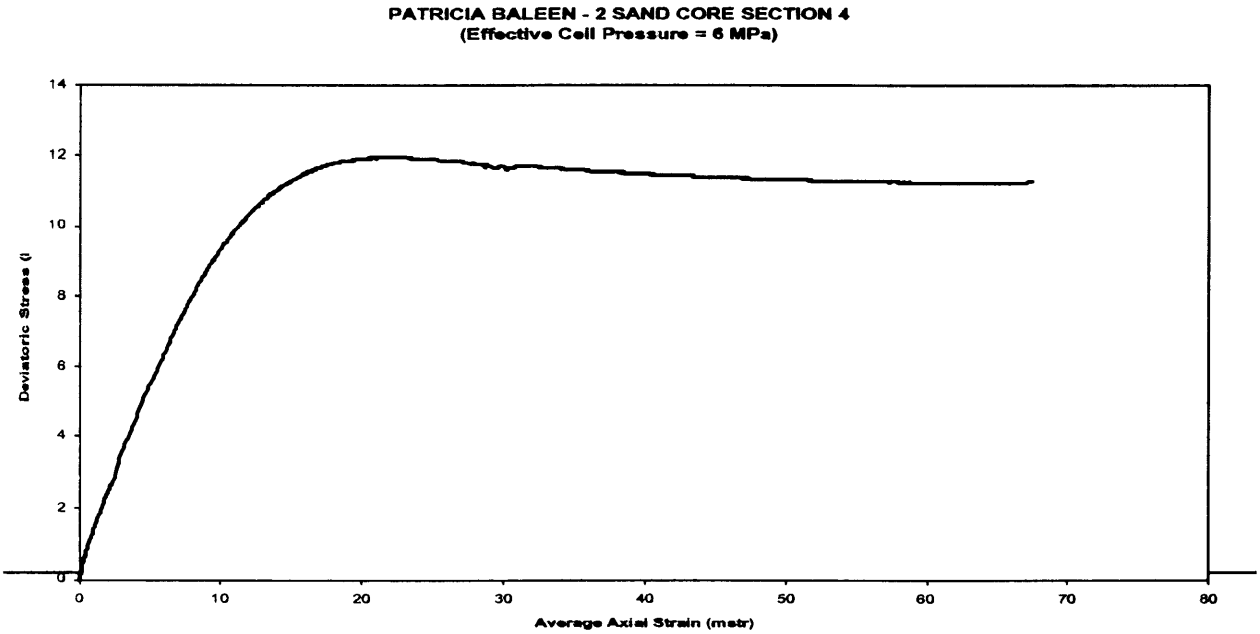

Figure 15a : Radial Strain vs Axial Strain : 9 MPa confinement : Test 4 - Baleen-2, 769.67m

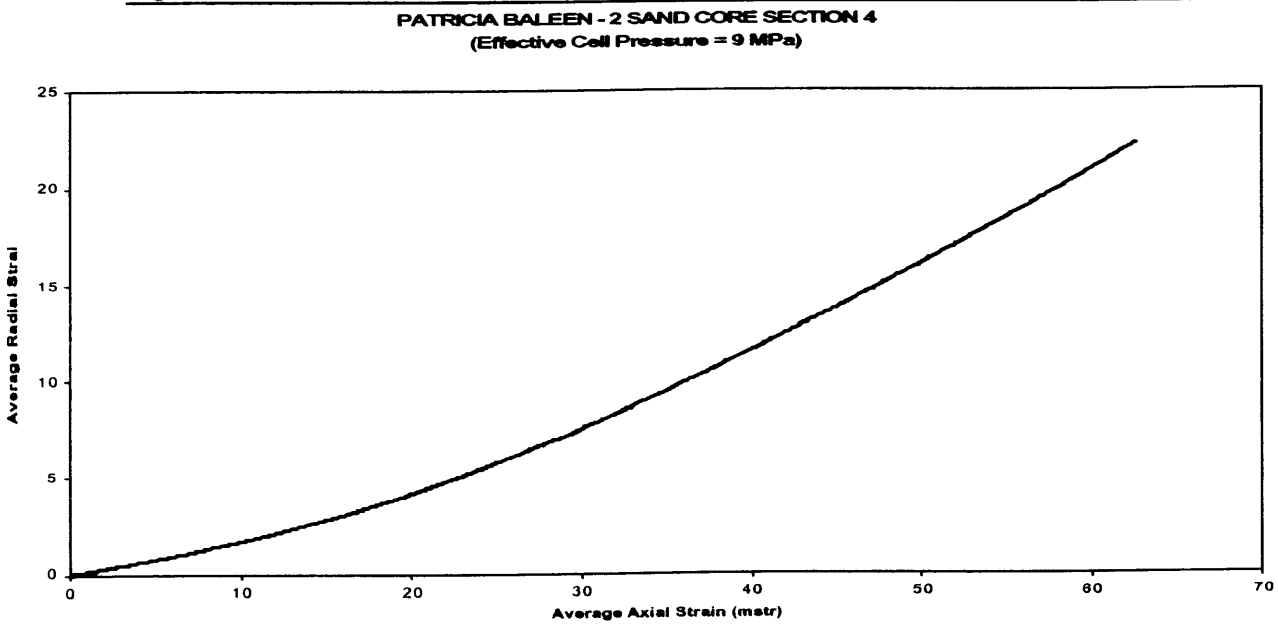

Figure 15b : Axial Stress vs Strain : 9 MPa confinement : Test 4 - Baleen-2, 769.67m

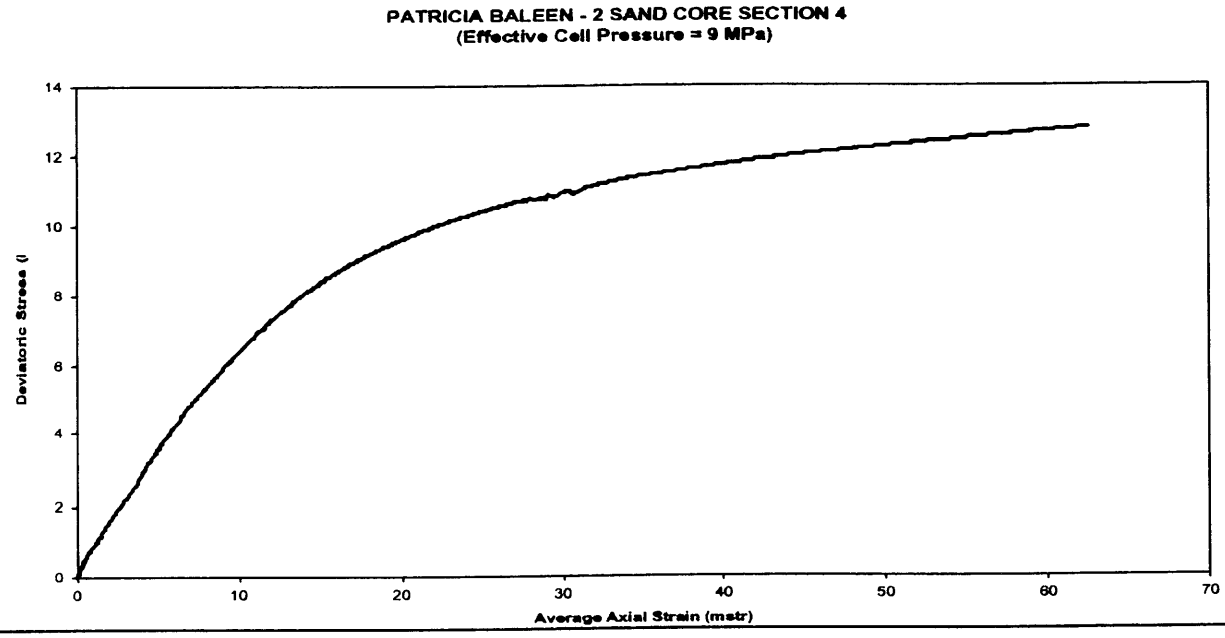

Figure 16a: Radial Strain vs Axial Strain : Multi-Stage Tests : Test 4 - Baleen-2, 769.67m

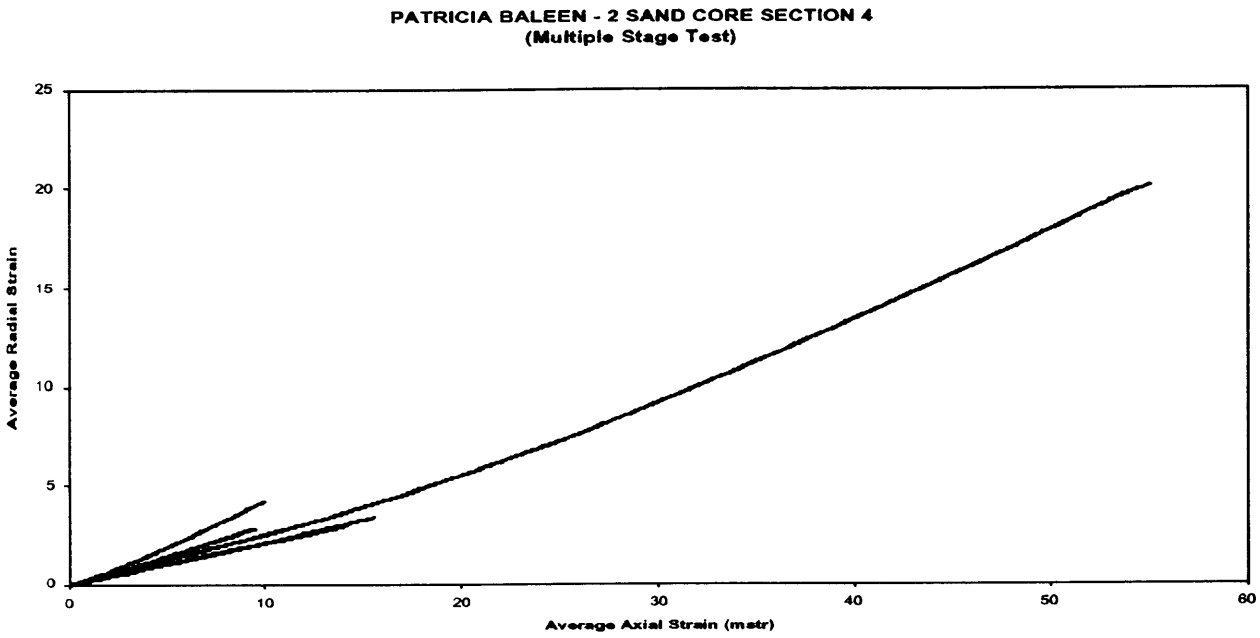

Figure 16b: Axial Stress vs Strain : Multi-Stage Tests : Test 4 - Baleen-2, 769.67m

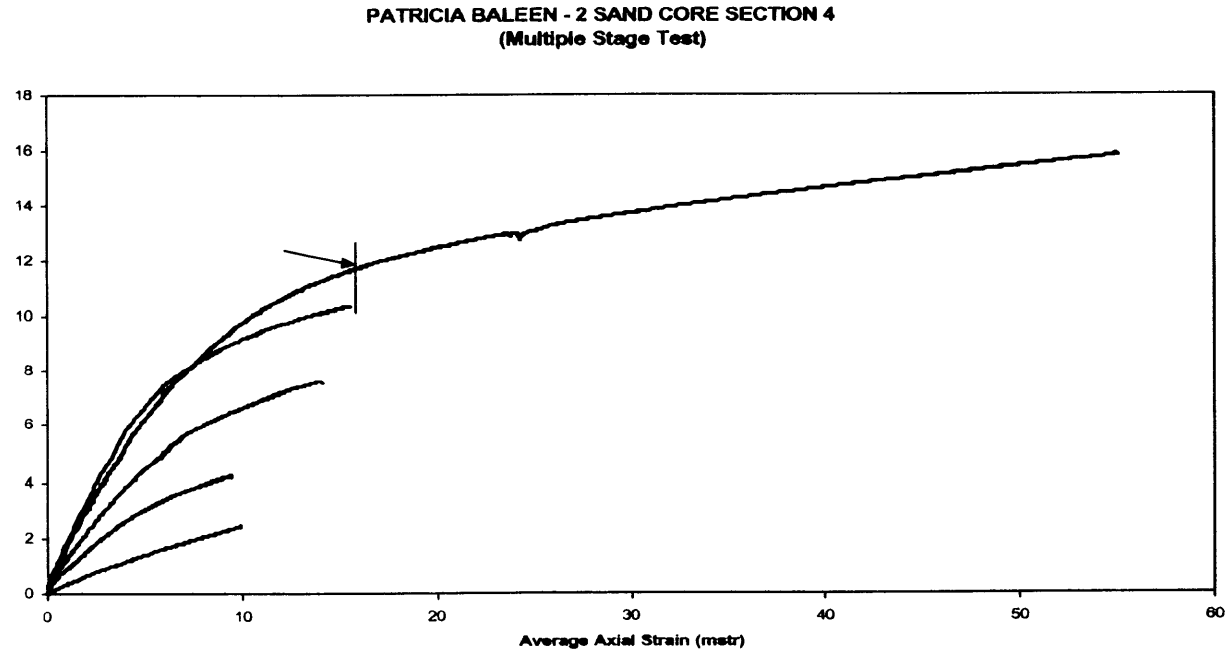

Figure 17a: Young's Modulus & Poisson's Ratio for Multi-Stage:Test 4 - Baleen-2, 769.67m

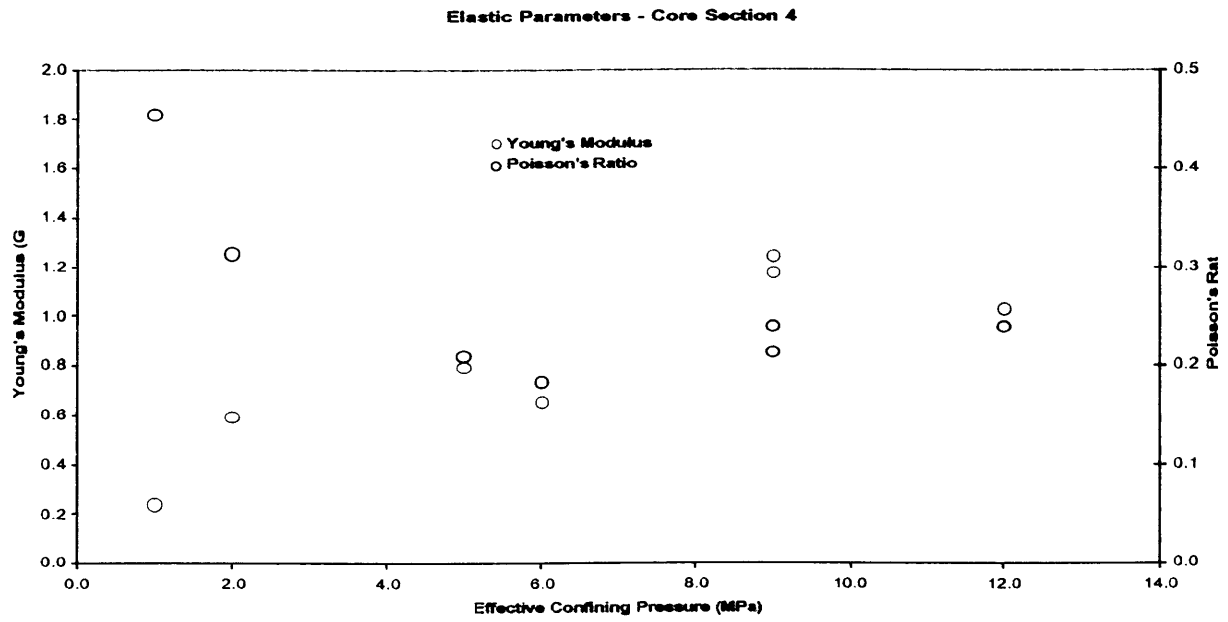

Figure 17b: Mohr's Circles of Strength for Multi-Stage : Test 4 - Baleen-2, 769.67m

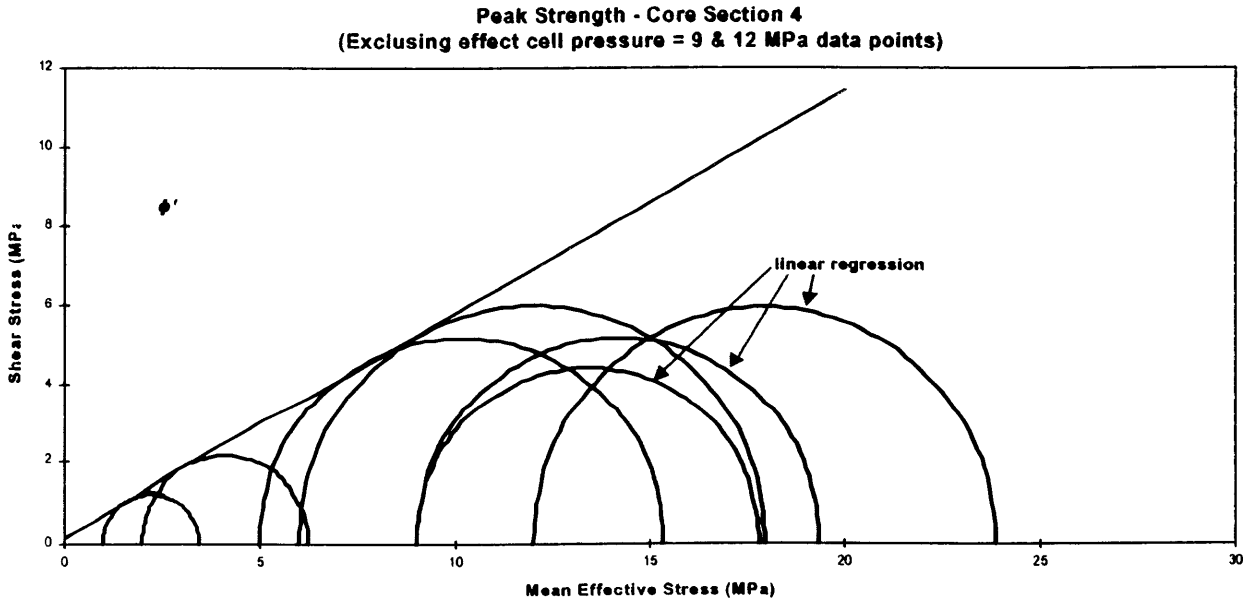

Figure 17c: Elasto-plastic Modelling for 6 MPa Test: Test 4 - Baleen-2, 769.67m

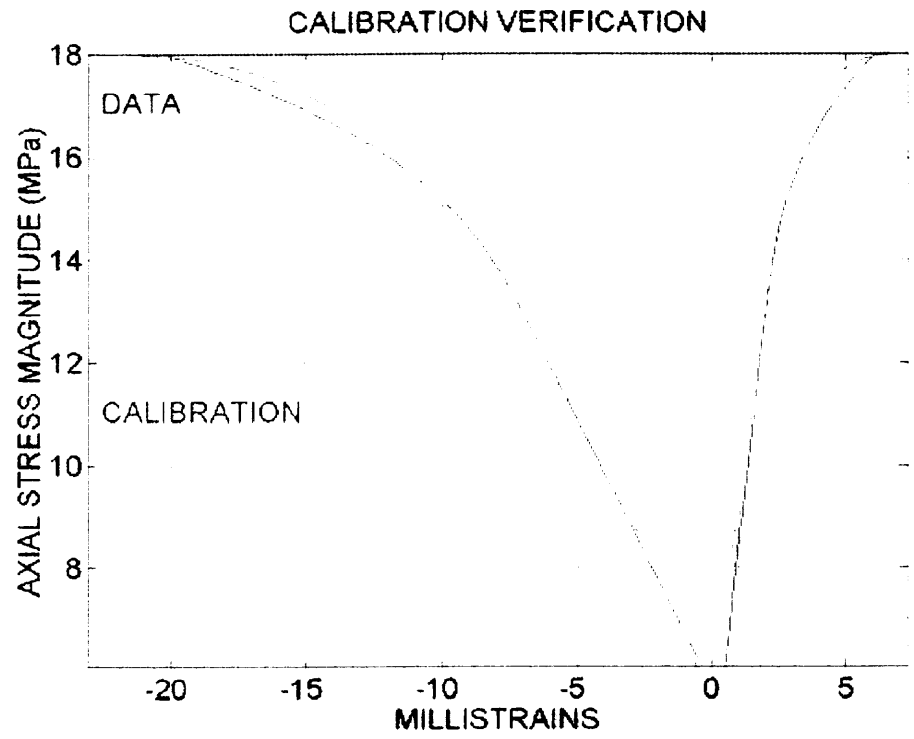

Figure 18a : Radial Strain vs Axial Strain : 6 MPa confinement : Test 5 - Baleen-2, 777.00m

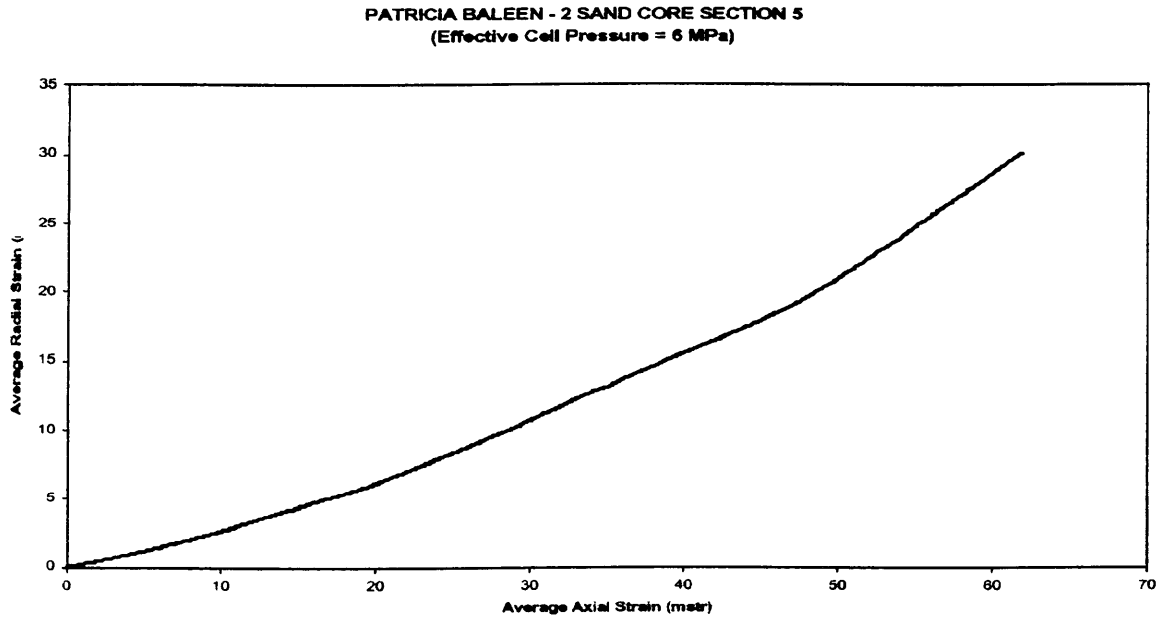

Figure 18b : Axial Stress vs Strain : 6 MPa confinement : Test 5 - Baleen-2, 777.00m

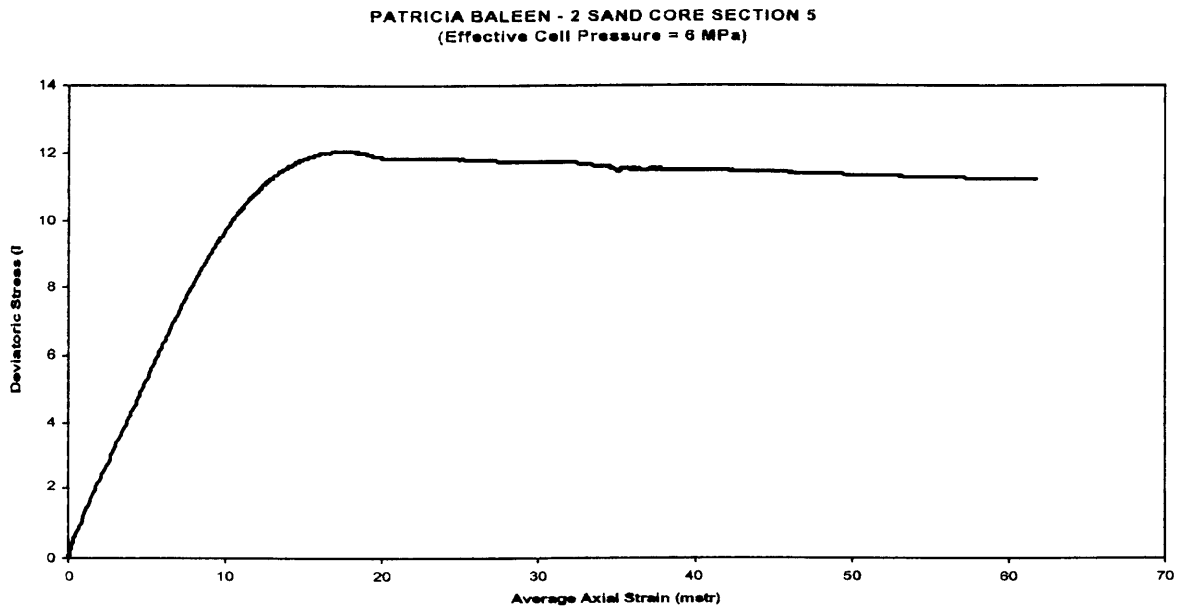

Figure 19a : Radial Strain vs Axial Strain : 9 MPa confinement : Test 5 - Baleen-2, 777.00m

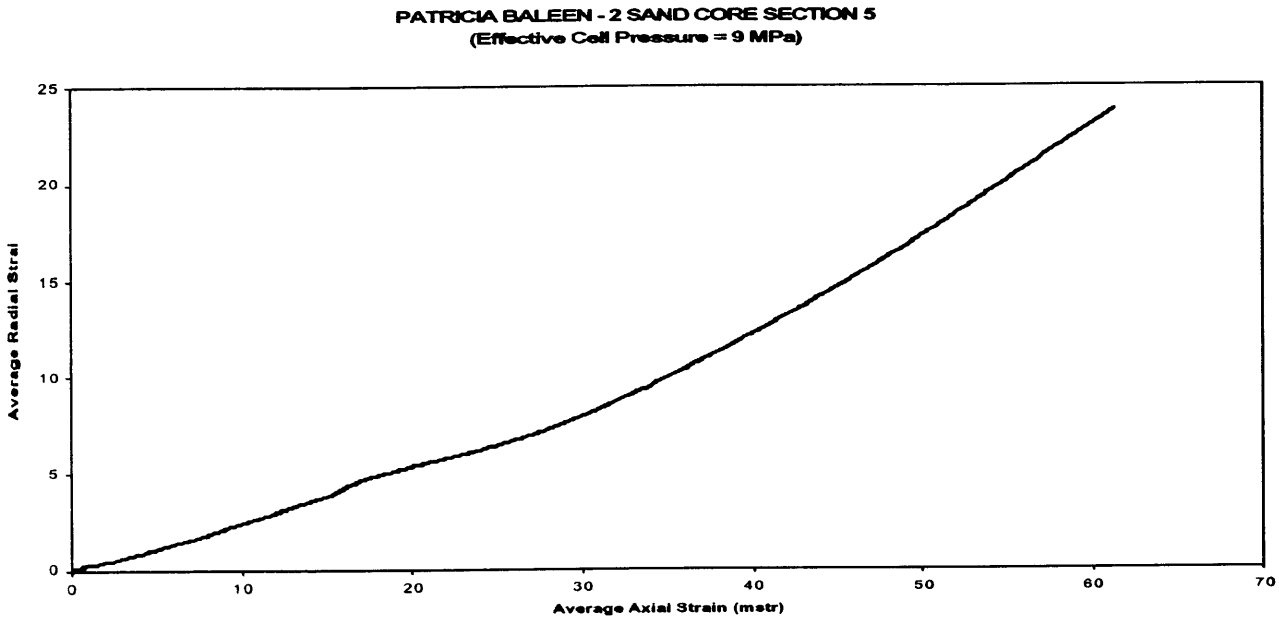

Figure 19b : Axial Stress vs Strain : 9 MPa confinement : Test 5 - Baleen-2, 777.00m

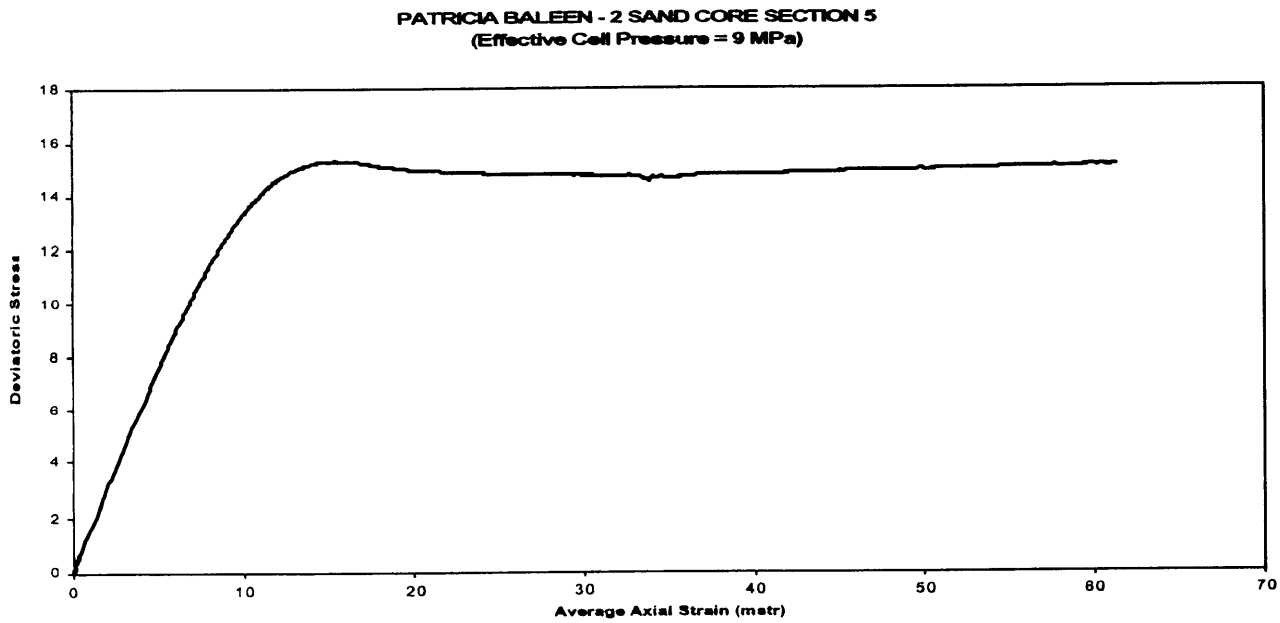

Figure 20a: Radial Strain vs Axial Strain : Multi-Stage Tests : Test 5 - Baleen-2, 777.00m

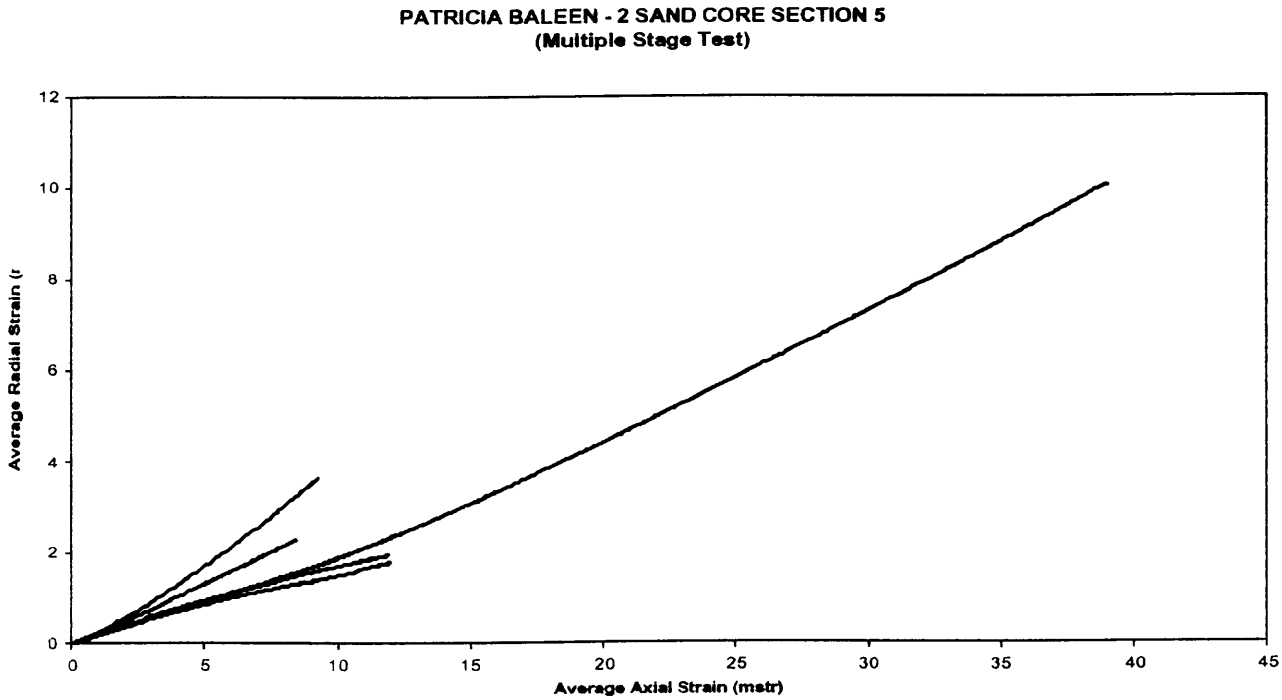

Figure 20b: Axial Stress vs Strain : Multi-Stage Tests : Test 5 - Baleen-2, 777.00m

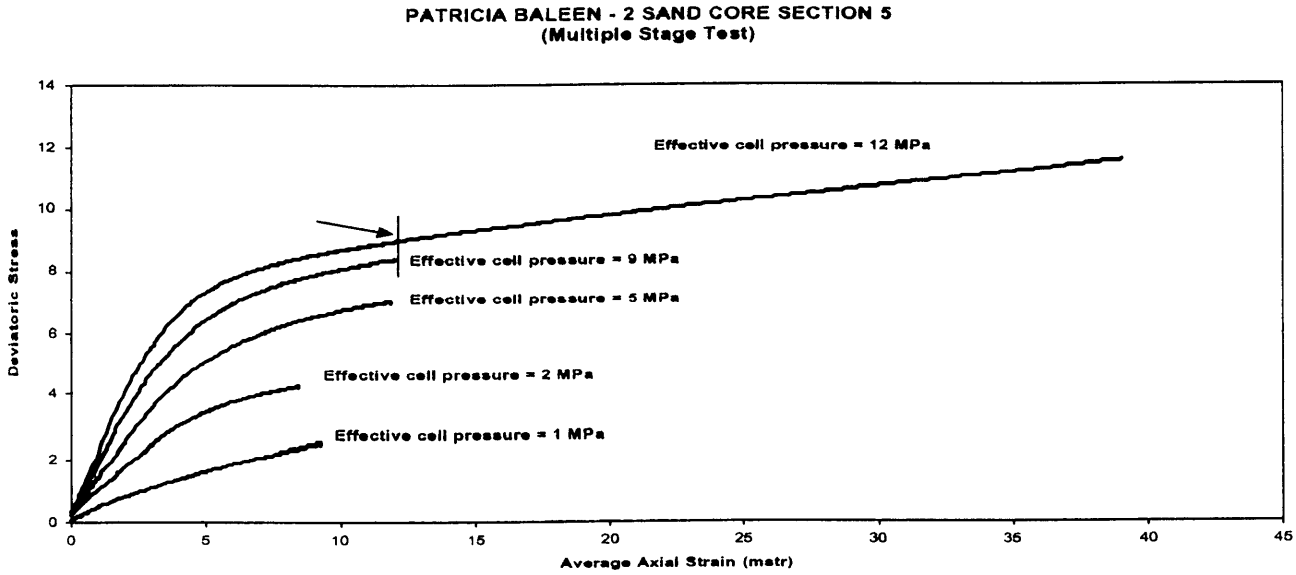

Figure 21a: Young's Modulus & Poisson's Ratio for Multi-Stage:Test 5 - Baleen-2, 777.00m

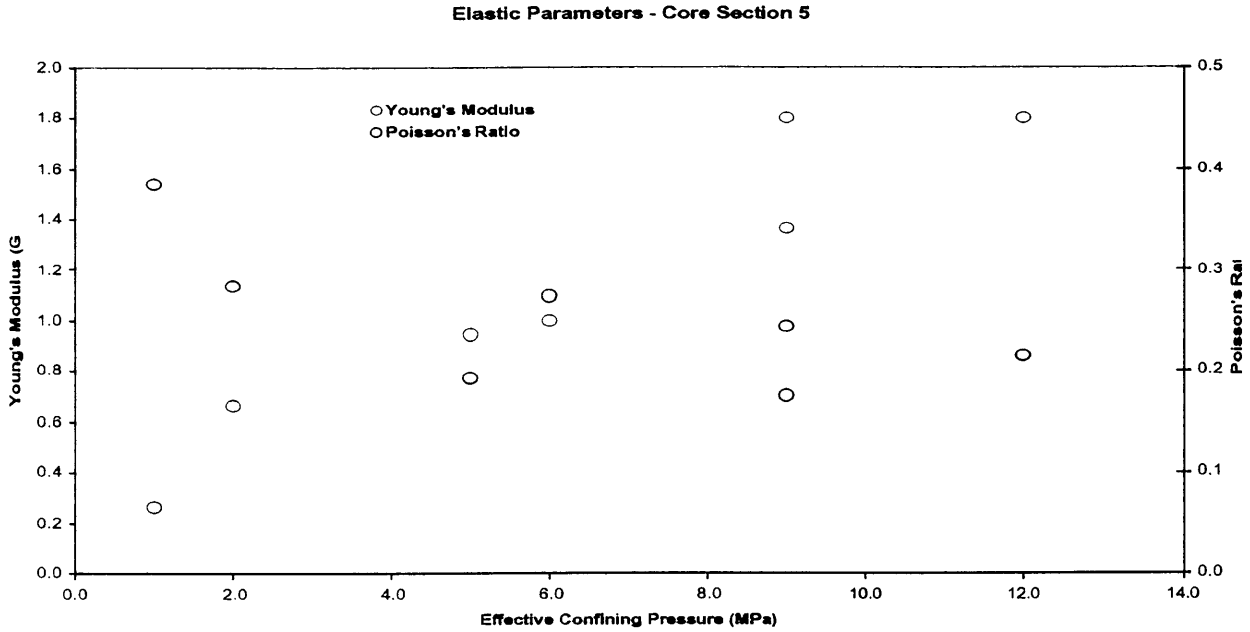

Figure 21b: Mohr's Circles of Strength for Multi-Stage : Test 5 - Baleen-2, 777.00m

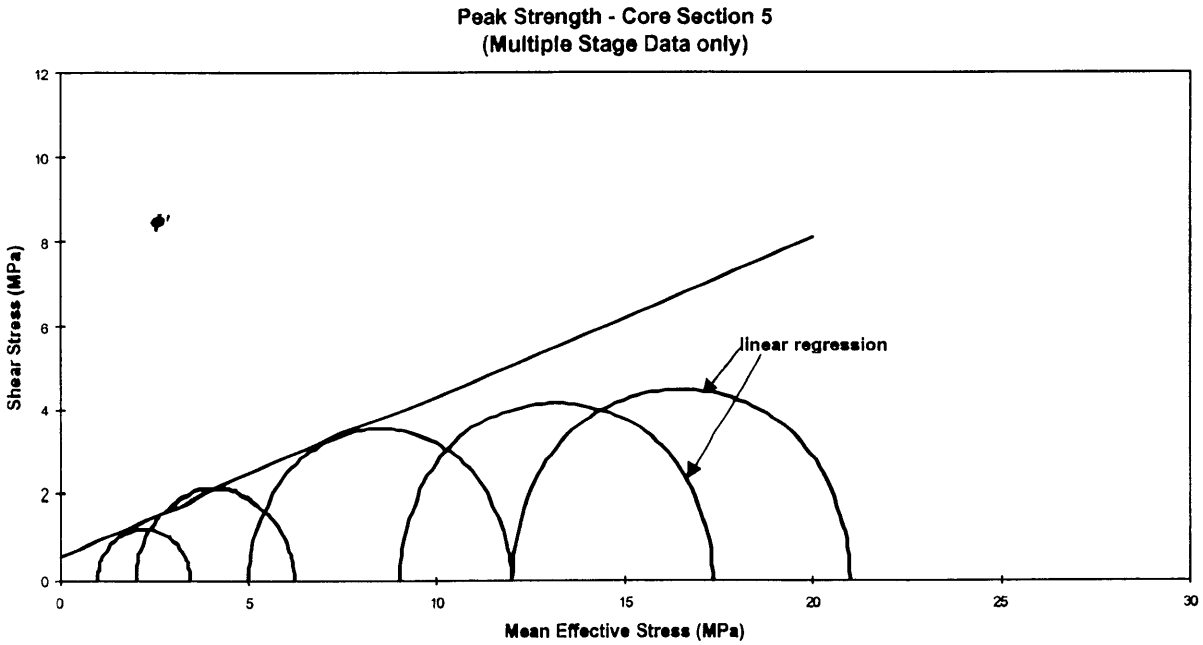

Figure 21c: Elasto-plastic Modelling for 6 MPa Test: Test 5 - Baleen-2, 777.00m

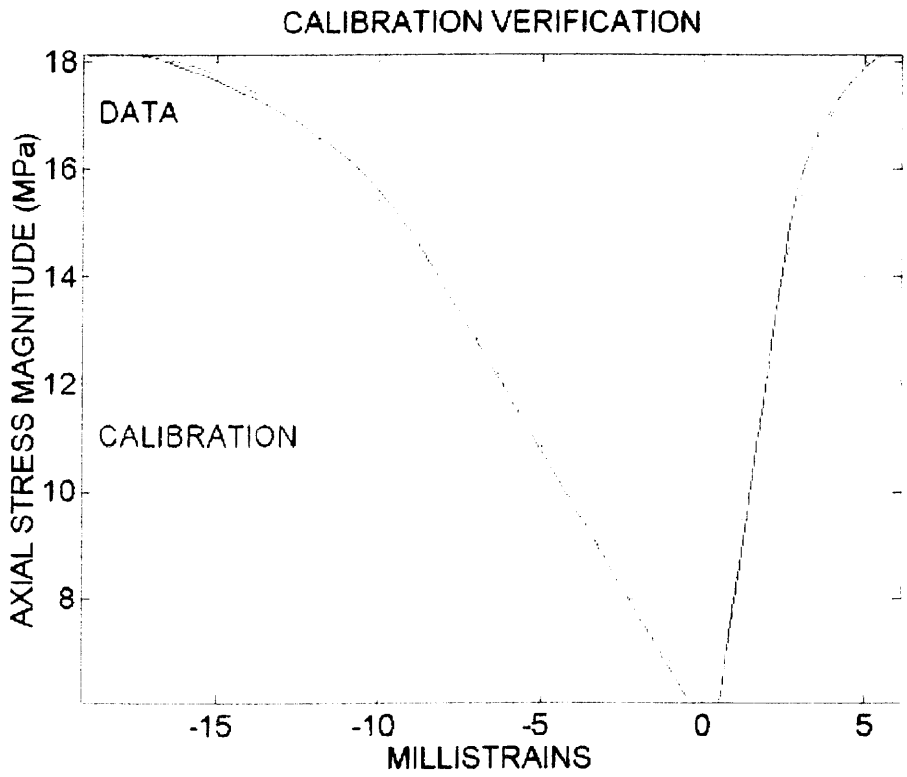

APPENDIX 3

REFERENCES

Biot M.A., - Theory of Elastic Waves in a Fluid Saturated Porous Solid, Journ. Acoust. Soc. Am. 28, 1956

Bradford I.D.R., Cook J.M., - A semi-analytic elastoplastic model for wellbore stability with applications to sanding , SPE/ISRM Eurock 94, Delft, 1994

Bradford I.D.R., Fuller J.A., Thompson P.J., Walsgrove T.R., Benefits of assessing the solids production risk in a North Sea reservoir using elastoplastic modeling, SPE 47360, Trondheim, July 1998

Cook J.M., A Study of Physical Mechanisms of Sanding and Application to Sand Production Prediction, SPE, 1993

Deere D.U. and Miller R.P., 1966, Engineering Classification and Index Properties for Intact Rock, Technical Report No. AFWL-TR-65-116, Air Force Weapons Laboratory, Kirtland, New Mexico.

Nicholson E.D., Goldsmith G., Cook J. - Direct observation and modelling of sand production processes in weak sandstone. SPE 47328, Trondheim, July 1998

Papanastasiou P, Nicholson E.D., Goldsmith G., Cook J. - Sanding prediction: Experimental results and numerical modelling. Poromechanics a tribune to M.Biot, 457-462, Balkema, Rotterdam (1998)

Papamichos E., van den Hoek P. - Size dependency of Castlegate and Berea sandstone hollow cylinder strength on the basis of bifurcation theory, Proc. 35th US Symp. Rock Mechanics (1995)

Plumb R.A., - Influence of Composition and Texture on the Failure Properties of Clastic Rocks, SPE/ISRM 28022, Eurock Aug. 1994

Plumb R.A., Thiercelin M., - Stress Estimation: Progress and Future Research Direction, research communication, SCR/SR/1989/027/DRM/C, 1989

Tronvoll J, Papamichos E, Kessler N. - Perforation cavity stability: Investigation of failure mechanisms. Proc. Symp. On hard soils and soft rocks, Athens, (1993)

Unander T.E., Papamichos E, Tronvoll J, Skjaerstein A. - Flow geometry effects on sand productionfrom oil producing perforation cavity. Int. J. Rock Mech. & Min Sci. 34: 3-4, No. 231, (1997)

White J.E. Underground Sound, published by Elsevier, 1983

Wu B., Addis M.A., Last N.C., Stress Estimation in Faulted Regions: The Effect of Residual Friction, SPE/ISRM 47210, Trondheim, July 1998.

APPENDIX 4

BALEEN-2

30 CENTIMETRE CORE PHOTOGRAPHY

-ACS LABORATORIES-

ACS

LABORATORIES

PTY. LTD.

White Light

30cm FORMAT CORE PHOTOGRAPHY

of

BALEEN-2

for

OMV AUSTRALIA PTY LTD

OMV Australia Pty Ltd.

BALEEN 2

ACS LABORATORIES PTY LTD

746.45m

CORE No. 1

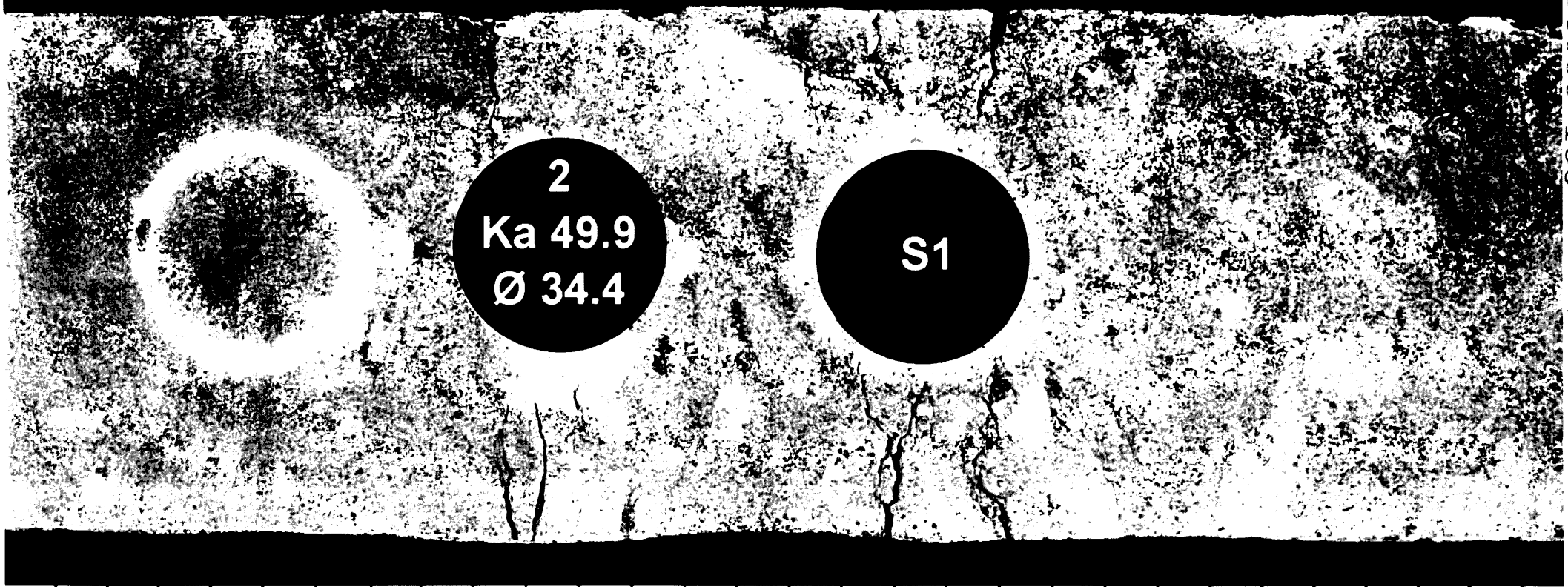

0 5 10 15 20 25 30

903080 136

Pe908080_colour 040

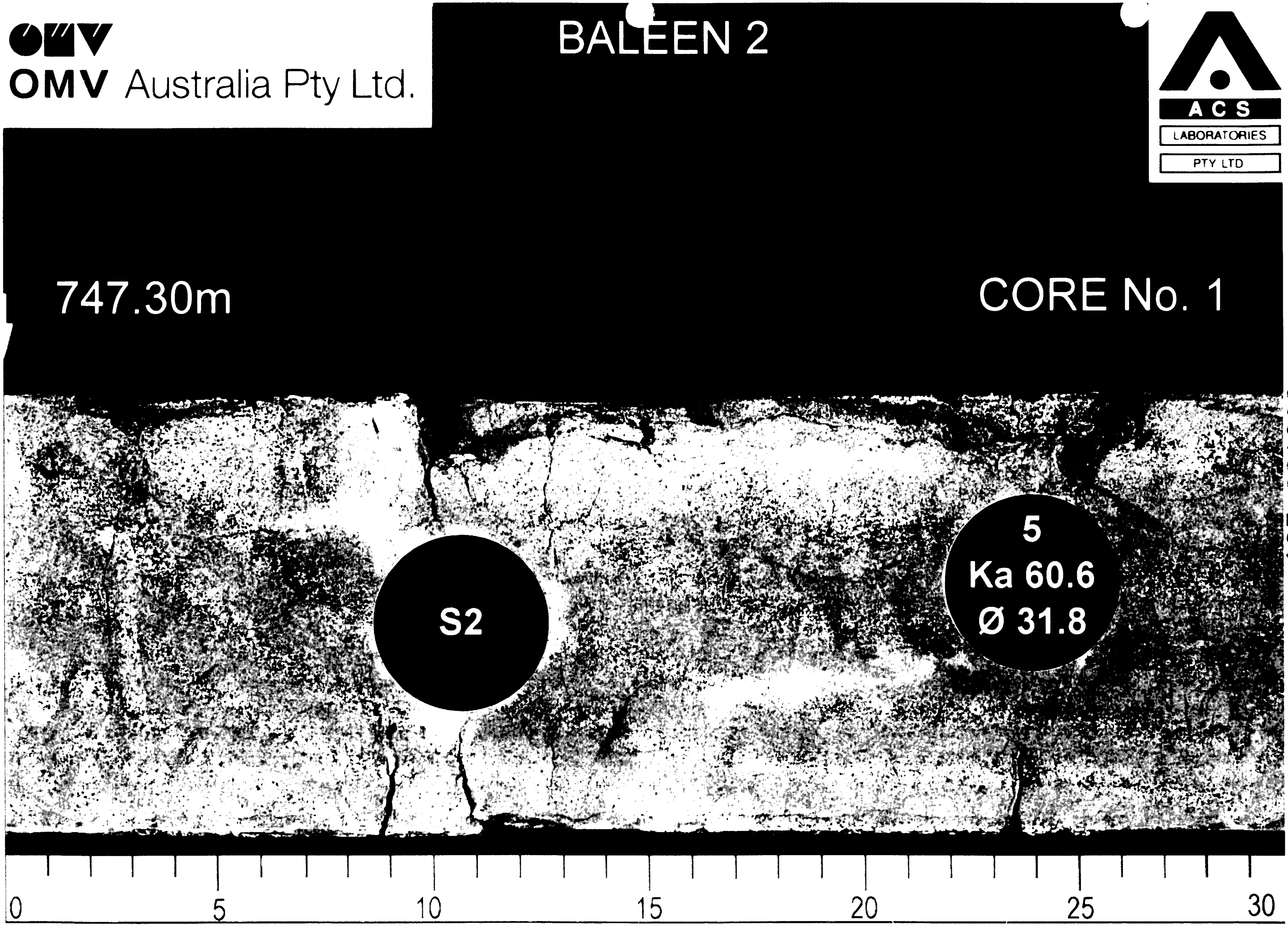

OMV Australia Pty Ltd.

BALEEN 2

ACS LABORATORIES PTY LTD

748.25m

CORE No. 1

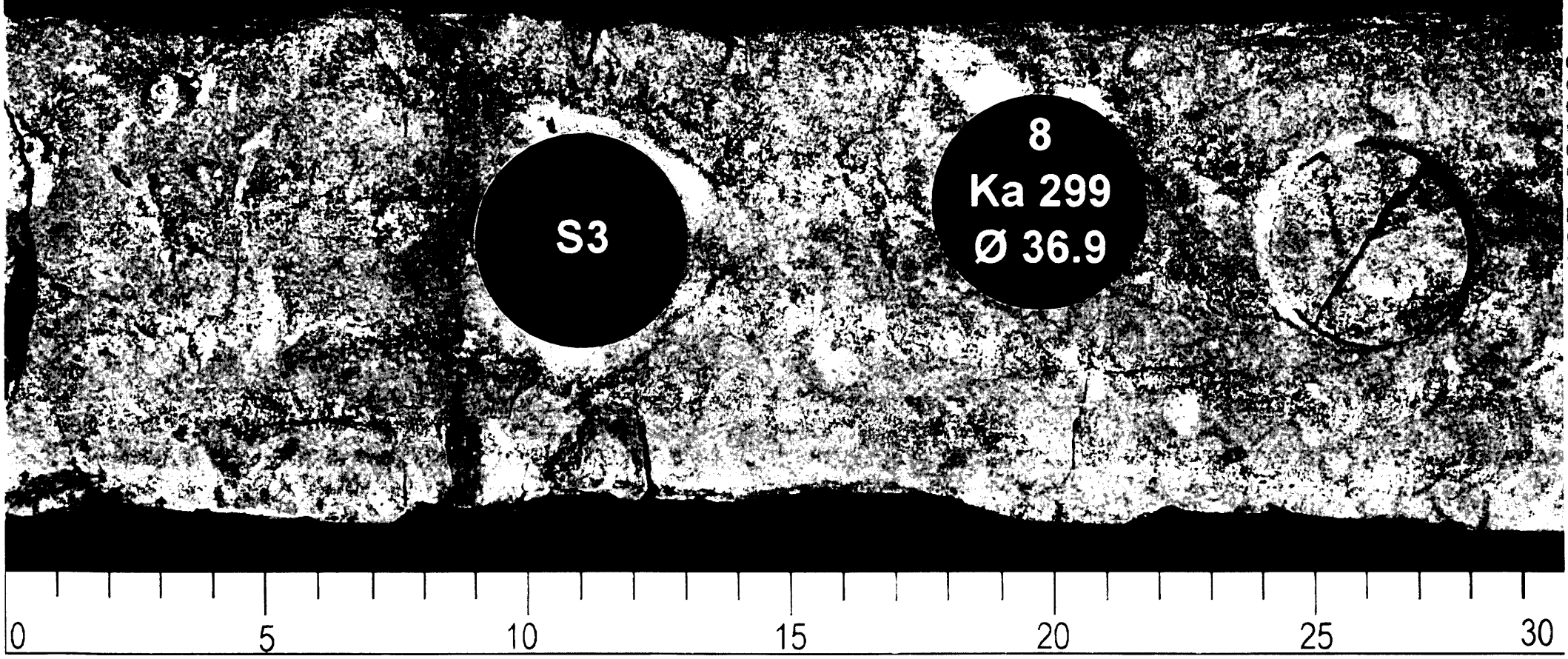

903080 187

OMV Australia Pty Ltd.

BALEEN 2

ACS LABORATORIES PTY LTD

749.30m

CORE No. 1

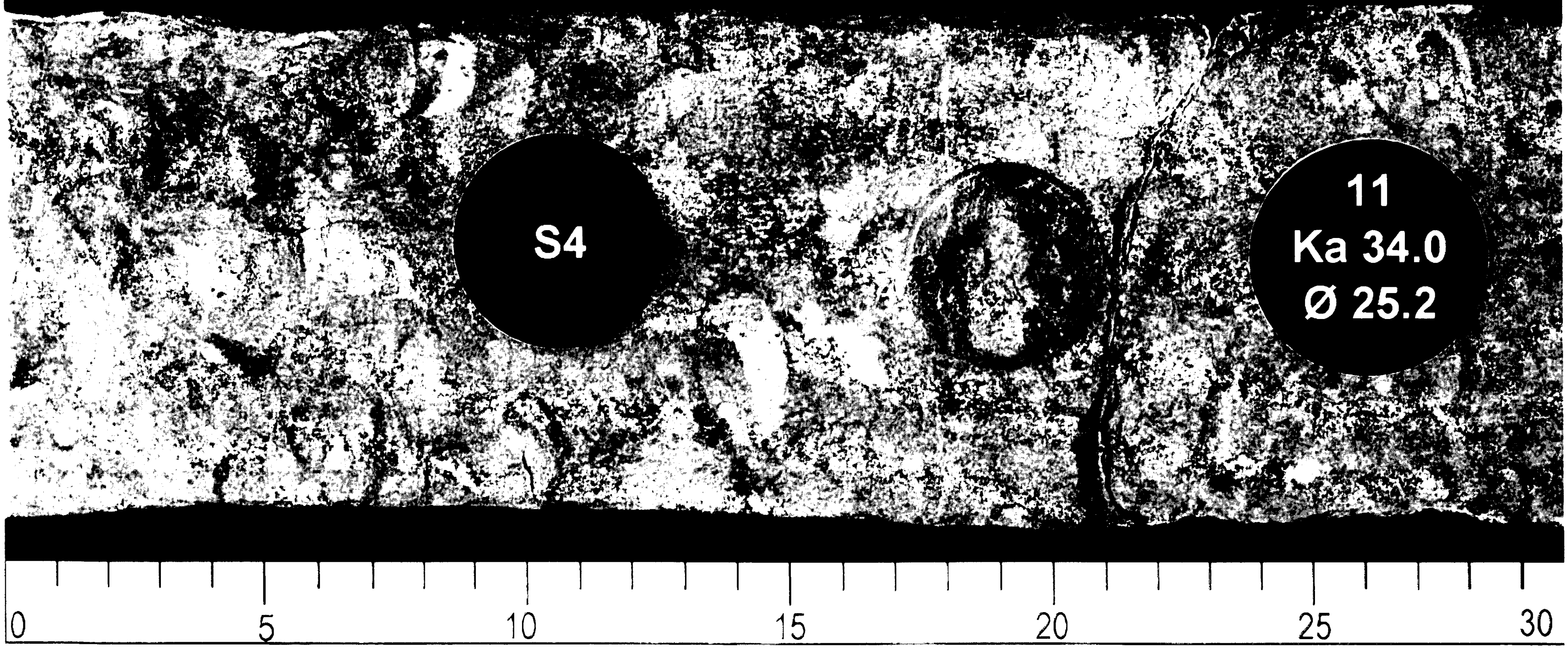

908080 188

PE908080_colour 042

OMV Australia Pty Ltd.

BALEEN 2

ACS LABORATORIES PTY LTD

750.30m

CORE No. 1

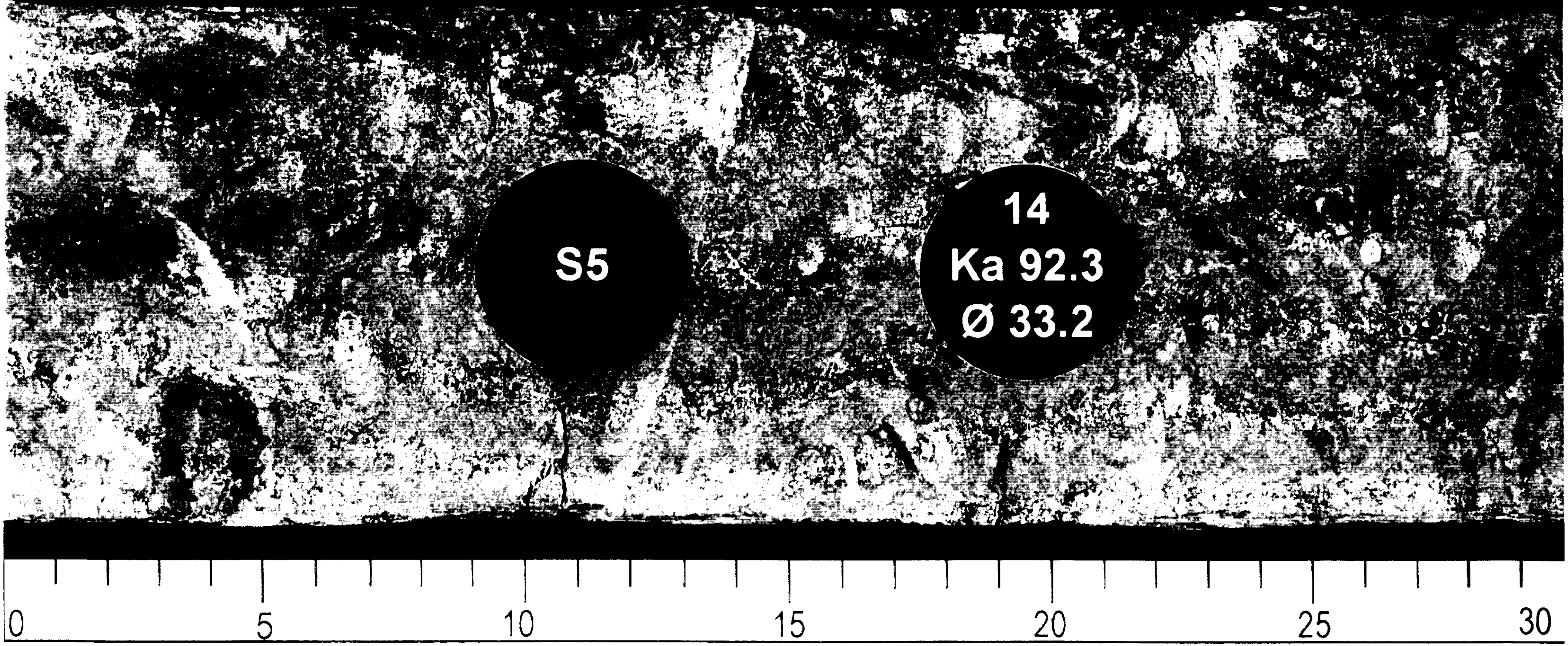

903080 189

PE 908080 - colour 043

OMV Australia Pty Ltd.

BALEEN 2

ACS LABORATORIES PTY LTD

751.35m

CORE No. 1

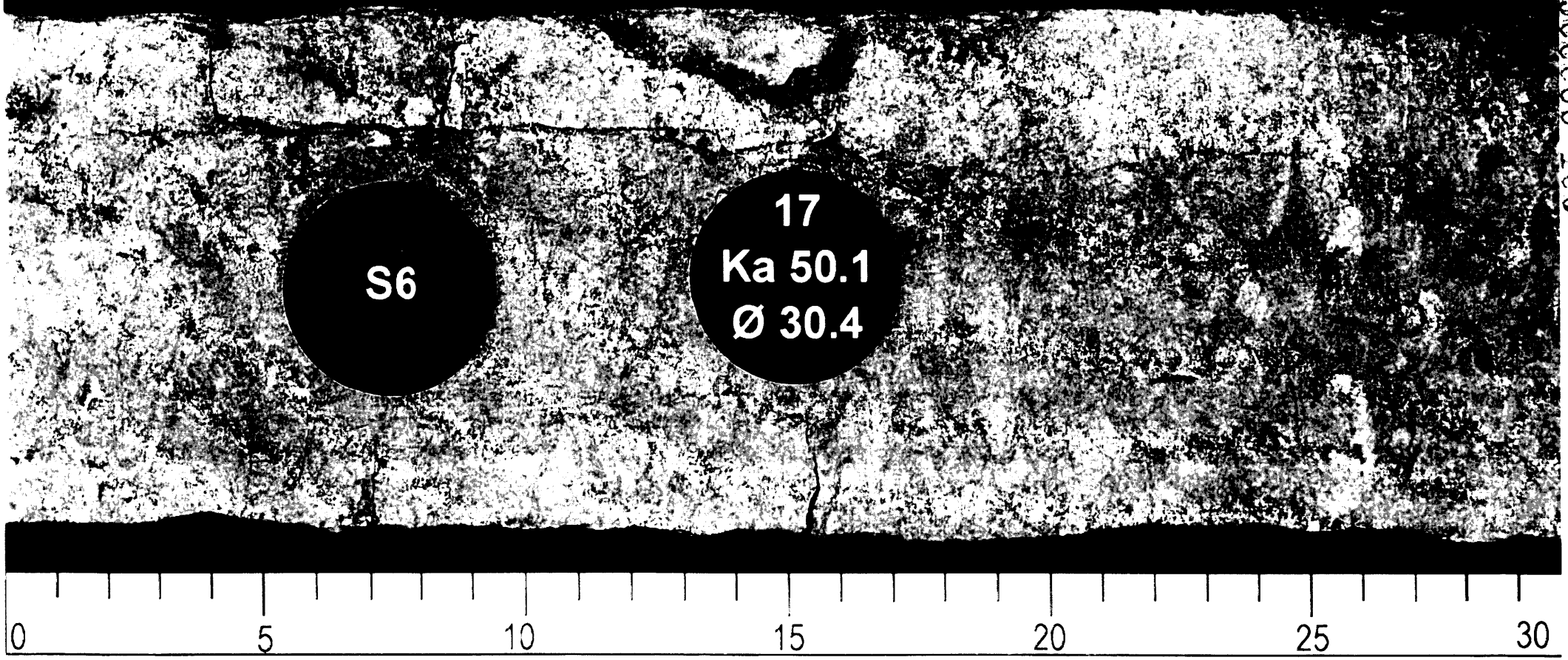

OMV Australia Pty Ltd.

BALEEN 2

ACS LABORATORIES PTY LTD

752.30m

CORE No. 1

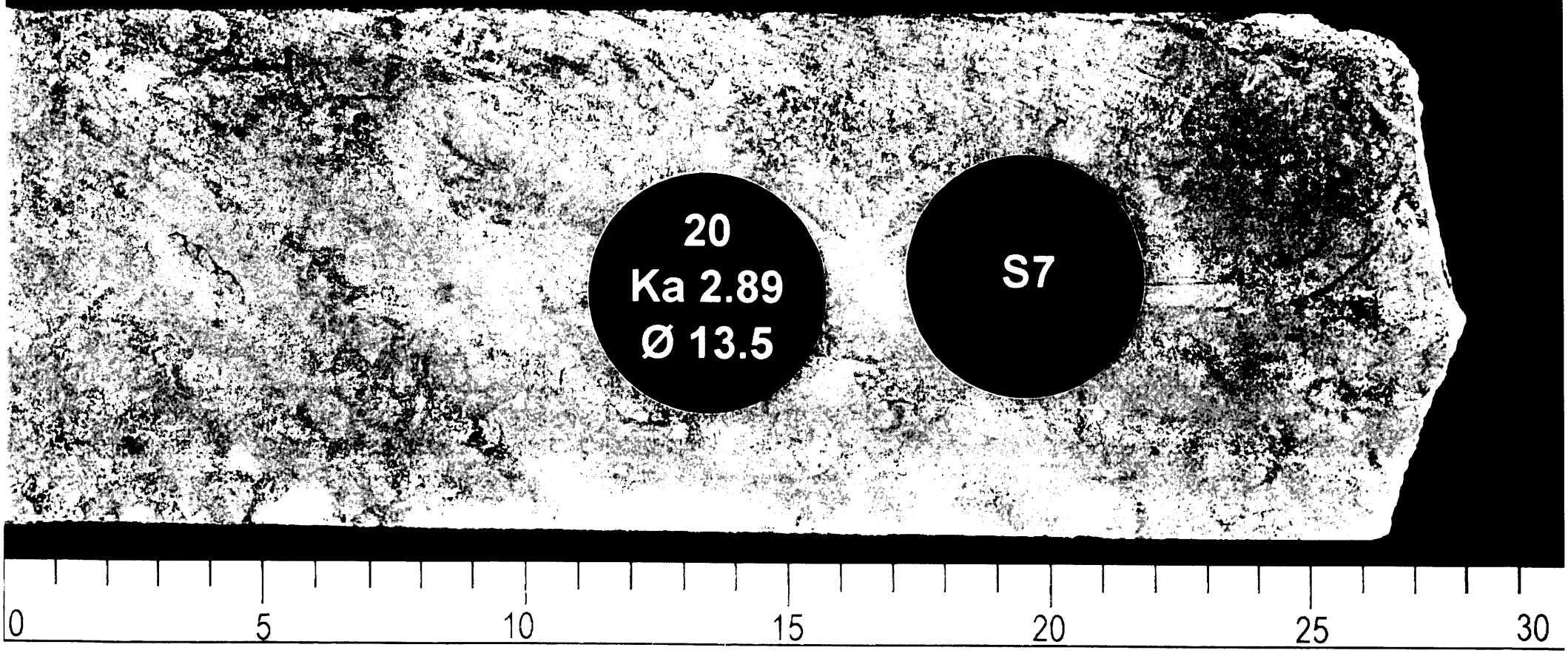

OMV Australia Pty Ltd.

BALEEN 2

ACS LABORATORIES PTY LTD

753.30

CORE No. 1

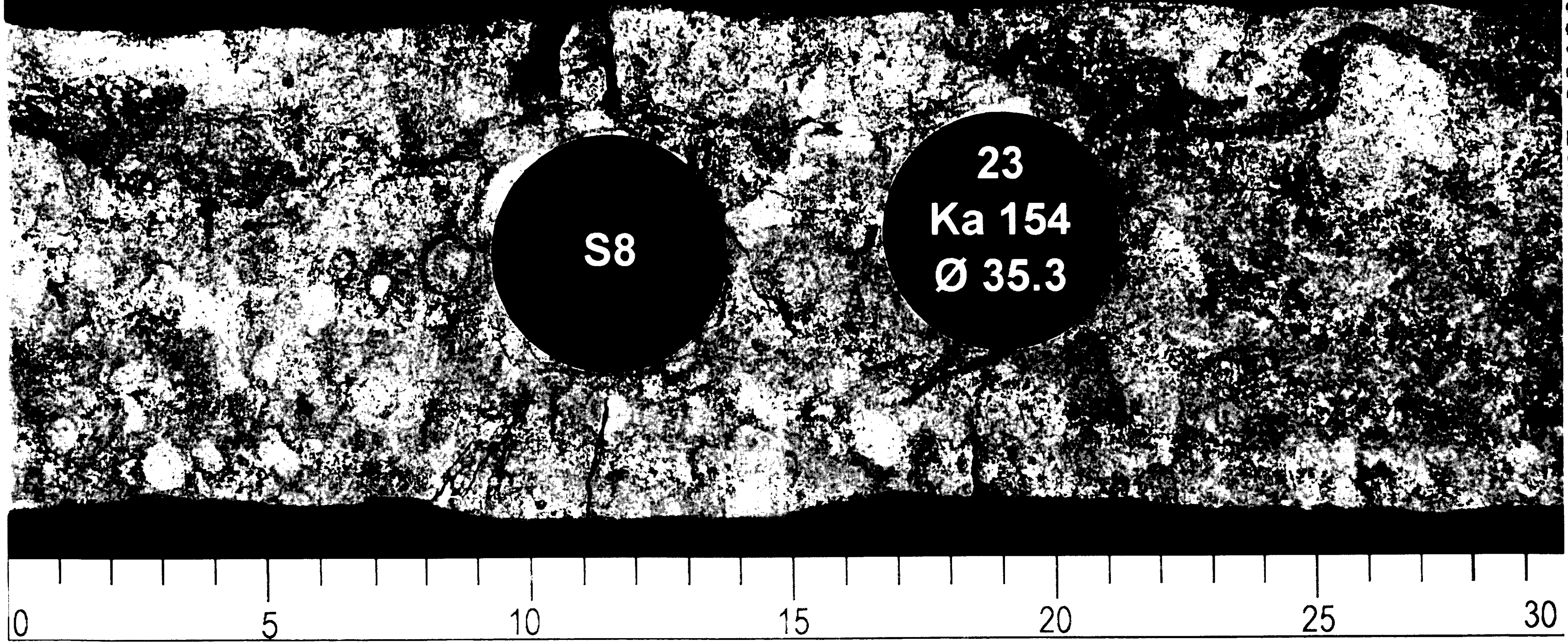

908080 192

PE908080-colour046

OMV Australia Pty Ltd.

BALEEN 2

ACS LABORATORIES PTY LTD

754.30m

CORE No. 1

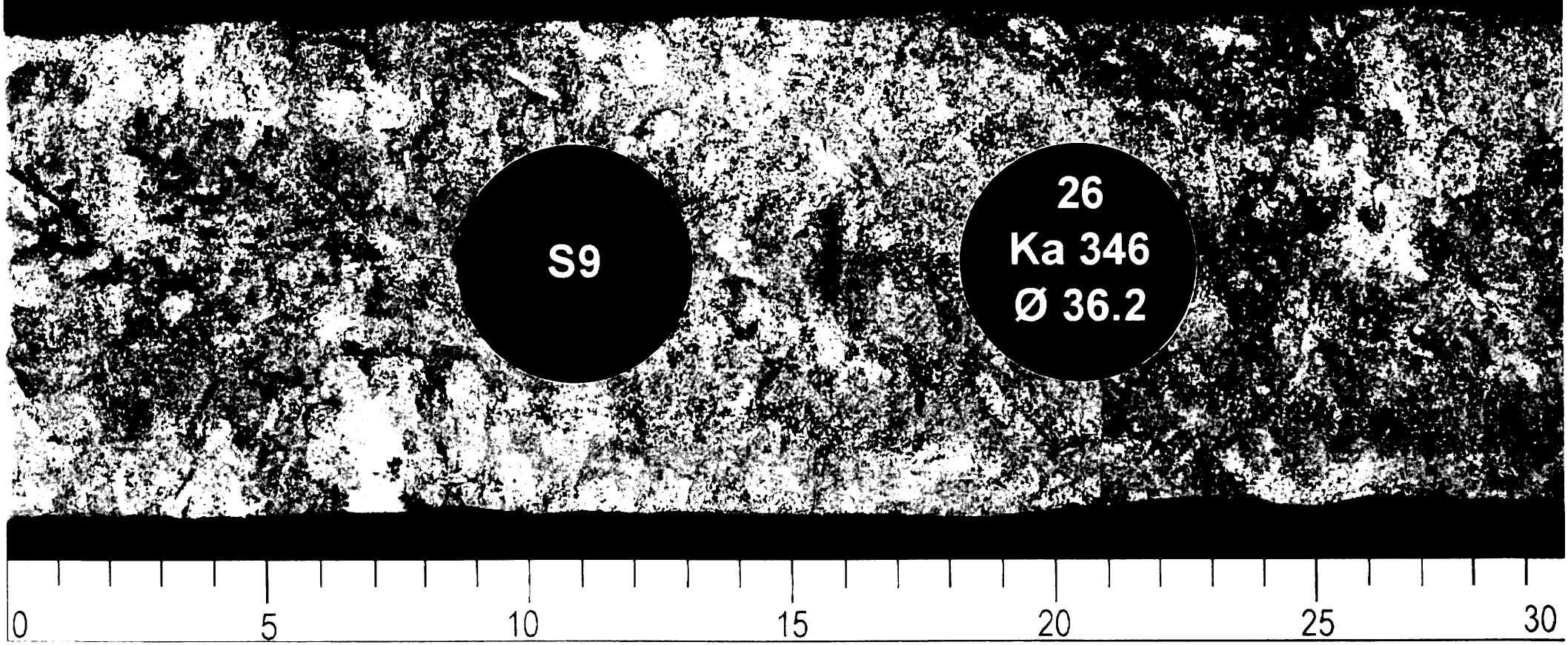

OMV Australia Pty Ltd.

BALEEN 2

ACS LABORATORIES PTY LTD

755.30m

CORE No. 1

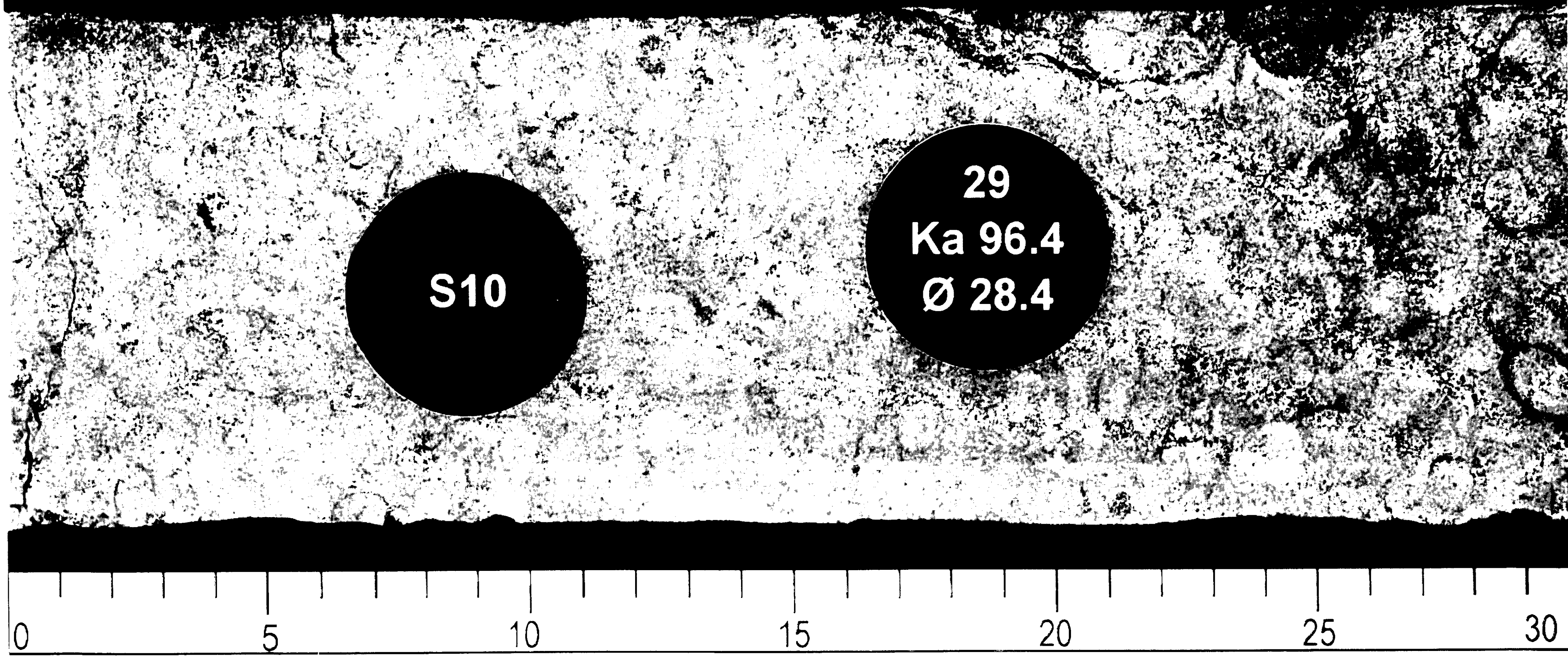

908080 104

PE908080_colour 048

OMV Australia Pty Ltd.

BALEEN 2

ACS LABORATORIES PTY LTD

756.25m

CORE No. 1

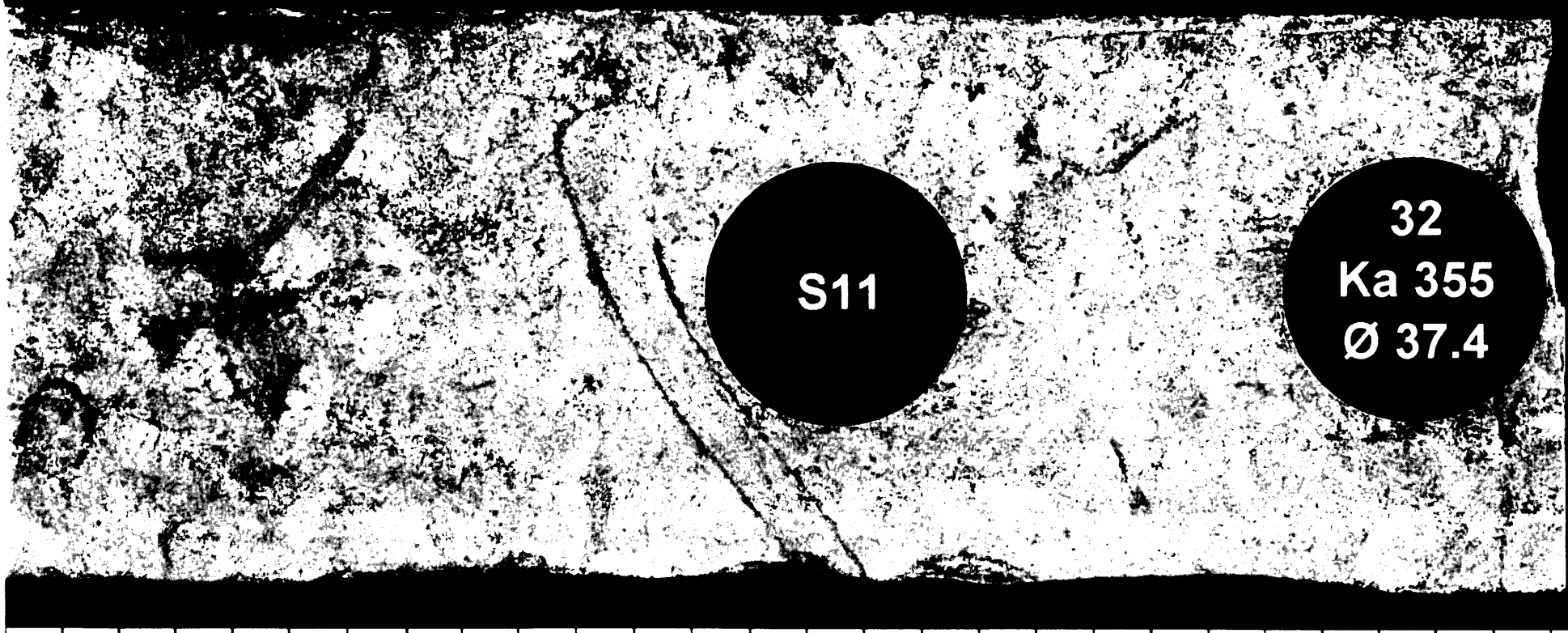

0 5 10 15 20 25 30

903080 135

Pt 90 8080 - Coloured

OMV Australia Pty Ltd.

BALEEN 2

ACS LABORATORIES PTY LTD

757.30m

CORE No. 1

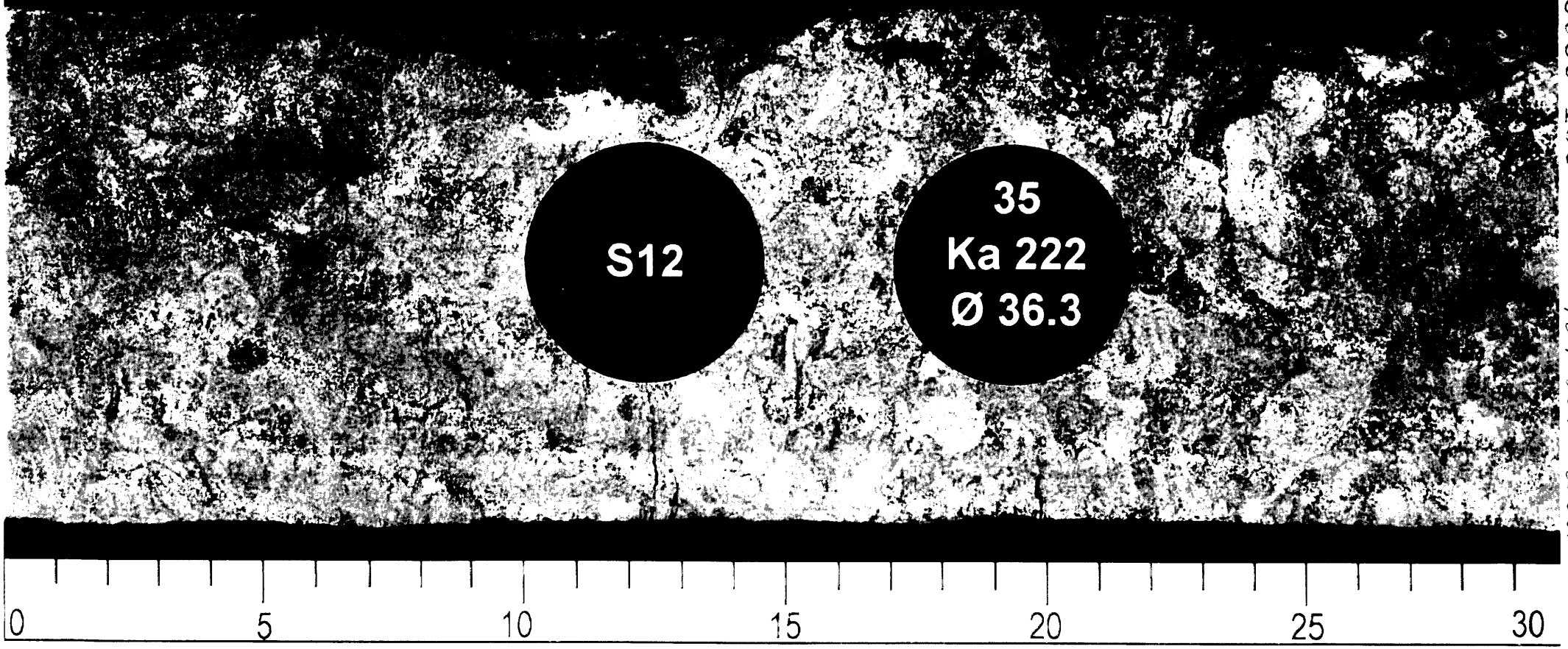

908080 1[illegible]

PE 9CSC SC - colour CSC

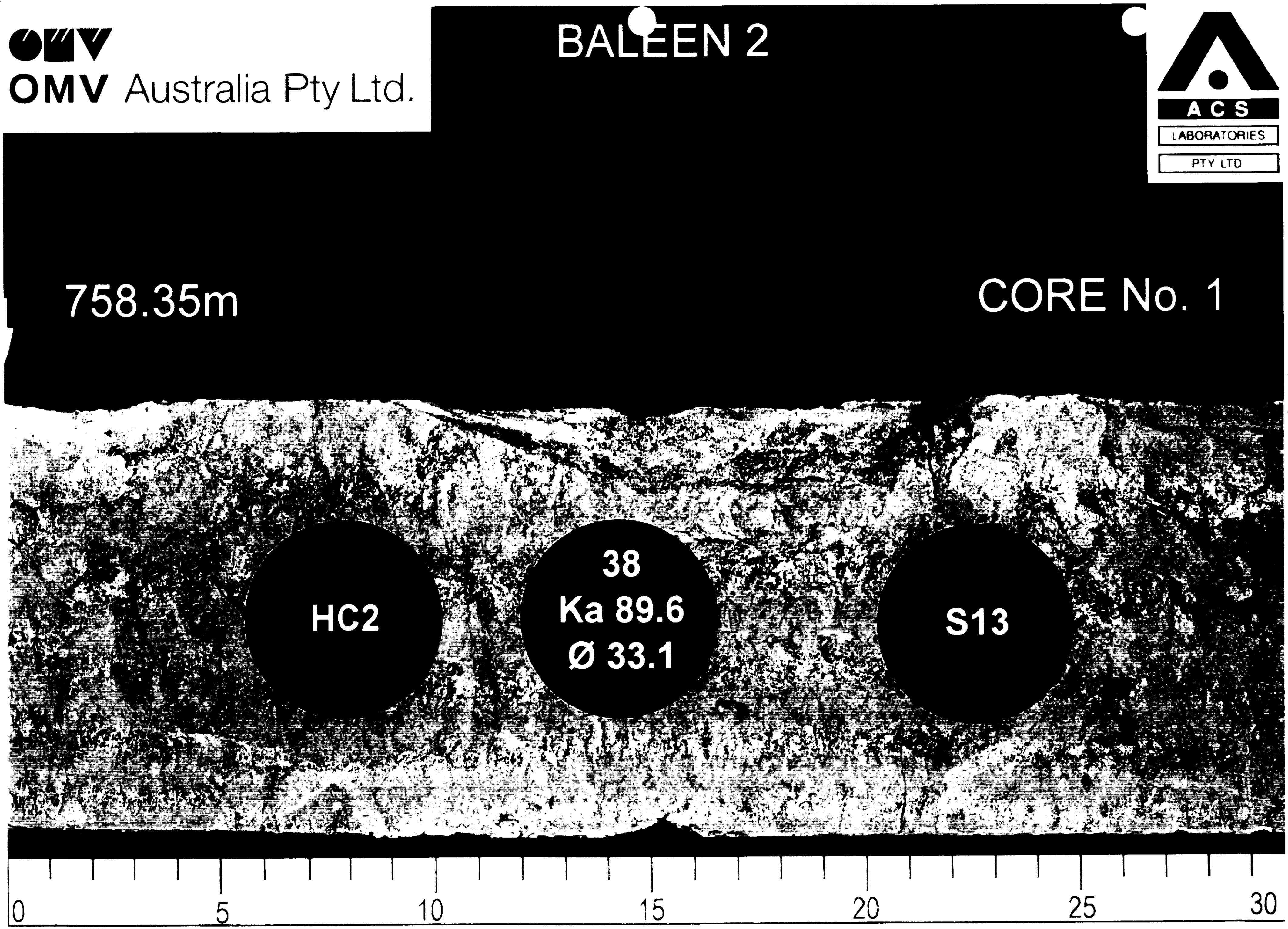

908080 137

PE908080 - colour 051

OMV Australia Pty Ltd.

BALEEN 2

ACS LABORATORIES PTY LTD

759.30m

CORE No. 1

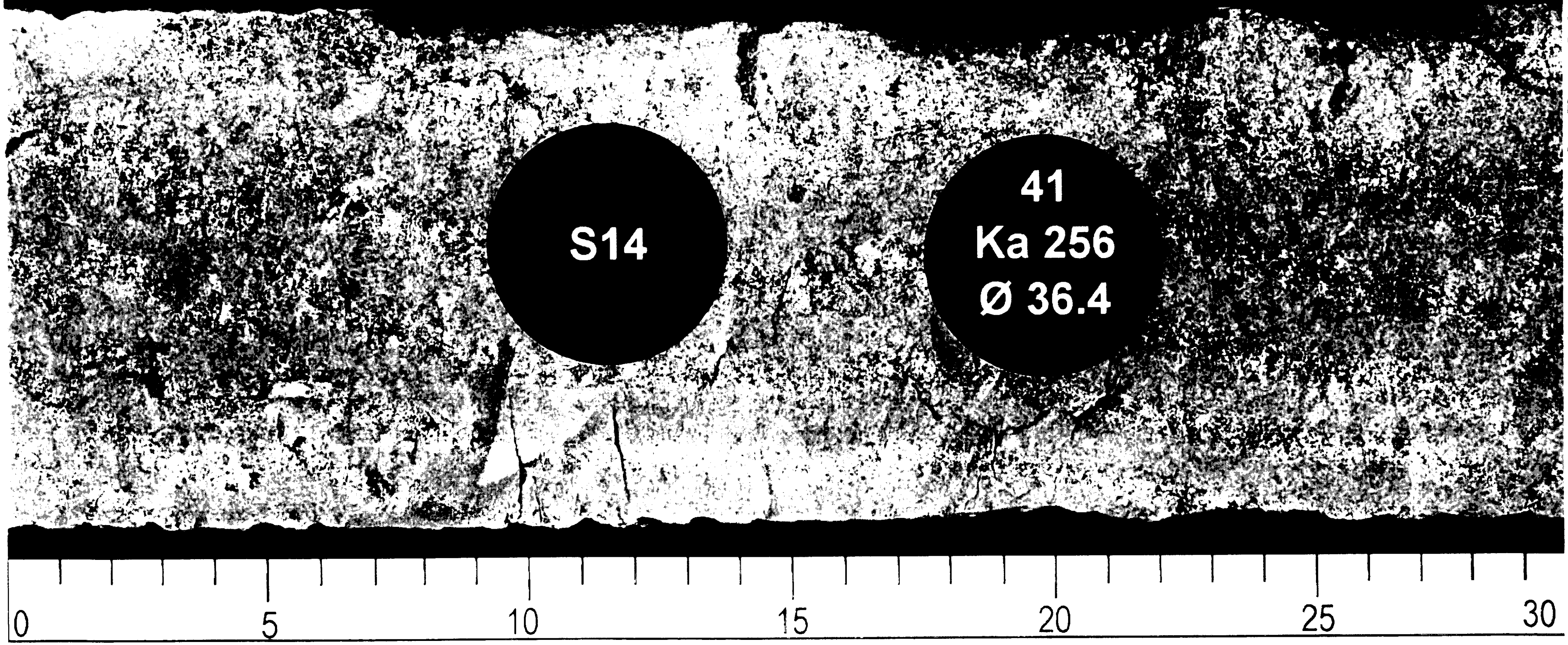

OMV Australia Pty Ltd.

BALEEN 2

ACS LABORATORIES PTY LTD

763.70m

CORE No. 2

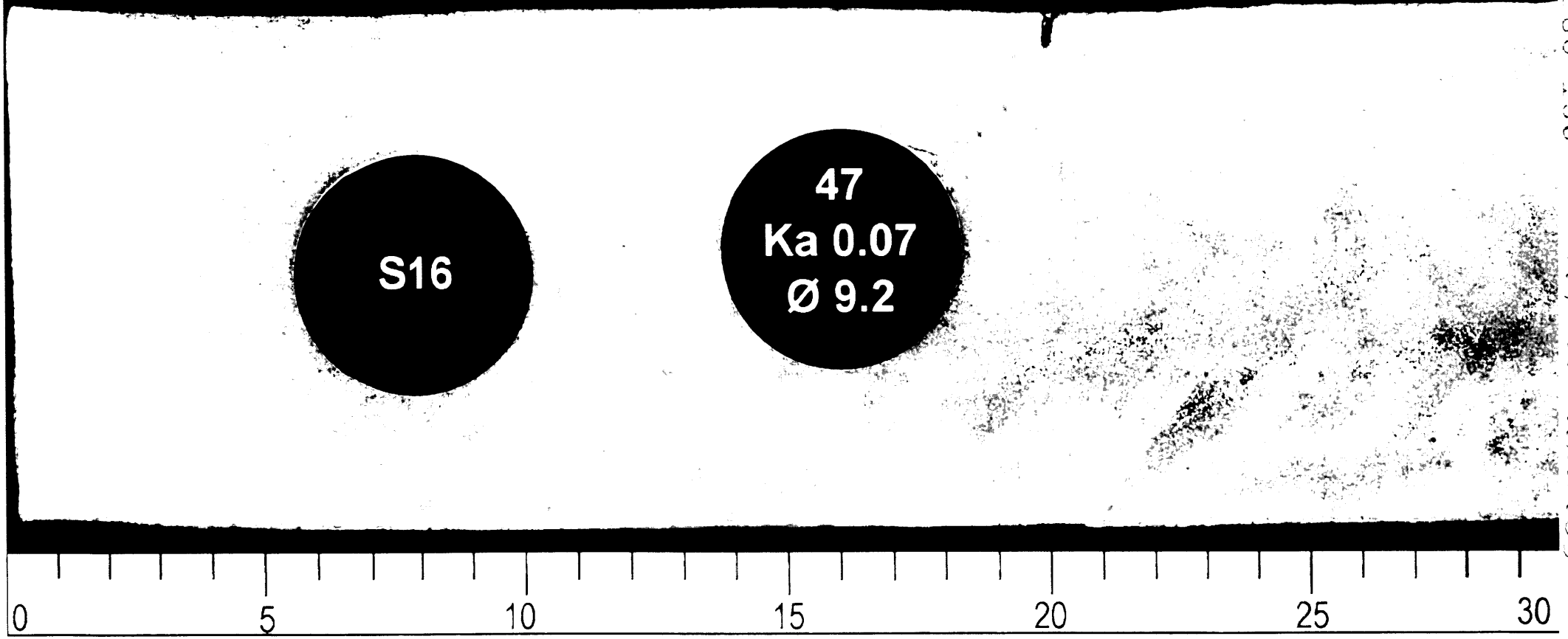

OMV Australia Pty Ltd.

BALEEN 2

ACS LABORATORIES PTY LTD

764.70m

CORE No. 2

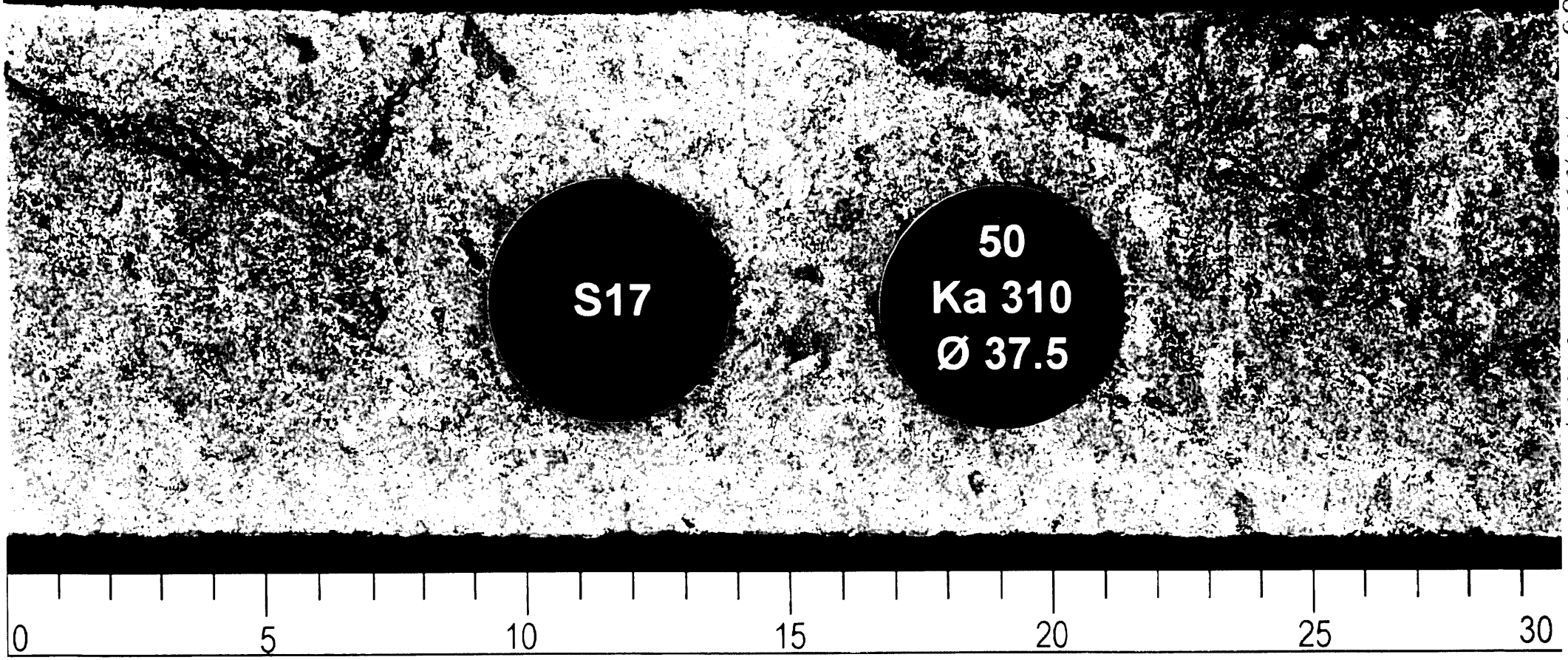

903680 200

Pe 903680 - colour CS4

908080 201

PE908080 - colour 055

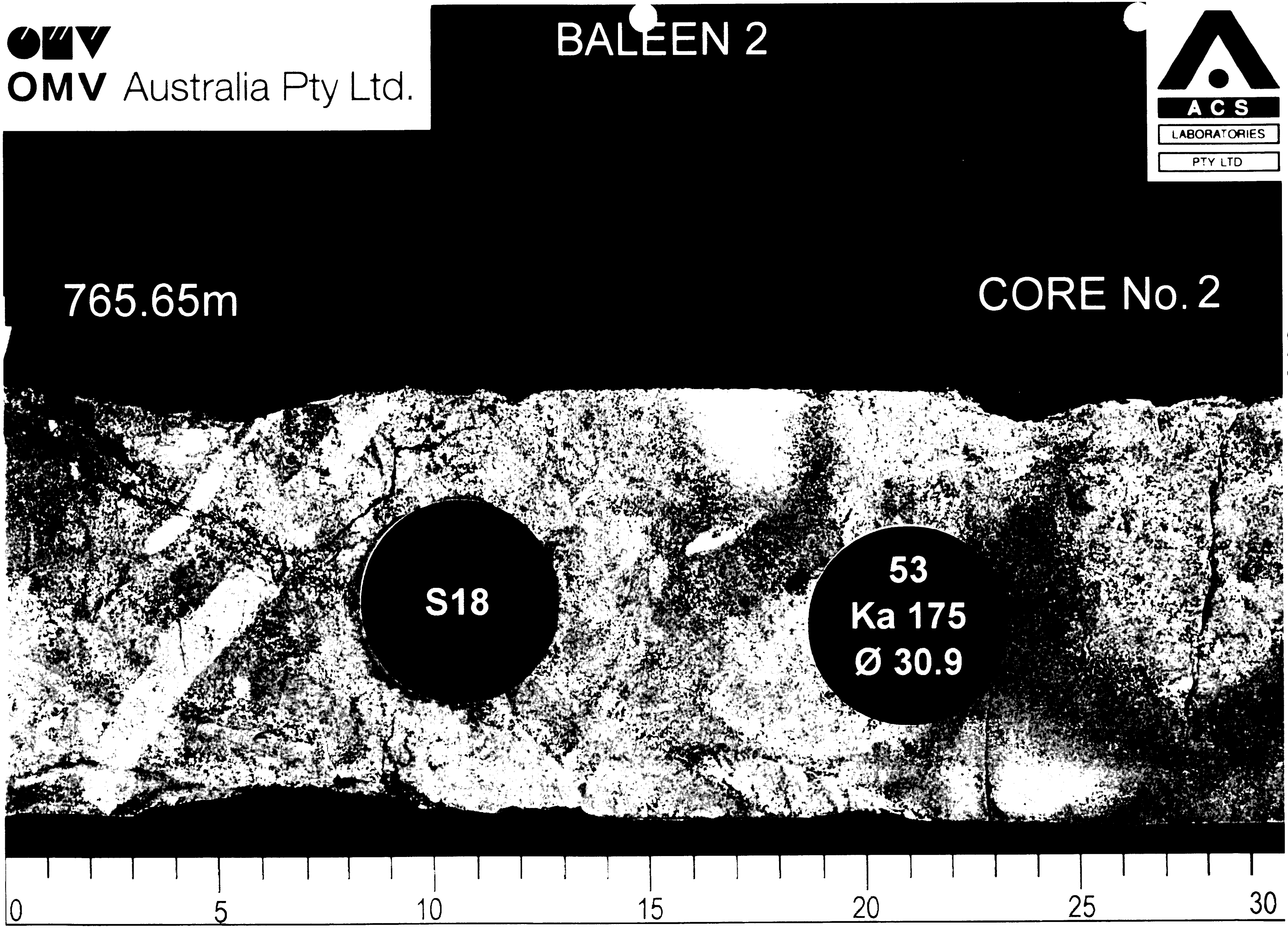

OMV Australia Pty Ltd.

BALEEN 2

ACS LABORATORIES PTY LTD

766.70

CORE No. 2

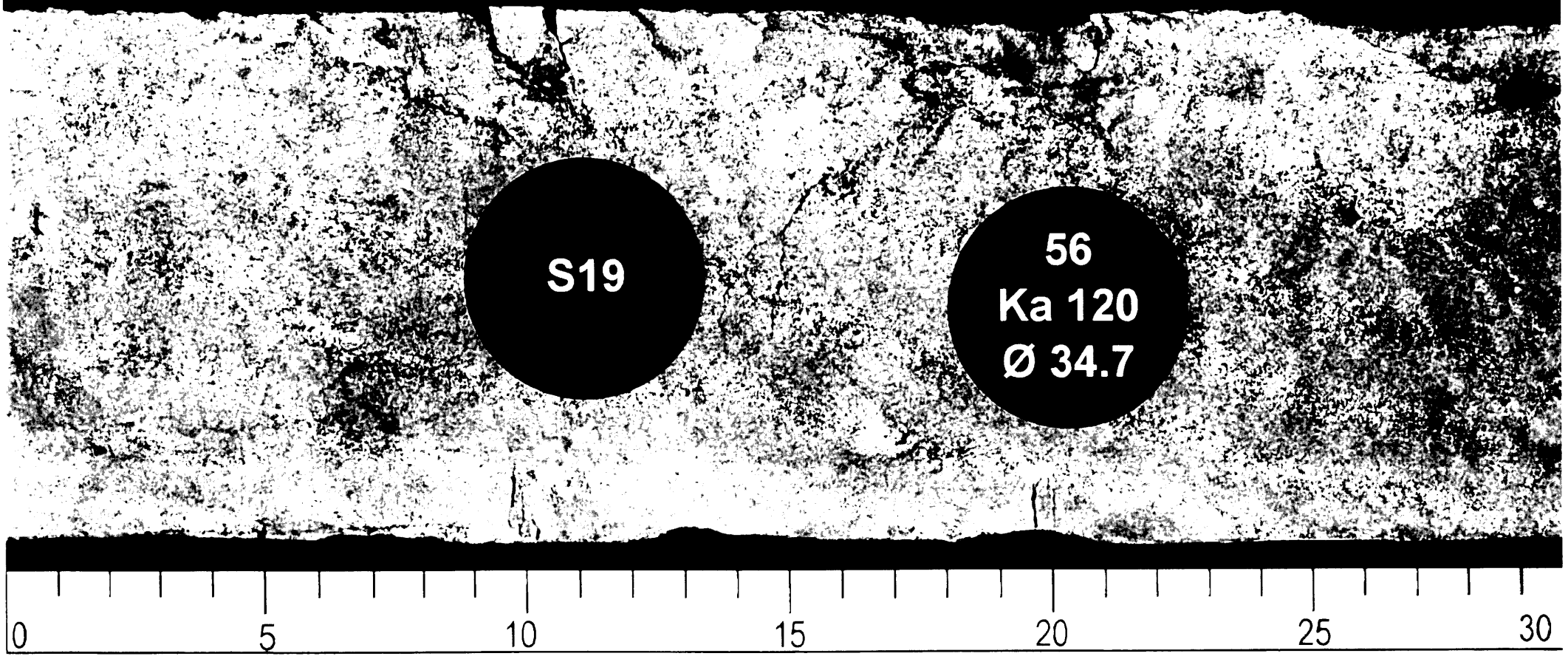

908080 202

903080 203

PE908080 colour 057

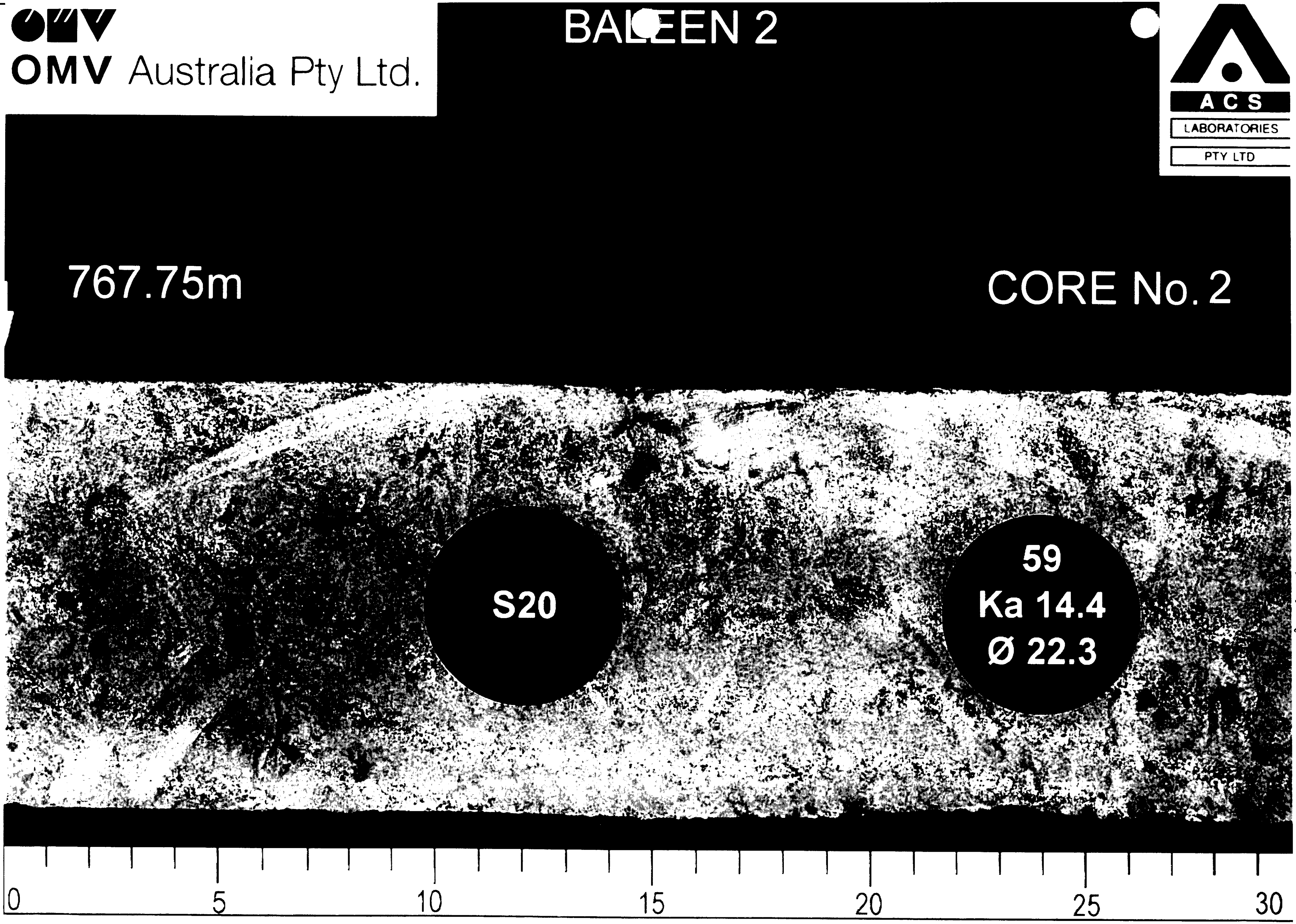

OMV Australia Pty Ltd.

BALEEN 2

ACS LABORATORIES PTY LTD

768.70m

CORE No. 2

903080 204

Pt 903080 - colour core

OMV Australia Pty Ltd.

BALEEN 2

ACS LABORATORIES PTY LTD

769.85m

CORE No. 2

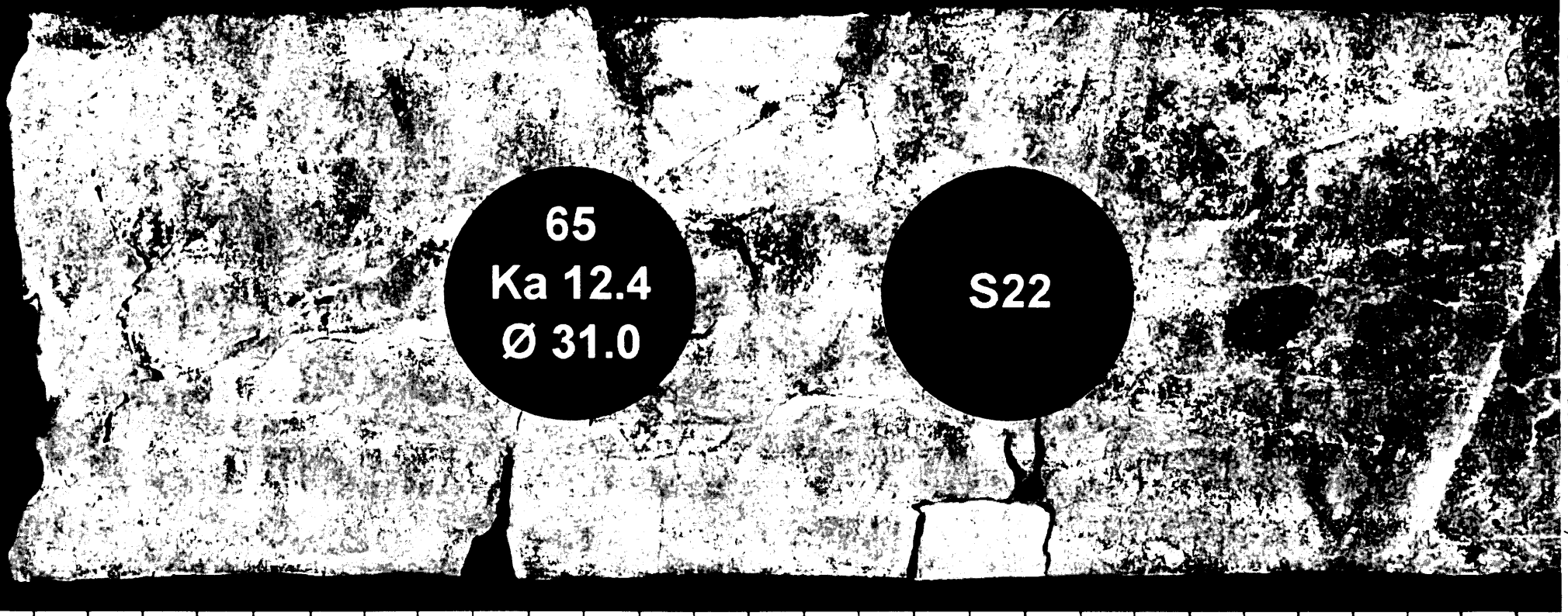

0 5 10 15 20 25 30

9030080 205

PE610858 - colour core

OMV Australia Pty Ltd.

BALEEN 2

ACS LABORATORIES PTY LTD

770.80m

CORE No. 2

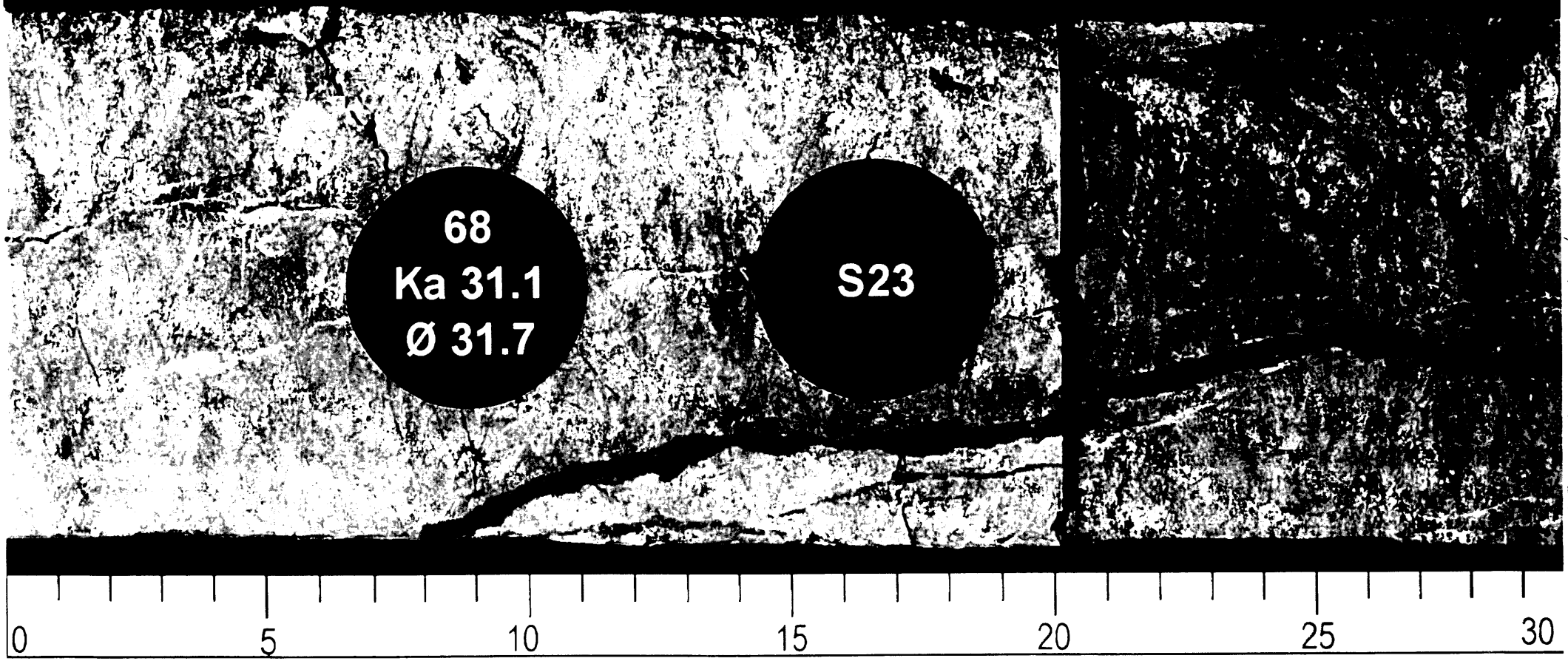

908080 206

Fe 908080 - colour UEC

OMV Australia Pty Ltd.

BALEEN 2

ACS LABORATORIES PTY LTD

771.70m

CORE No. 2

903080 207

PE908080_colour061

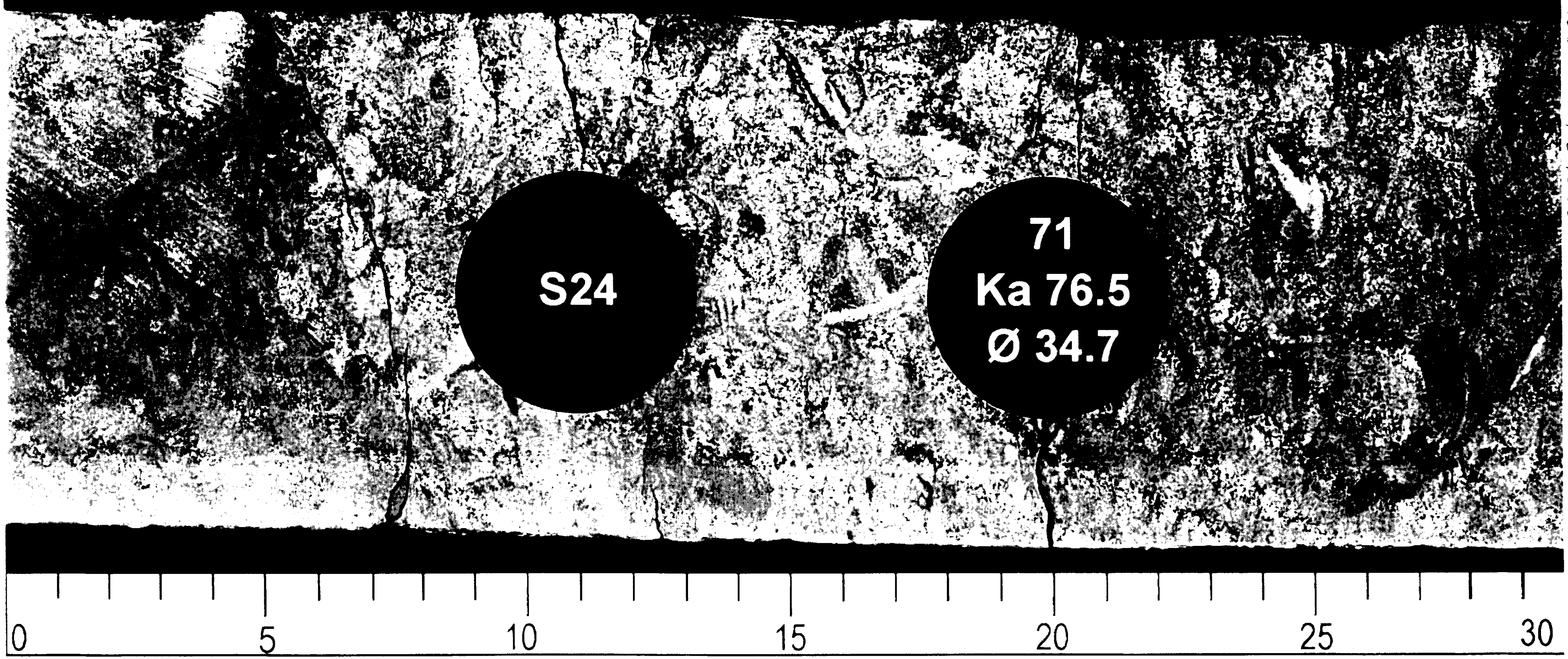

OMV Australia Pty Ltd.

BALEEN 2

ACS LABORATORIES PTY LTD

772.80m

CORE No. 2

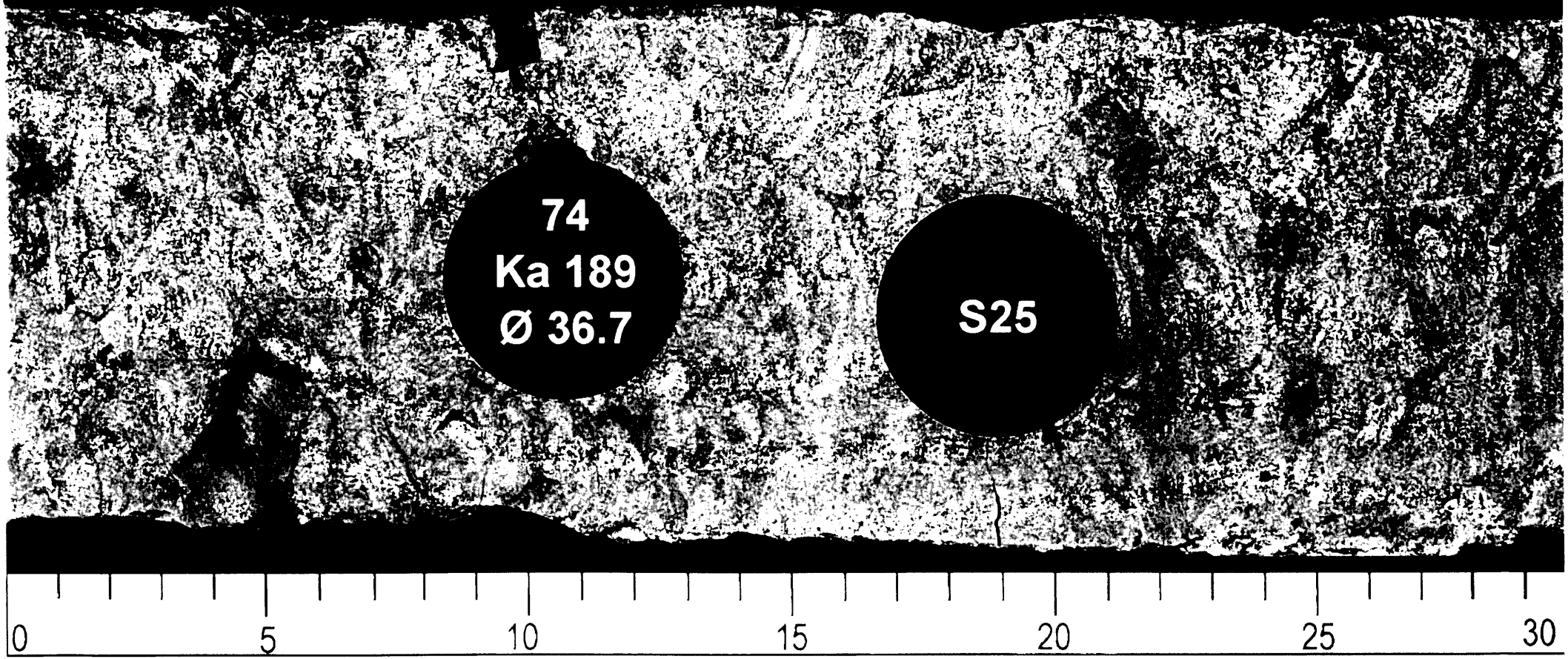

903080 208

P/903080 colour 042

OMV Australia Pty Ltd.

BALEEN 2

ACS LABORATORIES PTY LTD

773.70

CORE No. 2

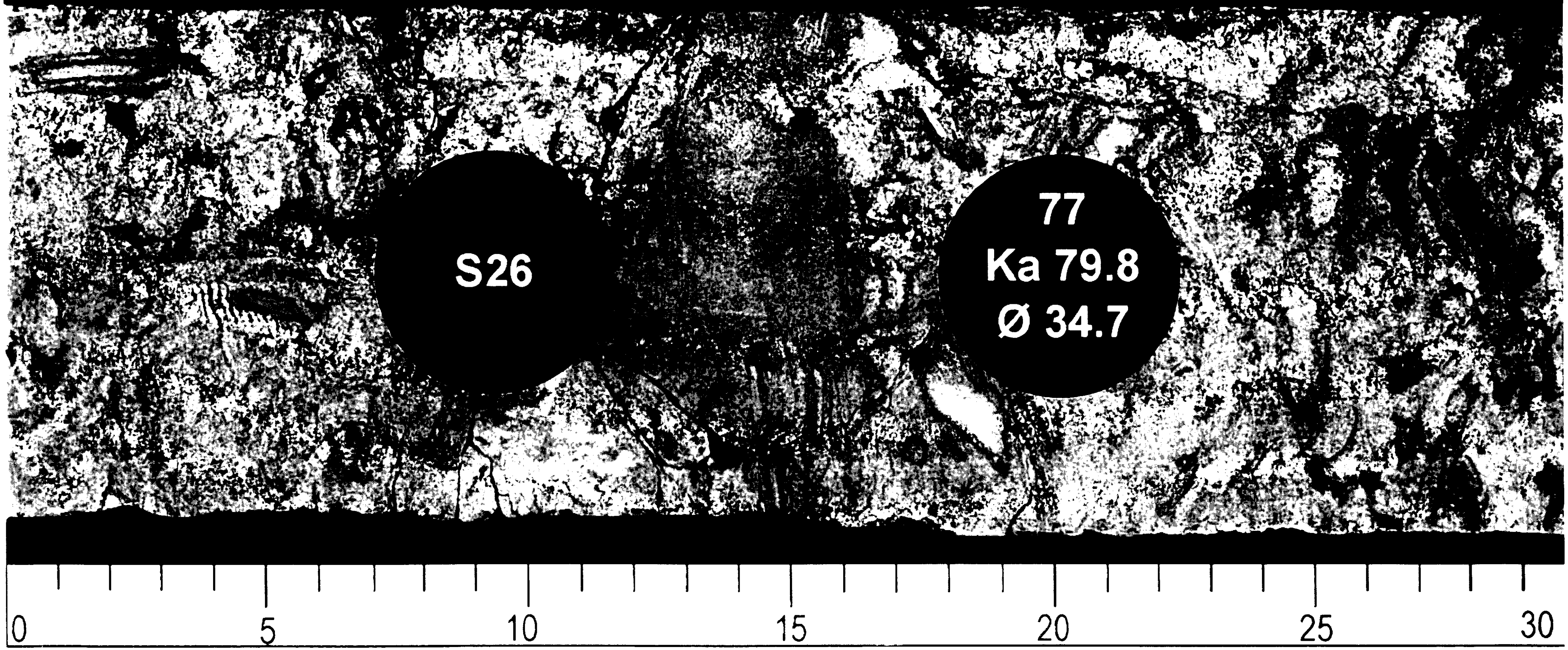

908080 209

PE908080_colour063

908080 210 PE908080_colour064

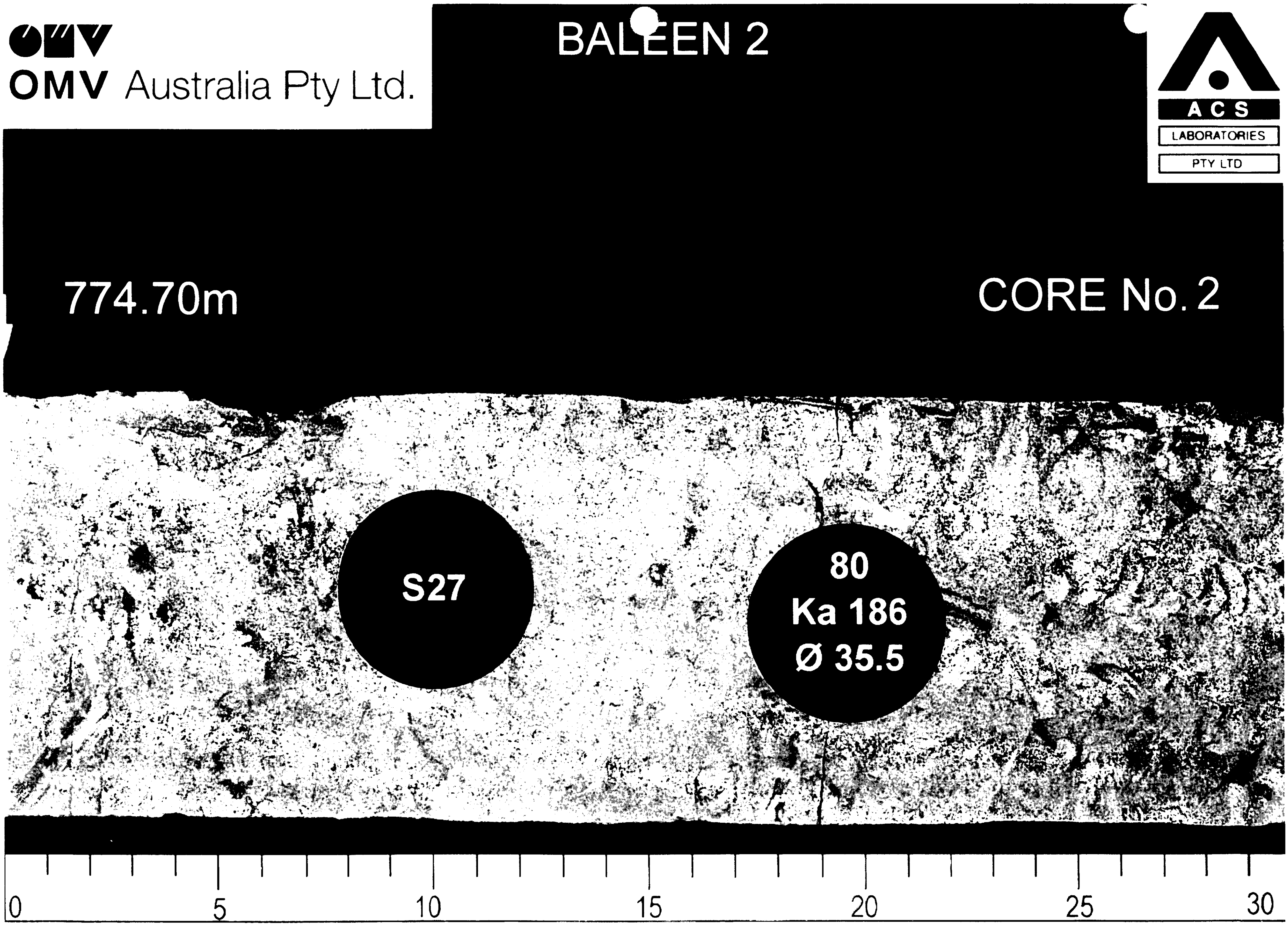

OMV Australia Pty Ltd.

BALEEN 2

ACS LABORATORIES PTY LTD

775.70m

CORE No. 2

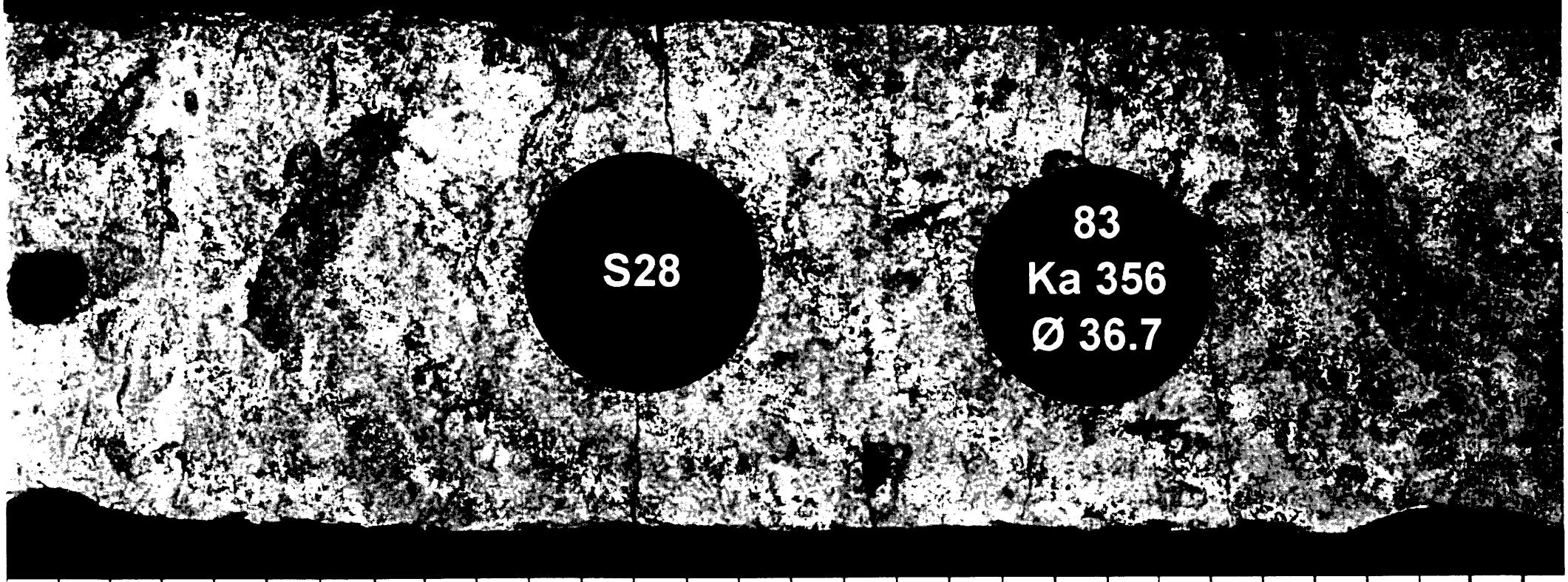

0 5 10 15 20 25 30

908080 211

PE 908080 - colour CBS

OMV Australia Pty Ltd.

BALEEN 2

ACS LABORATORIES PTY LTD

777.70m

CORE No. 2

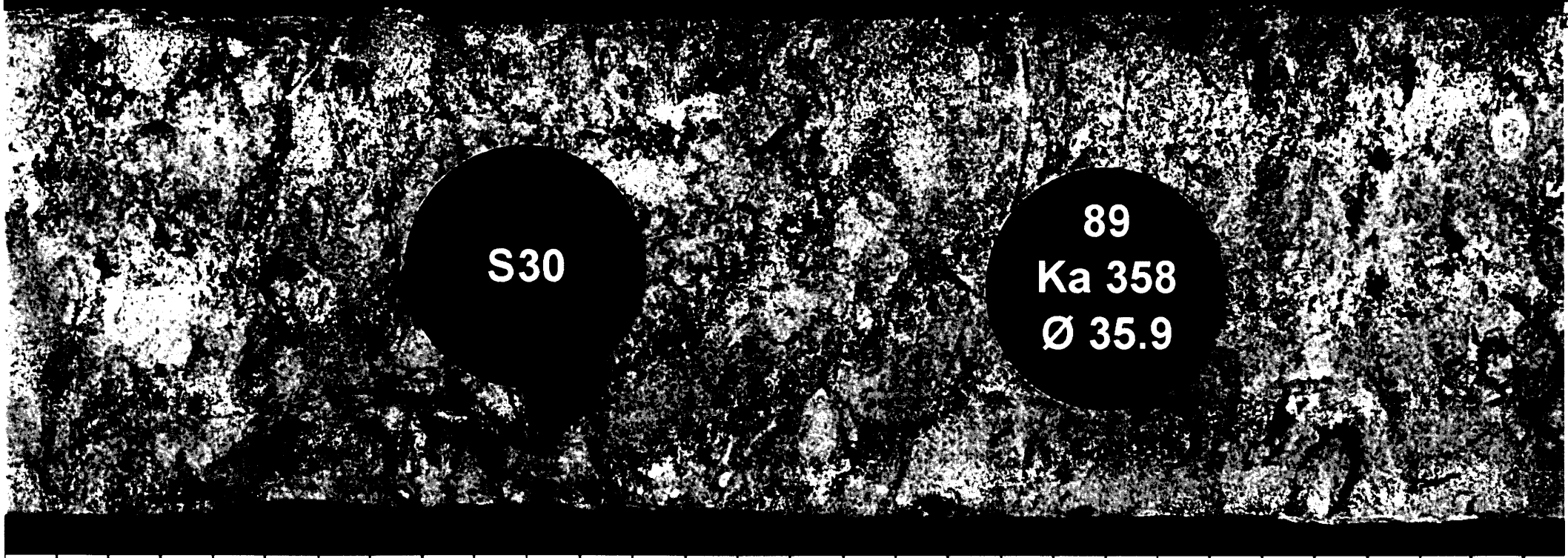

0 5 10 15 20 25 30

908080 212

APPENDIX 5

BALEEN-2

CT SCAN REPORT

-ACS LABORATORIES-

ACS
LABORATORIES
PTY. LTD.

CT SCAN REPORT

of

BALEEN-2

for

OMV AUTRALIA PTY LTD

by

ACS LABORATORIES PTY LTD

3 April 2000

ACS LABORATORIES PTY. LTD.

OMV Australia Pty Ltd
Level 29, St Martins Tower
44 St Georges Tce
PERTH WA 6000

Attention: Mark Adamson

CT SCAN REPORT: 0445-08

CLIENT REFERENCE:	OSA-1999-008
MATERIAL:	Core Plugs
LOCALITY:	Baleen-2
WORK REQUIRED:	Special Core Analysis

Please direct technical enquiries regarding this work to the signatories below under whose supervision the work was carried out.

PETER CROZIER
Operations Manager

CONTENTS

CHAPTER 1

INTRODUCTION

1. INTRODUCTION

This report presents images of the samples selected for analyses as part of a special core analysis study of core samples from Baleen-2. CT Scanning images have been digitally superimposed onto single pages (for easier comparison) in Chapter 3 of this report.

The imaging forms part of the screening process for special core analysis sample selection. OMV Australia Pty Ltd Purchase Order No. OSA-1999-008 supports this program.

All other special core analysis results are to be presented in a separate final report.

CHAPTER 2

CT SCANNING PROCEDURE

2. CT SCANNING PROCEDURE

CT Scanning was undertaken in order that internal inhomogeneities and/or drilling fluid invasion zones may be noted. Typical inhomogeneities may be clasts, bedding sedimentary structures, cementation, fractures and any other discontinuities that may not be readily visible to the naked eye.

The principle of CT Scanning and its applications is presented by Hove et al, 1987 and Wellington and Vinegar, 1987.

CT Scanners generate cross-sectional image slices through the sample by revolving an X-ray tube around the sample and obtaining projections at many different angles (Appendix I). From these image slices, a cross-sectional image was reconstructed by a back projection algorithm in the scanner's computer.

Prior to analysis, an arbitrary orientation line was inscribed onto the sample using a marker to facilitate subsequent re-orientation. The sample was placed vertically within the scanner, with the orientation arrow left, and longitudinal section image obtained. The sample was then rotated through exactly 90° to the initial orientation, and another section image recorded. These two images were labelled '0' and '90' on the prints.

All images are presented here in a standard ACS format and are stored digitally.

CHAPTER 3

CT SCANNING IMAGES

OMV Australia Pty Ltd.

Baleen-2
CT Scans

ACS LABORATORIES PTY LTD

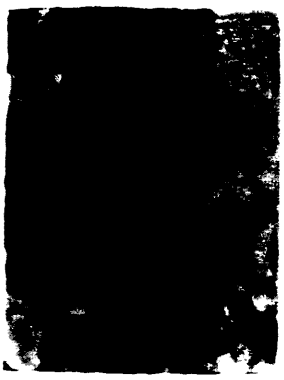

0° 90°

Sample No:	S1
Depth:	746.63 m
Permeability:	81mD
Porosity:	32.7%

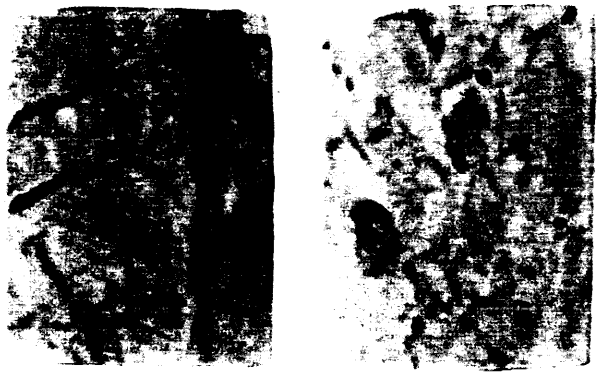

0° 90°

Sample No:	S2
Depth:	747.41 m
Permeability:	74mD
Porosity:	32.8%

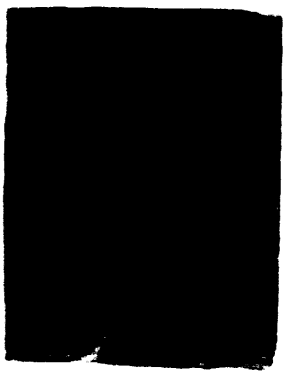

0° 90°

Sample No:	S5
Depth:	750.41 m
Permeability:	131mD
Porosity:	33.1%

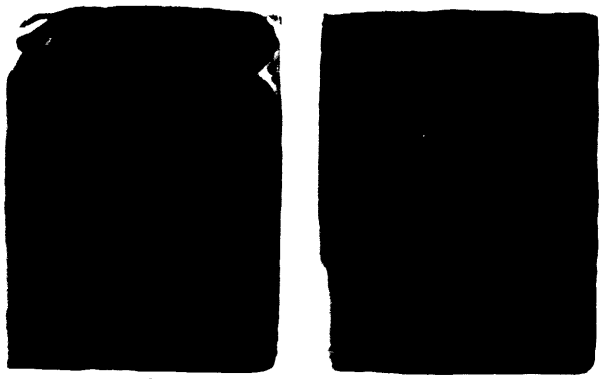

0° 90°

Sample No:	S6
Depth:	751.42 m
Permeability:	127mD
Porosity:	33.5%

Pe 908080 - colour 06 8

908080 224

OMV Australia Pty Ltd.

Baleen-2
CT Scans

ACS LABORATORIES PTY LTD

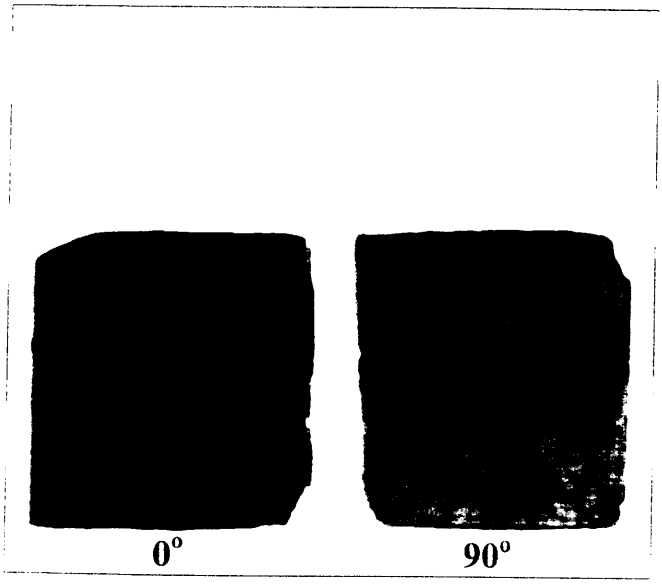

Sample No:	S8
Depth:	753.42 m
Permeability:	735mD
Porosity:	38.3%

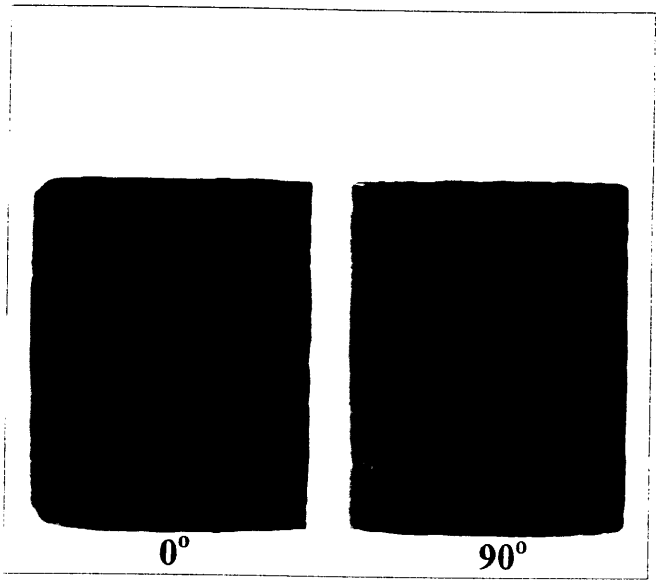

Sample No:	S9
Depth:	754.41 m
Permeability:	467mD
Porosity:	36.7%

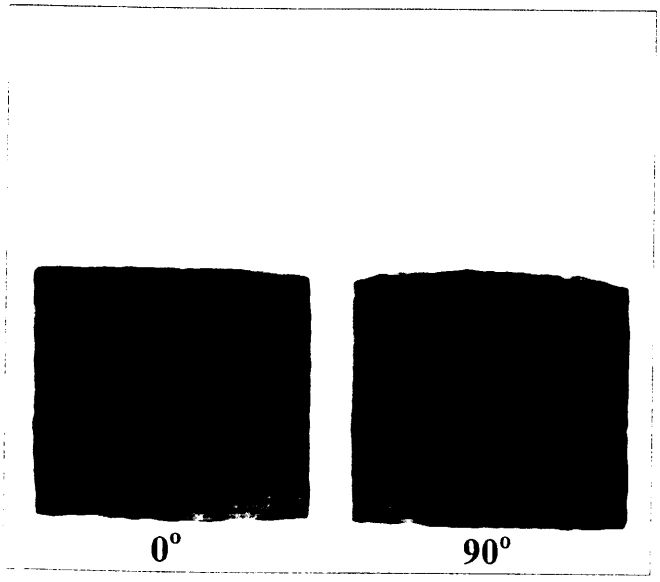

Sample No:	S10
Depth:	755.39 m
Permeability:	272mD
Porosity:	33.6%

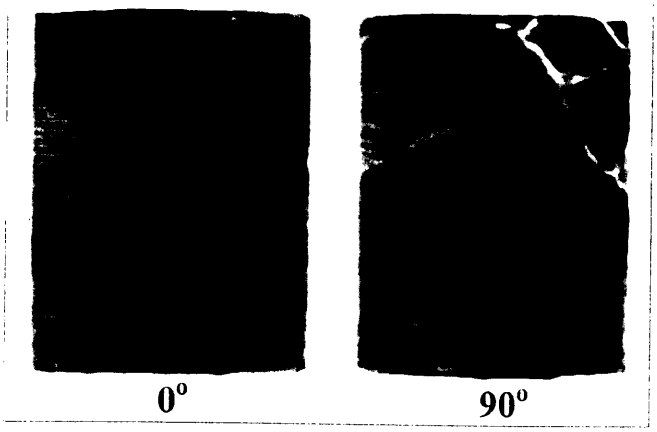

Sample No:	S11
Depth:	756.40 m
Permeability:	238mD
Porosity:	35.2%

Pe908080_colour 069

908080 225

OMV Australia Pty Ltd.

Baleen-2
CT Scans

ACS LABORATORIES PTY LTD

Sample No:	S12
Depth:	757.42 m
Permeability:	337mD
Porosity:	36.1%

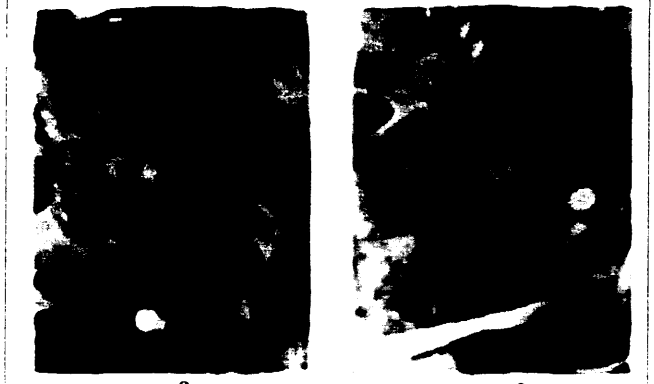

Sample No:	S20
Depth:	767.87 m
Permeability:	46mD
Porosity:	23.6%

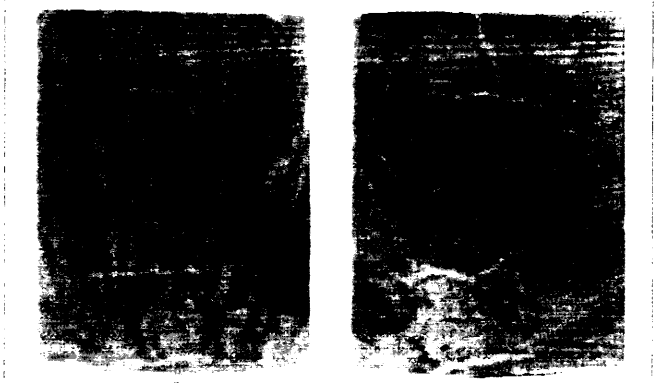

Sample No:	S21
Depth:	768.79 m
Permeability:	33mD
Porosity:	31.3%

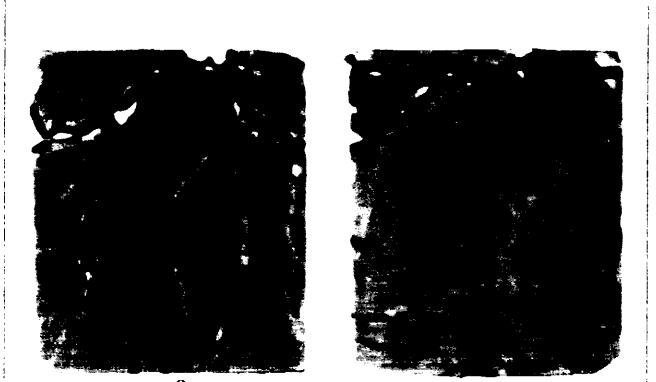

Sample No:	S22
Depth:	770.05 m
Permeability:	
Porosity:	

OMV Australia Pty Ltd.

Baleen-2
CT Scans

ACS LABORATORIES PTY LTD

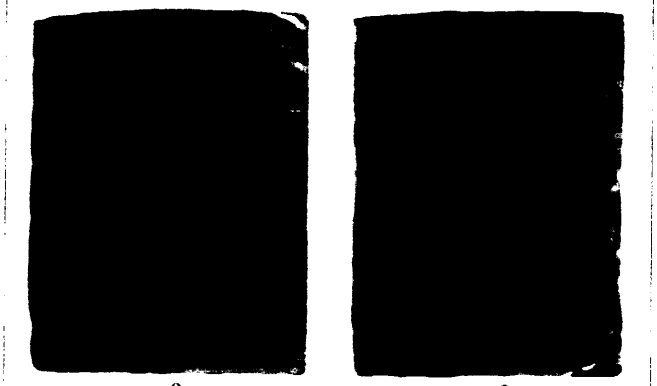

Sample No:	S23
Depth:	770.97 m
Permeability:	27mD
Porosity:	30.2%

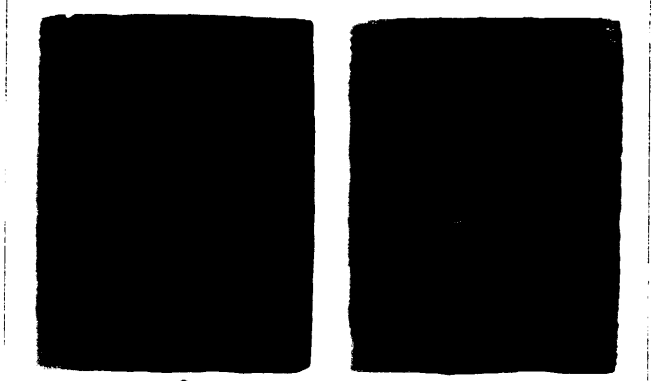

Sample No:	S24
Depth:	771.81 m
Permeability:	82mD
Porosity:	32.8%

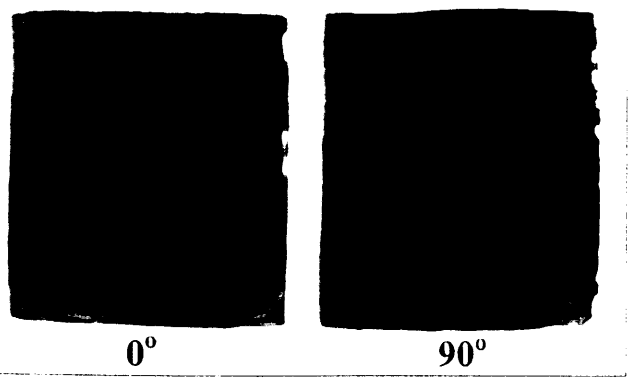

Sample No:	S25
Depth:	772.99 m
Permeability:	112mD
Porosity:	33.9%

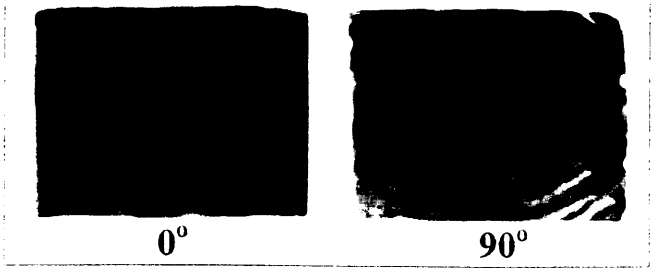

Sample No:	S26
Depth:	773.79 m
Permeability:	119mD
Porosity:	35.6%

OMV Australia Pty Ltd.

Baleen-2
CT Scans

ACS LABORATORIES PTY LTD

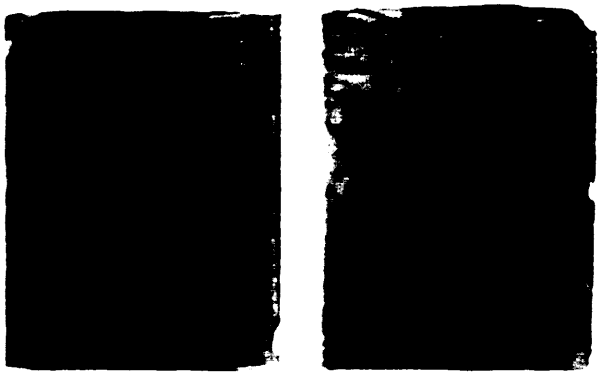

0° 90°

Sample No:	S27
Depth:	774.80 m
Permeability:	346mD
Porosity:	37.1%

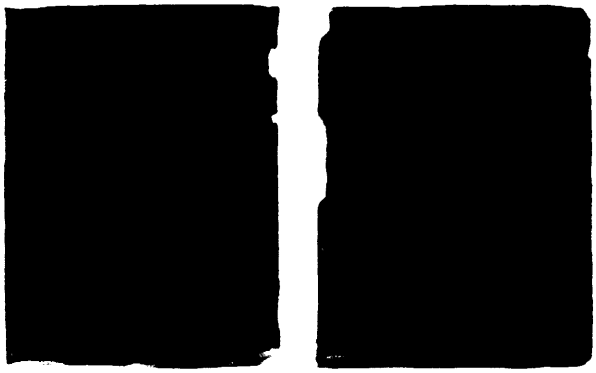

0° 90°

Sample No:	S28
Depth:	775.82 m
Permeability:	396mD
Porosity:	36.1%

0° 90°

Sample No:	S29
Depth:	776.80 m
Permeability:	528mD
Porosity:	36.7%

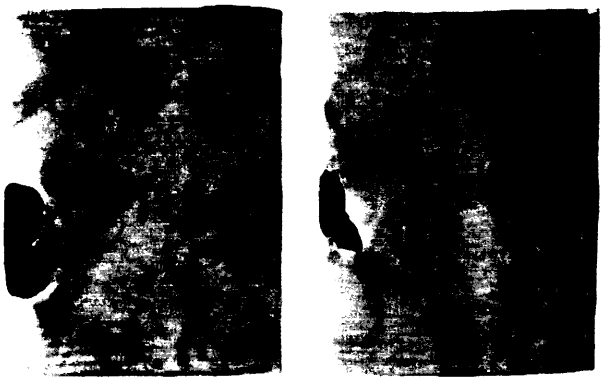

0° 90°

Sample No:	S30
Depth:	777.80 m
Permeability:	563mD
Porosity:	35.6%

APPENDIX I

CT SCANNER SCHEMATIC

PE908080_color#72

908080 229

CT SCANNER SCHEMATIC

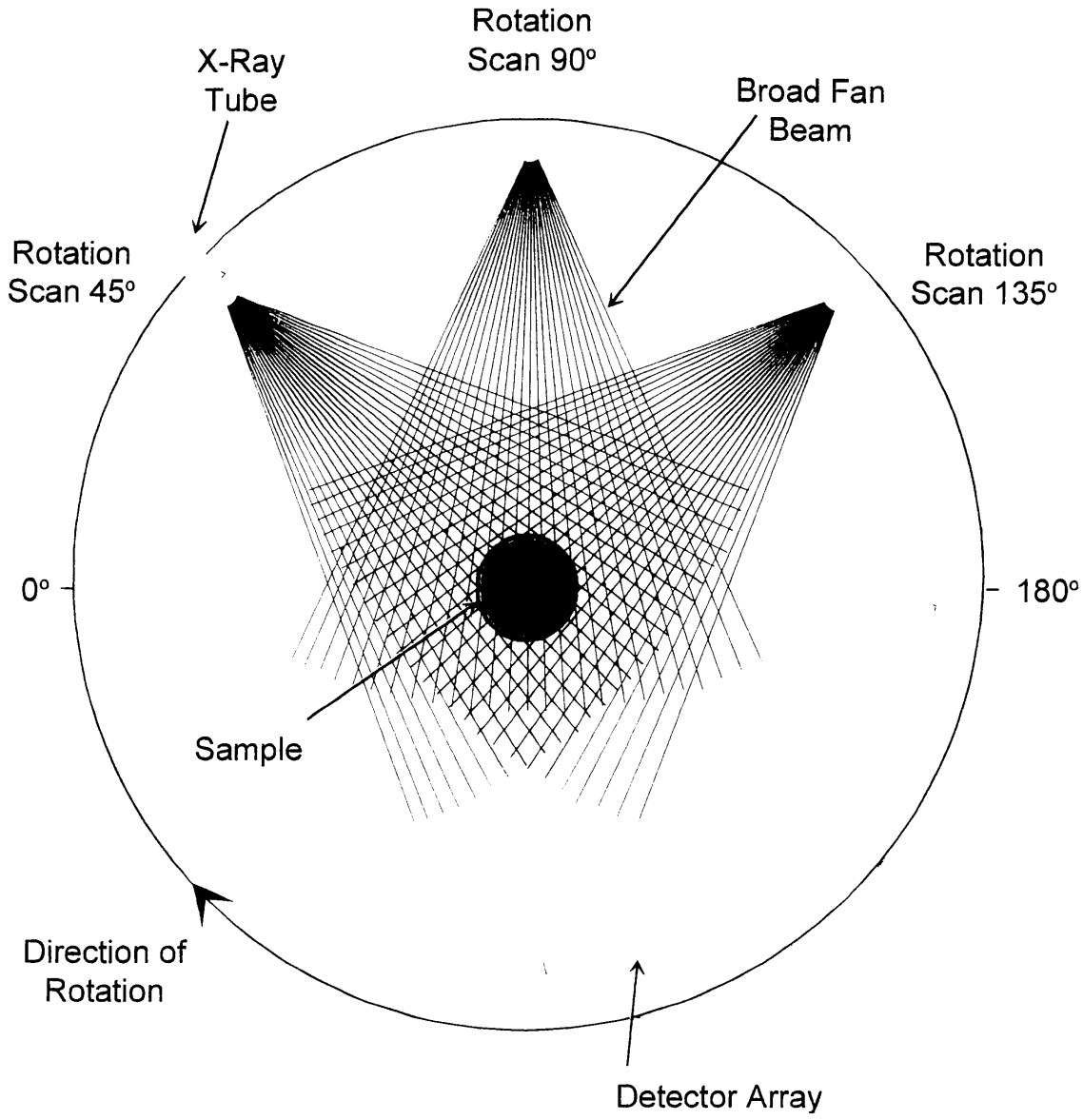

APPENDIX 6

BALEEN-2

SPECIAL CORE ANALYSIS REPORT

-ACS LABORATORIES-

ACS
LABORATORIES
PTY. LTD.

SPECIAL CORE ANALYSIS FINAL REPORT

of

BALEEN-2

for

OMV AUSTRALIA PTY LTD

by

ACS LABORATORIES PTY LTD

14 August, 2000

ACS LABORATORIES PTY. LTD.

OMV Australia Pty Ltd
Level 29, St Martins Tower
44 St Georges Tce
PERTH WA 6000

Attention: Mark Adamson

FINAL REPORT: 0445-08

CLIENT REFERENCE:	Contract Ref: OSA-1999-008 RFS No. Basin 001
MATERIAL:	Core Plugs
LOCALITY:	Baleen-2
WORK REQUIRED:	Special Core Analysis

Please direct technical enquiries regarding this work to the signatories below under whose supervision the work was carried out.

PETER N CROZIER
Operations Manager

Chermside Laboratory
P O Box 396, Chermside South Qld 4032, Australia
Telephone: 61 7 3350 1222 Facsimile: 61 7 3359 0666
E-mail: acs.bris@acslabs.com.au
ACS Laboratories Pty Ltd
ABN: 81 008 273 005

CONTENTS

CHAPTERS **PAGE**

CONTENTS (cont)

CHAPTERS **PAGE**

APPENDICES

CHAPTER 1

INTRODUCTION

1. INTRODUCTION

This final report details the procedures and presents the results of a special core analysis study on a suite of samples from Baleen-2.

Subsequent to discussions between ACS and OMV representatives a final SCA program was received on 14 February 2000. Chapter 2 of this report summarises the test program and the following chapters detail test procedures and results. The Appendices include ancillary information pertinent to the study.

The effective overburden stress of 1040psi used in this study was calculated using reservoir information supplied, and confirmed, by OMV. The calculation is found in Appendix I.

CHAPTER 2

SUMMARY OF TEST PROGRAM

TEST SCHEDULE

Client: OMV Australia Pty Ltd
Well: Baleen-2

F = failed
C = cancelled

Sample	Depth	Test Sequence																	
		Teflon Sleeve	*CT Scan*	*Clean*	*Dry*	*Ambient Base Parameters*	*Saturate*	*Permeability to brine*	*Desat. To Swirr*	*Basic waterflood*	*Clean and Dry*	*Formation factor*	*Multi-Salinity Formation Factor*	*RI*	*Pc*	*Post Testing Base Parameters*	*Klinkenberg permeability*	*Petrology*	*Cation Exchange Capacity*
S1	746.63	S1	S1	S1	S1	S1	S1					S1	S1	S1	S1	S1	S1		S1
S2	747.41	S2	S2	S2	S2	S2	S2	S2	S2	S2	S2					S2	S2		
S5	750.41	S5	S5	S5	S5	S5	S5					S5	S5	S5	S5	S5	S5	S5	S5
S6	751.42	S6	S6	S6	S6	S6	S6	S6	S6	S6	S6					S6	S6	S6	
S8	753.42	S8	S8	S8	S8	S8													
S9	754.41	S9	S9	S9	S9	S9	S9					S9	S9	S9	S9	S9	S9	S9	S9
S10	755.39	S10	S10	S10	S10	S10	S10					S10	S10	S10	S10	S10	S10		S10
S11	756.40	S11	S11	S11	S11	S11	S11	S11	S11	S11	S11					S11	S11		
S12	757.42	S12	S12	S12	S12	S12	S12	S12	S12	S12	S12					S12	S12	S12	
S20	767.87	S20	S20	S20	S20	S20	S20					S20	S20	S20	S20	S20	S20		S20
S21	768.79	S21	S21	S21	S21	S21	S21	S21	S21	S21	S21					S21	S21	S21	
S22	770.05	S22	S22															S22	
S23	770.97	S23	S23	S23	S23	S23	S23					S23	S23	F					S23
S24	771.81	S24	S24	S24	S24	S24	S24	S24	S24	S24	S24					S24	S24	S24	
S25	772.99	S25	S25	S25	S25	S25	S25					S25	S25	S25	S25	S25	S25		S25
S26	773.79	S26	S26	S26	S26	S26	S26	S26	S26	S26	S26					S26	S26	S26	
S27	774.80	S27	S27	S27	S27	S27	S27					S27	F						S27
S28	775.82	S28	S28	S28	S28	S28	S28	S28	C			S28	S28	S28	S28	S28	S28	S28	S28
S29	776.80	S29	S29	S29	S29	S29	S29					S29	F						S29
S30	777.80	S30	S30	S30	S30	S30	S30	S30	S30	S30	S30					S30	S30	S30	
	Total	20	20	19	19	19	18	9	8	8	8	10	8	7	7	15	15	10	10

FLOW CHART

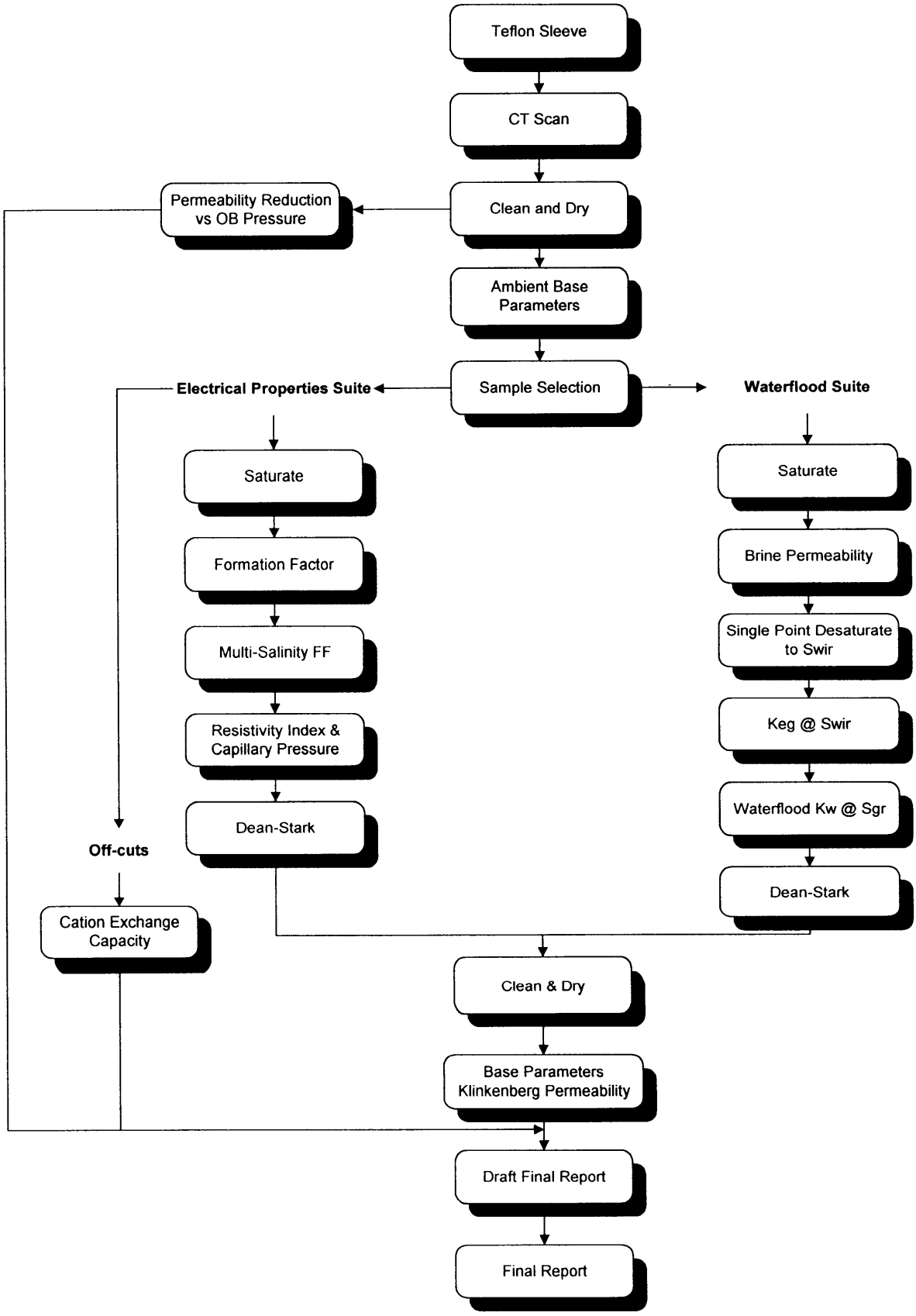
Teflon Sleeve
CT Scan
Clean and Dry
Permeability Reduction vs OB Pressure
Ambient Base Parameters
Sample Selection
Electrical Properties Suite
Waterflood Suite
Saturate
Formation Factor
Multi-Salinity FF
Resistivity Index & Capillary Pressure
Dean-Stark
Off-cuts
Cation Exchange Capacity
Saturate
Brine Permeability
Single Point Desaturate to Swir
Keg @ Swir
Waterflood Kw @ Sgr
Dean-Stark
Clean & Dry
Base Parameters Klinkenberg Permeability
Draft Final Report
Final Report

CHAPTER 3

SAMPLE PREPARATION AND BASE PARAMETER DETERMINATIONS

3.1 Test and Calculation Procedures

3. SAMPLE PREPARATION AND BASE PARAMETER DETERMINATIONS

3.1 Test and Calculation Procedures

3.1.1 Sample Sleeving

Teflon sleeving allows the samples to maintain their integrity and can be utilized for electrical properties testing. Each sample was carefully wrapped in PTFE (teflon) tape of a known weight and density. Subsequently, each sample was placed into an appropriate length of heat shrink Teflon tubing. Prior to shrinking the tubing, a set of stainless steel mesh screens were placed at each end of the plug. Shrinking the tubing holds the screens in place (Appendix III).

3.1.2 CT Scanning

CT Scanning was undertaken in order that internal inhomogeneities and/or drilling fluid invasion zones may be noted. Typical inhomogeneities may be clasts, bedding sedimentary structures, cementation, fractures and any other discontinuities that may not be readily visible to the naked eye.

The principle of CT Scanning and its applications is presented by Hove et al, 1987 and Wellington and Vinegar, 1987.

CT Scanners generate cross-sectional image slices through the sample by revolving an X-ray tube around the sample and obtaining projections at many different angles (Appendix III). From these image slices, a cross-sectional image was reconstructed by a back projection algorithm in the scanner's computer.

Prior to analysis, arbitrary orientation lines were inscribed onto the sample using a marker to facilitate subsequent re-orientation. The sample was placed vertically within the scanner, with the orientation arrow left to right, and a longitudinal section image obtained. The sample was then rotated through exactly 90° to the initial orientation, and another section image recorded. These two images are labelled '0' and '90' on the prints.

All images have been reported previously.

3.1.3 Cleaning and Drying

Cleaning was performed in a modified soxhlet system (Appendix III) ensuring the samples were continuously submersed in solvents. Cleaning continued until tests for oil (fluorescence under UV light) and salt (silver nitrate precipitation) showed negative.

On completion of cleaning the solvent-saturated samples were immersed under methanol in a critical point drying apparatus (Appendix III). The cell was pressured with liquid carbon dioxide ensuring the temperature was kept below the critical point. The methanol was removed by diffusion through the liquid carbon dioxide and vented off, while ensuring the pressure did not drop below the critical point. Once all methanol was removed, the temperature of the cell was raised above the critical point, thus avoiding an apparent phase change or front passing through the samples. The carbon dioxide gas was then slowly vented off and the dry samples removed.

3.1.4 Ambient Base Parameters

Porosity

Porosity was determined in two stages. Initially each sample was placed in a sealed matrix cup. Helium held at 100 psi reference pressure was then introduced to the cup. From the resultant pressure drop the unknown grain volume was determined from Boyle's Law.

$$P_1 V_1 = P_2 V_2$$
$$\Rightarrow P_1 Vr = P_2 (Vr + Vc + Vl - Vg)$$

where

	P_1	=	*initial pressure (psig)*
	Vr	=	*reference cell volume (cm^3)*
	Vc	=	*matrix cup volume (cm^3)*
	Vl	=	*line volume (cm^3)*
	Vg	=	*grain volume (cm^3)*
	P_2	=	*final pressure (psig)*

and

$$\rho = \frac{Wt}{Vg}$$

where

	ρ	=	*grain density (g/cm^3)*
	Wt	=	*weight of sample (g)*
	Vg	=	*grain volume (cm^3)*

The samples were then placed into individual thick walled rubber sleeves and the assembly loaded into a hydrostatic cell. With an ambient pressure (400 psi) applied to the sample, helium held at 100 psi reference pressure was released into the samples pore volume. The resultant pressure drop was used to determine pore volume at ambient.

$$Vb = Vp + Vg$$

$$Ambient\ Porosity\ \% = \frac{Vp}{Vb} x\ 100$$

where

	Vp	=	*ambient pore volume (cm^3)*
	Vb	=	*ambient bulk volume (cm^3)*
	Vg	=	*grain volume (cm^3)*

Permeability to Air

The permeability to air was determined immediately after the helium was vented from the sample, after the pore volume determination described above. A confining pressure of 400 psi was used to prevent bypassing of air around the sample when the measurement was made. In order to determine permeability a known air pressure was applied to the upstream face of each sample, creating a flow of air through the core plug. Air permeability for each core sample was calculated using Darcy's Law through knowledge of the upstream pressure, flow rate, viscosity of air and sample dimensions.

$$Ka = \frac{2000.BP.\mu.q.L}{(P_1^2 - P_2^2).A}$$

where

Ka	=	*air permeability (milliDarcy's)*
BP	=	*barometric pressure (atmospheres)*
μ	=	*gas viscosity (cP)*
q	=	*flow rate (cm^3/s)*
L	=	*sample length (cm)*
P_1	=	*upstream pressure (atmospheres)*
P_2	=	*downstream pressure (atmospheres)*
A	=	*sample cross sectional area (cm^2)*

3.1.5 Sample Saturation

The selected samples were initially vacuum saturated with synthetic formation brine (composition as supplied), followed by pressure saturation at 2000 psi for a minimum of 12 hours. To determine complete saturation, the pore volume of each sample was ascertained by mass balance and compared with that of porosimetry. In all cases, the saturation levels were within 2% (of 100% Sw) and therefore deemed suitable to proceed with the scheduled analysis program.

CHAPTER 3

SAMPLE PREPARATION AND BASE PARAMETER DETERMINATIONS

3.2 Test Results

POROSITY and AIR PERMEABILITY

Client OMV Australia Pty Ltd

Well Baleen-2

Ambient

Sample Number	Depth (metres)	Permeability to Air (milliDarcy's)	Porosity (percent)	Grain Density (g/cm^3)
S1	746.63	81	32.7	2.83
S2	747.41	74	32.8	2.71
S5	750.41	131	33.1	2.69
S6	751.42	127	33.5	2.68
S8	753.42	735	38.3	2.68
S9	754.41	467	36.7	2.68
S10	755.39	272	33.6	2.73
S11	756.40	238	35.2	2.68
S12	757.42	337	36.1	2.68
S20	767.87	46	23.6	2.99
S21	768.79	33	31.3	2.69
S23	770.97	27	30.2	2.68
S24	771.81	82	32.8	2.71
S25	772.99	112	33.9	2.74
S26	773.79	119	35.6	2.71
S27	774.80	346	37.1	2.69
S28	775.82	396	36.1	2.68
S29	776.80	528	36.7	2.68
S30	777.80	563	35.6	2.72

POROSITY and AIR PERMEABILITY

Client OMV Australia Pty Ltd

Well Baleen-2

Ambient

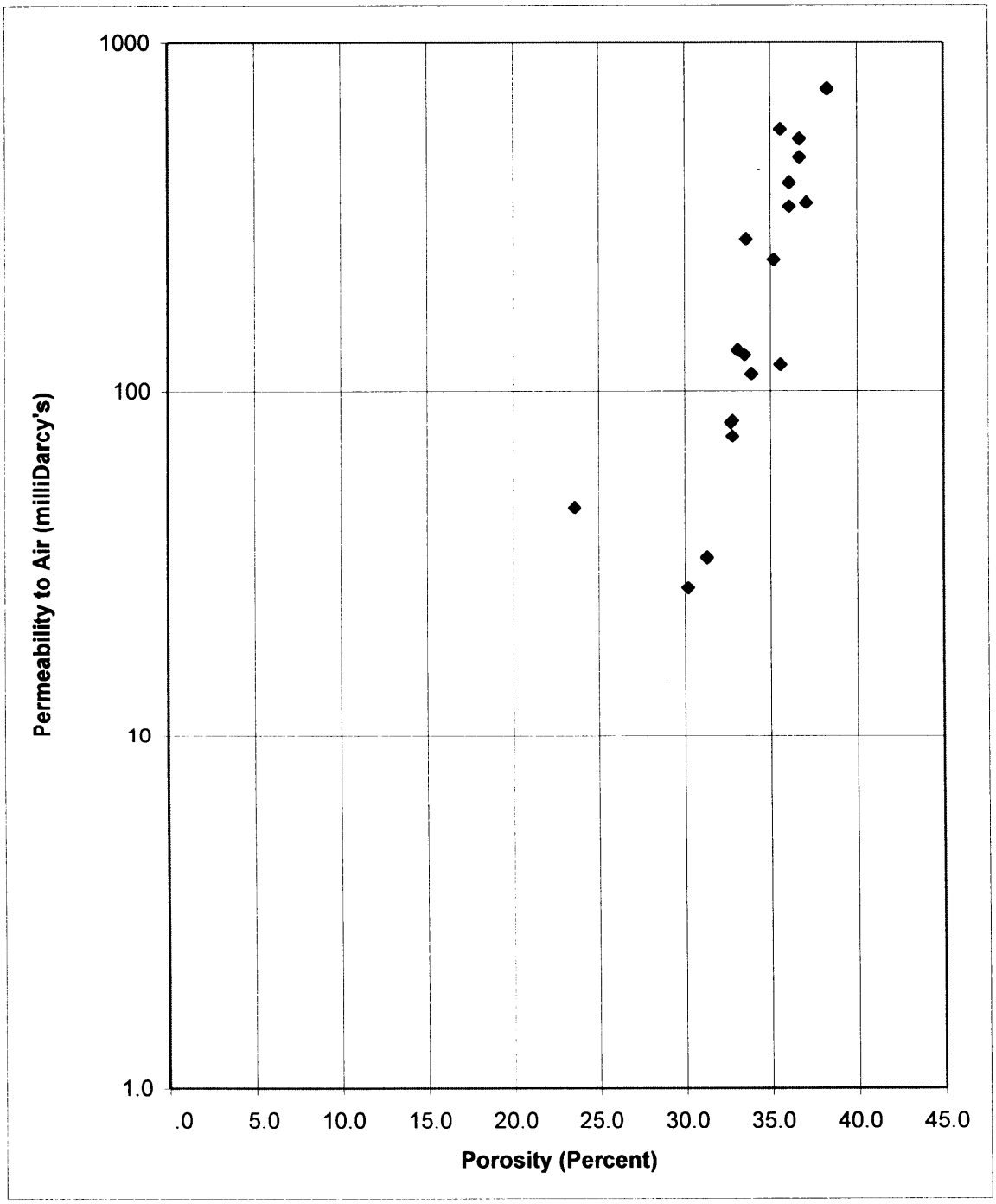

CHAPTER 4

WATERFLOOD

4.1 Test and Calculation Procedures

4. WATERFLOOD

4.1 Test and Calculation Procedures

4.1.1 Brine Permeability

On completion of saturation the selected samples were individually loaded into a hydrostatic core holder (Appendix III) with an overburden confining pressure of 1040 psi applied. Brine was flowed through each sample and the permeability to brine was calculated through knowledge of upstream pressure, brine viscosity, sample dimensions and flow rate.

$$Kw = \frac{14696 \,.\, Q.\, L.\, \mu T}{\Delta p \,.\, A}$$

where 14696 = *units conversion*
Q = *flow rate (cm^3/s)*
Δp = *flooding pressure (psig)*
L = *sample length (cm)*
A = *sample cross sectional area (cm^2)*
μT = *brine viscosity (cP) at T (°C)*

4.1.2 Single Point Desaturation to Swir

The saturated samples were placed onto a brine saturated ceramic porous plate in an ambient capillary pressure cell. Diatomaceous earth was used to ensure a capillary contact (between the sample and the porous plate) to facilitate drainage.

At the applied pressure of 150 psi each sample was allowed to reach stable saturation, as defined by no further production of effluent brine. The samples were unloaded and saturations determined by mass balance.

4.1.3 Basic Waterflood

Each sample was loaded into a hydrostatic core holder and permeability to humidified air was determined using procedures as described in section 3.1.4 of this report.

On completion of air permeability each sample was flooded with synthetic formation brine (Appendix II) at a flow rate of 4 cm^3 per hour. Once the sample had reached stable saturation (defined as no further production of gas) the flow rate was increased to 2 cm^3 per minute. On completion of the gas production, the gas produced was recorded and brine permeability at residual gas saturation was determined using procedures as described above. The sample then proceeded for Dean-Stark analysis to confirm final saturations.

CHAPTER 4

WATERFLOOD

4.2 Test Results

SUMMARY OF WATERFLOOD RESULTS

Client OMV Australia Pty Ltd
Well Baleen-2

Overburden Pressure 1040 psi

				Initial Conditions			Water Flood		
Sample Number	Overburden Permeability to Air (milliDarcy's)	Overburden Permeability to Brine (milliDarcy's)	Overburden Porosity (percent)	Brine Saturation Swir (percent)	Effective Permeability to Air Keg @ Swir (milliDarcy's)	Relative Permeability to Air	Gas Saturation Sgr (percent)	Effective Permeability to Brine Kw @ Sgr (milliDarcy's)	Relative Permeability to Brine
S2	42	0.49	31.5	37.6	25	0.595	16.8	0.26	0.531
S6	84	10	31.4	29.1	76	0.905	16.0	2.1	0.210
S11	149	20	33.9	27.7	134	0.899	14.8	2.3	0.117
S12	268	39	34.8	21.2	245	0.914	13.9	6.2	0.159
S21	22	1.3	29.9	39.6	5.8	0.264	12.3	0.53	0.408
S24	61	5.7	32.0	31.6	47	0.770	16.9	2.3	0.405
S26	86	7.7	34.2	35.2	63	0.733	15.8	1.7	0.221
S30	493	80	34.5	16.4	447	0.907	10.3	21	0.263

RELATIVE PERMEABILITY

Client OMV Australia Pty Ltd
Well Baleen-2

Overburden Pressure 1040 psi

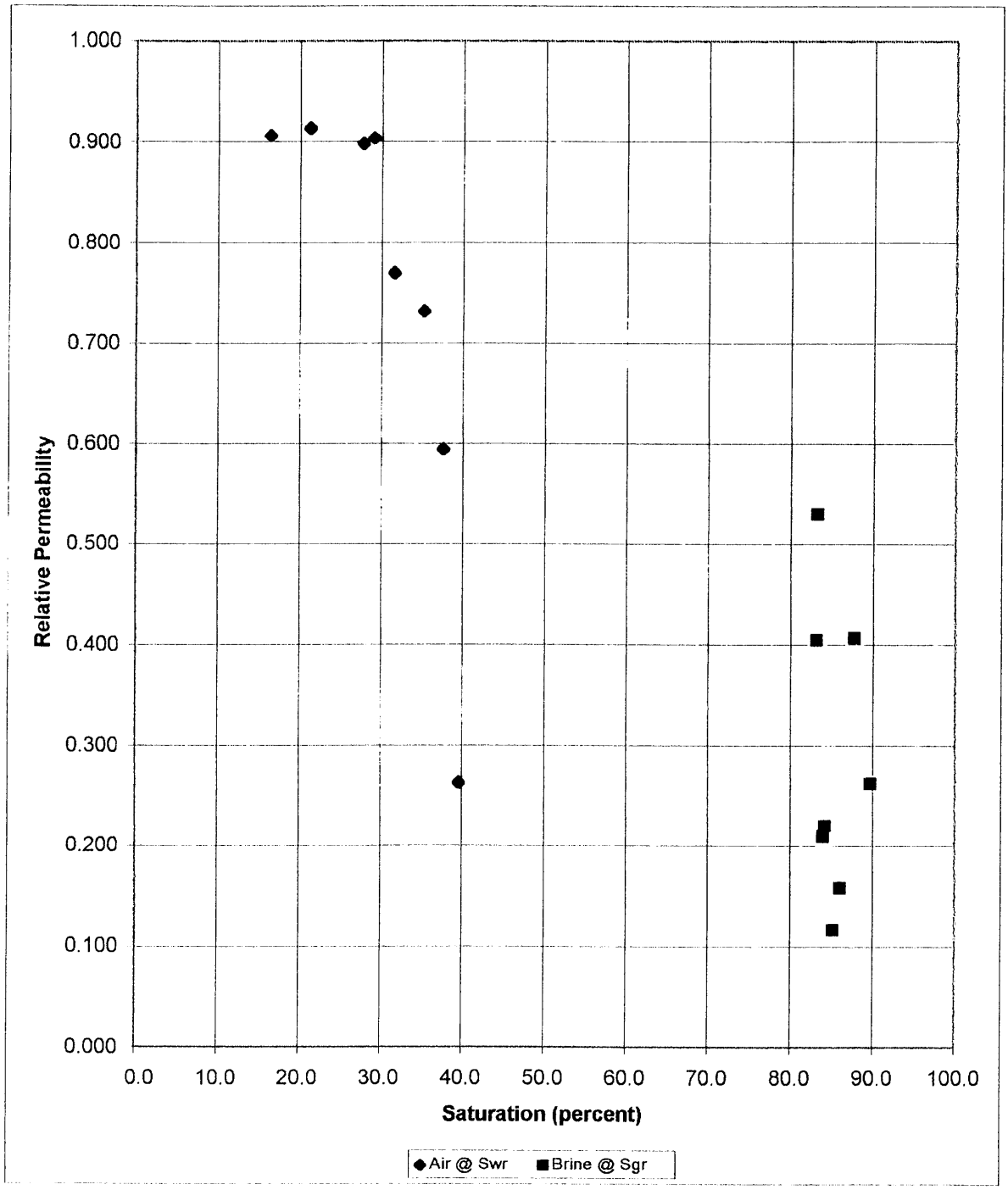

CHAPTER 5

ELECTRICAL PROPERTIES AND CAPILLARY PRESSURE

5.1 Test and Calculation Procedures

5. ELECTRICAL PROPERTIES AND CAPILLARY PRESSURE

5.1 Test and Calculation Procedures

5.1.1 Formation Factor

On completion of base parameter and pressure saturation with synthetic formation brine, the samples continued on for formation resistivity factor analyses.

Each fully brine saturated sample was sandwiched between a pair of stainless steel core holder platens. These platens also act as the current carrying and potential electrodes. A thin silver leaf was also placed between the plug endfaces and electrodes, to ensure electrical contact. A strongly hydrophilic membrane was placed at the bottom end of the sample. This assembly was placed into a snugly fitting rubber overburden sleeve and then loaded into a Hydrostatic type core holder. A confining pressure of 1040 psi was gradually applied as an effective overburden pressure (see Appendix III for schematic).

Synthetic brine (Appendix II) was slowly flowed through each sample at a rate of 0.5cm^3/min. During this process sample resistivity was monitored on a digi-bridge capable of measuring sample resistance to 0.001 (ohms) accuracy. In each case the current frequency was selected to yield minimum phase angles, thus ensuring maximum electrical contact (between each sample and the current carrying and potential electrodes). Values of sample resistance (Rc) and effluent brine resistivity (Rw) were recorded daily. Each sample was deemed to be at ionic equilibrium when three consecutive daily readings were recorded within 1%.

From these stable data, the following results were recorded:

$$Ro = \frac{A \,.\, Rc}{100L}$$

where Ro = *sample resistivity (ohm.m)*
Rc = *sample resistance (ohms)*
L = *electrode gap (sample length - cm)*
A = *cross sectional area (cm^2)*
100 = *units conversion*

Formation resistivity factor was calculated using the following equations:

$$FF = \frac{a}{\Phi^m}$$

and

$$FF = \frac{Ro}{Rw}$$

where Rw = *brine resistivity (ohm.m)*
a = *intercept (assumed = 1)*
m = *cementation exponent*
and Φ = *porosity (fraction)*

The brine resistivity (Rw) was accurately determined by a NATA certified fluids laboratory.

5.1.2 Multi-Salinity Formation Factor

On completion of formation resistivity factor, a series of brines of various salinities (therefore conductivities) were flowed through each sample in the following sequence: 120000 ppm, 50000 ppm and formation brine. Each sample was connected in turn to a resistivity digi-bridge capable of measuring sample resistance to 0.001 accuracy. In each case the current frequency was selected to yield a minimum phase angle, thus ensuring maximum electrical contact between each sample and the current carrying and potential electrode. Values of sample resistance (Rc) and effluent brine resistivity (Rw) were recorded daily. Each sample was deemed to be at ionic equilibrium when three consecutive readings were recorded within 1%.

$$Ro = \frac{A \,.\, Rc}{100L}$$

where Ro = *sample resistivity (ohm.m)*
Rc = *sample resistance (ohms)*
L = *electrode gap (sample length - cm)*
A = *sample cross sectional area (cm^2)*
100 = *units conversion*

also $Co = \frac{1}{Ro}$

where Co = *conductivity of fully brine saturated sample (mho/m)*

and $Cw = \frac{1}{Rw}$

where Cw = *conductivity of saturant (mho/m)*

This process was then repeated with all brines scheduled.

The entire data set of multi-salinity resistivity data were plotted on linear graphs and a 'best-fit' (least squares) line was placed through the data set. As per standard practices, brines < 20,000 ppm were excluded from the trend line. The equation of the resulting line was calculated as:

$$y = mx + c$$

where y = *Co data points*
x = *Cw data points*
m = *gradient*
c = *intercept*

From the x-axis negative intercept a shaly sand equivalent value of formation resistivity factor (FRF*) and cementation factor (m*) were calculated for each of the samples, in accordance with Waxman-Thomas.

5.1.3 Formation Resistivity Index and Capillary Pressure

Upon completion of the preceding multi-salinity formation resistivity factor analyses, each sample was flooded with 150000 ppm brine before continuing with formation resistivity index analyses in conjunction with drainage capillary pressure curves. The top endface port was connected to a supply of humidified air and the bottom port connected to a graduated receiving tube (Appendix III). The samples were desaturated by gradually increasing the displacing fluid pressure to the samples. The actual pressures utilised were inversely proportional to the individual sample permeability data. A small amount of oil was placed into the collection tubes to prevent any potential brine loss by evaporation. Sample resistances were measured at successive decreasing brine saturations, which were calculated from the following equation:

$$Water\ Saturation\ (\%) = \frac{Pore\ Volume\ @\ OB\ (cm^3) - Brine\ Expelled\ (cm^3)}{Pore\ Volume\ @\ OB\ (cm^3)} \times 100$$

Capillary pressure curves plot water saturation (x-axis) against applied displacing fluid pressure. A hyperbolic curve is used to define this relationship. The ratio of the sample resistance (Rc) values to the previously determined FF values (at 100% saturation) were used to calculate the formation resistivity indices.

$$Rt = \frac{A \,.\, Rc}{100L}$$

where Rt = *resistivity of partially brine saturated sample (ohm.m)*
Rc = *sample resistance (ohms)*

and $$RI = \frac{Rt}{Rw \,.\, FF}$$

where RI = *resistivity index*
Rw = *resistivity of brine (ohm.m)*

(modified from standard Archie equation to include Rw).

These RI values (for each sample) were plotted against brine saturation (Sw) on graphs with logarithmic axes and the gradient of the best-fit line through the co-ordinate (1.0, 1.0) was calculated. Each gradient is quoted as the saturation exponent (n) for that sample, in accordance with Archie's formula.

$$RI = \frac{1}{Sw^n}$$

Terminal water saturations were confirmed by Dean-Stark analysis (Appendix III).

5.1.4 Cation Exchange Capacity

Cation exchange capacity was determined on approximately 5 grams of sample (off-cuts) using the wet chemistry method. The samples were first washed with an ammonium chloride solution to exchange ions with the available clay cations. An exchange reagent was then washed through the sample and the resultant solution titrated. Where a smaller sample is used the limit of detection becomes greater and a minimum value is reported.

Values of exchangeable cations (theoretical minimum of zero) present in the samples are reported as milliequivalents per 100 grams of dry sample (meq/100 g). Values of Q_v have been calculated using the following equation:

$$Q_v = \frac{CEC\,(1-\Phi)\rho}{100\,\Phi}$$

where

ρ = *grain density (g/cm^3)*

Φ = *porosity (fraction)*

Q_v = *volume concentration of clay exchange cations (meq/cm^3 pore space)*

CEC = *cation exchange capacity (meq/100 g dry sample)*

Based on these CEC/Qv data, values of shaly sand equivalent formation factor (FF*), cementation factor (m*) and saturation exponent (n*) were calculated using the following equations:

$$FF^* = FF\,.(1 + B.Qv.Rw)$$

$$m^* = \frac{\log FF^*}{-\log \Phi}$$

$$n^* = \frac{\log\left[\frac{1 + Rw.B.Qv}{1 + Rw.B.Qv\,/\,Sw}\right] - \log FRI}{\log Sw}$$

where

FF = *formation resistivity factor*

FF^* = *shaly sand equivalent formation resistivity factor*

m^* = *shaly sand equivalent cementation factor*

Φ = *porosity (fraction)*

n^* = *shaly sand equivalent saturation exponent*

Rw = *brine resistivity (ohm.m @ 25°C)*

Qv = *volume concentration of clay exchange cations (meq/cm^3 pore space)*

Sw = *brine saturation (fraction)*

B = *equivalent conductance of clay exchange cations (mho.cm^2.meq^{-1})*

FRI = *formation resistivity index*

CHAPTER 5

ELECTRICAL PROPERTIES AND CAPILLARY PRESSURE

5.2 Test Results

5.2.1 Formation Factor

FORMATION RESISTIVITY FACTOR

Client	OMV Australia Pty Ltd	**Saturant**	Formation Brine
Well	Baleen-2	**Rw of Saturant**	0.826 at 25°C
		Overburden	1040 psi
		Average m	1.62

Sample Number	Depth (metres)	Permeability to Air (milliDarcy's)	Porosity (percent)	Formation Factor FF	Cementation Exponent m
S1	746.63	27	31.2	7.2	1.72
S5	750.41	76	32.1	6.2	1.61
S9	754.41	313	35.8	5.6	1.68
S10	755.39	240	33.1	6.8	1.73
S20	767.87	30	23.3	12.2	1.73
S23	770.97	27 *	30.2 *	8.2	1.70
S25	772.99	79	33.3	6.3	1.67
S27	774.80	346 *	37.1 *	3.8	1.15
S28	775.82	213	35.3	5.5	1.64
S29	776.80	528 *	36.7 *	4.9	1.54

* Ambient Data

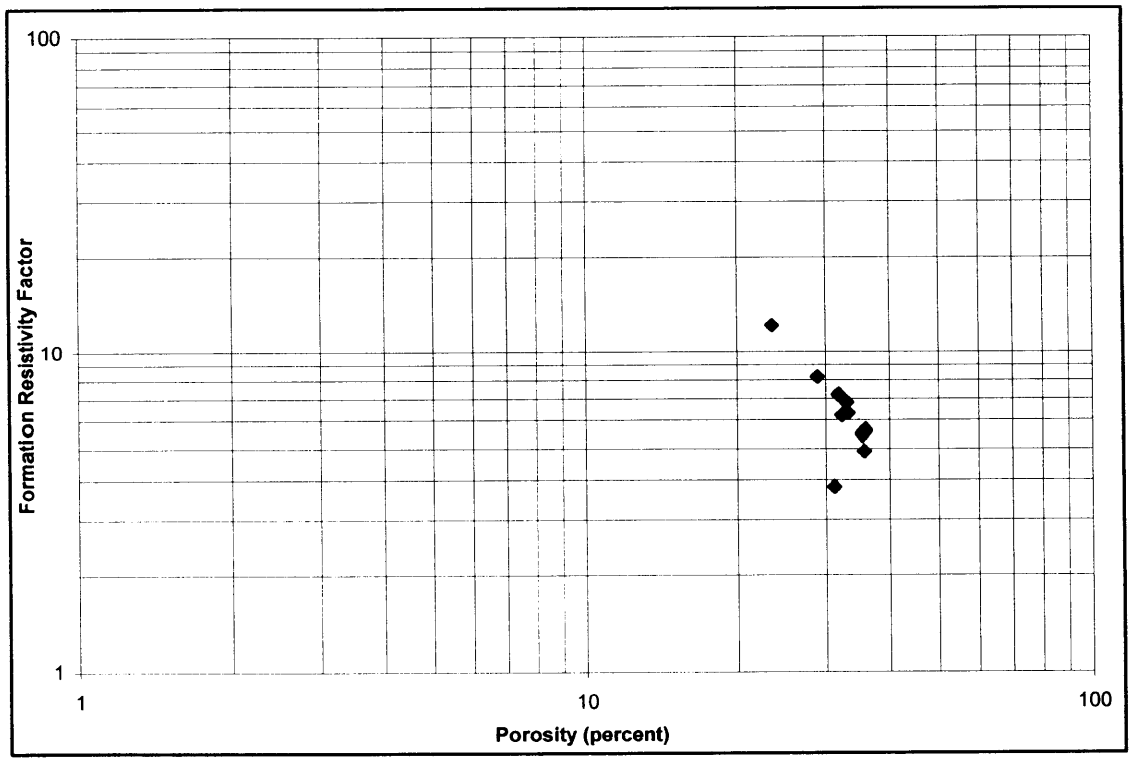

CHAPTER 5

ELECTRICAL PROPERTIES AND CAPILLARY PRESSURE

5.2 Test Results

5.2.2 Multi-Salinity Formation Factor

MULTI-SALINITY RESISTIVITY ANALYSES

Client	OMV Australia Pty Ltd		
Well	Baleen-2		
Sample	S1	**Air Permeability**	27 mD
Depth	746.63 m	**Porosity**	31.2 %
Overburden	1040 psi		

Formation Factor, FF	7.2	**Shaly Sand Equivalent FF***	13.3
Cementation Exponent, m	1.72	**Shaly Sand Equivalent m***	2.26

Brine	Brine Resistivity, Rw (ohm.m)	Sample Resistivity, Ro (ohm.m)	Brine Conductivity, Cw (mho/m)	Sample Conductivity, Co (mho/m)
Formation	0.885	6.38	1.13	0.157
120000	0.078	0.930	12.8	1.08
50000	0.155	1.66	6.45	0.602
Formation	0.900	5.88	1.11	0.170

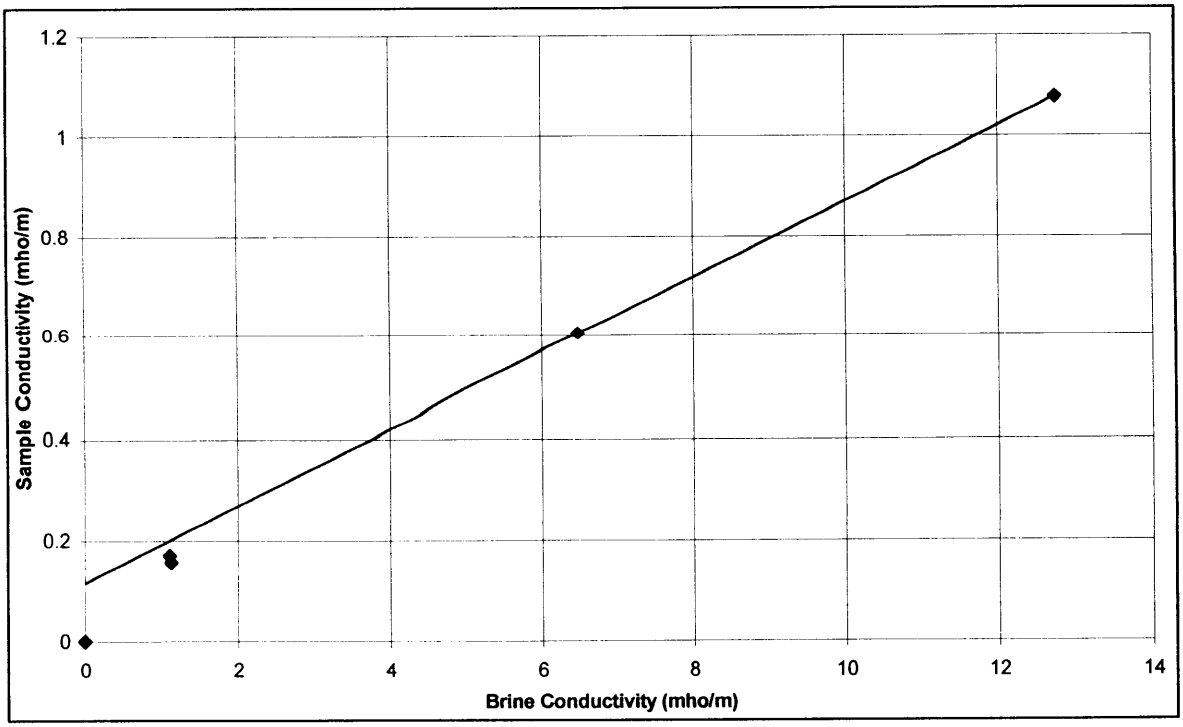

MULTI-SALINITY RESISTIVITY ANALYSES

Client	OMV Australia Pty Ltd		
Well	Baleen-2		
Sample	S5	**Air Permeability**	76 mD
Depth	750.41 m	**Porosity**	32.1 %
Overburden	1040 psi		

Formation Factor, FF	6.2	**Shaly Sand Equivalent FF***	8.5
Cementation Exponent, m	1.61	**Shaly Sand Equivalent m***	1.89

Brine	Brine Resistivity, Rw (ohm.m)	Sample Resistivity, Ro (ohm.m)	Brine Conductivity, Cw (mho/m)	Sample Conductivity, Co (mho/m)
Formation	0.900	5.60	1.11	0.179
120000	0.078	0.630	12.8	1.59
50000	0.157	1.19	6.37	0.840
Formation	0.900	5.12	1.11	0.195

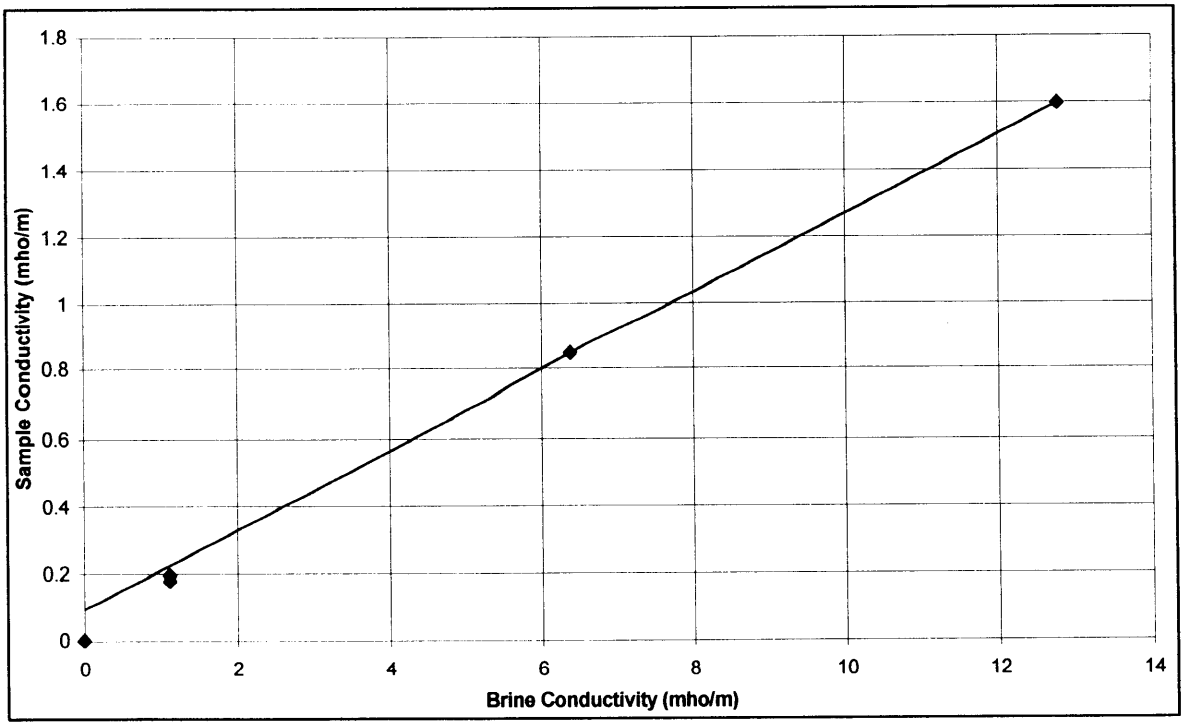

MULTI-SALINITY RESISTIVITY ANALYSES

Client	OMV Australia Pty Ltd		
Well	Baleen-2		
Sample	S9	**Air Permeability**	313 mD
Depth	754.41 m	**Porosity**	35.8 %
Overburden	1040 psi		

Formation Factor, FF	5.6	**Shaly Sand Equivalent FF***	7.6
Cementation Exponent, m	1.68	**Shaly Sand Equivalent m***	1.98

Brine	Brine Resistivity, Rw (ohm.m)	Sample Resistivity, Ro (ohm.m)	Brine Conductivity, Cw (mho/m)	Sample Conductivity, Co (mho/m)
Formation	0.826	5.06	1.21	0.198
120000	0.078	0.560	12.8	1.79
50000	0.158	1.07	6.33	0.935
Formation	0.828	4.92	1.21	0.203

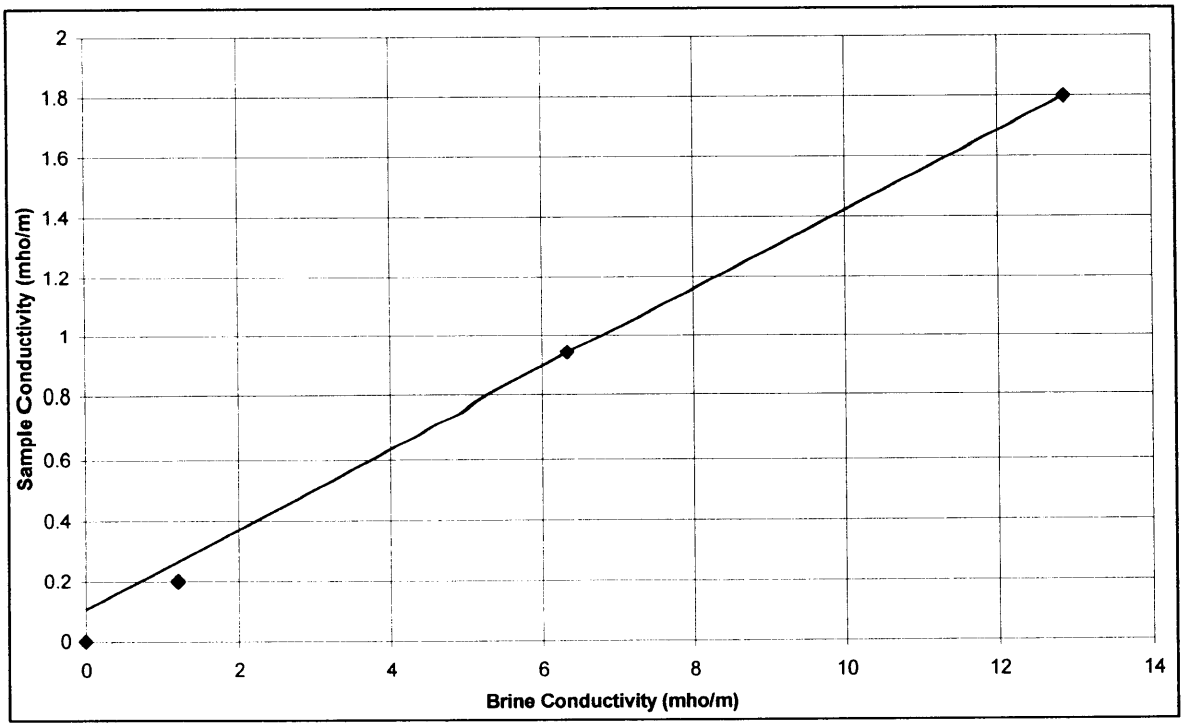

MULTI-SALINITY RESISTIVITY ANALYSES

Client	OMV Australia Pty Ltd		
Well	Baleen-2		
Sample	S10	**Air Permeability**	240 mD
Depth	755.39 m	**Porosity**	33.1 %
Overburden	1040 psi		

Formation Factor, FF	6.8	**Shaly Sand Equivalent FF***	9.7
Cementation Exponent, m	1.73	**Shaly Sand Equivalent m***	2.06

Brine	Brine Resistivity, Rw (ohm.m)	Sample Resistivity, Ro (ohm.m)	Brine Conductivity, Cw (mho/m)	Sample Conductivity, Co (mho/m)
Formation	0.894	6.11	1.12	0.164
120000	0.077	0.700	13.0	1.43
50000	0.159	1.35	6.29	0.741
Formation	0.887	6.09	1.13	0.164

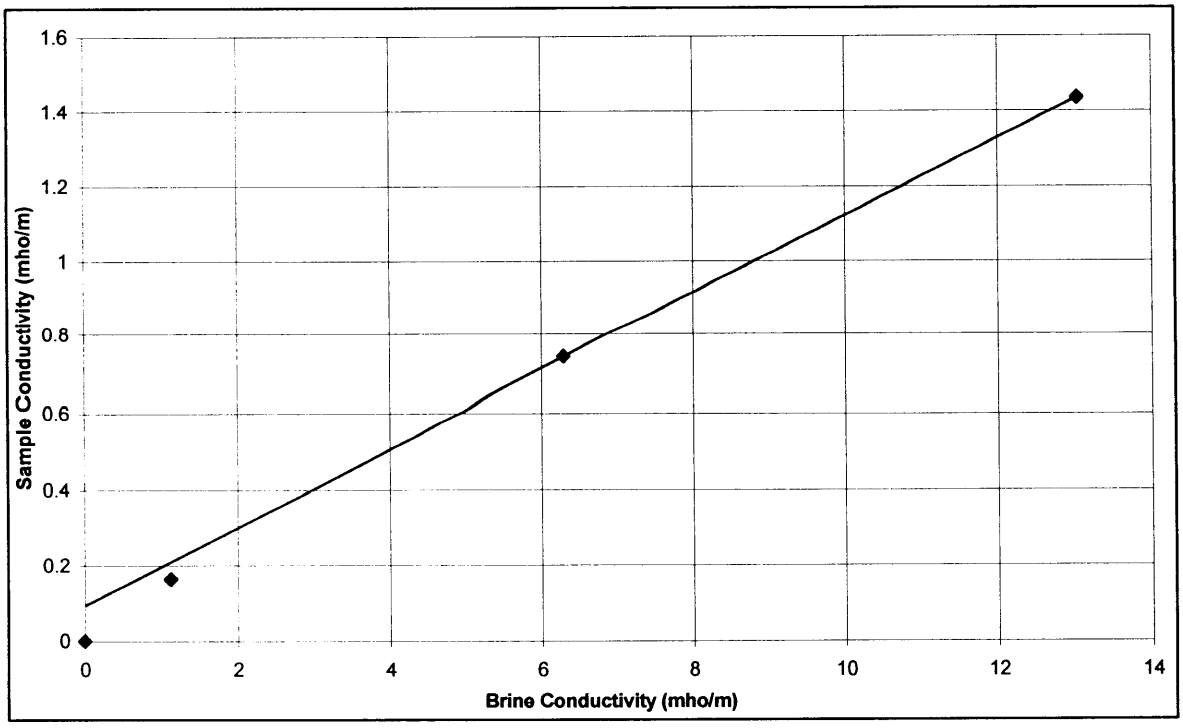

MULTI-SALINITY RESISTIVITY ANALYSES

Client	OMV Australia Pty Ltd		
Well	Baleen-2		
Sample	S20	**Air Permeability**	30 mD
Depth	767.87 m	**Porosity**	23.3 %
Overburden	1040 psi		

Formation Factor, FF	12.2	**Shaly Sand Equivalent FF***	20.3
Cementation Exponent, m	1.73	**Shaly Sand Equivalent m***	2.08

Brine	Brine Resistivity, Rw (ohm.m)	Sample Resistivity, Ro (ohm.m)	Brine Conductivity, Cw (mho/m)	Sample Conductivity, Co (mho/m)
Formation	0.887	10.8	1.13	0.092
120000	0.077	1.46	13.0	0.685
50000	0.155	2.74	6.45	0.365
Formation	0.887	10.5	1.13	0.095

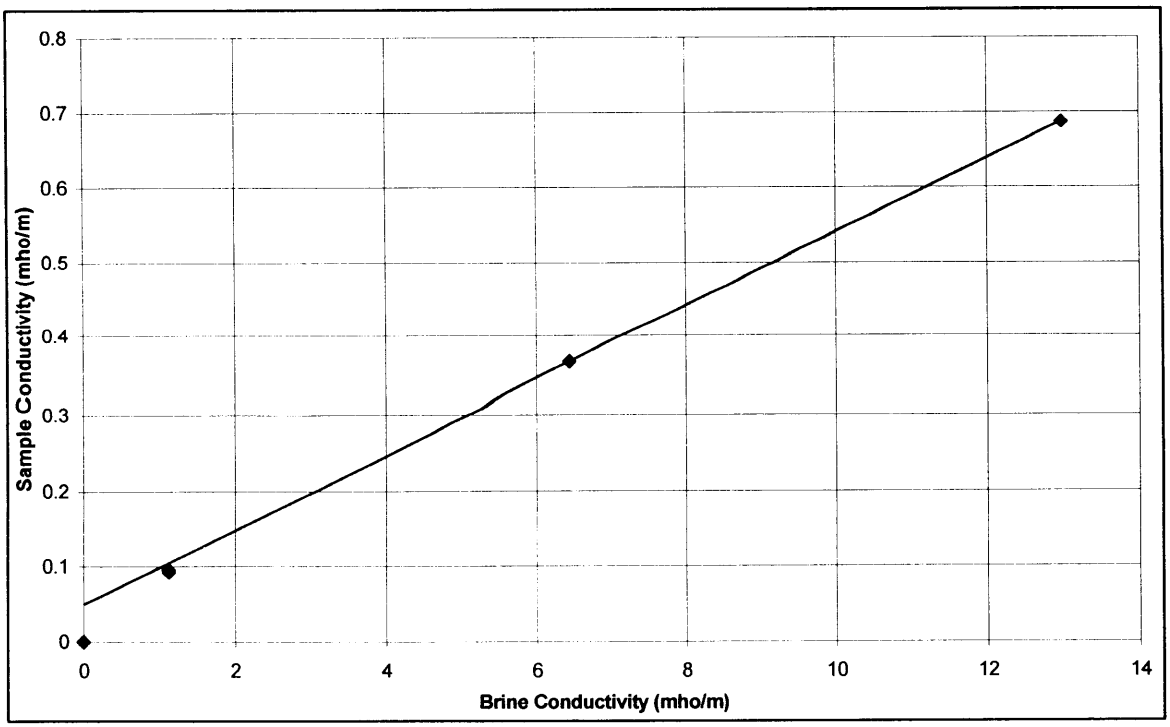

MULTI-SALINITY RESISTIVITY ANALYSES

Client	OMV Australia Pty Ltd		
Well	Baleen-2		
Sample	S23	**Ambient Air Permeability**	27 mD
Depth	770.97 m	**Ambient Porosity**	30.2 %
Overburden	1040 psi		

Formation Factor, FF	8.2	**Shaly Sand Equivalent FF***	12.9
Cementation Exponent, m	1.70	**Shaly Sand Equivalent m***	2.14

Brine	Brine Resistivity, Rw (ohm.m)	Sample Resistivity, Ro (ohm.m)	Brine Conductivity, Cw (mho/m)	Sample Conductivity, Co (mho/m)
Formation	0.887	7.28	1.13	0.137
120000	0.077	0.900	13.0	1.11
50000	0.154	1.65	6.49	0.606
Formation	0.898	7.24	1.11	0.138

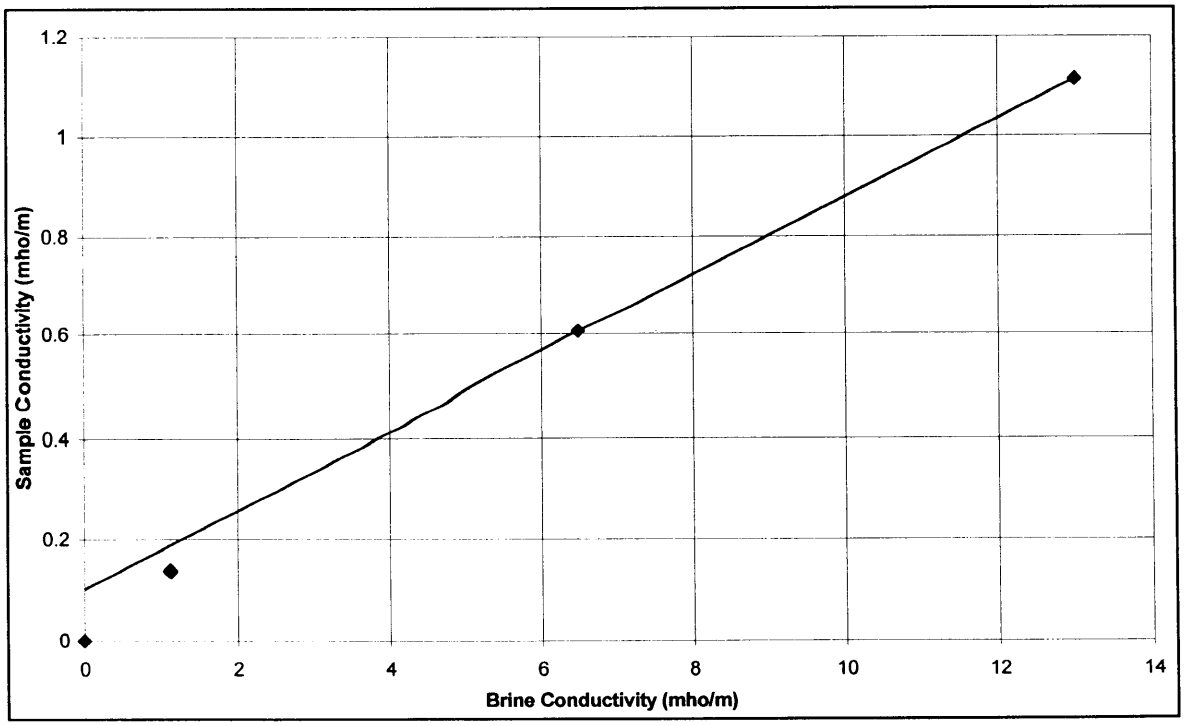

MULTI-SALINITY RESISTIVITY ANALYSES

Client	OMV Australia Pty Ltd		
Well	Baleen-2		
Sample	S25	**Air Permeability**	79 mD
Depth	772.99 m	**Porosity**	33.3 %
Overburden	1040 psi		

Formation Factor, FF	6.3	**Shaly Sand Equivalent FF***	9.2
Cementation Exponent, m	1.67	**Shaly Sand Equivalent m***	2.02

Brine	Brine Resistivity, Rw (ohm.m)	Sample Resistivity, Ro (ohm.m)	Brine Conductivity, Cw (mho/m)	Sample Conductivity, Co (mho/m)
Formation	0.894	5.62	1.12	0.178
120000	0.078	0.670	12.8	1.49
50000	0.151	1.25	6.62	0.800
Formation	0.887	5.44	1.13	0.184

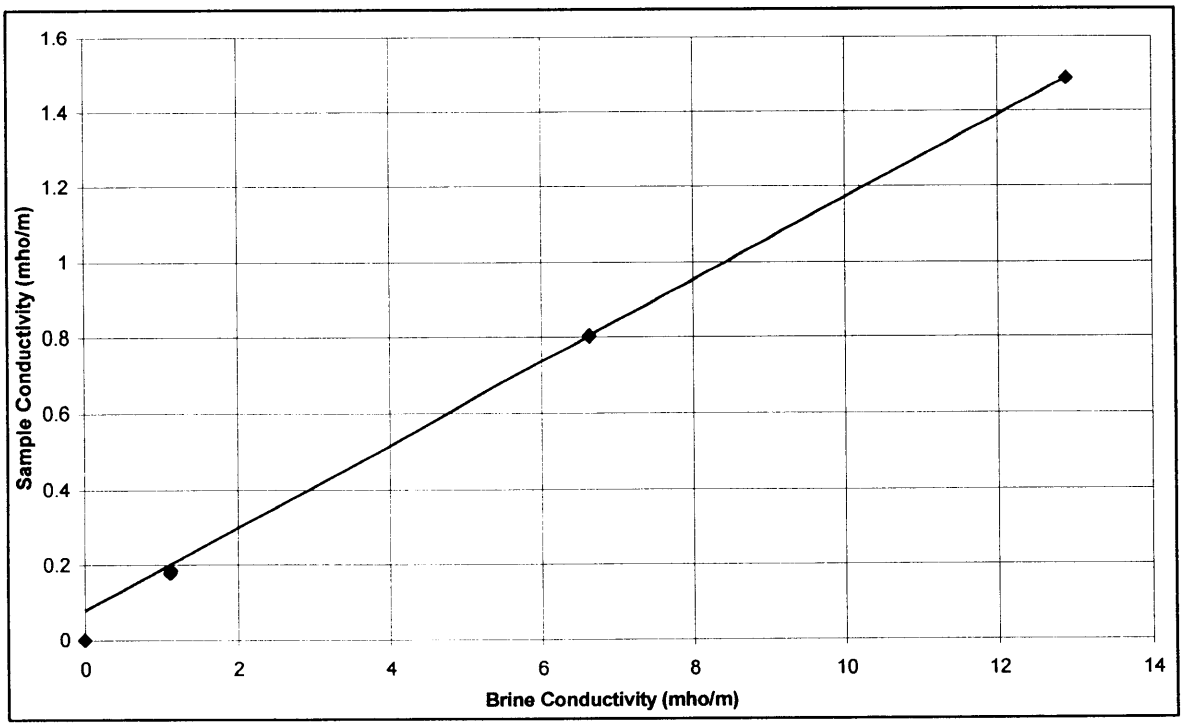

MULTI-SALINITY RESISTIVITY ANALYSES

Client	OMV Australia Pty Ltd		
Well	Baleen-2		
Sample	S27	**Ambient Air Permeability**	346 mD
Depth	774.80 m	**Ambient Porosity**	37.1 %
Overburden	1040 psi		
Formation Factor, FF	3.8	**Shaly Sand Equivalent FF***	11.0
Cementation Exponent, m	1.15	**Shaly Sand Equivalent m***	2.42

Brine	Brine Resistivity, Rw (ohm.m)	Sample Resistivity, Ro (ohm.m)	Brine Conductivity, Cw (mho/m)	Sample Conductivity, Co (mho/m)
Formation	0.894	3.64	1.12	0.275
120000	0.078	0.530	12.8	1.89
50000	0.151	0.760	6.62	1.32
Formation	Failed			

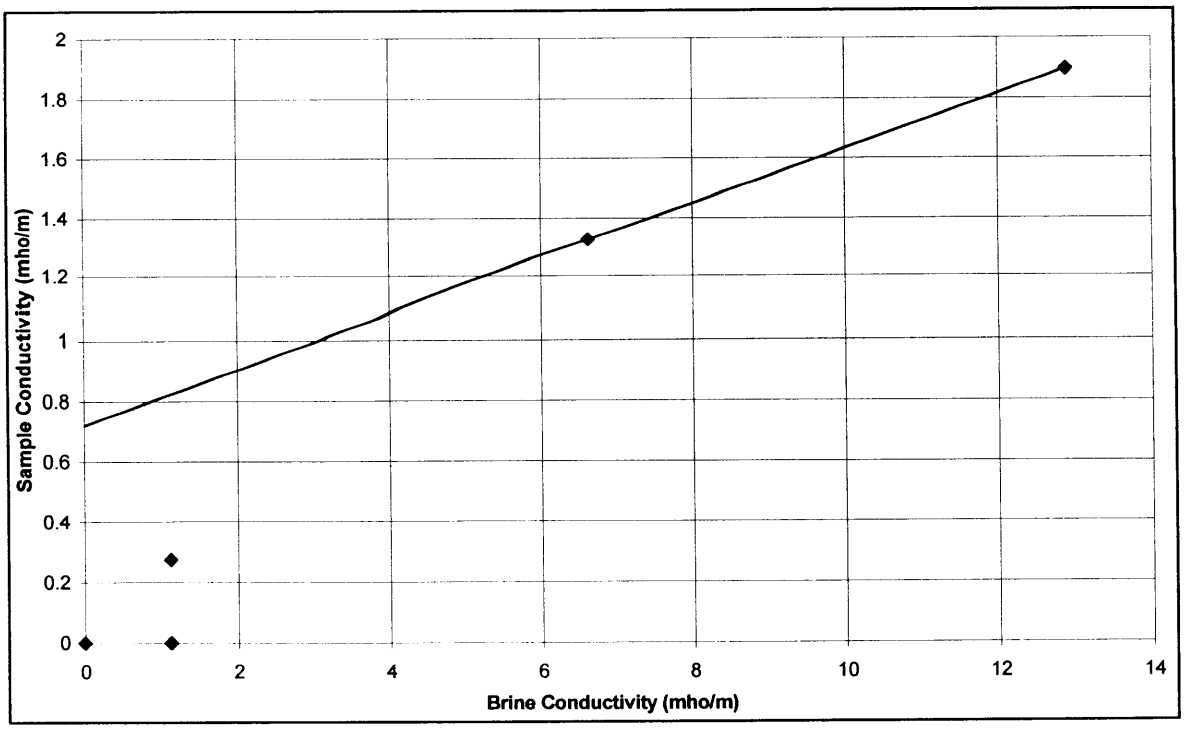

MULTI-SALINITY RESISTIVITY ANALYSES

Client	OMV Australia Pty Ltd		
Well	Baleen-2		
Sample	S28	**Air Permeability**	213 mD
Depth	775.82 m	**Porosity**	35.3 %
Overburden	1040 psi		

Formation Factor, FF	5.5	**Shaly Sand Equivalent FF***	7.2
Cementation Exponent, m	1.64	**Shaly Sand Equivalent m***	1.94

Brine	Brine Resistivity, Rw (ohm.m)	Sample Resistivity, Ro (ohm.m)	Brine Conductivity, Cw (mho/m)	Sample Conductivity, Co (mho/m)
Formation	0.889	4.91	1.13	0.204
120000	0.076	0.540	13.2	1.85
50000	0.150	1.04	6.67	0.962
Formation	0.894	5.22	1.12	0.192

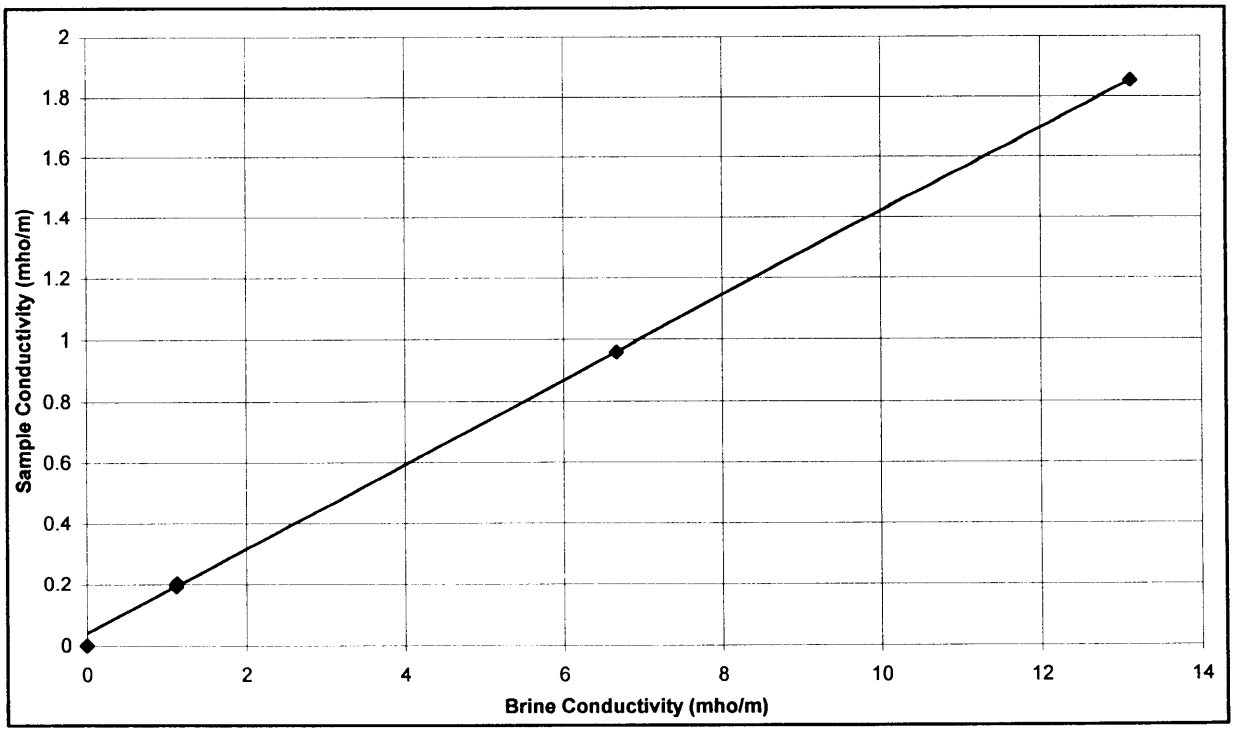

MULTI-SALINITY RESISTIVITY ANALYSES

Client	OMV Australia Pty Ltd		
Well	Baleen-2		
Sample	S29	**Ambient Air Permeability**	528 mD
Depth	776.80 m	**Ambient Porosity**	36.7 %
Overburden	1040 psi		

Formation Factor, FF	4.9	**Shaly Sand Equivalent FF***	11.1
Cementation Exponent, m	1.54	**Shaly Sand Equivalent m***	2.40

Brine	Brine Resistivity, Rw (ohm.m)	Sample Resistivity, Ro (ohm.m)	Brine Conductivity, Cw (mho/m)	Sample Conductivity, Co (mho/m)
Formation	0.894	4.73	1.12	0.211
120000	0.077	0.750	13.0	1.33
50000	0.150	1.33	6.67	0.752
Formation	Failed			

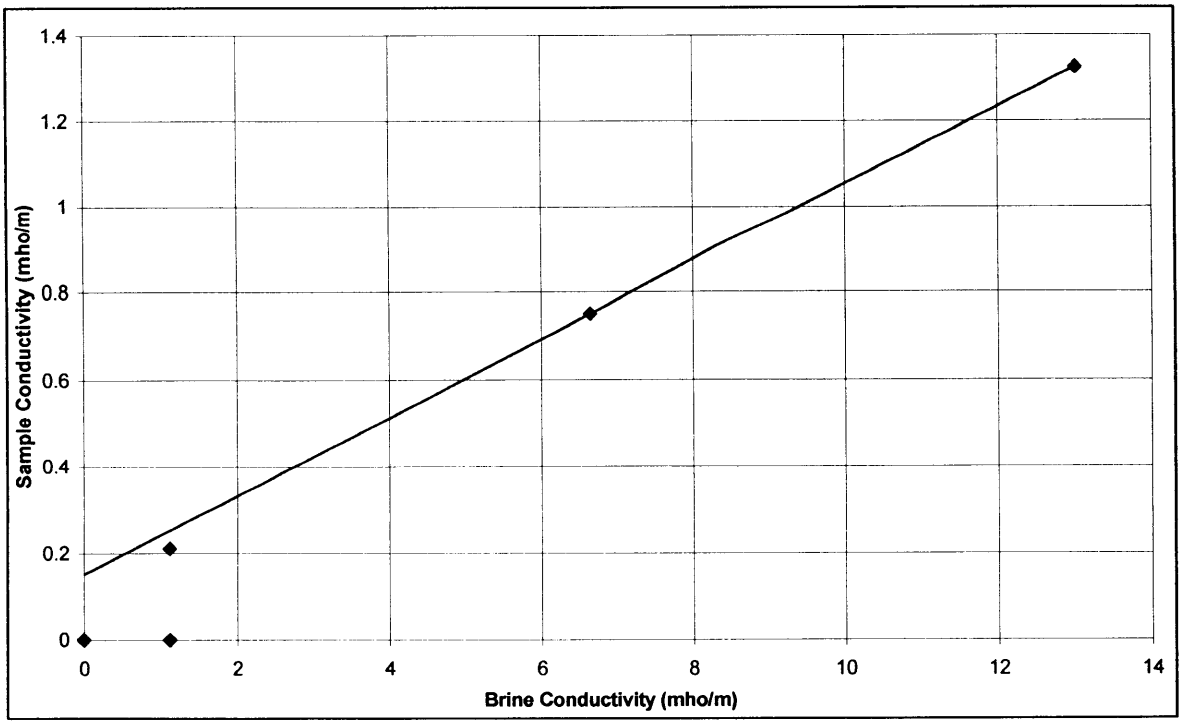

CHAPTER 5

ELECTRICAL PROPERTIES AND CAPILLARY PRESSURE

5.2 Test Results

5.2.3 Resistivity Index

RESISTIVITY INDEX

Client OMV Australia Pty Ltd
Well Baleen-2

Rw of Saturant 0.072 @25C
Method Air/Brine Porous Plate @ Overburden

Sample Number	Depth (metres)	Permeability to Air (milliDarcy's)	Porosity (percent)	Formation Factor FF	Brine Saturation (fraction)	Resistivity Index RI	Saturation Exponent n
S1	746.63	27	31.2	12.1	1.000	1.00	
					0.975	1.07	
					0.922	1.11	
					0.860	1.21	
					0.816	1.37	
					0.793	1.48	
					0.771	1.66	
					0.754	1.73	
					0.738	1.81	1.81

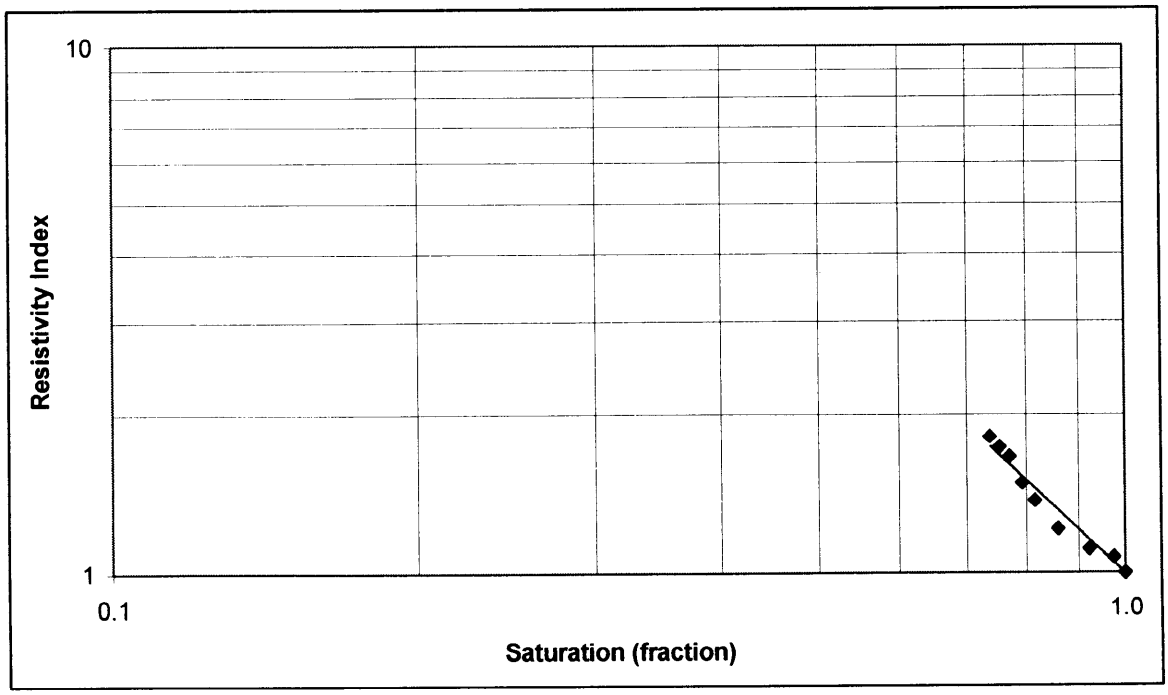

RESISTIVITY INDEX

Client OMV Australia Pty Ltd
Well Baleen-2

Rw of Saturant 0.072 @25C
Method Air/Brine Porous Plate @ Overburden

Sample Number	Depth (metres)	Permeability to Air (milliDarcy's)	Porosity (percent)	Formation Factor FF	Brine Saturation (fraction)	Resistivity Index RI	Saturation Exponent n
S5	750.41	76	32.1	8.00	1.000	1.00	
					0.989	1.02	
					0.925	1.13	
					0.745	1.64	
					0.602	2.31	
					0.507	3.21	
					0.413	4.74	
					0.380	5.27	
					0.358	5.90	1.72

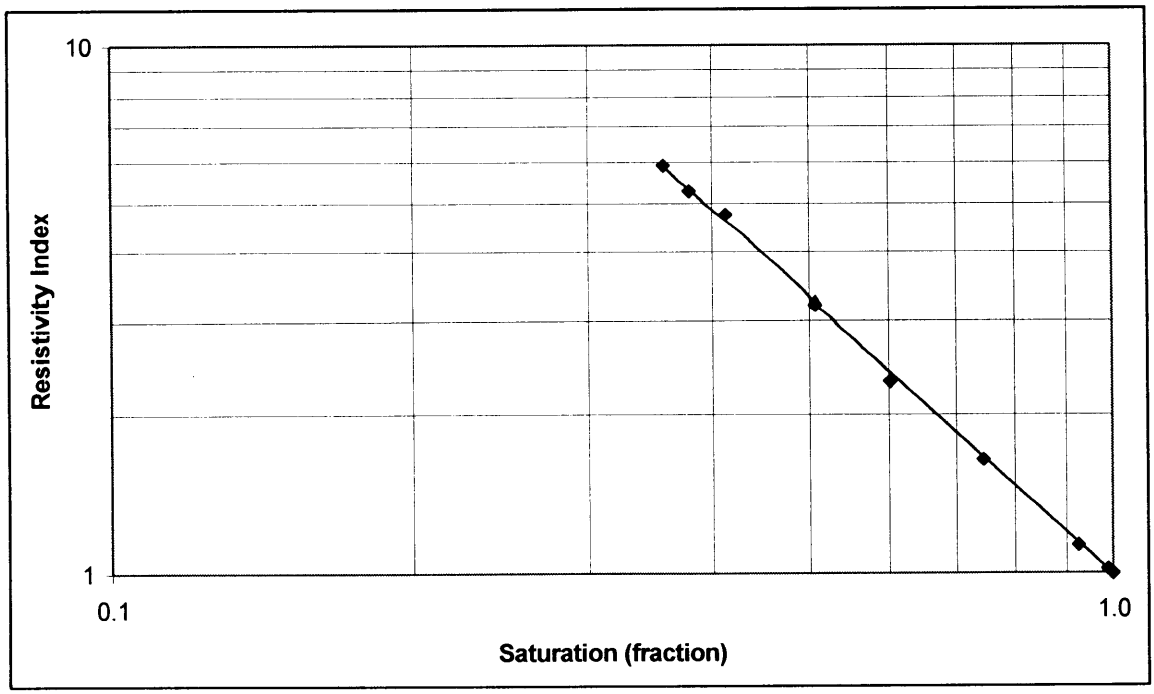

RESISTIVITY INDEX

Client OMV Australia Pty Ltd
Well Baleen-2

Rw of Saturant 0.072 @25C
Method Air/Brine Porous Plate @ Overburden

Sample Number	Depth (metres)	Permeability to Air (milliDarcy's)	Porosity (percent)	Formation Factor FF	Brine Saturation (fraction)	Resistivity Index RI	Saturation Exponent n
S9	754.41	313	35.8	7.20	1.000	1.00	
					0.987	1.02	
					0.674	2.04	
					0.549	2.84	
					0.423	4.00	
					0.348	5.72	
					0.313	7.84	
					0.288	8.67	
					0.273	9.20	1.71

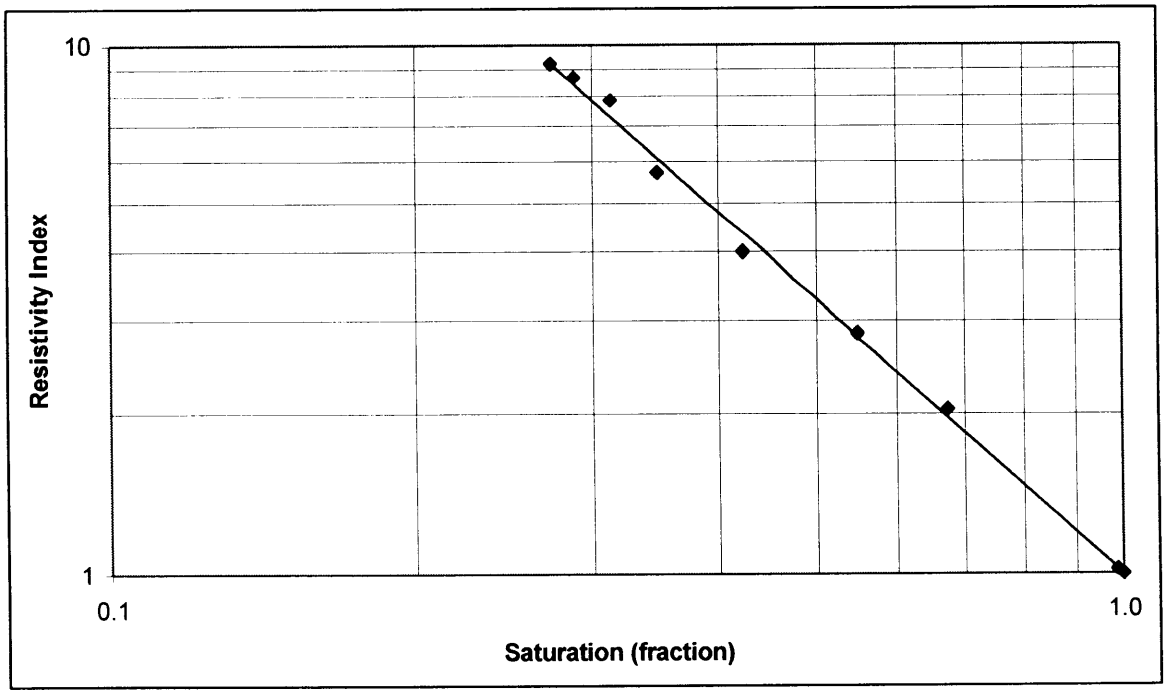

RESISTIVITY INDEX

Client OMV Australia Pty Ltd
Well Baleen-2

Rw of Saturant 0.072 @25C
Method Air/Brine Porous Plate @ Overburden

Sample Number	Depth (metres)	Permeability to Air (milliDarcy's)	Porosity (percent)	Formation Factor FF	Brine Saturation (fraction)	Resistivity Index RI	Saturation Exponent n
S10	755.39	240	33.1	9.10	1.000	1.00	
					0.992	1.01	
					0.699	1.90	
					0.563	2.68	
					0.451	3.98	
					0.368	5.19	
					0.323	6.74	
					0.308	7.41	
					0.300	7.88	1.70

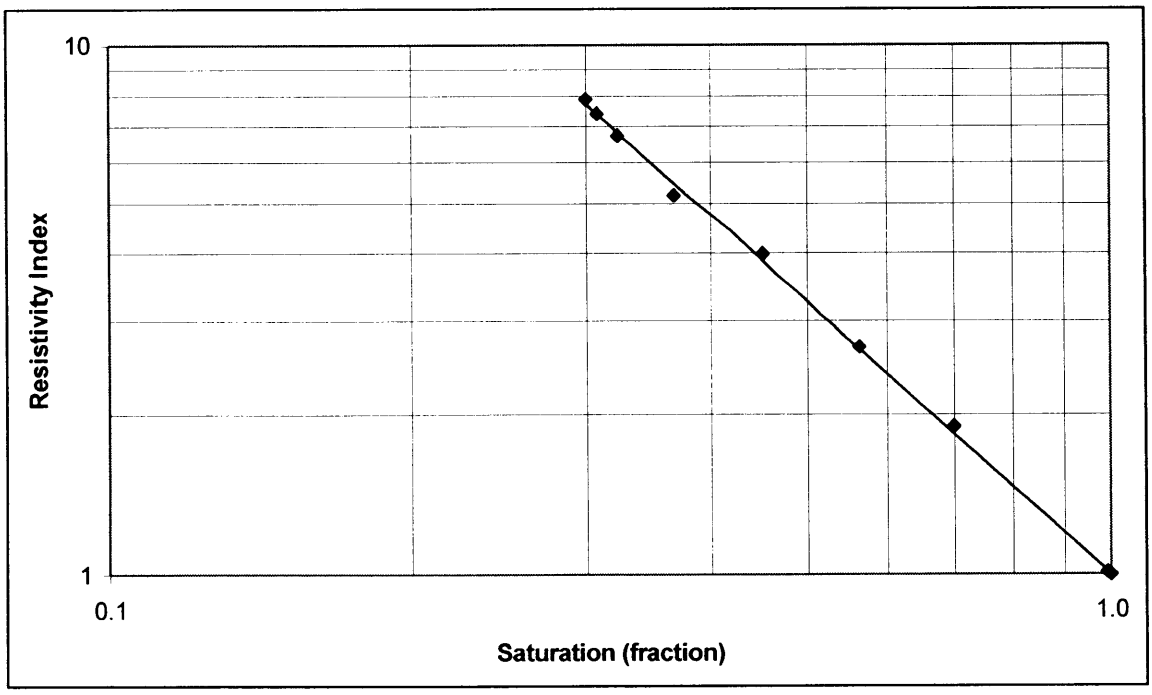

RESISTIVITY INDEX

Client OMV Australia Pty Ltd
Well Baleen-2

Rw of Saturant 0.072 @25C
Method Air/Brine Porous Plate @ Overburden

Sample Number	Depth (metres)	Permeability to Air (milliDarcy's)	Porosity (percent)	Formation Factor FF	Brine Saturation (fraction)	Resistivity Index RI	Saturation Exponent n
S20	767.87	30	23.3	18.9	1.000	1.00	
					0.971	1.03	
					0.890	1.19	
					0.773	1.51	
					0.627	2.15	
					0.546	2.86	
					0.517	3.28	
					0.495	3.41	
					0.480	3.62	1.74

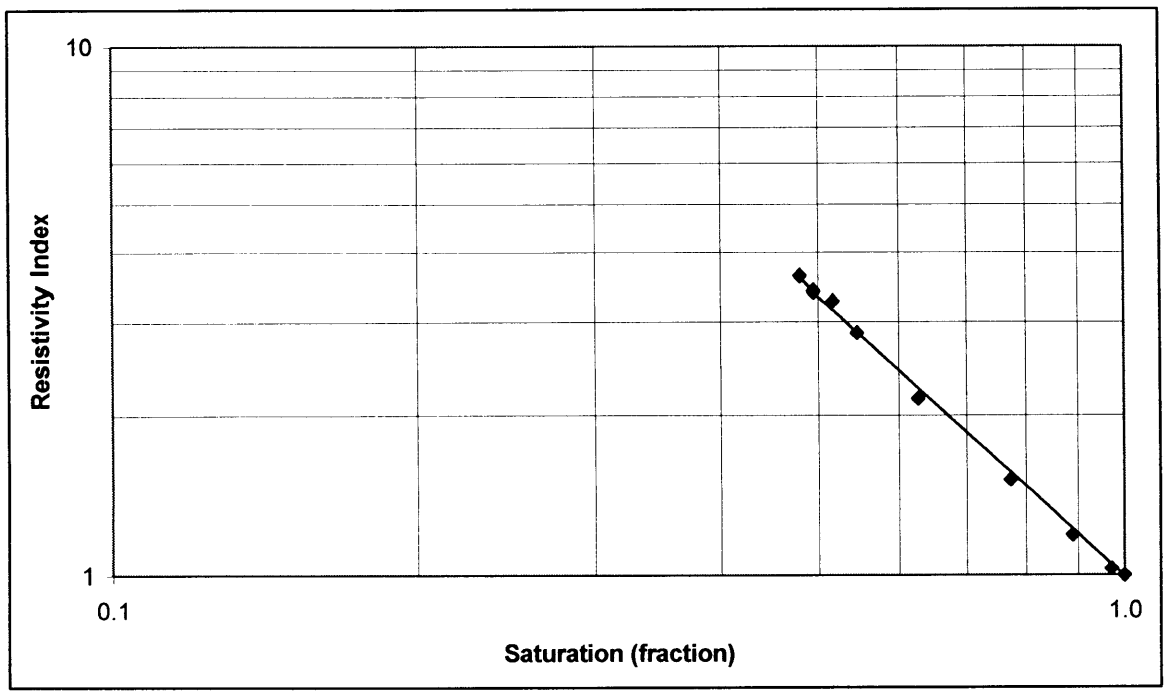

RESISTIVITY INDEX

Client OMV Australia Pty Ltd
Well Baleen-2

Rw of Saturant 0.072 @25C
Method Air/Brine Porous Plate @ Overburden

Sample Number	Depth (metres)	Permeability to Air (milliDarcy's)	Porosity (percent)	Formation Factor FF	Brine Saturation (fraction)	Resistivity Index RI	Saturation Exponent n
S25	772.99	79	33.3	8.70	1.000	1.00	
					0.999	1.03	
					0.984	1.08	
					0.768	1.65	
					0.549	3.11	
					0.468	3.81	
					0.414	5.68	
					0.395	5.93	
					0.386	6.12	1.90

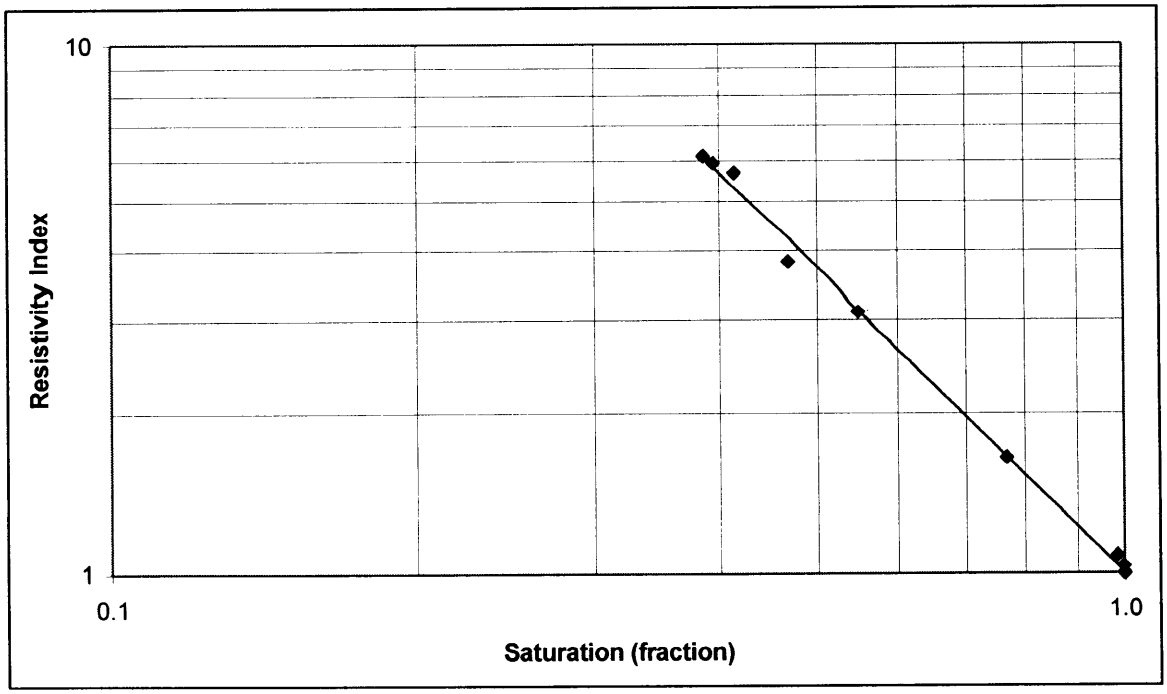

RESISTIVITY INDEX

Client OMV Australia Pty Ltd
Well Baleen-2

Rw of Saturant 0.072 @25C
Method Air/Brine Porous Plate @ Overburden

Sample Number	Depth (metres)	Permeability to Air (milliDarcy's)	Porosity (percent)	Formation Factor FF	Brine Saturation (fraction)	Resistivity Index RI	Saturation Exponent n
S28	775.82	213	35.3	7.10	1.000	1.00	
					0.938	1.06	
					0.659	1.86	
					0.551	2.59	
					0.473	3.44	
					0.396	4.83	
					0.344	6.82	
					0.328	7.20	
					0.318	7.58	1.73

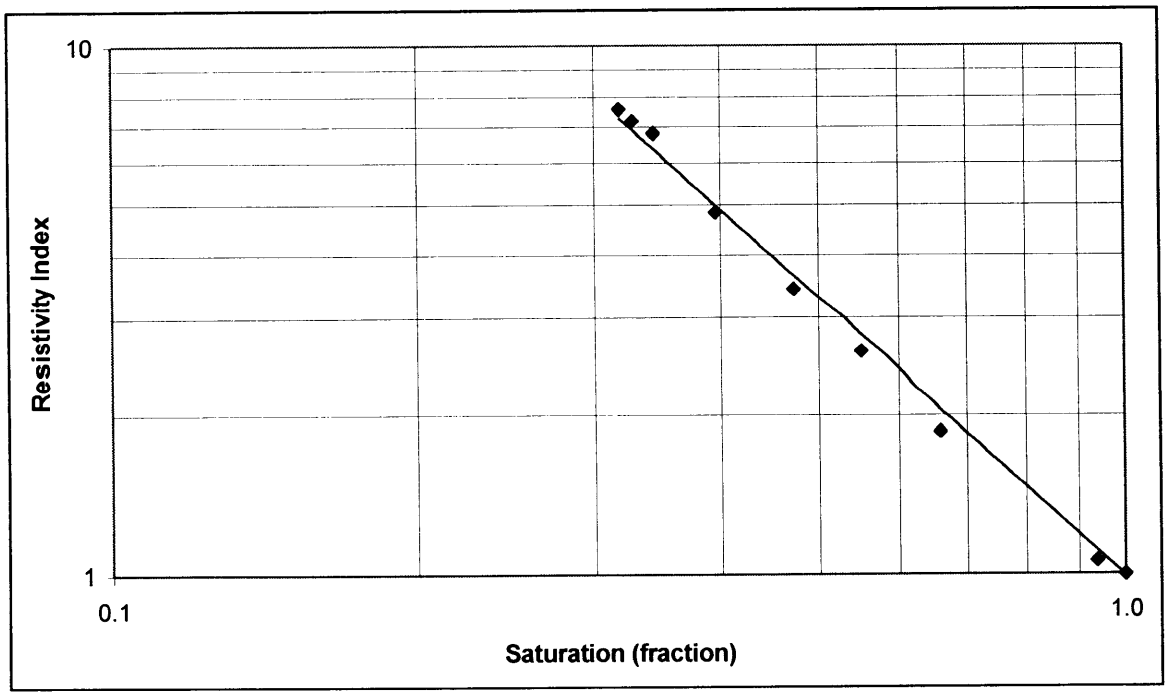

RESISTIVITY INDEX

Client OMV Australia Pty Ltd
Well Baleen-2

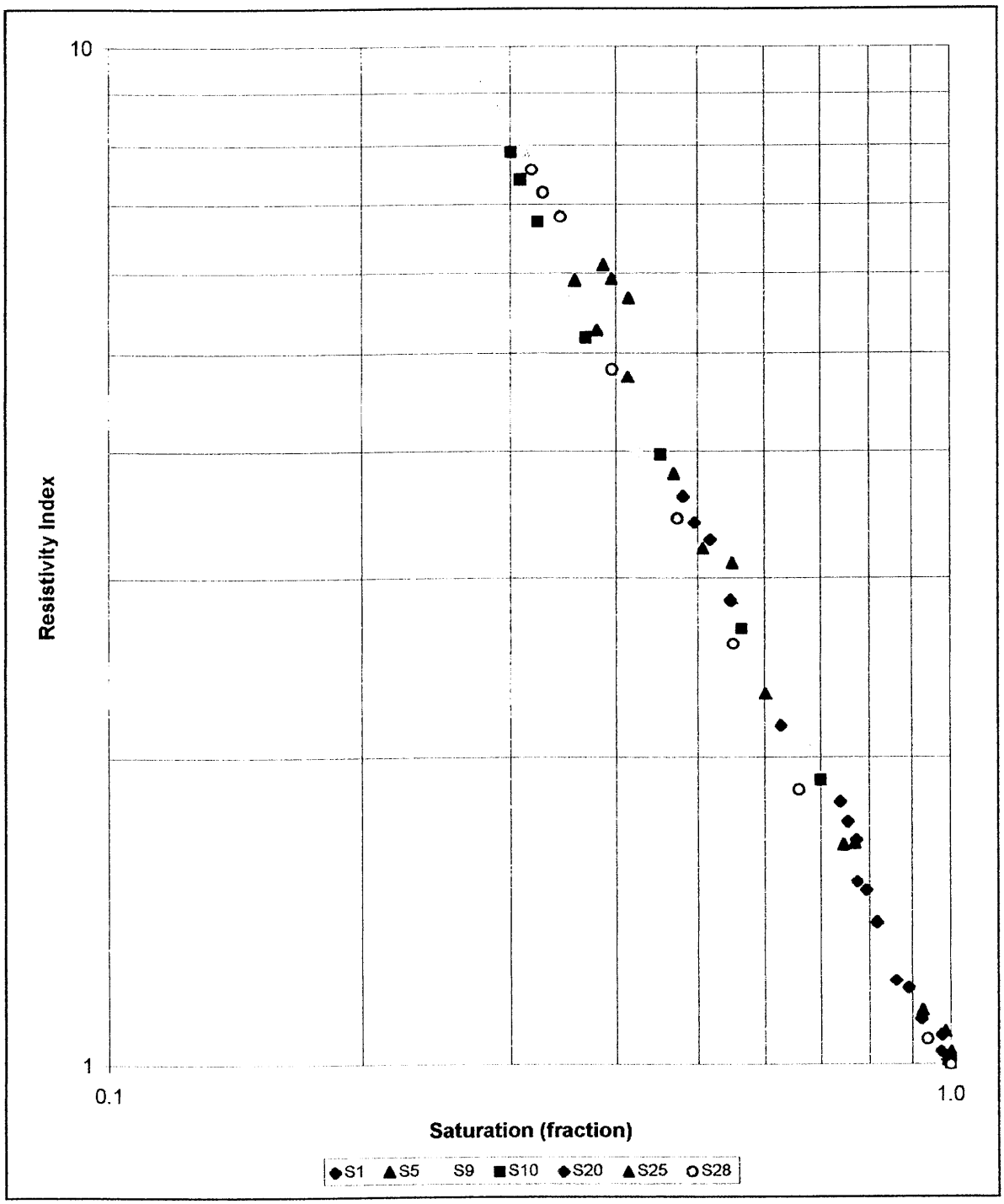

CHAPTER 5

ELECTRICAL PROPERTIES AND CAPILLARY PRESSURE

5.2 Test Results

5.2.4 Capillary Pressure

CAPILLARY PRESSURE
Overburden

Client	OMV Australia Pty Ltd	**Air Permeability**	27 milliDarcy's
Well	Baleen-2	**Porosity**	31.2 percent
Sample	S1		
Depth	746.63 metres		
Test Method	Air/Brine Porous Plate @ Overburden		
Overburden	1040 psi		

Capillary Pressure (psi)	Brine Saturation (percent)
4.0	97.5
8.0	92.2
16	86.0
24	81.6
32	79.3
64	77.1
100	75.4
150	73.8

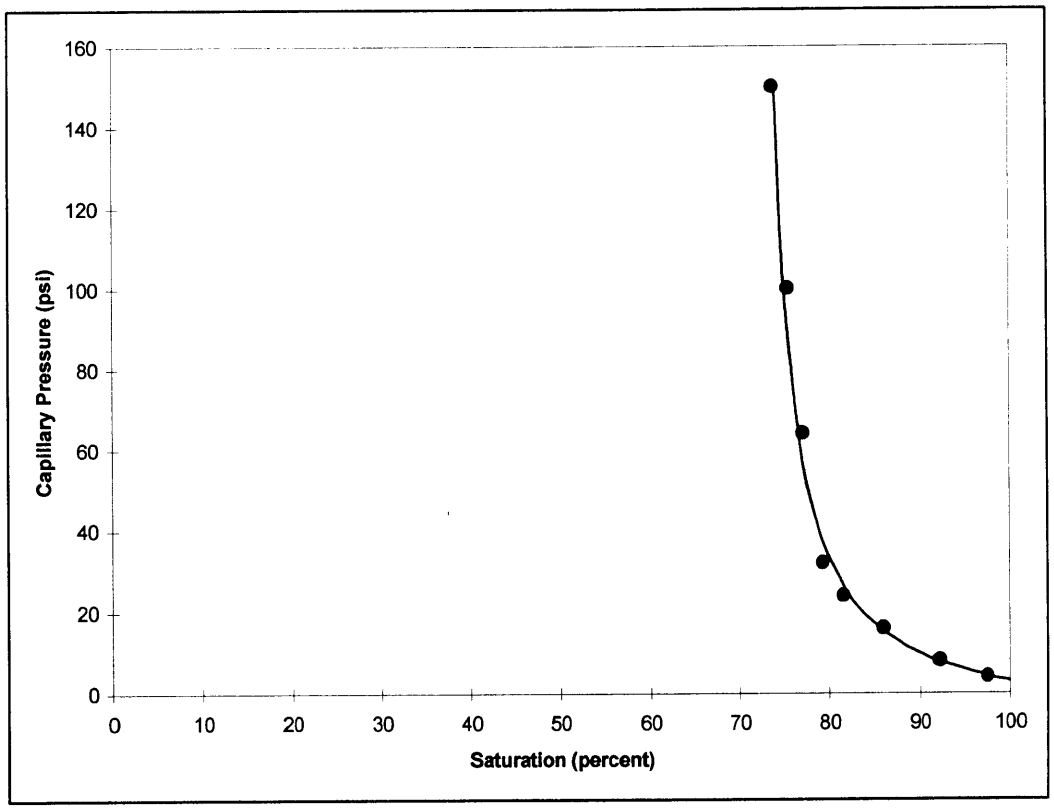

9030080 280

CAPILLARY PRESSURE
Overburden

Client	OMV Australia Pty Ltd	**Air Permeability**	76 milliDarcy's
Well	Baleen-2	**Porosity**	32.1 percent
Sample	S5		
Depth	750.41 metres		
Test Method	Air/Brine Porous Plate @ Overburden		
Overburden	1040 psi		

Capillary Pressure (psi)	Brine Saturation (percent)
2.0	98.9
4.0	92.5
8.0	74.5
16	60.2
32	50.7
64	41.3
100	38.0
150	35.8

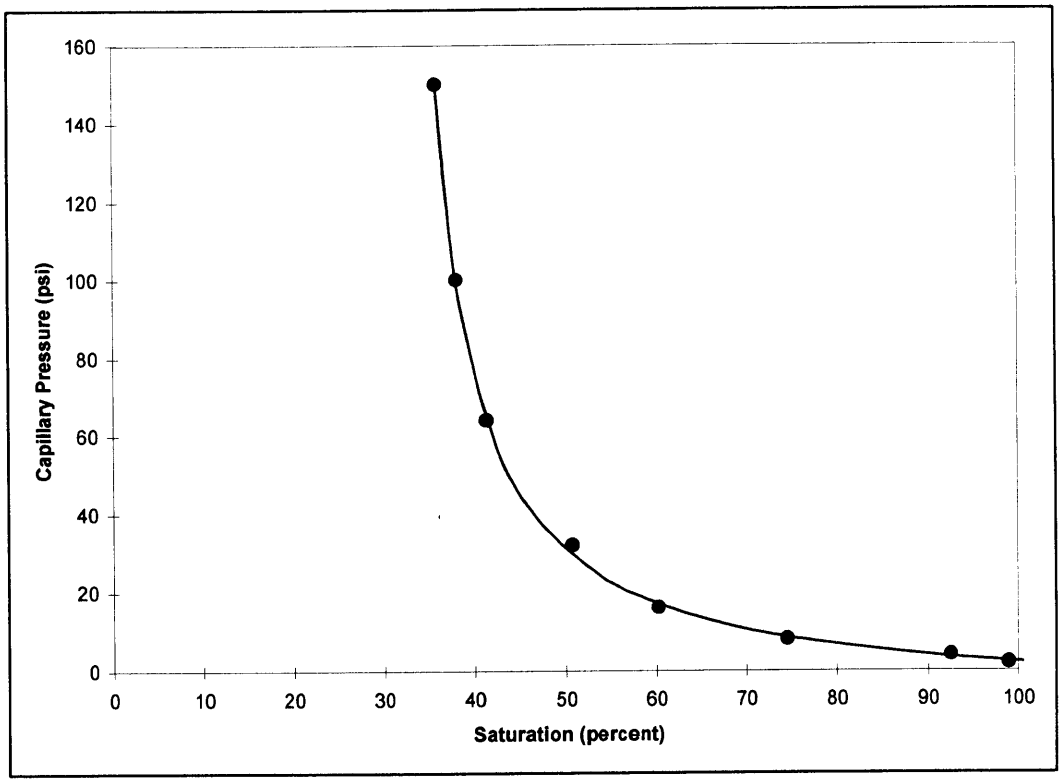

9030080 281

CAPILLARY PRESSURE
Overburden

Client	OMV Australia Pty Ltd	**Air Permeability**	313 milliDarcy's
Well	Baleen-2	**Porosity**	35.8 percent
Sample	S9		
Depth	754.41 metres		
Test Method	Air/Brine Porous Plate @ Overburden		
Overburden	1040 psi		

Capillary Pressure (psi)	Brine Saturation (percent)
2.0	98.7
4.0	67.4
8.0	54.9
16	42.3
32	34.8
64	31.3
100	28.8
150	27.3

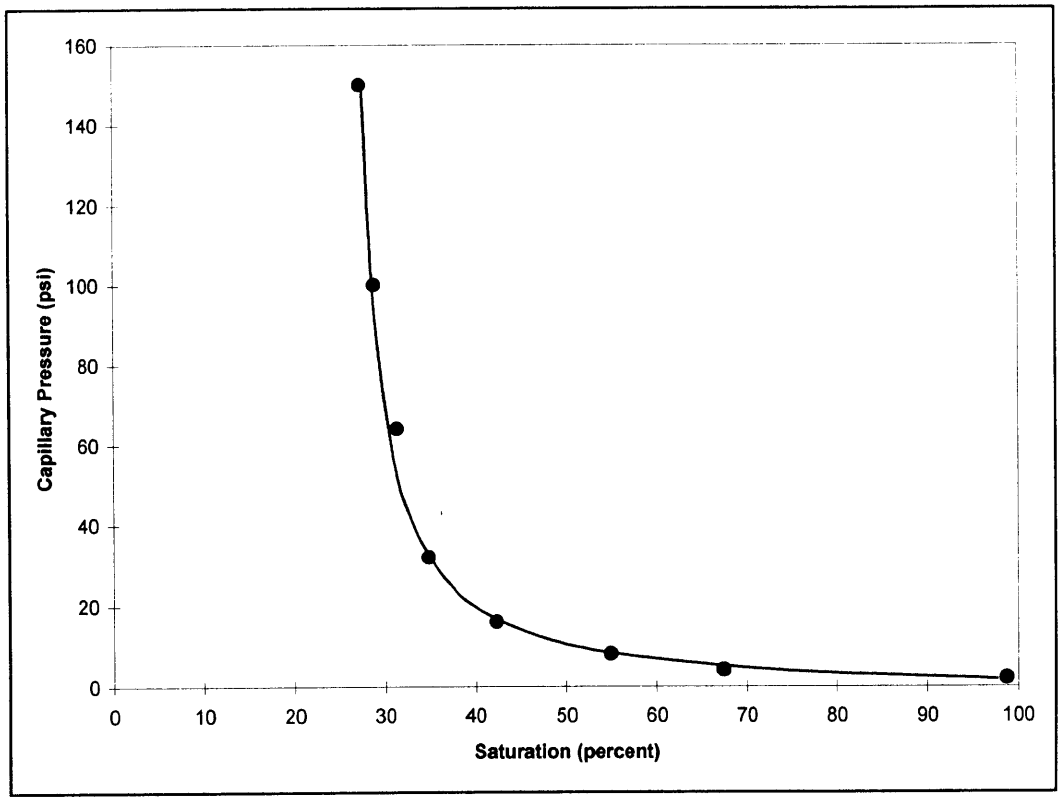

9030080 282

CAPILLARY PRESSURE
Overburden

Client	OMV Australia Pty Ltd	**Air Permeability**	240 milliDarcy's
Well	Baleen-2	**Porosity**	33.1 percent
Sample	S10		
Depth	755.39 metres		
Test Method	Air/Brine Porous Plate @ Overburden		
Overburden	1040 psi		

Capillary Pressure (psi)	Brine Saturation (percent)
2.0	99.2
4.0	69.9
8.0	56.3
16	45.1
32	36.8
64	32.3
100	30.8
150	30.0

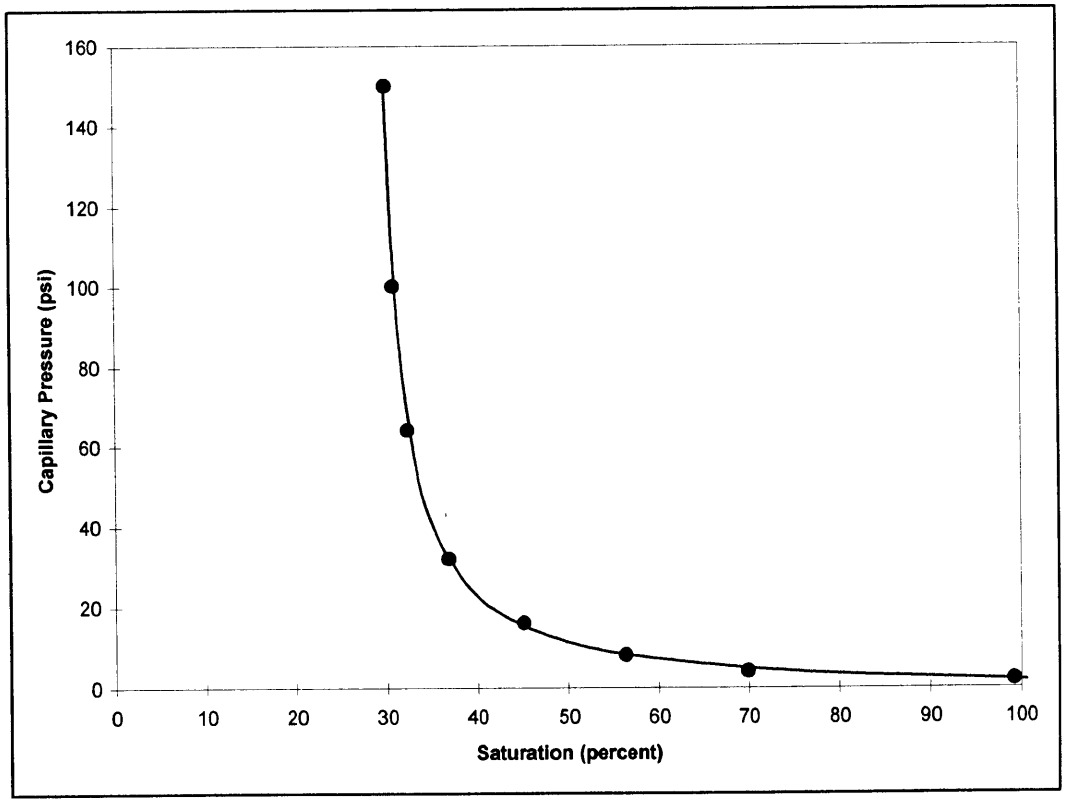

CAPILLARY PRESSURE
Overburden

Client	OMV Australia Pty Ltd	**Air Permeability**	30 milliDarcy's
Well	Baleen-2	**Porosity**	23.3 percent
Sample	S20		
Depth	767.87 metres		
Test Method	Air/Brine Porous Plate @ Overburden		
Overburden	1040 psi		

Capillary Pressure (psi)	Brine Saturation (percent)
2.0	97.1
4.0	89.0
8.0	77.3
16	62.7
32	54.6
64	51.7
100	49.5
150	48.0

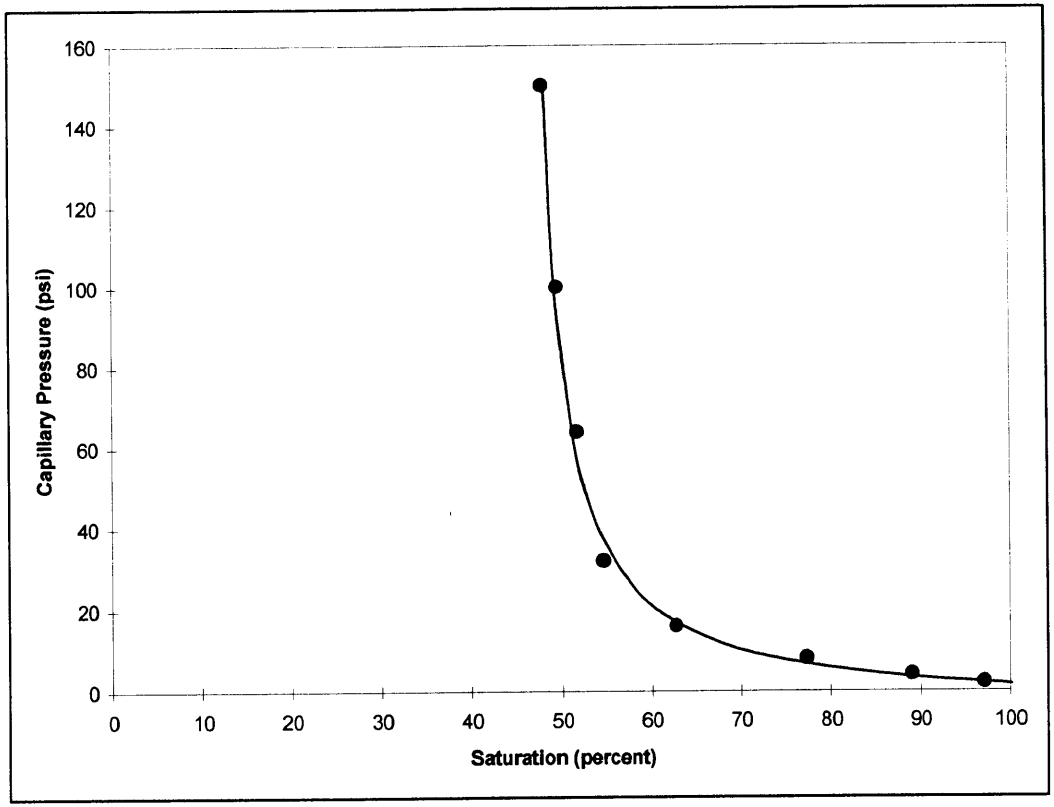

903080 281

CAPILLARY PRESSURE
Overburden

Client	OMV Australia Pty Ltd	**Air Permeability**	79 milliDarcy's
Well	Baleen-2	**Porosity**	33.3 percent
Sample	S25		
Depth	772.99 metres		
Test Method	Air/Brine Porous Plate @ Overburden		
Overburden	1040 psi		

Capillary Pressure (psi)	Brine Saturation (percent)
2.0	99.9
4.0	98.4
8.0	76.8
16	54.9
32	46.8
64	41.4
100	39.5
150	38.6

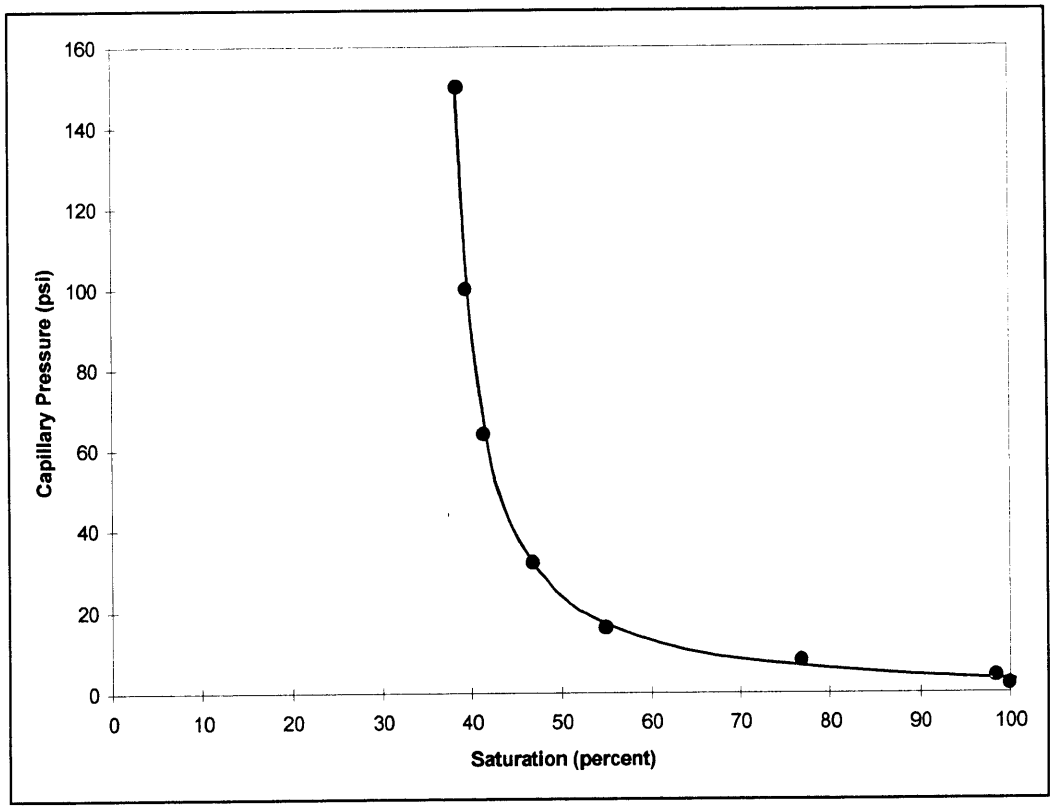

CAPILLARY PRESSURE
Overburden

Client	OMV Australia Pty Ltd	**Air Permeability**	213 milliDarcy's
Well	Baleen-2	**Porosity**	35.3 percent
Sample	S28		
Depth	775.82 metres		
Test Method	Air/Brine Porous Plate @ Overburden		
Overburden	1040 psi		

Capillary Pressure (psi)	Brine Saturation (percent)
2.0	93.8
4.0	65.9
8.0	55.1
16	47.3
32	39.6
64	34.4
100	32.8
150	31.8

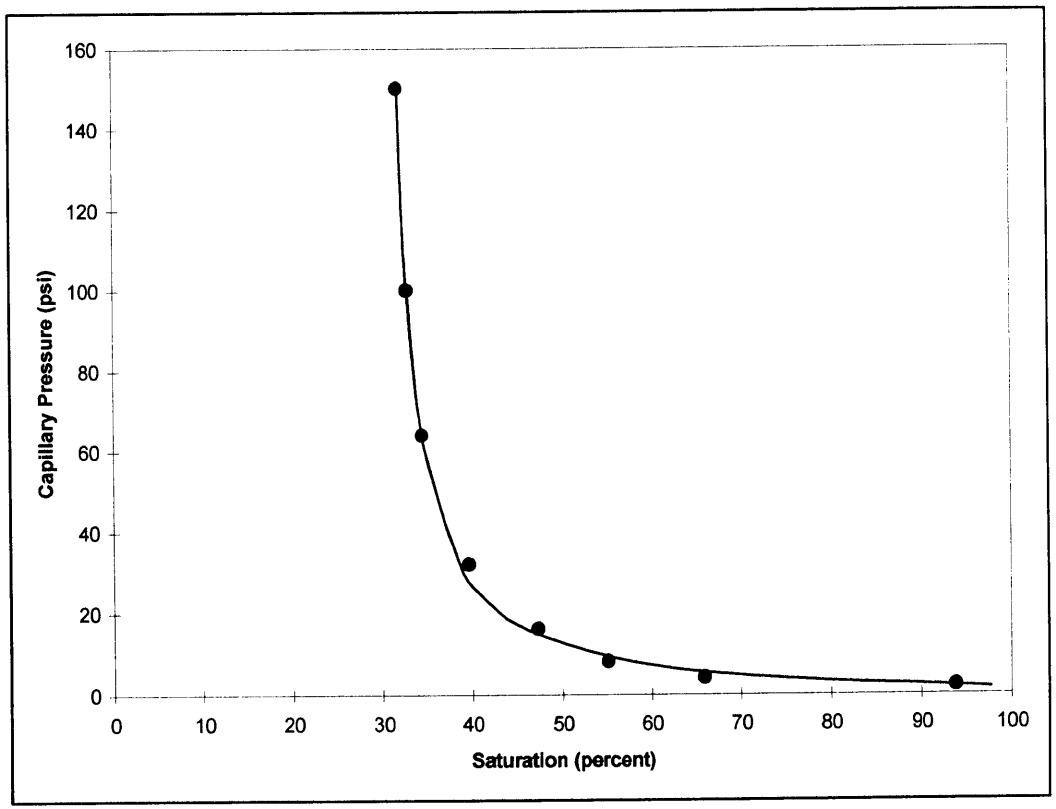

9030080 286

CAPILLARY PRESSURE

Client OMV Australia Pty Ltd
Well Baleen-2

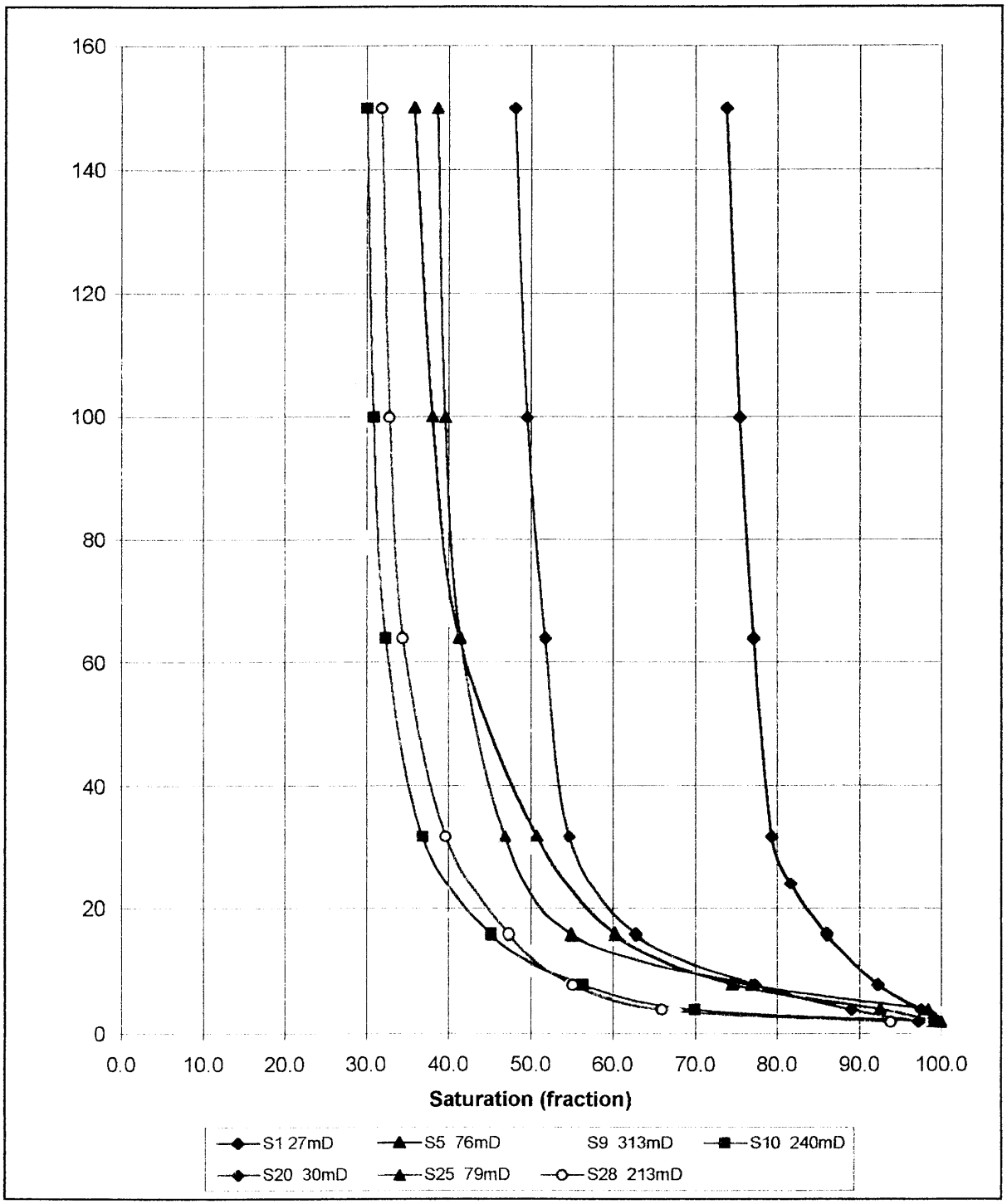

CHAPTER 5

ELECTRICAL PROPERTIES AND CAPILLARY PRESSURE

5.2 Test Results

5.2.5 Cation Exchange Capacity

CATION EXCHANGE CAPACITY

Client OMV Australia Pty Ltd
Well Baleen-2

Sample Number	Depth (metres)	Porosity (percent)	Grain Density (g/cm^3)	Cation Exchange Capacity (meq/100g)		Quantity of Cation Exchangeable Clay Qv (meq/cm^3)	
				Uncrushed	Crushed	Uncrushed	Crushed
S1	746.63	32.7	2.83	5.29	5.46	0.31	0.32
S5	750.41	33.1	2.69	1.99	2.34	0.11	0.13
S9	754.41	36.7	2.68	2.64	2.52	0.12	0.12
S10	755.39	33.6	2.73	1.27	2.54	0.07	0.14
S20	767.87	23.6	2.99	1.77	2.68	0.17	0.26
S23	770.97	30.2	2.68	2.82	3.09	0.17	0.19
S25	772.99	33.9	2.74	2.96	2.86	0.16	0.15
S27	774.80	37.1	2.69	2.60	2.58	0.12	0.12
S28	775.82	36.1	2.68	2.89	2.83	0.14	0.13
S29	776.80	36.7	2.68	2.24	2.21	0.10	0.10

CHAPTER 5

ELECTRICAL PROPERTIES AND CAPILLARY PRESSURE

5.2 Test Results

5.2.6 Summary

FORMATION RESISTIVITY FACTOR

Client OMV Australia Pty Ltd
Well Baleen-2

Saturant Formation Brine
Rw of Saturant 0.826 at 25°C
Overburden 1040 psi

Average m 1.62

Sample Number	Depth (metres)	Permeability to Air (milliDarcy's)	Porosity (percent)	Formation Factor FF	Cementation Exponent m	Saturation Exponent n	Residual Saturation (percent)	Shaley-Sand Equivalent † Formation Factor FF*	Shaley-Sand Equivalent † Cementation Exponent m*	Shaley-Sand Equivalent † Saturation Exponent n*
S1	746.63	27	31.2	7.2	1.72	1.81	73.8	13.3	2.26	1.91
S5	750.41	76	32.1	6.2	1.61	1.72	35.8	8.5	1.89	1.84
S9	754.41	313	35.8	5.6	1.68	1.71	27.3	7.6	1.98	1.86
S10	755.39	240	33.1	6.8	1.73	1.70	30.0	9.7	2.06	1.83
S20	767.87	30	23.3	12.2	1.73	1.74	48.0	20.3	2.08	1.80
S23	770.97	27 *	30.2 *	8.2	1.70			12.9	2.14	
S25	772.99	79	33.3	6.3	1.67	1.90	38.6	9.2	2.02	2.00
S27	774.80	346 *	37.1 *	3.8	1.15			11.0	2.42	
S28	775.82	213	35.3	5.5	1.64	1.73	31.8	7.2	1.94	1.74
S29	776.80	528 *	36.7 *	4.9	1.54			11.1	2.40	

* Ambient Data
† Calculated from Multi-Salinity Analysis

9030080 291

FORMATION RESISTIVITY FACTOR

Client OMV Australia Pty Ltd
Well Baleen-2

Saturant Formation Brine
Rw of Saturant 0.826 at 25°C
Overburden 1040 psi

Average m 1.62

Sample Number	Depth (metres)	Permeability to Air (milliDarcy's)	Porosity (percent)	Formation Factor FF	Cementation Exponent m	Saturation Exponent n	Residual Saturation (percent)	Shaley-Sand Equivalent ‡ Formation Factor FF*	Shaley-Sand Equivalent ‡ Cementation Exponent m*	Shaley-Sand Equivalent ‡ Saturation Exponent n*
S1	746.63	27	31.2	7.2	1.72	1.81	73.8	10.3	2.04	1.81
S5	750.41	76	32.1	6.2	1.61	1.72	35.8	7.2	1.75	1.72
S9	754.41	313	35.8	5.6	1.68	1.71	27.3	6.6	1.84	1.71
S10	755.39	240	33.1	6.8	1.73	1.70	30.0	7.5	1.82	1.70
S20	767.87	30	23.3	12.2	1.73	1.74	48.0	15.0	1.87	1.74
S23	770.97	27 *	30.2 *	8.2	1.70			10.2	1.87	
S25	772.99	79	33.3	6.3	1.67	1.90	38.6	7.7	1.85	1.90
S27	774.80	346 *	37.1 *	3.8	1.15			4.7	1.33	
S28	775.82	213	35.3	5.5	1.64	1.73	31.8	6.6	1.82	1.78
S29	776.80	528 *	36.7 *	4.9	1.54			5.6	1.67	

* Ambient Data
‡ Calculated from Cation Exchange Capacity

9030080 2927

CHAPTER 6

POST-TESTING BASE PARAMETERS

6.1 Test and Calculation Procedures

6. POST-TESTING BASE PARAMETERS

6.1 Test and Calculation Procedures

6.1.1 Sample Preparation

On completion of all preceding analysis each sample was cleaned in a modified soxhlet system until tests for salt (silver nitrate precipitation) showed negative. The clean samples were then dried to constant weight in a humidity oven at 60°C and 40% relative humidity. Once dry, the samples were cooled to room temperature in an airtight chamber.

6.1.2 Porosity

Porosity was determined in two stages. Initially each sample was placed in a sealed matrix cup. Helium held at 100 psi reference pressure was then introduced to the cup. From the resultant pressure drop the unknown grain volume was determined from Boyle's Law.

$$P_1 V_1 = P_2 V_2$$
$$\Rightarrow P_1 Vr = P_2 (Vr + Vc + Vl - Vg)$$

where

	P_1	=	*initial pressure (psig)*
	Vr	=	*reference cell volume (cm^3)*
	Vc	=	*matrix cup volume (cm^3)*
	Vl	=	*line volume (cm^3)*
	Vg	=	*grain volume (cm^3)*
	P_2	=	*final pressure (psig)*

and

$$\rho = \frac{Wt}{Vg}$$

where

	ρ	=	*grain density (g/cm^3)*
	Wt	=	*weight of sample (g)*
	Vg	=	*grain volume (cm^3)*

The samples were then placed into individual thick walled rubber sleeves and the assembly loaded into a hydrostatic cell. With an ambient pressure (400 psi) applied to the sample, helium held at 100 psi reference pressure was released into the samples pore volume. The resultant pressure drop was used to determine pore volume at ambient. The confining pressure was then increased to the overburden pressure of 1040 psi and the resultant change in internal pore pressure was monitored and used to determine pore volume at overburden conditions.

$$Vb = Vp + Vg$$

$$Ambient\ Porosity\ \% = \frac{Vp}{Vb} x\ 100$$

$$Overburden\ Porosity\ \% = \frac{Vp - \Delta Vp}{Vb - \Delta Vp} x\ 100$$

where
Vp = *ambient pore volume (cm^3)*
Vb = *ambient bulk volume (cm^3)*
Vg = *grain volume (cm^3)*
ΔVp = *change in pore volume (cm^3)*

6.1.3 Permeability to air

The permeability of each sample was determined on completion of the porosity measurement. The confining pressure of 400 psi was used to prevent bypassing of air around the sample when the measurement was made. In order to determine permeability a known air pressure was applied to the upstream face of each sample, creating a flow of air through the core plug. Air permeability for each core sample was calculated using Darcy's Law through knowledge of the upstream pressure, flow rate, viscosity of air and sample dimensions.

$$Ka = \frac{2000.BP.\mu.q.L}{(P_1^2 - P_2^2).A}$$

where
Ka = *air permeability (milliDarcy's)*
BP = *barometric pressure (atmospheres)*
μ = *gas viscosity (cP)*
q = *flow rate (cm^3/s)*
L = *sample length (cm)*
P_1 = *upstream pressure (atmospheres)*
P_2 = *downstream pressure (atmospheres)*
A = *sample cross sectional area (cm^2)*

The confining pressure was then increased to the overburden pressure of 1040 psi and the above procedure repeated to give permeability at overburden conditions.

6.1.4 Klinkenberg Permeability

The Klinkenberg permeability of the samples was determined after the overburden permeability. With the sample still under overburden conditions, a known upstream pressure of oxygen free nitrogen (measured by an electronic transducer) was introduced to the sample. A back pressure regulator placed at the core outlet created an elevated differential pressure within the core. The differential pressure, monitored by a transducer, was adjusted to a pressure at which laminar flow occurred. When the flow of gas through the sample was stable, a reading was taken with flow meters connected to the gas outflow line. Several readings were made for each sample, successively increasing the upstream pressure while maintaining a constant differential pressure. All flow rates were sufficiently low to maintain laminar flow.

Klinkenberg permeability was calculated through knowledge of the upstream pressure, differential pressure, flow rate and the samples dimensions. The resulting data was then plotted and the line of best fit (of the form $y = mx + c$) was used to calculate Klinkenberg permeability at zero inverse mean pressure.

y	=	*gas permeability*
x	=	*inverse mean pressure*
m	=	bKl
c	=	Kl

CHAPTER 6

POST-TESTING BASE PARAMETERS

6.2 Test Results

POROSITY and AIR PERMEABILITY

Client OMV Australia Pty Ltd

Well Baleen-2

Sample Number	Depth (metres)	Pre-Testing Ambient Permeability to Air (milliDarcy's)	Pre-Testing Ambient Porosity (percent)	Post-Testing Ambient Permeability to Air (milliDarcy's)	Post-Testing Ambient Porosity (percent)	Post-Testing Overburden 1040 psi Permeability to Air (milliDarcy's)	Post-Testing Overburden 1040 psi Klinkenberg Permeability (milliDarcy's)	Post-Testing Overburden 1040 psi Porosity (percent)	Grain Density (g/cm^3)
S1	746.63	81	32.7	39	31.8	27	22	31.2	2.83
S2	747.41	74	32.8	53	32.3	42	33	31.5	2.71
S5	750.41	131	33.1	85	32.6	76	63	32.1	2.69
S6	751.42	127	33.5	111	32.9	84	69	31.4	2.68
S8	753.42	735	38.3						2.68
S9	754.41	467	36.7	342	36.4	313	280	35.8	2.68
S10	755.39	272	33.6	256	33.5	240	215	33.1	2.73
S11	756.40	238	35.2	160	34.5	149	128	33.9	2.68
S12	757.42	337	36.1	306	35.5	268	224	34.8	2.68
S20	767.87	46	23.6	32	23.6	30	25	23.3	2.99

9003080 298

POROSITY and AIR PERMEABILITY (cont.)

Sample Number	Depth (metres)	Pre-Testing Ambient Permeability to Air (milliDarcy's)	Pre-Testing Ambient Porosity (percent)	Post-Testing Ambient Permeability to Air (milliDarcy's)	Post-Testing Ambient Porosity (percent)	Post-Testing Overburden 1040 psi Permeability to Air (milliDarcy's)	Post-Testing Overburden 1040 psi Klinkenberg Permeability (milliDarcy's)	Post-Testing Overburden 1040 psi Porosity (percent)	Grain Density (g/cm^3)
S21	768.79	33	31.3	26	30.6	22	17	29.9	2.69
S23	770.97	27	30.2						2.68
S24	771.81	82	32.8	74	32.6	61	45	32.0	2.71
S25	772.99	112	33.9	91	33.8	79	64	33.3	2.74
S26	773.79	119	35.6	99	34.9	86	73	34.2	2.71
S27	774.80	346	37.1						2.69
S28	775.82	396	36.1	240	35.9	213	176	35.3	2.68
S29	776.80	528	36.7						2.68
S30	777.80	563	35.6	516	34.9	493	462	34.5	2.72

PORE VOLUME REDUCTION

Client OMV Australia Pty Ltd

Well Baleen-2

		Pre-Testing		Post-Testing					
		Ambient		Ambient			Overburden 1040 psi		
Sample Number	Depth (metres)	Porosity (percent)	Pore Volume (cm^3)	Porosity (percent)	Pore Volume (cm^3)	Pore Volume Reduction (cm^3)	Porosity (percent)	Pore Volume (cm^3)	Grain Density (g/cm^3)
S1	746.63	32.7	18.40	31.8	17.89	0.51	31.2	17.56	2.83
S2	747.41	32.8	18.34	32.3	18.06	0.28	31.5	17.62	2.71
S5	750.41	33.1	18.50	32.6	18.22	0.28	32.1	17.94	2.69
S6	751.42	33.5	18.21	32.9	17.89	0.32	31.4	17.07	2.68
S8	753.42	38.3	16.99						2.68
S9	754.41	36.7	20.41	36.4	20.24	0.17	35.8	19.91	2.68
S10	755.39	33.6	13.51	33.5	13.47	0.04	33.1	13.31	2.73
S11	756.40	35.2	19.23	34.5	18.85	0.38	33.9	18.52	2.68
S12	757.42	36.1	20.05	35.5	19.72	0.33	34.8	19.33	2.68
S20	767.87	23.6	13.74	23.6	13.72	0.02	23.3	13.57	2.99

PORE VOLUME REDUCTION (cont)

		Pre-Testing		Post-Testing					
		Ambient		Ambient			Overburden 1040 psi		
Sample Number	Depth (metres)	Porosity (percent)	Pore Volume (cm^3)	Porosity (percent)	Pore Volume (cm^3)	Pore Volume Reduction (cm^3)	Porosity (percent)	Pore Volume (cm^3)	Grain Density (g/cm^3)
S21	768.79	31.3	17.38	30.6	16.99	0.39	29.9	16.60	2.69
S23	770.97	30.2	16.45						2.68
S24	771.81	32.8	18.43	32.6	18.32	0.11	32.0	17.98	2.71
S25	772.99	33.9	16.30	33.8	16.26	0.04	33.3	16.02	2.74
S26	773.79	35.6	13.04	34.9	12.79	0.25	34.2	12.53	2.71
S27	774.80	37.1	20.20						2.69
S28	775.82	36.1	19.83	35.9	19.72	0.11	35.3	19.39	2.68
S29	776.80	36.7	19.94						2.68
S30	777.80	35.6	19.91	34.9	19.52	0.39	34.5	19.29	2.72

CHAPTER 7

PERMEABILITY vs OVERBURDEN STRESS ANALYSIS

7.1 Test and Calculation Procedures

7. PERMEABILITY vs OVERBURDEN STRESS ANALYSIS

7.1 Test and Calculation Procedures

This study was commissioned on completion of the main study to investigate the permeability reduction with respect to increased effective overburden stress. It was performed on five samples from the original SCA sample set that had not been utilized in the main study (ie these samples had not been subjected to overburden stress in the laboratory prior to this study).

The samples were initially cleaned and critical point dried as per the procedures set out in Chapter 3.1.3.

Once dried, permeabilities were measured on each sample at 100 psi overburden stress increments from ambient (200 psi) to 500 psi over the overburden stress used in the main study (1540 psi). The permeabilities were measured as per the procedure set out in Chapter 3.1.4. A stabilized flow rate was obtained at each overburden stress before moving onto the next pressure.

CHAPTER 7

PERMEABILITY vs OVERBURDEN STRESS ANALYSIS

7.2 Test Results

PERMEABILITY vs OVERBURDEN STRESS

Client OMV Australia Pty Ltd
Well Baleen-2

Sample Number	Depth (metres)	Permeability to Air (milliDarcy's) Confining Pressure (psi) 200	300	400	500	600	700	800	900	1040	1140	1240	1340	1440	1540
S4	749.40	105	96.0	87.9	83.2	78.8	76.0	73.4	70.9	68.2	66.6	65.1	63.3	62.2	60.9
S13	758.58	90.5	87.1	83.8	80.5	77.8	75.4	73.2	71.6	69.6	69.6	69.6	65.6	64.4	63.3
S14	759.42	159	149	142	137	134	131	129	126	124	122	120	118	117	115
S17	764.82	302	291	284	278	272	268	264	261	257	255	252	249	247	245
S18	765.76	169	157	149	141	135	130	127	125	122	119	116	114	112	109

PERMEABILITY vs OVERBURDEN STRESS

Client OMV Australia Pty Ltd
Well Baleen-2

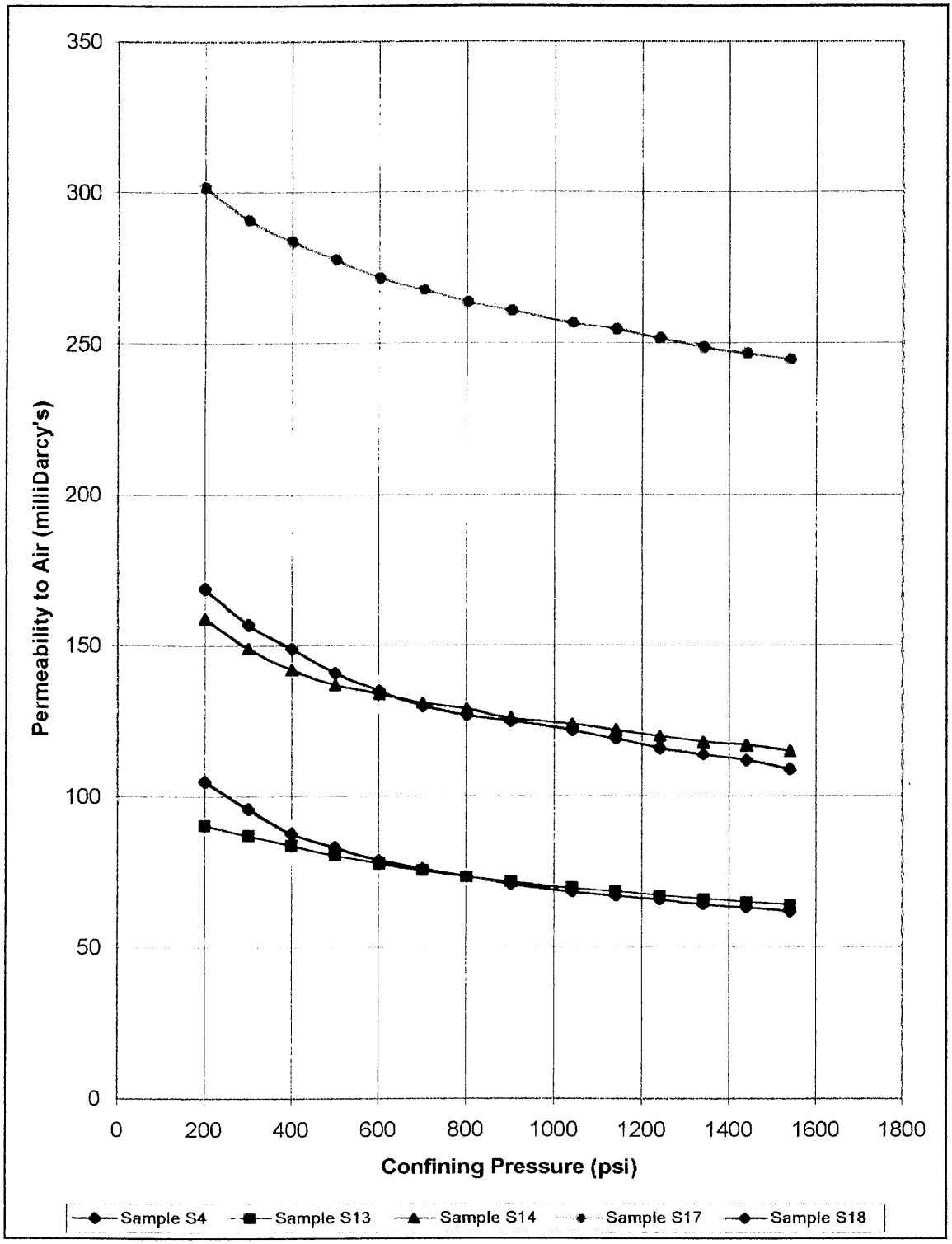

RELATIVE PERMEABILITY vs OVERBURDEN STRESS

Client OMV Australia Pty Ltd
Well Baleen-2

Sample Number	Depth (metres)	Relative Permeability — Confining Pressure (psi)													
		200	300	400	500	600	700	800	900	1040	1140	1240	1340	1440	1540
S4	749.40	1.000	0.913	0.836	0.791	0.749	0.723	0.698	0.674	0.649	0.633	0.619	0.602	0.591	0.579
S13	758.58	1.000	0.962	0.925	0.889	0.860	0.832	0.808	0.791	0.769	0.769	0.769	0.725	0.711	0.699
S14	759.42	1.000	0.938	0.895	0.864	0.845	0.828	0.810	0.796	0.778	0.767	0.756	0.744	0.735	0.727
S17	764.82	1.000	0.965	0.941	0.921	0.903	0.888	0.877	0.867	0.853	0.844	0.834	0.827	0.819	0.812
S18	765.76	1.000	0.928	0.881	0.833	0.803	0.771	0.752	0.743	0.720	0.704	0.690	0.674	0.662	0.648

RELATIVE PERMEABILITY vs OVERBURDEN STRESS

Client OMV Australia Pty Ltd
Well Baleen-2

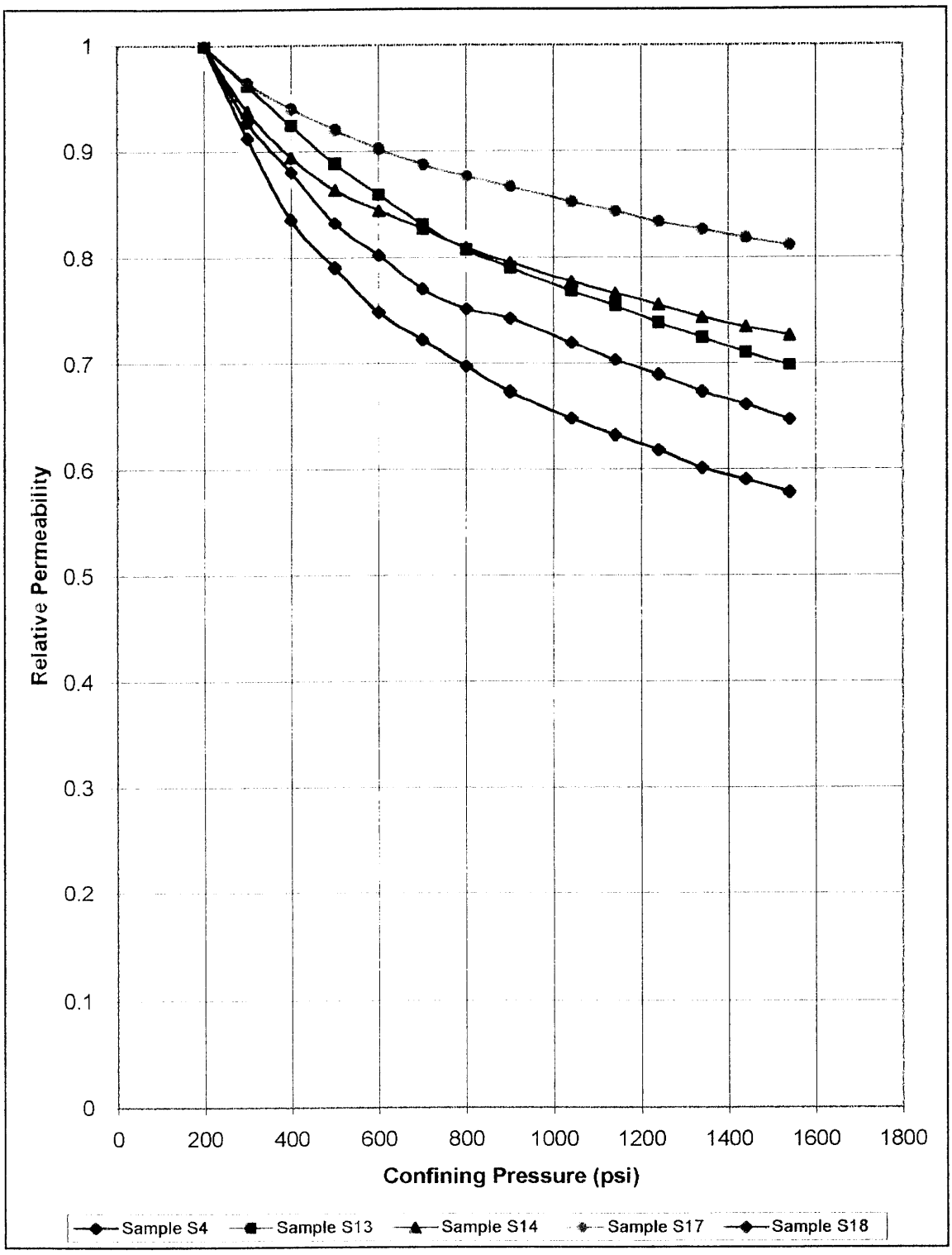

CHAPTER 8

SIEVE ANALYSIS

8.1 Test and Calculation Procedures

8. SIEVE ANALYSIS

8.1 Test and Calculation Procedures

Sieve analysis was performed on the five samples chosen for rock strength testing. They were performed on the sample remaining after the rock strength plugs had been cut from the designated whole core.

The samples were initially extracted and dried as described previously, and crushed, using a mortar and pestle, to grain size.

The entire sample was accurately weighed and then poured into the top sieve of a nest of six sieves, plus pan. Sieve sizes were selected so as to best represent the grain size distribution within the samples.

The nest of sieves, plus pan, were shaken for a minimum of twenty minutes or until the weights of each individual sieve had stabilized.

On completion, each sieve was unloaded and brushed thoroughly to remove all sand grains. A weight of sand retained on each of the sieves and pan was determined. Weight retained by each sieve was calculated as a percentage of the initial total weight.

CHAPTER 8

SIEVE ANALYSIS

8.2 Test Results

SIEVE ANALYSIS

Client OMV Australia Pty Ltd
Well Baleen-2
Sample 1
Depth 750.82m - 751.17m

Sieve Size (µm)	Incremental Weight (%)	Cumulative Weight (%)
250	0.1	0.1
180	0.6	0.7
125	15.4	16.1
75	51.7	67.8
53	21.8	89.7
PAN	10.3	100.0

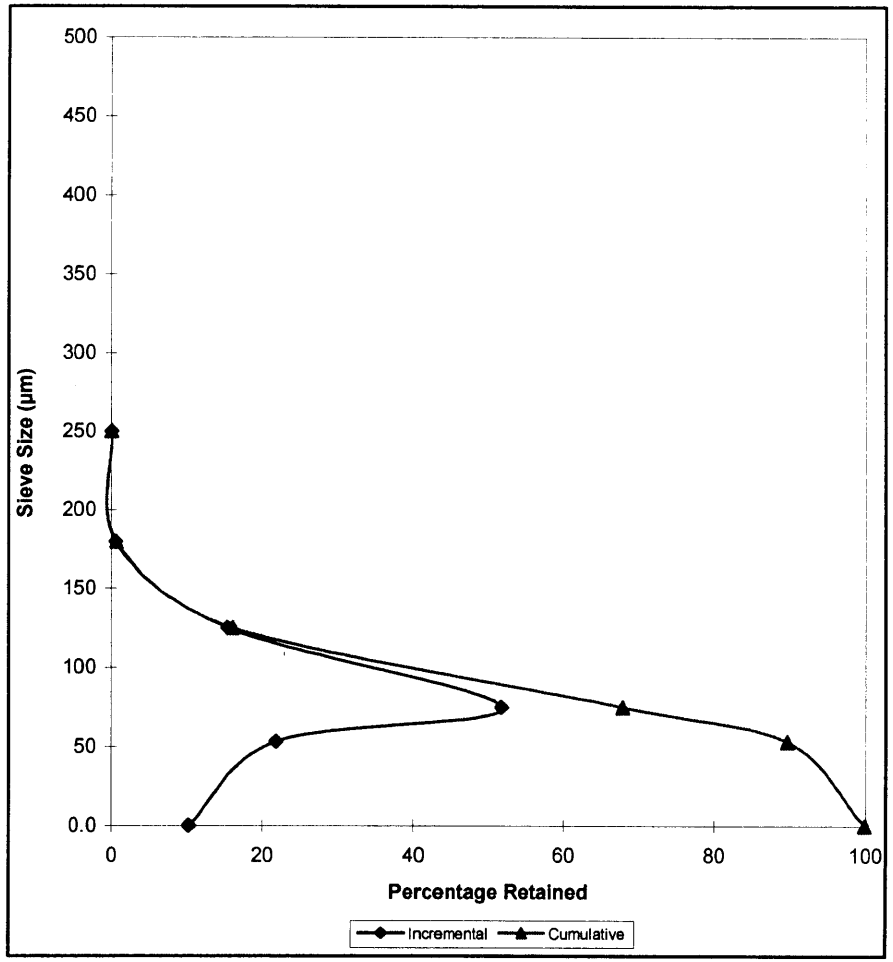

9030080 312

SIEVE ANALYSIS

Client OMV Australia Pty Ltd
Well Baleen-2
Sample 2
Depth 756.50m - 756.80m

Sieve Size (µm)	Incremental Weight (%)	Cumulative Weight (%)
250	0.0	0.0
180	0.6	0.6
125	21.1	21.7
75	57.3	79.0
53	10.7	89.7
PAN	10.3	100.0

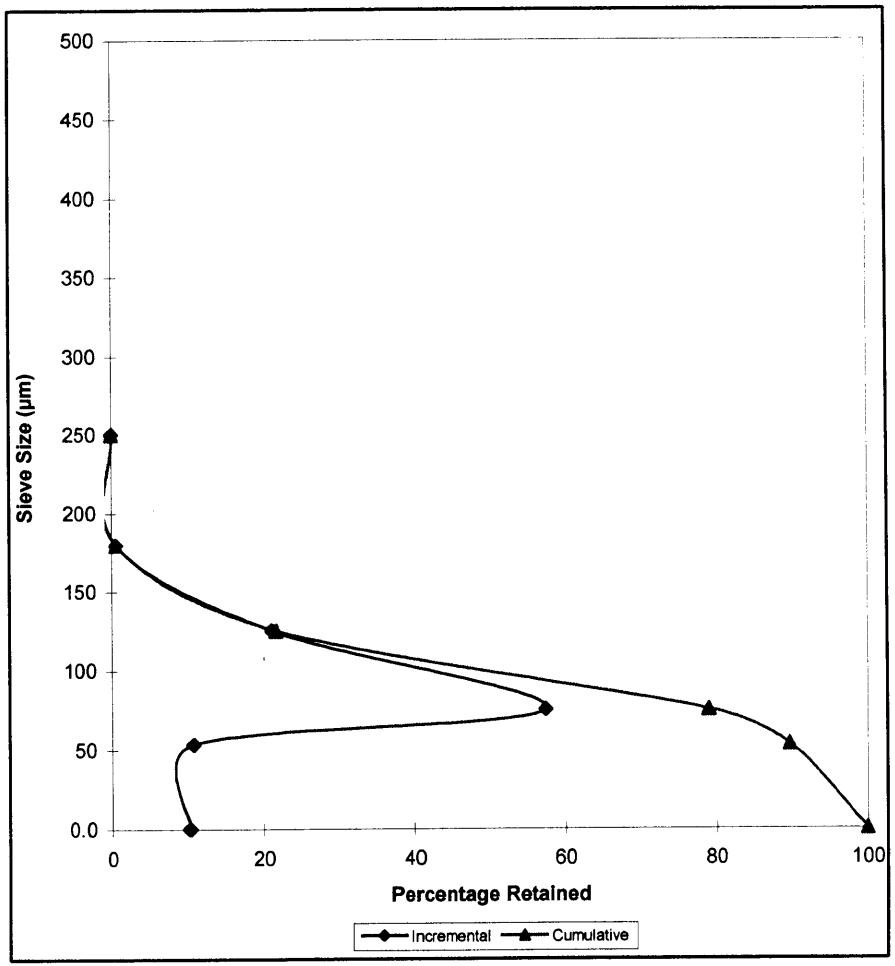

SIEVE ANALYSIS

Client OMV Australia Pty Ltd
Well Baleen-2
Sample 3
Depth 760.20m - 760.46m

Sieve Size (µm)	Incremental Weight (%)	Cumulative Weight (%)
250	0.0	0.0
180	1.3	1.3
125	19.0	20.4
75	54.1	74.5
53	13.4	88.0
PAN	12.0	100.0

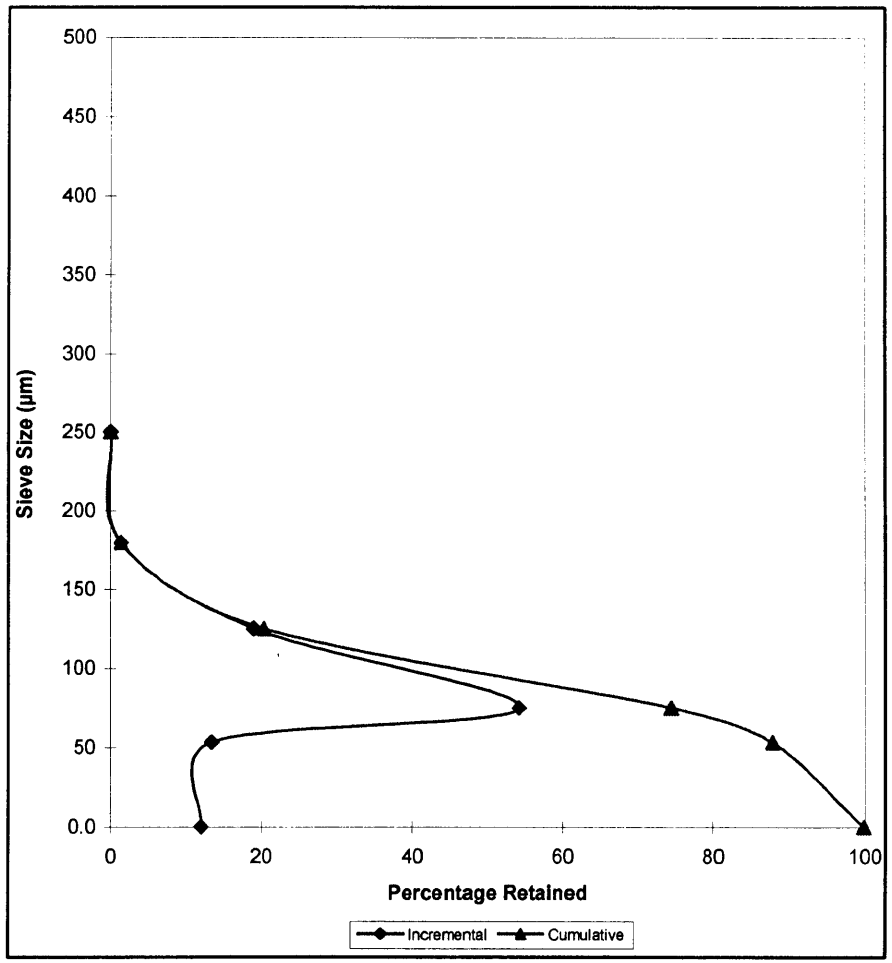

SIEVE ANALYSIS

Client OMV Australia Pty Ltd
Well Baleen-2
Sample 4
Depth 770.88m - 771.28m

Sieve Size (µm)	Incremental Weight (%)	Cumulative Weight (%)
250	0.0	0.0
180	0.1	0.1
125	2.6	2.7
75	40.5	43.3
53	35.7	79.0
PAN	21.0	100.0

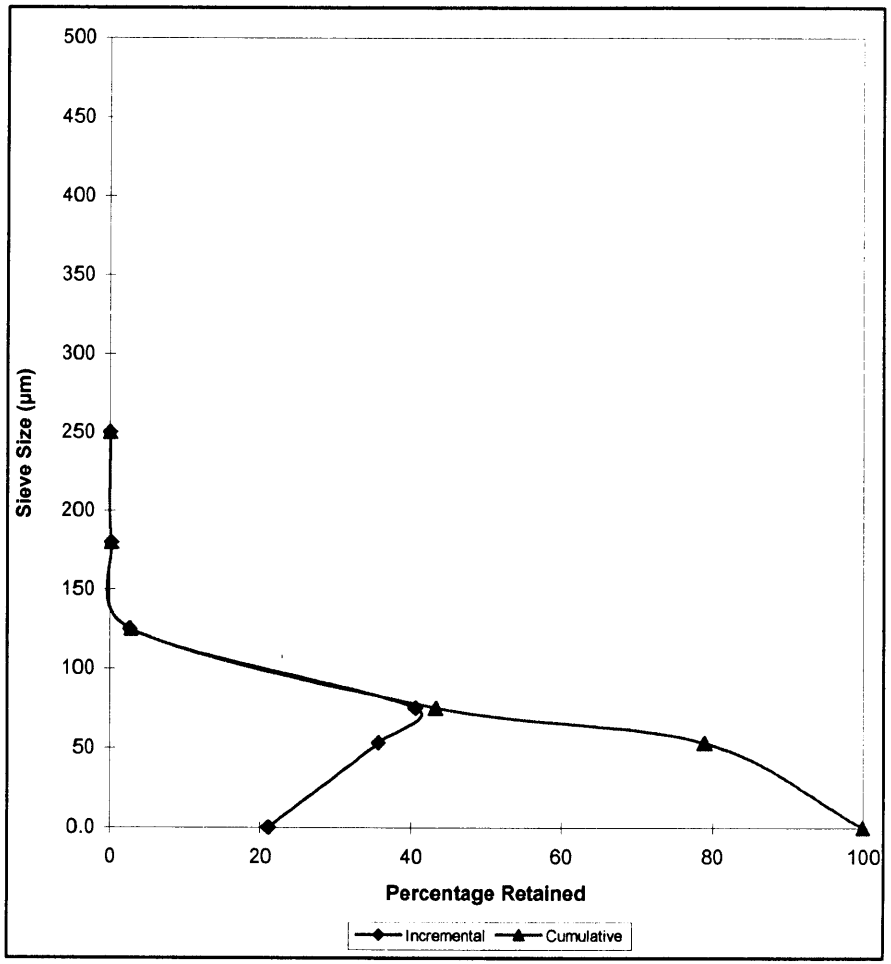

SIEVE ANALYSIS

Client OMV Australia Pty Ltd
Well Baleen-2
Sample 5
Depth 776.69m - 776.90m

Sieve Size (µm)	Incremental Weight (%)	Cumulative Weight (%)
250	0.0	0.0
180	0.3	0.3
125	5.5	5.8
75	67.7	73.6
53	13.1	86.7
PAN	13.3	100.0

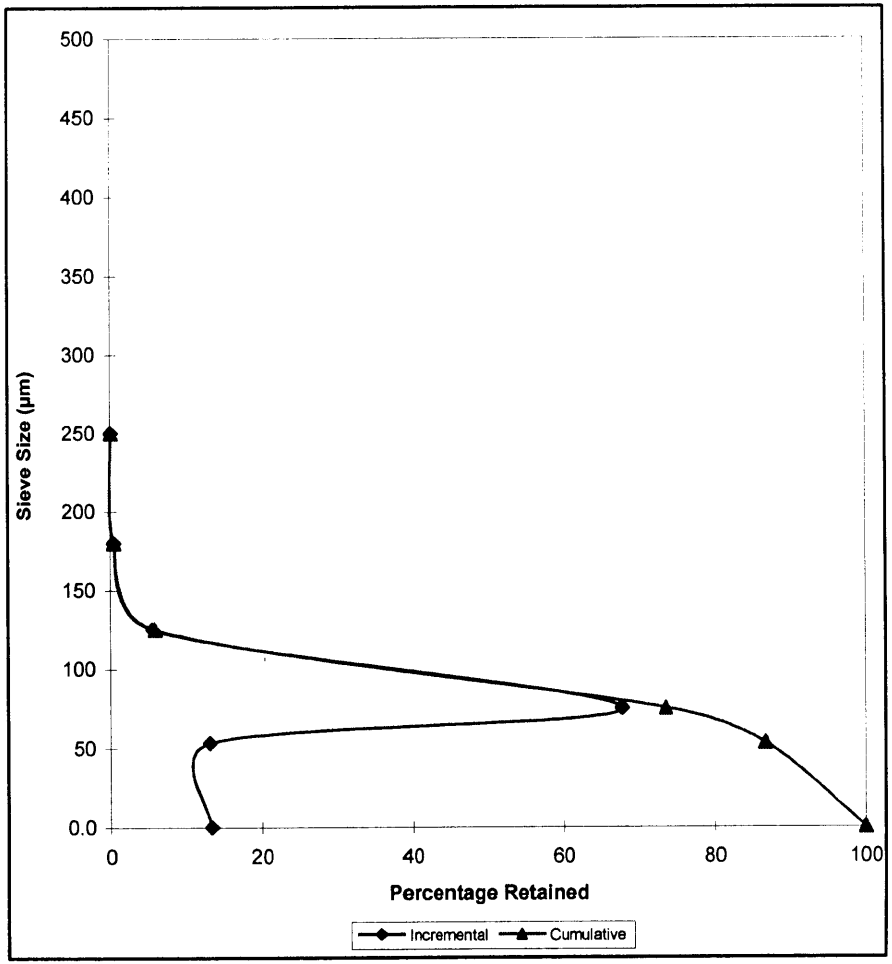

SIEVE ANALYSIS

Client OMV Australia Pty Ltd
Well Baleen-2

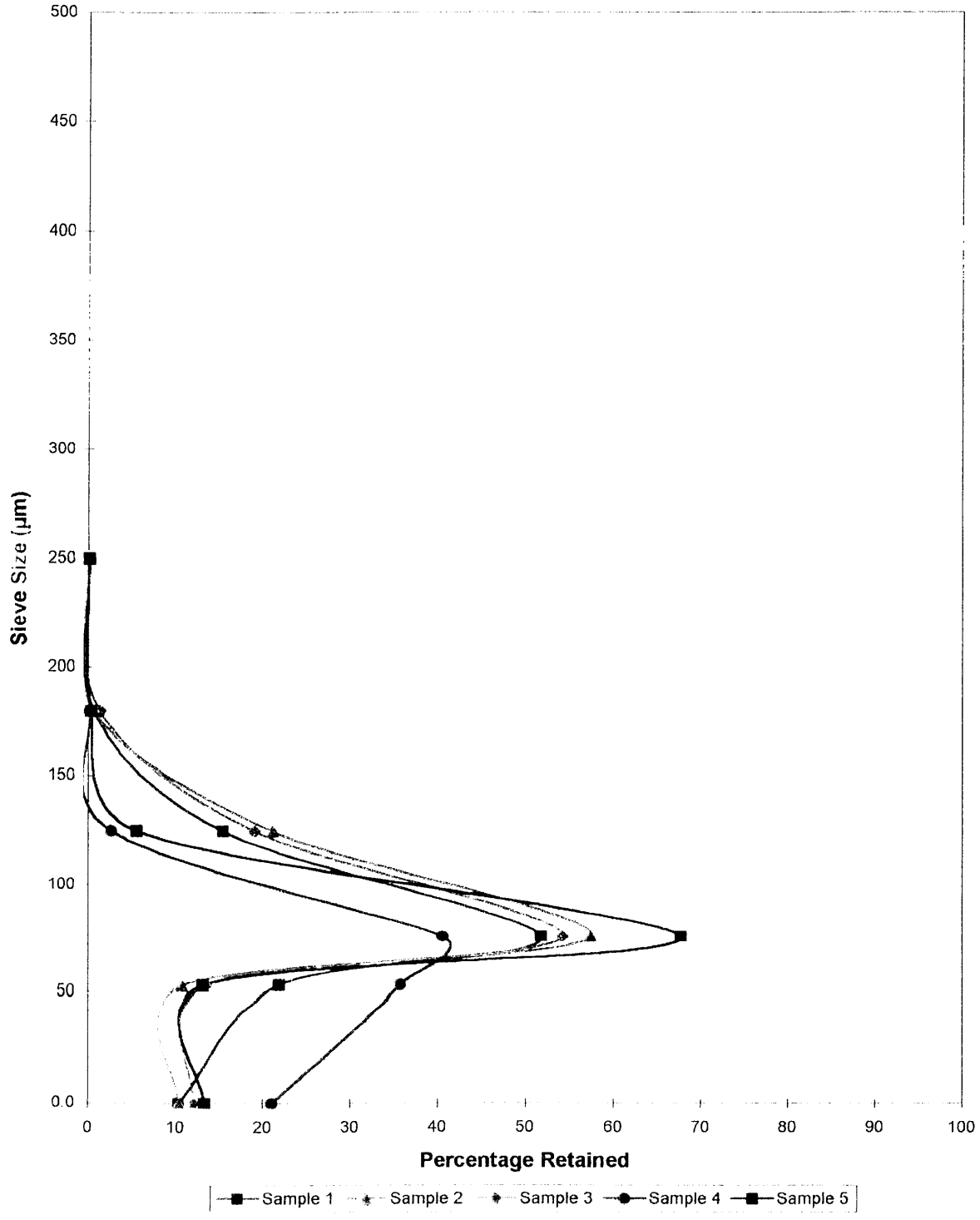

APPENDIX I

EFFECTIVE OVERBURDEN STRESS CALCULATION

EFFECTIVE OVERBURDEN STRESS CALCULATION

Core Depth:	720m – 750m (av. 735m)
Water Depth:	52m
Reservoir Pressure:	1100 psi

Total Vertical OB Stress	=	(52 * 3.281 * 0.45)+((735 - 52) * 1 * 3.281)
	=	2317.7 psi
Minimum Horizontal Stress	=	2317.7 * 0.75
	=	1738.3 psi
Maximum Horizontal Stress	=	2317.7 * 0.875
	=	2028.0 psi
Average Total Stress	=	(2317.7 + 1738.3 + 2028.0) / 3
	=	2028 psi
Laboratory Effective Stress (Nieto Eqn)[1]	=	2028 – (0.9 * 1100)
	=	1038 psi

[1] Nieto, J A, Yale, D P, Evans, R J:"Improved Methods for Correcting Core Porosity to Reservoir Conditions", The Log Analyst, May-June 94, p21-30.

APPENDIX II

FLUID PROPERTIES

FLUID PROPERTIES

Synthetic Formation Brine (composition as supplied)

Cations	mg/L	Anions	mg/L
Sodium	3000	Chloride	4610
Calcium	76	Bicarbonate	618
Magnesium	82	Sulphate	79
Potassium	142	Carbonate	0

Density = 0.999 g/cm^3 @ 25°C
Resistivity = 0.826 ohm.m @ 25°C
Viscosity = 0.956 cP @ 25°C

Multi Salinity Brines

120000 ppm NaCl equivalent
Resistivity = 0.072 ohm.m @ 25°C

50000 ppm NaCl equivalent
Resistivity = 0.141 ohm.m @ 25°C

APPENDIX III

EQUIPMENT SCHEMATICS

PE9080_color076

903080 323

CT SCANNER SCHEMATIC

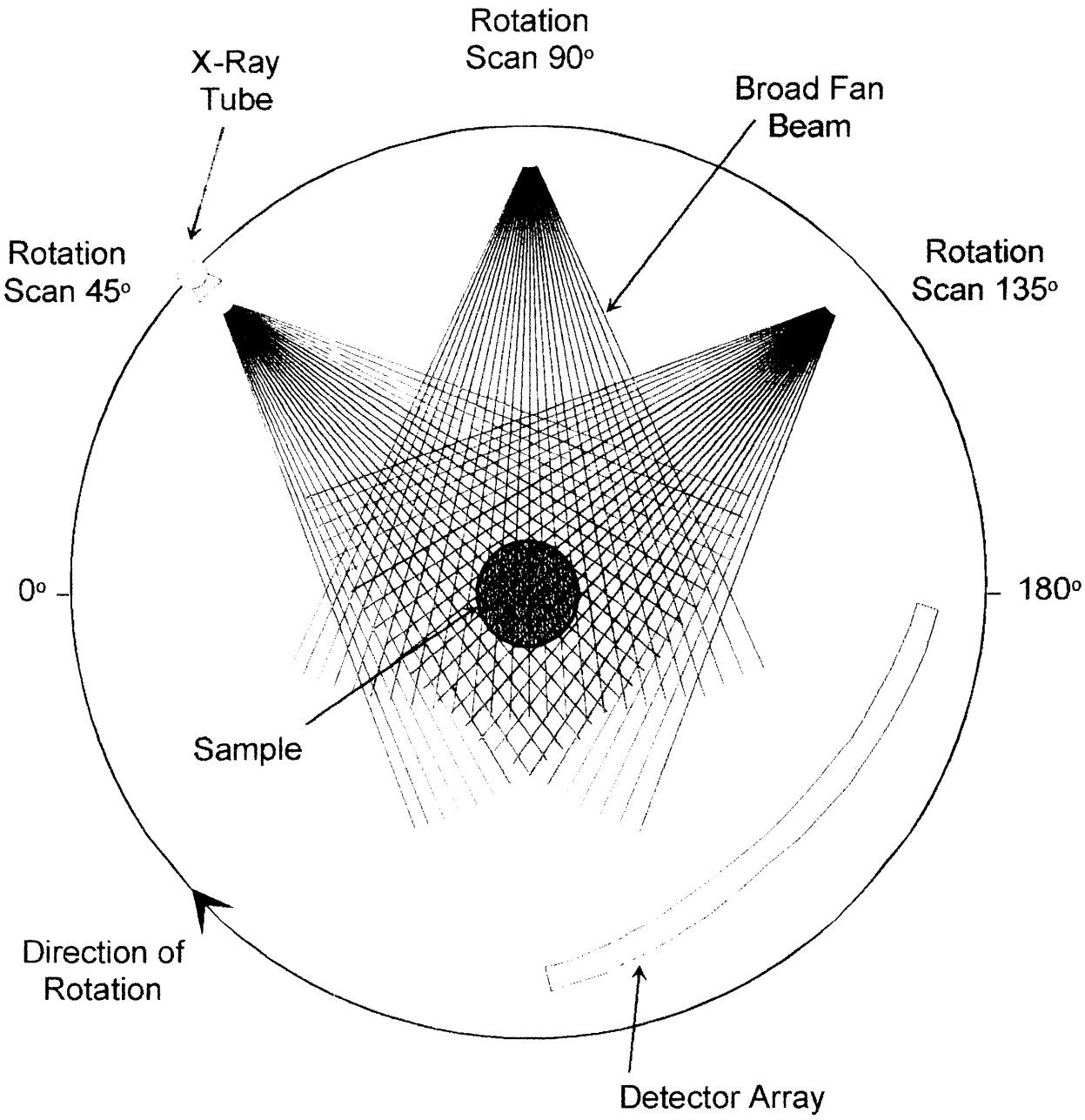

ACS Laboratories Pty Ltd
ABN: 81 008 273 005

PE908pe0_color077

903080 321

SAMPLE SLEEVE SCHEMATIC (Exploded View)

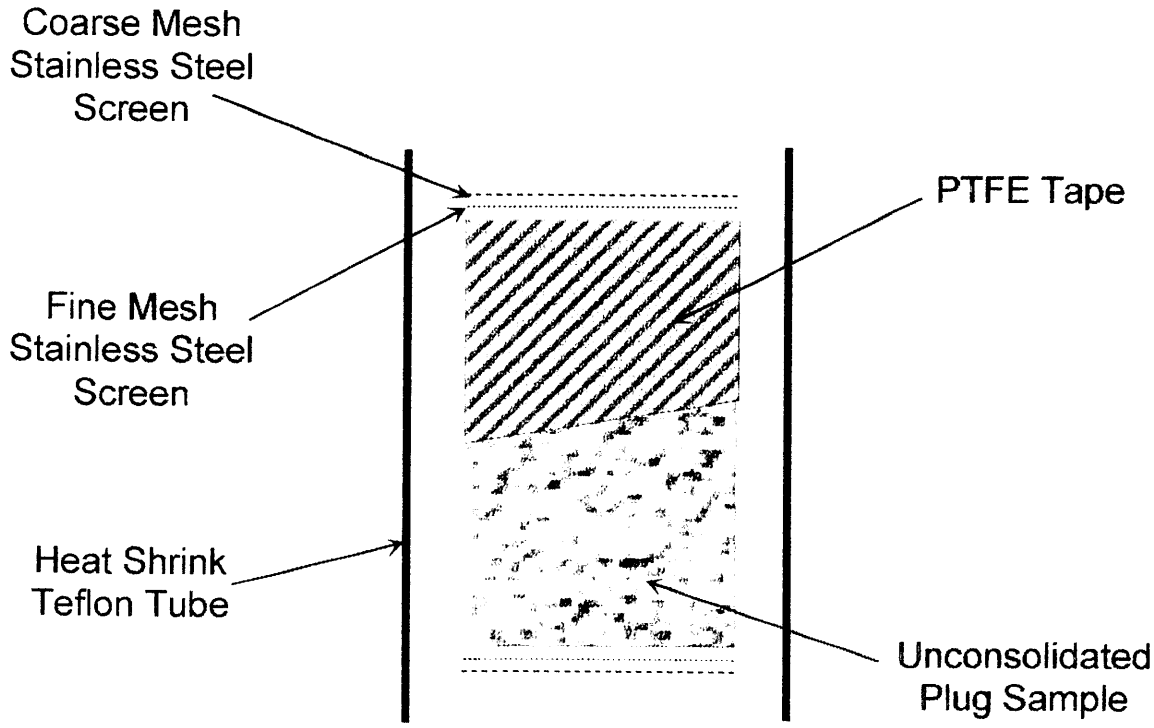

PE9Φ8Φ8Φ - color Φ 78

903080 325

COLD SOLVENT SOXHLET APPARATUS

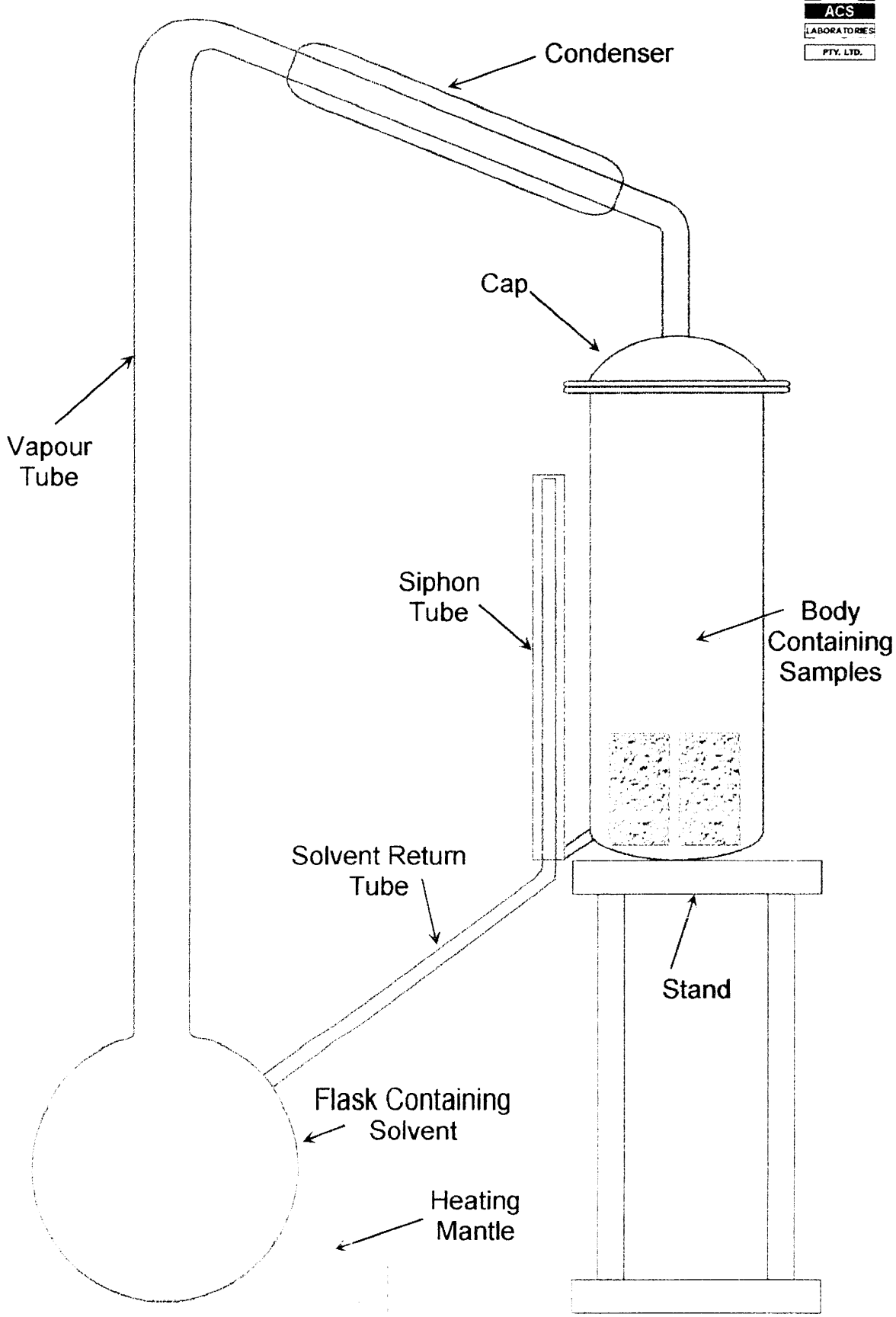

ACS Laboratories Pty Ltd
ABN: 81 008 273 005

PE9ΦEΦE¢ - color ¢79

903080 326

CRITICAL POINT DRYING APPARATUS

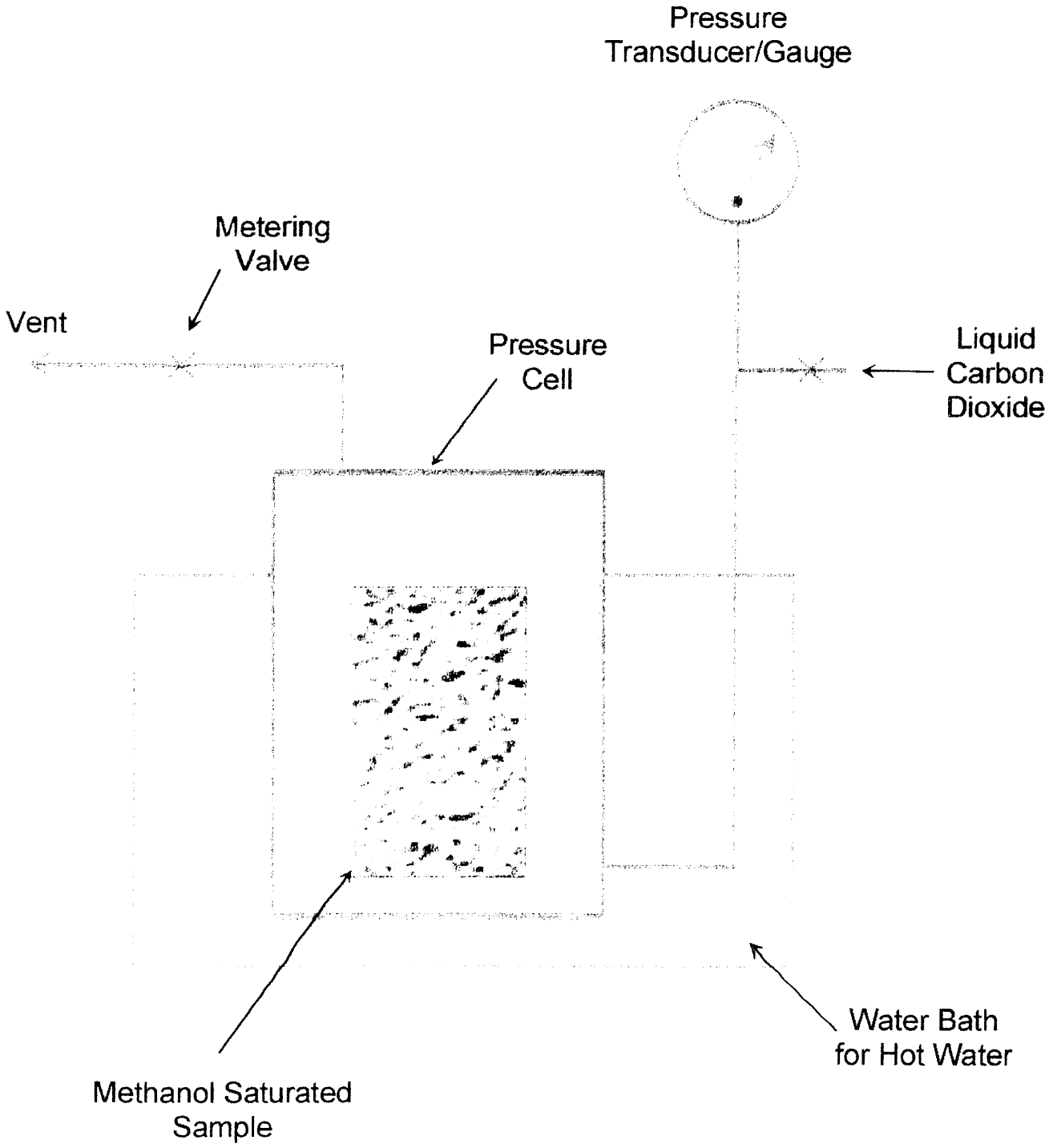

ACS Laboratories Pty Ltd
ABN: 81 008 273 005

POROSIMETER SCHEMATIC

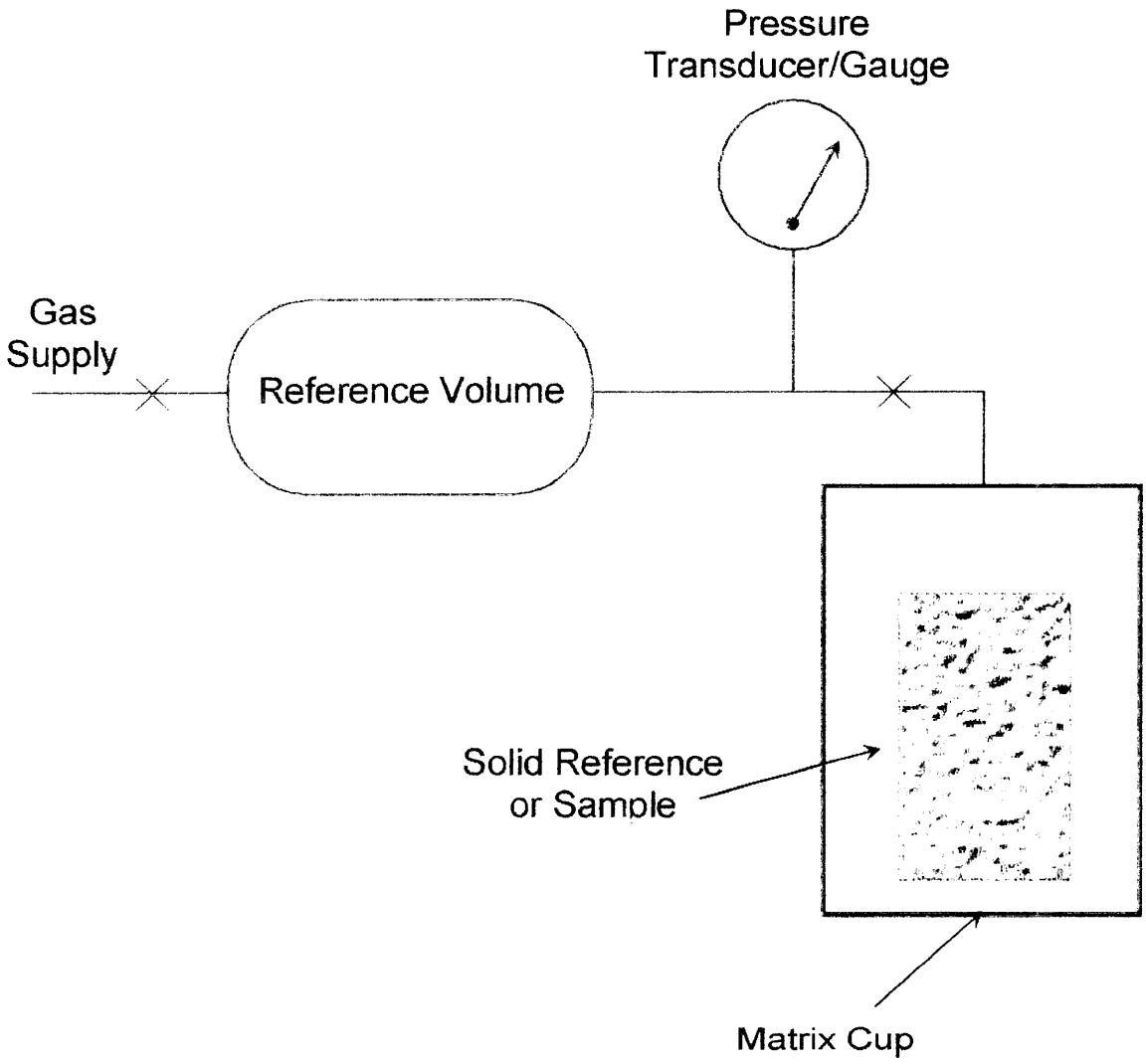

P1.V1 (reference) = P2.V2 (sample)

PE908080_color 81

903080 328

GAS PERMEAMETER SCHEMATIC (Hydrostatic)

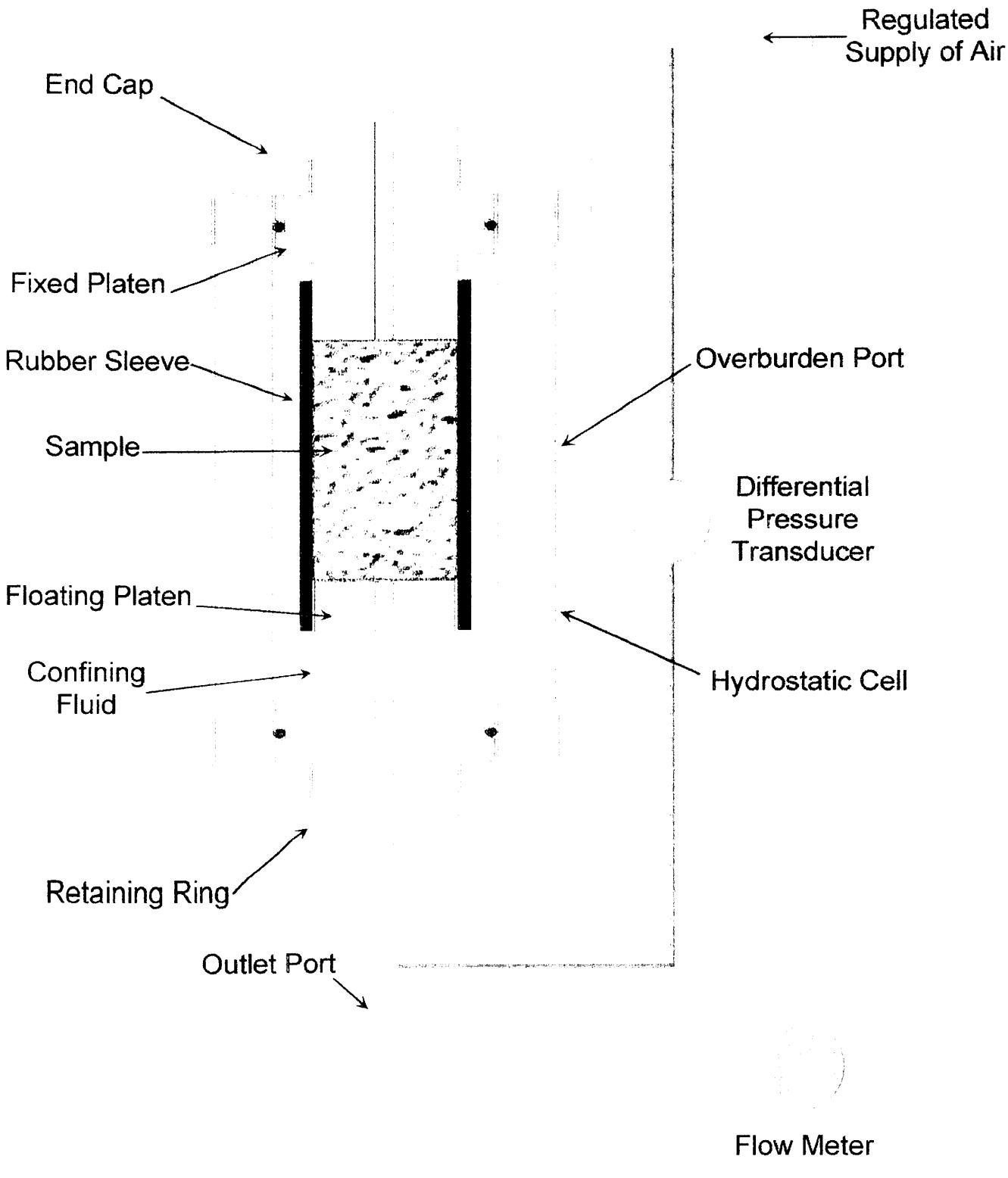

PE900880 - color 082

903080 329

KLINKENBERG PERMEAMETER SCHEMATIC

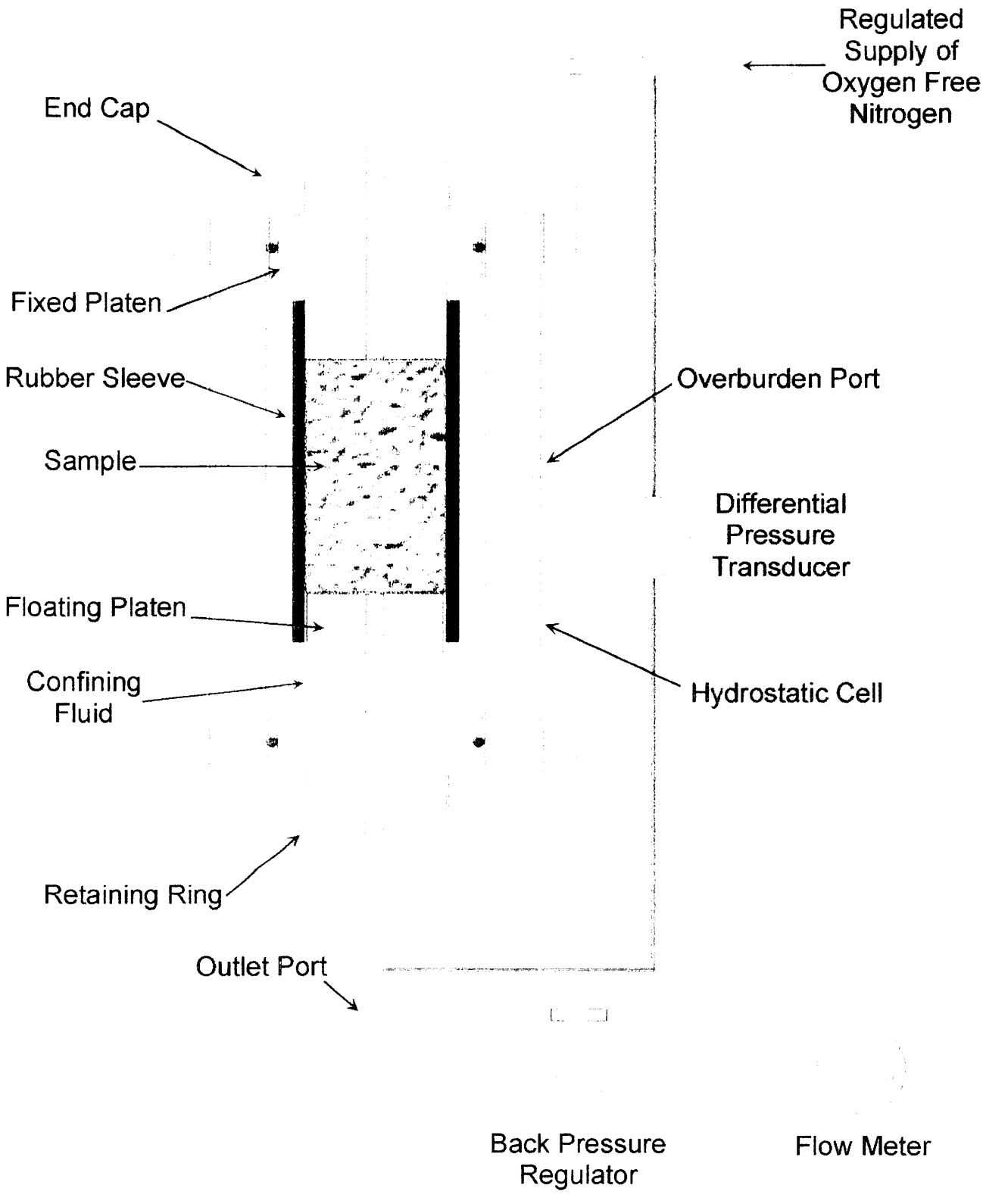

HYDROSTATIC CORE HOLDER

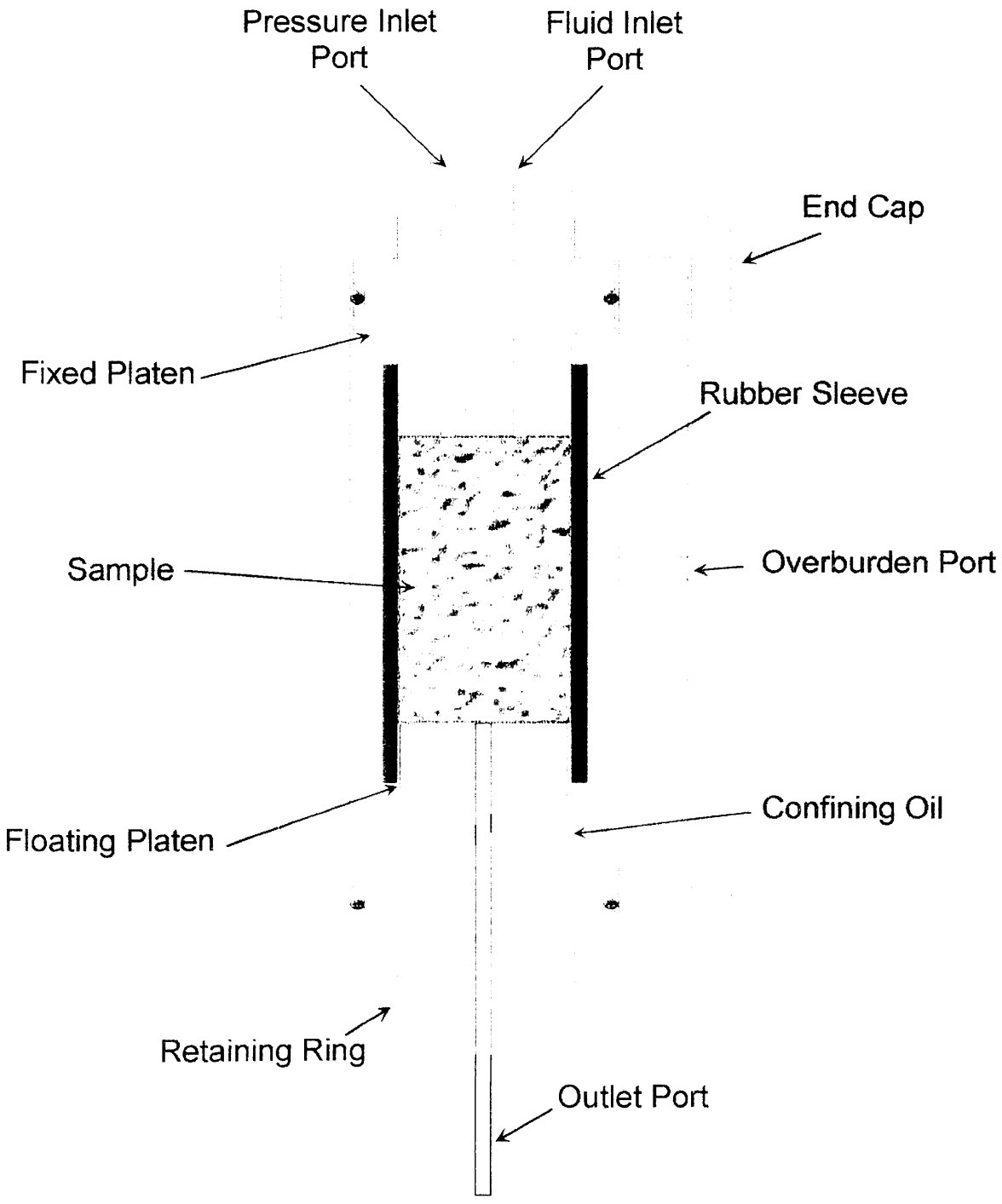

PE900800 - color 84

903080 331

AMBIENT POROUS PLATE CAPILLARY PRESSURE CELL

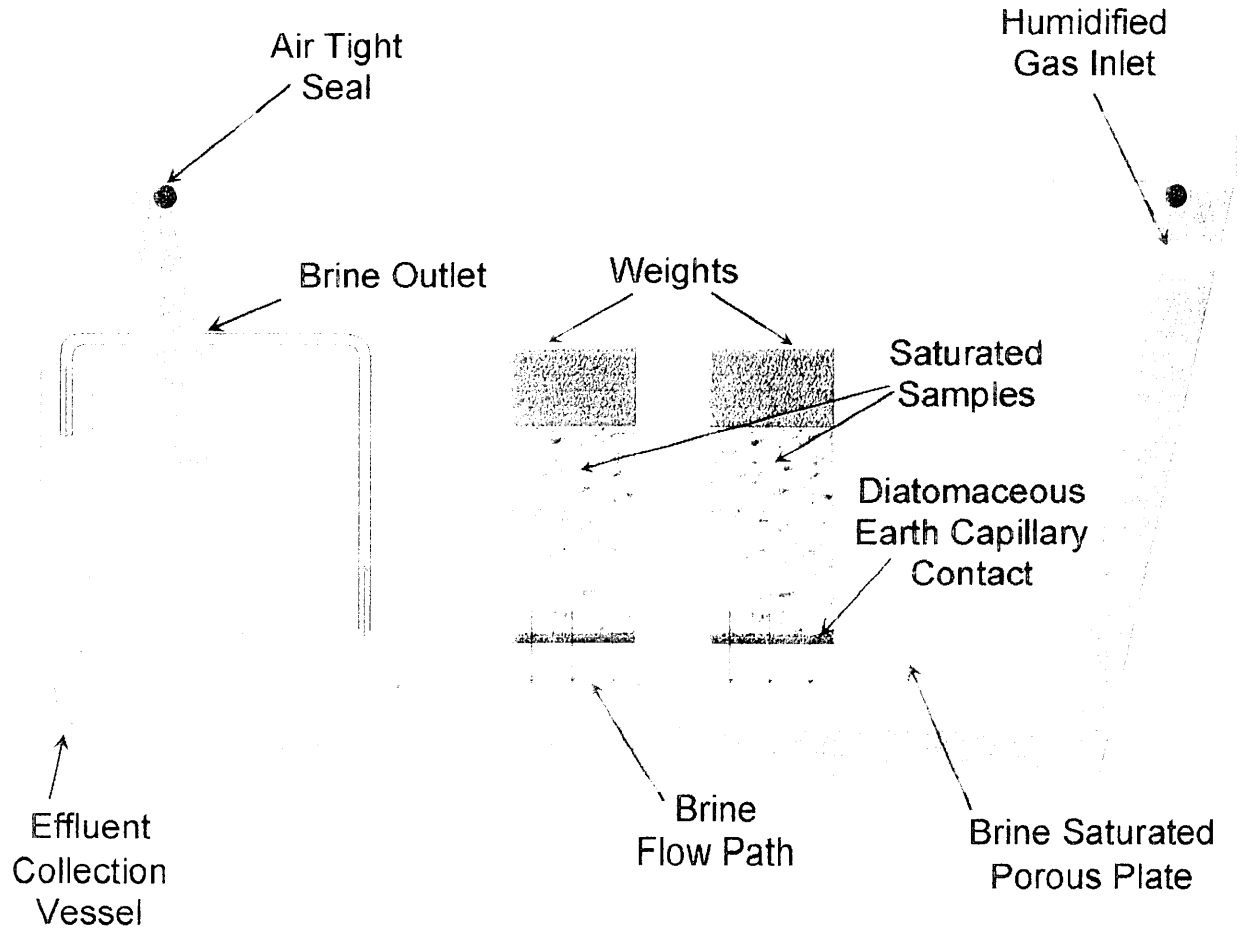

PE908080_color085

903080 332

LIQUID PERMEABILITY SCHEMATIC

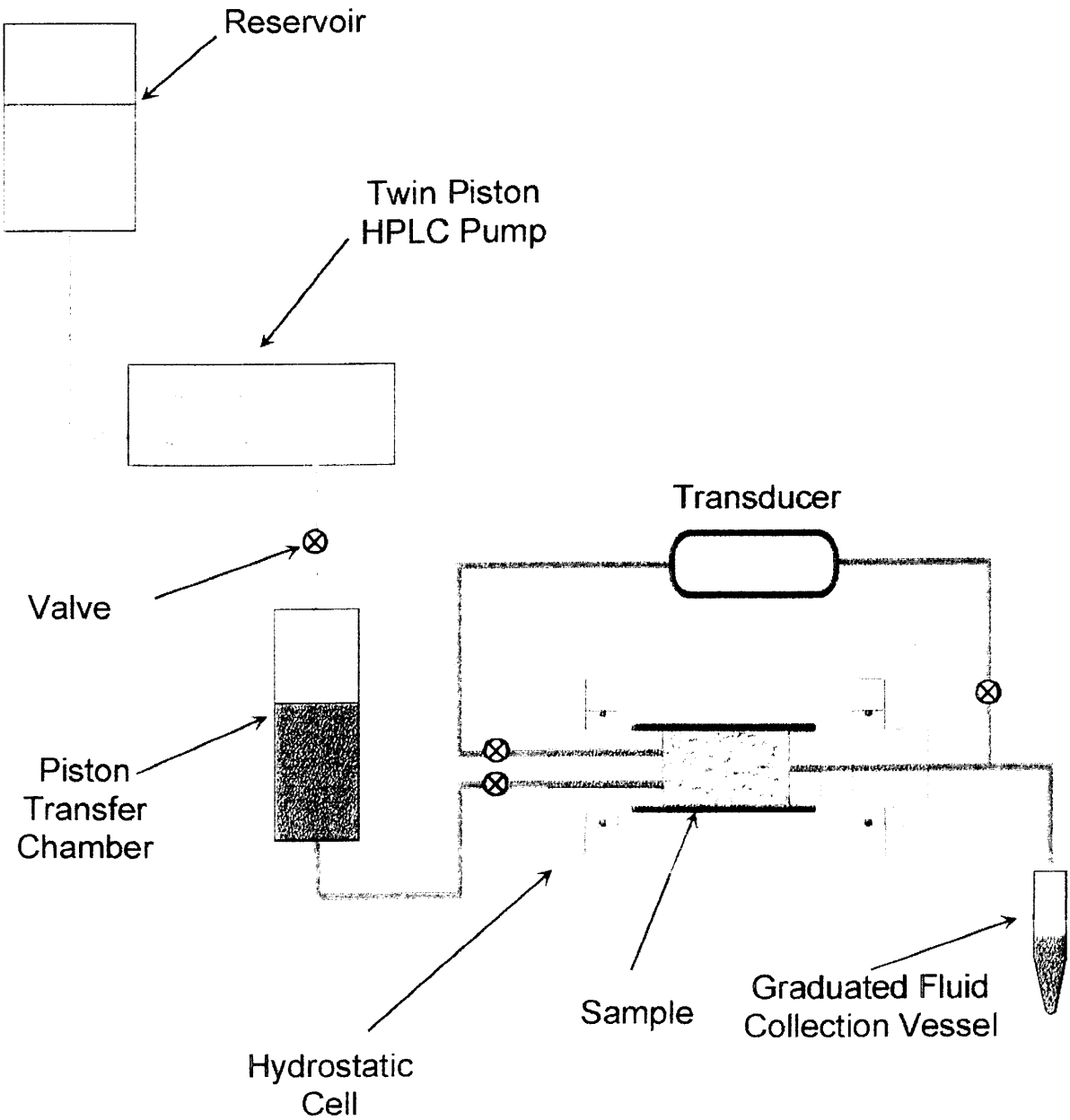

APPENDIX IV

FINAL STATUS REPORT

ACS LABORATORIES PTY LTD: SPECIAL CORE ANALYSIS STATUS REPORT

Status Report Number	10

Company:	Attention:	Copy to:	Date:
OMV Australia Pty Ltd	**Mark Adamson**		**12 June 00**
Well/Work:	Fax No.:	Fax No.:	ACS File No.:
Baleen-2	**08 9223 5004**		**0445-08**

Analysis	No	Date Started	Number Complete	Completion Dates		Invoice Number	Details	Comments
				Expected	Actual			
Sample screening and Preparation								
CT Scanning	20	21 Feb 00	20		25 Feb 00			Complete
Cold Solvent Extraction	19	29 Feb 00	19	4 Mar 00	5 Mar 00			Complete
Critical Point Drying	19	5 Mar 00	19	12 Mar 00	13 Mar 00			Complete
Ambient Base Parameters	19	13 Mar 00	19	13 Mar 00	14 Mar 00			Complete
Electrical Properties / Pc								
Saturate	9	16 Mar 00	9	16 Mar 00	17 Mar 00			Complete
Multi Salinity Formation Factor	10	23 Mar 00	10	31 Mar 00	31 Mar 00			Complete See Note 1,2 & 3
RI @ OB	7	4 Apr 00	7	19 Jun 00	16 Jun 00			Complete See Note 3
Pc A/B p.p. @ OB	7	4 Apr 00	7	19 Jun 00	16 Jun 00			Complete
Dean Stark	7	26 May 00	7	20 Jun 00	17 Jun 00			Complete
Clean & Dry	7	28 May 00	7	23 May 00	26 Jun 00			Complete
OB base parameters	7	1 Jun 00	7	26 Jun 00	26 Jun 00			Complete
Cation Exchange Capacity	10		10	15 May 00	18 May 00			Complete and Reported
Residual Gas								
Saturate	9	16 Mar 00	9	16 Mar 00	17 Mar 00			Complete
Permeability to brine	9	23 Mar 00	9	24 Mar 00	27 Mar 00			Complete

ACS LABORATORIES PTY LTD: SPECIAL CORE ANALYSIS STATUS REPORT

Status Report Number	10

Company:	Attention:	Copy to:	Date:
OMV Australia Pty Ltd	**Mark Adamson**		**12 June 00**
Well/Work:	Fax No.:	Fax No.:	ACS File No.:
Baleen-2	**08 9223 5004**		**0445-08**

Analysis	No	Date Started	Number Complete	Completion Dates		Invoice Number	Details	Comments
				Expected	Actual			
Desat. to Swi	8	27 Mar 00	8	24 May 00	24 May 00			Complete
Basic water flood	8	2 May 00	8	30 May 00	28 May 00			Complete
- Keg @ Swi								
- Kw @ Sgr								
Clean & Dry	8	28 May 00	8	1 Jun 00	1 Jun 00			Complete
OB base parameters	8	3 Jun 00	8	3 Jun 00	3 Jun 00			Complete
Klinkenberg permeability	8	3 Jun 00	8	3 Jun 00	5 Jun 00			Complete
Permeability vs OB stress	5	21 Aug 00	5	29 Aug 00	31 Aug 00			Complete
Petrology	12	19 Feb 00	12	24 Mar 00	7 Apr 00			Complete
Sand Stability Study								
Sieve Analysis	5	24 Mar 00	5	30 Mar 00	31 Mar 00			Complete
Critical Velocities	3							Cancelled by OMV
Draft Final Report	1		1		14 Aug 00			
Final Report	3		3		6 Oct 00			

Additional Comments/Notes:

1. **Samples #27 & #29 failed during Co/Cw measurements.**
2. **Sample #28 moved from residual gas suite to electrical properties suite.**
3. **Sample #S23 Failed**

PETER CROZIER
Operations Manager
Ph: 07 3350 1222
Fax: 07 3359 0666
Email: p.crozier@acslabs.com.au

APPENDIX V

ABBREVIATIONS

ABBREVIATIONS for CORE PROPERTIES

a	Intercept (assumed = 1)
A	Sample Cross Sectional Area (cm^2)
ABPc	Air-Brine Capillary Pressure
Amb	Ambient Conditions (No Overburden Pressure)
B	Equivalent Conductance of Clay Exchange Cations ($mho/m.cm^2.meq^{-1}$)
β	Beta Factor (ft^{-1})
BF	Basic Flood
BHN	Brinell Hardness Number (kg/mm^2)
BP	Barometric Pressure (atm)
CEC	Cation Exchange Capacity (meq/100g dry sample)
Cent	Centrifuge
Co	Conductivity of Fully Brine Saturated Sample (mho/m)
cP	Centipoise
Cw	Conductivity of Brine (mho/m)
Dr	Drainage (i.e. draining of the wetting fluid - usually brine)
Φ	Porosity
FF	Formation Factor
*FF**	Shaly Sand Equivalent Formation Factor
g	grams
HeInj	Helium Injection
HgInj	Mercury Injection Capillary Pressure
Imb	Imbibition (i.e. imbibition of the wetting fluid - usually brine)
K	Permeability (mD)
Ka	Air Permeability (mD)
Keg	Effective Permeability to Gas (mD)
Keo	Effective Permeability to Oil (mD)
Kew	Effective Permeability to Water (mD)
Kg	Gas Permeability (mD)
KgKo	Gas-Oil Relative Permeability

ACS Laboratories Pty Ltd
ABN: 81 008 273 005

ABBREVIATIONS for CORE PROPERTIES

KgKw	Gas-Water Relative Permeability
Klink or Kl	Klinkenberg Permeability (mD)
Ko	Oil Permeability (mD)
Krg	Relative Gas Permeability
Kro	Relative Oil Permeability
Krw	Relative Water Permeability
Kw	Brine Permeability (mD)
KwKo	Oil-Water Relative Permeability
L	Sample Length (cm)
m	Cementation Factor
*m**	Shaly Sand Equivalent Cementation Factor
mD	milliDarcy's
n	Saturation Exponent
*n**	Shaly Sand Equivalent Saturation Exponent
OB	Overburden Pressure (psig)
OBPc	Oil-Brine Capillary Pressure
P	Pressure (psi)
Pc	Capillary Pressure (psig)
PP	Porous Plate
PvComp	Pore Volume Compressibility
PVR	Pore Volume Reduction (cm^3)
ρ	Density (g/cm^3)
q	Flow Rate (cm^3/s)
θ	Contact Angle (degrees)
Qv	Volume Concentration of Clay Exchange Cations (meq/cm^3)
r	Radius (cm)
Rc	Sample Resistance (ohm)
RCA	Routine Core Analysis

ABBREVIATIONS for CORE PROPERTIES

ResCon	Reservoir Conditions
RI	Resistivity Index
RICP	Resistivity Index & Capillary Pressure
Ro	Resistivity of Fully Brine Saturated Sample (ohm.m)
Rt	Resistivity of Partially Saturated Sample (ohm.m)
Rw	Resistivity of Brine (ohm.m)
S	Saturation
s	Seconds
SCA	Special Core Analysis
Sg	Gas Saturation
Sgr	Residual Gas Saturation
SngPt	Single Point
So	Oil Saturation
Sor	Irreducible Oil Saturation (or Residual Oil Saturation)
SS	Steady State
Sw	Brine Saturation
Swi	Initial Water Saturation
Swir	Irreducible Water Saturation
Swr	Residual Water Saturation
T	Temperature (^{o}C)
USS	Unsteady State
μ	Viscosity (cP)
Vb	Bulk Volume (cm^3)
Vg	Grain Volume (cm^3)
Vp	Pore Volume (cm^3)
ω	Angular Velocity (rad/s)
Wett	Wettability
Wt	Weight (g)

ACS Laboratories Pty Ltd
ABN: 81 008 273 005

APPENDIX 7

BALEEN-2

COMMUNICATION FROM SCHLUMBERGER

-REGARDING MDT PRESSURE DISCREPANCY-

-SCHLUMBERGER-

From: Michel Claverie [Claverie@Perth.Oilfield.SLB.COM]
Sent: Thursday, 7 September 2000 10:17
To: Mark Adamson
Cc: Michel Claverie; Patrick Foale; Jack-King Ting
Subject: RE: Baleen-2 Pressure Data

Importance: High

Mark,

We investigated the calibration history of the MDT pressure gau ges used on
Baleen-2, in order to try and reduce the uncertainty on the abs olute
formation pressure.

Strain Gauge 181745: A new Master Calibration was performed on this gauge on
11 December 1999, and indicates a drift of -0.1 psia to -0.6 ps ia from the
Master Calbration used for the job (19 March 1999) for the down hole
conditions of Baleen-2 (1300 psi and 150 degF).

CQG Gauge 0351: A new Master Calibration was performed on this gauge on 6
June 2000, and indicates a drift of -1 psia from the Master Cal ibration used
for the job (9 February 1999) for the same downhole conditions of Baleen-2.

In view of these results, we advise that both gauges performed within
expected specifications and were accurately calibrated at the t ime of the
Baleen-2 survey.

We recommend that you should use the pressure estimates from th e CQG gauge
because of its intrinsic higher accuracy, and because its calib ration
procedures are more stringent than that of the strain gauge (th e CQG gauge
is re-calibrated in the laboratory of our manufacturing center, where the
Strain Gauge is re-calibrated at the field location).

With regards,
Michel

MICHEL CLAVERIE - Schlumberger Oilfield Australia

direct: 61 8 9420 4894
mobile: 61 412 026 966
mailto:claverie@perth.wireline.slb.com

-----Original Message-----
From: Michel Claverie
Sent: Tuesday, 18 July 2000 16:44
To: Mark Adamson
Cc: Michel Claverie; Zachariah John; Woodburn, Charles
Subject: RE: Baleen-2 Pressure Data

Mark,

We reviewed the MDT pressures from Baleen-2 on GeoFrame Polaris . The
attached Excel file contains the results of the processing, wit h all
pressures expressed in PSIA.

We compared CQG (quartz) and Strain Gauge readings for Mud Pres sure Before,
for Mud Pressure After and for Build-Up Pressure. The average difference in
reading is about 6 psi, with a maximum of 9 psi and a minimum o f 4.7 psi.

The specification for accuracy of the CQG gauge is +/- 2psi + 0 .01% of
reading, or about +/- 2.15 psi for this well. The specificatio n for
accuracy of the Strain Gauge is 0.1% of Full Scale reading (10k psi gauge),
or +/- 10 psi for this well.

The maximum acceptable difference is therefore 2.15 + 10 = 12.1 5 psi for
this well.

In this particular case, the readings of CQG quartz and Strain gauges are
within tolerance. I am sending you a copy of our published Pres sure Gauge
specifications for reference.

With regards,
Michel

MICHEL CLAVERIE - Schlumberger Oilfield Australia
direct: 61 8 9420 4894
mobile: 61 412 026 966
mailto:claverie@perth.wireline.slb.com

-----Original Message-----
From: Mark Adamson [mailto:mark.adamson@omv.com.au]
Sent: Thursday, 22 June 2000 17:21
To: Michel Claverie
Cc: Zachariah John; consulting
Subject: Baleen-2 Pressure Data

Michel,

As a log QC issue, I would like you to make an investigation of the Baleen-2
MDT run, (Suite-1 run 3 and 5, 16/10/99) and the data acquired.

The strain gauge reading (PSIG) reported on the log print reads 2-7 psi less
than the quartz gauge pressure reading (PSIA). This is evident for both the
formation and hydrostatic pressures on the various pre-tests. G iven that the
expected difference should be 14.7psi, it raises a question on the validity
of the data.

Please
i) review the data and the calibrations
ii) talk to us after your analysis, and
iii) finally provide us with a written explanation.

The gauge calibrations were 7 months and 8 months old for the s train and

quartz gauges respectively. Both should be reading within the accuracy
claimed (1 psi for strain and 0.1 psi for quartz).

The easy explanation of an incorrectly calibrated strain gauge will be
accepted by OMV cautiously. Rather, I request you to rigorously go through
the calibrations carried out on the quartz gauge and even check back to
determining that the correct calibration data for the Master ca libration was
used.

Regards,
Mark

Mark Adamson - Senior Operations Geologist
Tel +61-(0)8-9223 5000, Fax +61-(0)8-9223 5004
Level 29, 44 St Georges Terrace, Perth WA 6000, AUSTRALIA

ENCLOSURES

ENCLOSURES

903080 347

- **Enclosure 1** – Baleen-2 Well Composite Log - OMV
- **Enclosure 2** – 1:100 ELANPlus Wide Display Composite Plot (from Petrophysics Report: Appendix 2) – Schlumberger
- **Enclosure 3** – 1:200 ELANPlus Standard Display Composite Plot (from Petrophysics Report: Appendix 2) – Schlumberger
- **Enclosure 4** – 1:200 Dynamic Elastic Moduli and Rock Properties Plot (from Production Stability Evaluation Report Report: Appendix 3) – Schlumberger
- **Enclosure 5** – 1:200 Formation Integrity Sanding Production Plot (from Production Stability Evaluation Report Report: Appendix 3) – Schlumberger

PE908081

This is an enclosure indicator page.
The enclosure PE908081 is enclosed within the container PE908080 at this location in this document.

The enclosure PE908081 has the following characteristics:

ITEM_BARCODE	PE908081
CONTAINER_BARCODE	PE908080
NAME	Encl.1 Baleen-2 Composite Well Log
BASIN	GIPPSLAND
ONSHORE?	N
DATA_TYPE	WELL
DATA_SUB_TYPE	COMPOSITE_LOG
DESCRIPTION	Encl.1 Baleen-2 Composite Well Log, Scale 1:500, by OMV Australia, W1293, VIC/RL5.
REMARKS	
DATE_WRITTEN	
DATE_PROCESSED	
DATE_RECEIVED	25-JAN-2001
RECEIVED_FROM	OMV
WELL_NAME	Baleen-2
CONTRACTOR	OMV
AUTHOR	
ORIGINATOR	CULTUS
TOP_DEPTH	
BOTTOM_DEPTH	
ROW_CREATED_BY	DM35_TW

(Inserted by DNRE - Vic Govt Mines Dept)

PE908082

This is an enclosure indicator page.
The enclosure PE908082 is enclosed within the container PE908080 at this location in this document.

The enclosure PE908082 has the following characteristics:

ITEM_BARCODE	PE908082
CONTAINER_BARCODE	PE908080
NAME	Encl.2 Wide Display Composite Plot
BASIN	GIPPSLAND
ONSHORE?	N
DATA_TYPE	WELL
DATA_SUB_TYPE	MONTAGE_LOG
DESCRIPTION	Encl.2 Baleen-2 ELANPlus Wide Display Composite Plot 1:100, by Schlumberger for OMV Australia Pty Ltd, W1293, VIC/RL5.
REMARKS	
DATE_WRITTEN	
DATE_PROCESSED	
DATE_RECEIVED	25-JAN-2001
RECEIVED_FROM	CULTUS
WELL_NAME	Baleen-2
CONTRACTOR	Schlumberger
AUTHOR	
ORIGINATOR	OMV
TOP_DEPTH	
BOTTOM_DEPTH	
ROW_CREATED_BY	DM35_TW

(Inserted by DNRE - Vic Govt Mines Dept)

PE908083

This is an enclosure indicator page.
The enclosure PE908083 is enclosed within the container PE908080 at this location in this document.

The enclosure PE908083 has the following characteristics:

ITEM_BARCODE	PE908083
CONTAINER_BARCODE	PE908080
NAME	Encl.3 Standard Display Composite Plot
BASIN	GIPPSLAND
ONSHORE?	N
DATA_TYPE	WELL
DATA_SUB_TYPE	MONTAGE_LOG
DESCRIPTION	Encl.3 Baleen-2 ELANPlus Standard Display Composite Plot, Scale 1:200, by Schlumberger for OMV Australia Pty Ltd, W1293, VIC/RL5.
REMARKS	
DATE_WRITTEN	
DATE_PROCESSED	
DATE_RECEIVED	25-JAN-2001
RECEIVED_FROM	OMV
WELL_NAME	Baleen-2
CONTRACTOR	Schlumberger
AUTHOR	
ORIGINATOR	OMV
TOP_DEPTH	
BOTTOM_DEPTH	
ROW_CREATED_BY	DM35_TW

(Inserted by DNRE - Vic Govt Mines Dept)

PE908084

This is an enclosure indicator page.
The enclosure PE908084 is enclosed within the container PE908080 at this location in this document.

The enclosure PE908084 has the following characteristics:

ITEM_BARCODE	PE908084
CONTAINER_BARCODE	PE908080
NAME	Encl.4 Moduli & Rock Properties Plot
BASIN	GIPPSLAND
ONSHORE?	N
DATA_TYPE	WELL
DATA_SUB_TYPE	MONTAGE_LOG
DESCRIPTION	Encl.4 Baleen-2 Dynamic Elastic Moduli & Rock Properties Plot, Scale 1:200, by Schlumberger for OMV Australia Pty Ltd, W1293, VIC/RL5.
REMARKS	
DATE_WRITTEN	
DATE_PROCESSED	
DATE_RECEIVED	25-JAN-2001
RECEIVED_FROM	OMV
WELL_NAME	Baleen-2
CONTRACTOR	Schlumberger
AUTHOR	
ORIGINATOR	OMV
TOP_DEPTH	
BOTTOM_DEPTH	
ROW_CREATED_BY	DM35_TW

(Inserted by DNRE - Vic Govt Mines Dept)

PE908085

This is an enclosure indicator page.
The enclosure PE908085 is enclosed within the container PE908080 at this location in this document.

The enclosure PE908085 has the following characteristics:

ITEM_BARCODE	PE908085
CONTAINER_BARCODE	PE908080
NAME	Encl.5 Formation Intergrity Sanding
BASIN	GIPPSLAND
ONSHORE?	N
DATA_TYPE	WELL
DATA_SUB_TYPE	MONTAGE_LOG
DESCRIPTION	Encl.5 Baleen-2 Formation Integrity Sanding Production Plot, Scale 1:200, by Schlumberger for OMV Australia Pty Ltd, W1293, VIC/RL5.
REMARKS	
DATE_WRITTEN	
DATE_PROCESSED	
DATE_RECEIVED	25-JAN-2001
RECEIVED_FROM	OMV
WELL_NAME	Baleen-2
CONTRACTOR	Schlumberger
AUTHOR	
ORIGINATOR	OMV
TOP_DEPTH	
BOTTOM_DEPTH	
ROW_CREATED_BY	DM35_TW

(Inserted by DNRE - Vic Govt Mines Dept)